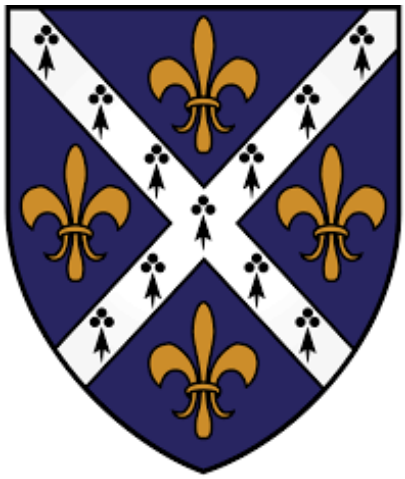
THE ROLE OF DLL4-NOTCH SIGNALLING IN ENDOTHELIAL CELL METABOLISM

Thesis submitted by:

Ulrike Harjes

St. Hugh's College



For the degree of:

Doctor of Philosophy

Department of Oncology

Trinity Term 2014

University of Oxford

Supervisor:

Professor Adrian L. Harris

Dr. Barbara Fielding

THESIS ABSTRACT

THE ROLE OF DLL4-NOTCH SIGNALLING IN ENDOTHELIAL CELL METABOLISM

Ulrike Harjes, St. Hugh's College, University of Oxford D.Phil. Candidate, TT 2014

Tumour tissue is characterised by fluctuating oxygen concentrations, decreased nutrient supply, and acidic pH. Angiogenic signalling pathways that drive a certain metabolic 'configuration' may give endothelial cells a selective advantage in the tumour environment. Previously it has been shown that glycolysis drives proliferation, migration and tip cell formation during sprouting of endothelial cells (De Bock, Georgiadou *et al.* 2013), and is increased by VEGFA. DLL4-NOTCH has been shown to limit angiogenesis and slow down proliferation of endothelial cells, and promote stalk cell formation during angiogenic sprouting, leading to sprout elongation. DLL4-NOTCH is implicated in tumour angiogenesis, and its overexpression is a potential mechanism of resistance to anti-VEGFA therapy (Li, Sainson *et al.* 2011). This thesis aimed at investigating the effect of the DLL4-NOTCH signalling pathway on endothelial metabolism and its implications in angiogenesis. Firstly, it was found that DLL4-NOTCH decreases the glycolytic rate and mitochondrial respiratory parameters in endothelial cells. When given exogenous fatty acids, DLL4-NOTCH activation caused increased fatty acid uptake, storage and oxidation. This shows that the induction of DLL4-NOTCH signalling results in increased fatty acid utilisation. Secondly, this research identified fatty acid oxidation as a target metabolism pathway for angiogenic therapy. More specifically, inhibition of fatty acid oxidation decreased proliferation of endothelial cells, decreased sprout elongation in the sprouting assay, and decreased sprouting from the axial vein in the zebrafish model. ATP production was not affected. Therefore, it was hypothesised that DLL4-NOTCH activation promotes and maintains the stalk cell phenotype through an increase of fatty acid oxidation, thereby promoting biomass production for endothelial cell proliferation and growth during angiogenic sprout elongation. Thirdly, a key fatty acid metabolism gene, *fatty acid binding protein 4* (*FABP4*), was identified, that is positively regulated by NOTCH at its promoter region. FABP4 is a candidate for mediating increased fatty acid flux in endothelial cells in response to DLL4-NOTCH. This study shows that FABP4 is induced by VEGFA in a manner dependent on DLL4-NOTCH, and the insulin-responsive transcription factor FOXO1 was required for FABP4 expression in response to DLL4-NOTCH. FABP4 is pro-angiogenic and implicated in tumour angiogenesis in ovarian cancer omental metastasis. Taken together, this study shows for the first time that DLL4-NOTCH signalling increases FABP4 induction, contributing to a key pro-angiogenic pathway, and also fatty acid utilisation in endothelial cells, and thereby contributes to the formation of blood vessels.

ACKNOWLEDGEMENTS

First and foremost I would like to thank Professor Adrian Harris for giving me the opportunity to do this D.Phil. project under his guidance and supervision. His mentorship has been invaluable, and the past years have been a great experience and an enjoyable challenge. My deepest gratitude also goes to Dr. Barbara Fielding for her very helpful advice and invaluable mentorship during the past few years.

I am deeply grateful to the members of the Harris laboratory, past and present. I have felt welcomed from the beginning of my M.Sc. project and the atmosphere in the lab has greatly contributed to my decision to stay on for my D.Phil,. I am deeply grateful to Esther Bridges. Her support and guidance were critical to the development and completion of the thesis. I am deeply grateful to Karim Bensaad and Alan McIntyre for being great scientists and for sharing their expertise. I am grateful to Simon Wigfield and Helen Sheldon, who are the heart and soul of the lab - I have stood in line to ask them for advice so many times, and they always have had time to listen and help. I am deeply grateful to Simon Lord, Ioanna Ledaki, Chris Blick, Dylan Jones, Massimo Masiero, Dean Singleton, Anassuya Ramachandran, Elena Favaro and Jon Williams, for being great colleagues, mentors and friends, and for all their help, advice, discussions, and thoughts they shared with me. Many thanks also to Peter Thomas, Sam Oats, Penny Berry, Sofia Santos, Matteo Morotti, Anand Sharma, Leonardo Motta, David Favara, Syed Haider, Christos Zois, Ruud van Stiphout and Laura Winchester, and of course to the rest of the Oncology floor.

I am grateful to Katherine Pinnick, Jane Cheeseman, Jennifer Collins, Professor Fredrik Karpe, and Katherine Kearney for their help and support with the fatty acid metabolism and adipocyte work, and to Ioannis Roxannis, Helen Turley, Fabrizio Miranda and Professor Ahmed Ahmed for supporting the ovarian cancer study.

My deepest gratitude goes to those who have been there for me along the way, especially Ghadeer for her unconditional friendship and support. I am grateful to Amy and Ruchi, and to Jon, Marta, Chrissy, Martin and Erica for being great friends. Also thanks to my past and present housemates (of course including the dog Graf), especially to Andi and Janina who have become dear friends. Lastly, I would like to thank my family, for their continuous love and support. I dedicate this thesis to my mother who never stops encouraging me to pursue my goals.

TABLE OF CONTENTS

COVER **1**

THESIS ABSTRACT **2**

ACKNOWLEDGEMENTS **3**

TABLE OF CONTENTS **4**

LIST OF FIGURES **7**

LIST OF TABLES **10**

LIST OF ABBREVIATIONS **11**

1 CHAPTER ONE Introduction and aims of the study **15**

1.1 The vasculature as a target in tumour therapy **16**

1.1.1 Tumour angiogenesis – a hallmark of cancer 16

1.1.2 Sprouting angiogenesis 17

1.1.3 Tumour angiogenic factors – regulation of VEGA in tumour tissue and anti-VEGFA therapy 20

1.1.4 The NOTCH signalling pathway 22

1.1.5 The interplay between VEGFA and NOTCH signalling 25

1.1.6 DLL4-NOTCH signalling in tumour angiogenesis and implications for tumour therapy 28

1.1.7 DLL4-NOTCH and mechanism of resistance to anti-tumour therapy 29

1.2 Metabolism as a target for tumour therapy **30**

1.2.1 Metabolic reprogramming in tumours - an emerging hallmark 30

1.2.2 Mechanisms of metabolic reprogramming 35

1.3 Endothelial cell metabolism **38**

1.3.1 Perspectives of metabolic reprogramming in tumour angiogenesis 38

1.3.2 Metabolism and endothelial cell plasticity 41

1.4 Aims **44**

2 CHAPTER TWO Material and Methods **45**

2.1 Cell culture techniques **46**

2.1.1 Cell growth conditions 46

2.1.2 Cell maintenance and passaging 46

2.1.3 Cell counting and seeding 46

2.1.4 Freezing and thawing cells 47

2.1.5 Growth factor stimulation 47

2.1.6 Hypoxia incubation 47

2.1.7 Drugs 48

2.1.8 RNA interference (RNAi) 48

2.2 Nucleic acid extraction and handling **49**

2.2.1 RNA extraction 49

2.2.2 RNA quantification 49

2.2.3 cDNA synthesis by reverse transcription 49

2.3 Real-time quantitative polymerase chain reaction (qrtPCR) **50**

2.4 Chromatin-Immunoprecipitation assay **52**

2.5 Protein analysis **53**

2.5.1 Preparation of cell lysate 53

2.5.2 Western blot analysis 54

2.5.3 Antibodies for Western blot 55

2.6 Cell-based assays **55**

2.6.1 Fluorescence- or luminescence-based assays 55
2.6.2 Luminescence-based assays 57
2.6.3 Absorbance-based assays 57
2.6.4 MitoStress test, Seahorse Bioscience, Denmark 60
2.6.5 ^{14}C-oleic acid utilisation assays 61
2.6.6 Gas chromatography/ mass spectrometry (GC/MS) techniques 65
2.6.7 Angiogenic assays 67
2.6.8 Zebrafish angiogenesis assay 68
2.7 Immunohistochemical (IHC) staining 68
2.7.1 IHC staining of in vitro cell pellets for antibody validation 68
2.7.2 IHC staining of patient samples 69
2.8 Statistical analysis 71
3 CHAPTER THREE DLL4-NOTCH signalling increases fatty acid utilisation 72
3.1 Introduction 73
3.2 Results 74
3.2.1 DLL4-NOTCH signalling decreases glycolysis 74
3.2.2 DLL4-NOTCH signalling decreases mitochondrial respiration 76
3.2.3 DLL4-NOTCH signalling leads to a substrate-dependent increase of oxygen consumption 79
3.2.4 Increased oxygen consumption in FA-enriched media is dependent on DLL4-NOTCH signalling, mitochondrial FA import, and glucose availability 82
3.2.5 Metabolism of ^{14}C-OA is increased by DLL4-NOTCH signalling 84
3.2.6 Accumulation of intracellular ^{14}C from exogenous ^{14}C-OA is increased by DLL4-NOTCH signalling 86
3.2.7 DLL4-NOTCH signalling activation leads to an increase of lipid droplet accumulation 88
3.2.8 DLL4-NOTCH activation leads to upregulation of intracellular triglyceride stores 90
3.2.9 PL-FA composition does not change in response to DLL4-NOTCH activation 92
3.2.10 Inhibition of FA oxidation by EX affects HUVEC proliferation but not migration 94
3.2.11 EX treatment depletes endothelial ATP levels at high concentrations 96
3.2.12 EX treatment affects mitochondrial respiration 98
3.2.13 Lipid droplets in sprouting HUVEC 103
3.2.14 Sprouting angiogenesis is decreased by EX 105
3.2.15 Inhibition of FA oxidation in zebrafish affects vascular plexus formation 107
3.3 Discussion 109
4 CHAPTER FOUR The regulation of FABP4 by DLL4-NOTCH 117
4.1 Introduction 118
4.2 Results 121
4.2.1 DLL4-NOTCH signalling regulates FABP4 121
4.2.2 FABP4 expression in response to DLL4-NOTCH is downregulated by γ-secretase inhibition and oxygen deprivation 125
4.2.3 FABP4 expression does not follow peroxisome proliferator-activated receptor expression in hypoxia 127
4.2.4 FABP4 expression in hypoxia is dependent on HIF-1α 131
4.2.5 Inhibition of DLL4-NOTCH binding by a DLL4 blocking antibody reduces FABP4 induction by VEGFA 133
4.2.6 VEGFA induced FABP4 is downregulated by γ-secretase inhibition. 135

4.2.7 Inhibition of ADAM 10 and ADAM 17 reduces FABP4 induction by VEGFA. 137
4.2.8 DLL4-NOTCH induced FABP4 expression is sensitive to rapamycin 139
4.2.9 AKT inhibition increases FABP4 expression 142
4.2.10 Regulation of FABP4 downstream of VEGFA or direct DLL4-NOTCH activation is dependent on FOXO1 144
4.2.11 NICD binds to specific FABP4 promoter regions adjacent to the FOXO1 binding motif 146
4.3 Discussion 149

5 CHAPTER FIVE The role of FABP4 in regulating fatty acid metabolism and angiogenesis 155
5.1 Introduction 156
5.2 Results 158
5.2.1 Role of FABP4 as a downstream target of DLL4-NOTCH signalling in angiogenesis 158
5.2.2 Role of FABP4 as a downstream target of DLL4-NOTCH signalling in FA utilisation 165
5.2.3 OA-derived ^{14}C-transfer from adipocytes to endothelial cells 167
5.3 Discussion 171
5.3.1 Role of FABP4 as a downstream target of DLL4-NOTCH in sprouting 171
5.3.2 Role of FABP4 as a downstream target of DLL4-NOTCH in FA utilisation. 173

6 CHAPTER SIX FABP4 in tumour angiogenesis – a pilot study 178
6.1 Introduction 179
6.2 Results 181
6.2.1 Expression of FABP4, NOTCH, DLL4 and VEGFR2 in ovarian tumours 181
6.3 Discussion 188

7 CHAPTER SEVEN Concluding remarks and future directions 191
7.1 Summary 192
7.2 FA metabolism - a metabolic niche for tumour endothelial cells? 195
7.3 Integration of FA metabolism by signalling pathways in the vasculature 196
7.3.1 VEGFB 196
7.3.2 PGC-1α 197
7.3.3 Nitric oxide (NO) 198
7.4 Potential of FA oxidation as a target in tumour therapy 199
7.4.1 Anti-inflammatory and pro-apoptotic properties of EX 199
7.4.2 Anti-angiogenic proterties of EX 200
7.5 Perspectives and future studies 203

APPENDIX I Supplementary data 205
MitoStress Test optimisation 206
Etomoxir effect on endothelial sprouting in fibrin gel 207
Gene expression data LDHA and SLC1A4 208
Lipolytic capacity of differentiated adipocytes 209
FABP4 antibody validation for IHC staining 210

APPENDIX II List of publications related to this thesis 211

REFERENCES 212

LIST OF FIGURES

Figure 1.1. Angiogenic sprouting in tumour tissue. 19
Figure 1.2 NOTCH signalling cascade activated by Delta-like ligand (DLL) 4. 24
Figure 1.3 The vascular endothelial growth factor (VEGFA) and NOTCH regulatory network during tip and stalk cell phenotype formation. 27
Figure 1.4 Overview of metabolic pathways important for tumour cell homeostasis.. 31
Figure 1.5 Endothelial cell metabolism in relation to the tumour metabolic environment. 43
Figure 3.1 DLL4-NOTCH signalling decreases glycolysis.. 75
Figure 3.2 DLL4-NOTCH signalling decreases mitochondrial respiration at 5 mM glucose. 78
Figure 3.3 DLL4-NOTCH signalling leads to a substrate-dependent increase of oxygen consumption. 81
Figure 3.4 Increased oxygen consumption in media with oleic acid (OA) is dependent on DLL4-NOTCH signalling, mitochondrial fatty acid (FA) import, and glucose availability.. 83
Figure 3.5 Metabolism of ^{14}C-oleic acid is increased by DLL4-NOTCH signalling. 85
Figure 3.7 DLL4-NOTCH signalling activation leads to an increase of lipid droplet accumulation... 89
Figure 3.8 DLL4-NOTCH activation leads to upregulation of intracellular triglyceride stores. 91
Figure 3.9 Phospholipid-fatty acid composition does not change in response to DLL4-NOTCH. 93
Figure 3.10 Inhibition of fatty acid oxidation by etomoxir does not affect HUVEC migration but does affect proliferation. 95
Figure 3.11 Etomoxir treatment depletes intracellular ATP levels at high concentrations. 97
Figure 3.12 Etomoxir treatment affects mitochondrial respiration. 102
Figure 3.13 Lipid droplets in sprouting HUVEC.. 104
Figure 3.14 Sprouting angiogenesis is decreased by EX in growth factor-reduced matrigel. 106
Figure 3.15 EX treatment affects caudal vein plexus (CVP) development and intersegmental vessel (ISV) number in zebrafish. 108
Figure 3.16 Schematic of effects of DLL4-NOTCH signalling on metabolism in endothelial stalk cells. 110
Figure 3.17 Model of DLL4-NOTCH effect on metabolism in sprouting endothelial cells. 115
Figure 4.1 Mechanisms of fatty acid uptake and utilisation. 119
Figure 4.2 DLL4-NOTCH signalling regulates fatty acid binding protein 4 (FABP4). 123
Figure 4.3 Fatty acid binding protein 4 (FABP4) in response to DLL4-NOTCH is downregulated by γ-secretase inhibition and by oxygen deprivation. 126

Figure 4.4 Fatty acid binding protein 4 (FABP4) expression does not follow peroxisome proliferator-activated receptor (PPAR) expression in hypoxia. 130
Figure 4.6 Inhibition of DLL4-NOTCH binding by a DLL4 blocking antibody reduces fatty acid binding protein 4 (FABP4) induction by VEGFA. 134
Figure 4.7 VEGFA-induced fatty acid binding protein 4 (FABP4) is downregulated by γ-secretase inhibition. 136
Figure 4.8 Inhibition of ADAM10 and ADAM17 reduces fatty acid binding protein 4 (FABP4) induction by VEGFA. 138
Figure 4.9 DLL4-NOTCH induced fatty acid binding protein 4 (FABP4) expression is sensitive to rapamycin. 140
Figure 4.10 VEGFA induced fatty acid binding protein 4 (FABP4) expression is sensitive to rapamycin.. 141
Figure 4.11 AKT inhibition increases fatty acid binding protein 4 (FABP4) expression. 143
Figure 4.12 Regulation of gene and protein expression of fatty acid binding protein 4 (FABP4) is dependent on FOXO1. 145
Figure 4.13 NOTCH intracellular domain (NICD) binds to specific fatty acid binding protein 4 (FABP4) promoter regions adjacent to the FOXO1 binding motif. 148
Figure 4.14 Regulation and mechanism of fatty acid binding protein 4 (FABP4) induction in endothelial cells is dependent on DLL4-NOTCH signalling and FOXO1. 150
Figure 5.1 Validation of *fatty acid binding protein 4 (FABP4)*-targeting siRNAs.. 159
Figure 5.2 *Fatty acid binding protein 4 (FABP4)* knockdown does not affect angiogenic sprouting in matrigel. 162
Figure 5.3 Fatty acid binding protein 4 (FABP4) inhibition by BMS309403 (F4I) and effect on endothelial proliferation, migration and sprouting. 164
Figure 5.4 FABP4 inhibition by RNAi or by BMS309403 (F4I) does not affect accumulation of ^{14}C derived from extracellular ^{14}C-oleate.. 166
Figure 5.5 Oleic acid-derived ^{14}C-transfer from adipocytes to endothelial cells. 170
Figure 6.1 Intensity scoring of immunohistochemial stainings of serial sections of human ovarian cancer specimen. 183
Figure 6.2 Extent scoring of immunohistochemial stainings of serial sections of human ovarian cancer specimen. 184
Figure 6.3 Representative immunohistochemical staining for fatty acid binding protein 4 (FABP4), NOTCH and VEGFR2 in epithelium of serial sections of ovarian serous borderline tumours (SBT), invasive implants (NII), and high grade serous carcinomas deposits (HGSC-D). 185
Figure 6.4 Representative immunohistochemical staining for fatty acid binding protein 4 (FABP4), NOTCH and VEGFR2 in epithelium-associated stroma of serial sections of ovarian serous borderline tumours (SBT), non-invasive implants (NII), and high greade serous carcinomas (HGSC). 186
Figure 6.5 Representative immunohistochemical staining for fatty acid binding protein 4 (FABP4), NOTCH, DLL4 and VEGFR2 in epithelium-associated vessels of serial sections of ovarian serous borderline tumours (SBT), invasive implants (NII), and high-grade serous carcinoma (HGSC). 187

Figure 7.1 DLL4-NOTCH-induced endothelial cell metabolism in relation to the tumour metabolic environment.....194
Figure 0.1 Optimisation of cell density and drug concentration for the MitoStress Test. 206
Figure 0.2 Sprouting angiogenesis is decreased by EX in fibrin gel.....207
Figure 0.3 DLL4-NOTCH signalling regulates lactate dehydrogenase A (LDHA) and the membranal glutamine transporter SLC1A4.....208
Figure 0.4 Lipolytic capacity of differentiated adipocytes used in coculture. 209
Figure 0.5 Validation of immunohistochemical staining for human fatty acid binding protein 4 (FABP4).....210

LIST OF TABLES

Table 1 Sequences of ON-TARGETplus siRNA targeting *FABP4* 48
Table 2 Sequences of primers used for detection of mRNA or for detection of immunoprecipitated (IP) DNA sequences 50
Table 3 Antibodies and conditions used for IHC staining of human tissues 71

LIST OF ABBREVIATIONS

AA	antimycin A
ACSL	long chain acyl-CoA synthetase
ACSVL	very long chain acyl-CoA synthetase
ADAM	a disintegrin and metalloprotease domain
ADAMTS10	A Disintegrin-Like And Metalloprotease (Reprolysin Type) With Thrombospondin Type 1 Motif, 10
AKT	Protein kinase B
AKTiX	AKT inhibitor X
AMP	adenosine monophosphate
AMPK	AMP-kinase
ANOVA	analysis of variance
ANS	8-anilino-1-napthalene-sulfonic acid
ATP	adenosine triphosphate
Bev	Bevazicumab
bFGF	basic fibroblast growth factor
BSA	bovine serum albumin
BSAc	BSA-coat
BRCA	Breast cancer 1, early onset gene
ChIP	Chromatin Immunoprecipitation
CoA	Coenzyme A
CPT	carnitine palmitoyl transferase
CTNNB1	Catenin (Cadherin-Associated Protein), Beta 1, 88kDa
DAB	3, 3'-diaminobenzidine
DAPI	4',6-diamidino-2-phenylindole
DBZ	dibenzazepine
DEPC	diethyl pyrocarbonate
DGAT	diacylglycerol O-acyltransferase 1
DLL4	Delta-like ligand 4
DLL4c	DLL4-coat
DMSO	dimethylsulfoxide
DNA	deoxyribonucleic acid
dNTP	deoxyribonucleotide triphosphate
EDTA	ethylenediaminetetraacetic acid
ERK	Extracellular signal-regulated kinase
EX	etomoxir
F4I	FABP4 inhibitor BMS 309403
FA	fatty acid
FABP	fatty acid binding protein
FACS	fluorescence-activated cell sorting
FAME	Fatty acid methyl ester

FASN	fatty acid synthase
FATP	fatty acid transport protein
FCCP	Carbonyl cyanide-4-(trifluoromethoxy)phenylhydrazone
FCS	fetal calf serum
FITC	fluorescein isothiocyanate
FOXO1	forkhead box protein O1
GC/MS	gas chromatography/ mass spectrometry
glc	glucose
gln	glutamine
GLUT1	glucose transporter 1
GPAT	glycerol-3-phosphate acyltransferase
HBSS	Hank's balanced salt solution
HES	hes family bHLH transcription factor
HEY	hes-related family bHLH transcription factor with YRPW motif 1
HGSC	high-grade serous carcinoma
HGSC-D	high grade serous carcinoma deposits
HIF	hypoxia-inducible factor
HK	hexokinase
HNSCC	head and neck squamous cell carcinoma
hpf	hours post fertilization
HRP	horse raddish peroxidase
HUVEC	human umbilical vein endothelial cells
IGF	Insulin growth factor
IHC	immunohistochemistry
II	invasive implants
IKK	inhibitor of kappa kinase
INCB3619	ADAM10/17 inhibitor
INCB4298	ADAM17 inhibitor
iNOS	inducible nitric oxide synthase
IP	Immunoprecipitation
lac	lactate
LD	lipid droplets
LDHA	lactate dehydrogenase A
LEF1	Lymphoid Enhancer-Binding Factor 1
LGSC	low-grade serous carcinoma
mADAM	mature ADAM
MAG	monoacylglycerol
MAGL	monoacylglycerol lipase
MAML1	Mastermind-like protein 1
MCT1	monocarboxylate transporter 1
MES	2-(N-morpholino)ethanesulfonic acid
mRNA	messenger ribonucleic acid
MTORC1	mammalian target of rapamycin complex 1
NAD	Nicotinamide adenine dinucleotide
NADP	Nicotinamide adenine dinucleotide phosphate

NEFA	non-esterified fatty acids
NF-kB	nuclear factor kB
NICD	NOTCH intracellular domain
NII	non-invasive implants
NO	Nitric oxide
NRARP	NOTCH-regulated ankyrin repeat protein
OA	oleic acid
OA-BSA	BSA-conjugated oleic acid
OCAR	oxygen consumption arbitrary rate
OCHRe	Oxford Centre for Histopathology Research
OCR	oxygen consumption rate
OxPhos	oxidative phosphorylation
pADAM	premature ADAM
PAGE	polyacrylamide gel electrophoresis
pAKT	phosphorylated AKT
PBS	phosphate-buffered saline
PDK1	pyruvate dehydrogenase kinase 1
PFA	paraformaldehyde
PFK1	phospho-fructo kinase 1
PFKFB3	6-phosphofructo-2-kinase/fructose-2,6-biphosphatase 3
PI3K	Phosphatidylinositol-4,5-bisphosphate 3-kinas
PL	phospholipid
PlGF	placental growth factor
PPAR	peroxisome proliferator-activated receptor
PVDF	polyvinylidene difluoride
RBPJk	recombination signal binding protein for immunoglobulin kappa J region
rhDLL4	recombinant human DLL4
RNA	Ribonucleic acid
RNAi	RNA interference
ROS	reactive oxygen species
Rot	rotenone
RT	reverse transcription
S.D.	standard deviation
SBT	serous borderline tumours
SCD	stearoylCoA-desaturase
SCF	stem cell factor
SDS	sodium dodecyl sulfate
siRNA	small interfering RNA
SIRT1	Sirtuin 1
SLC27A	solute carrier family member 27 A
TBST	Tris buffered saline – Tween 20
TCA	tricarboxylic acid
TG	triglyceride
Tg(kdrl:GFP)	transgenic product, Kinase Insert Domain Receptor tagged with green fluorescent protein

TLC	thin layer chromatography
UPR	unfolded protein response
VEGFA	vascular endothelial growth factor A
VEGFR	vascular endothelial growth factor receptor

1 CHAPTER ONE

Introduction and aims of the study

portions of the text, and figure 1.5, have been published in a modified form in Harjes, U., et al.* (2012). "Endothelial cell metabolism and implications for cancer therapy." Br J Cancer **107**(8): 1207-1212.

1.1 The vasculature as a target in tumour therapy

1.1.1 Tumour angiogenesis – a hallmark of cancer

Activation of oncogenes or inhibition of tumour suppressor genes leads to enhanced proliferation and reduced apoptosis of tumour cells and favours rapid growth of the tumour mass. A distance of <0.2 mm from the tumour cell to the next capillary lumen is the maximum tolerable distance for sufficient diffusion of oxygen. This distance is shorter for the diffusion of molecules like glucose. Beyond this distance, cells that cannot survive such harsh conditions will ultimately die, leaving the area within the tumour necrotic. Tumour angiogenesis, which is the growth of vasculature into the tumour from nearby existing vessels, occurs when the balance of pro- and anti-angiogenic signalling factors tips to the predominance of pro-angiogenic signalling (known as the angiogenic switch) and is crucial for tumour progression. Increased release of pro-angiogenic factors from cells in hypoxic areas, from tumour cells that increase production due to genetic aberrations, and invading cells such as macrophages, results in a sustained stimulation of the vasculature to proliferate and migrate, resulting in chronic tumour angiogenesis. The process of tumour angiogenesis has been more extensively reviewed by Harris (2002), Bridges, Oon *et al.* (2011), and Weis and Cheresh (2011).

Overall the increased number of blood vessels improves oxygen and nutrient supply in the tumour tissue and provides routes for metastasis through dissemination of tumour cells via the bloodstream. However, due to chronic vessel stimulation, tumour vasculature is typically abnormal, immature, characterised by hyperpermeable vessels, and without identifiable hierarchical organization of arterioles, capillaries and venules. The vessels are of uneven

diameter, have abnormal arteriolar-venous shunts, or blind ends and also unperfused channels can occur (Dewhirst, Kimura *et al.* 1996, Konerding, Fait *et al.* 2001).

The existence of non-functional vasculature in the growing tumour tissue leads to areas of insufficient oxygen and nutrient supply within the tumour mass, amplification of pro-angiogenic signalling, and more aggressive tumour growth due to activation of signalling pathways that promote survival of tumour cells in conditions of supply scarcity. Preventing the emergence of tumour angiogenesis at early, still avascularised stages can halt tumour growth, and improving tumour vasculature at more advanced stages can enhance chemotherapeutic drug delivery to the tumour and prevent aggressive transformation. The tumour vasculature and its regulation by angiogenic factors are therefore valuable targets for anti-tumour therapy.

1.1.2 Sprouting angiogenesis

The basic principles of sprouting angiogenesis have been described in a number of excellent reviews (Gerhardt 2008, Herbert and Stainier 2011, Potente, Gerhardt *et al.* 2011). For a schematic depiction of sprouting angiogenesis in tumour tissue please see figure 1.1.

In stable vessels, inactive endothelial cells line the vascular lumens in a cobblestone-like monolayer. Angiogenesis comprises firstly the formation of a sprout that elongates and moves towards the source of the angiogenic cue coming from the tumour tissue. In response to pro-angiogenic signals like the soluble vascular angiogenic growth factor A (VEGFA), a small proportion of endothelial cells in the monolayer become more motile and invasive. These cells detach from the cell layer and invade into the matrix, migrating towards the cue. Adjacent endothelial cells follow, adapting a less motile, more proliferative phenotype. This supports sprout elongation, while maintaining connectivity to the parental vessel. The leading cells are referred to as tip cells and the trailing cells are referred to as stalk cells. The tip cell phenotype is the default endothelial response to pro-angiogenic signals whereas the stalk cell phenotype is established by upregulation of Delta-like ligand 4 (DLL4)-NOTCH signalling (Fig. 1.1). Eventually the growing sprout reconnects with sprouts in close proximity, and

forms a network (anastomosis). Lumen formation follows. Upon the recruitment of mural cells (pericytes and smooth muscle cells), a basal membrane is established. During maturation of the new network, blood flow is initiated and endothelial cells go into quiescence. However if the pro-angiogenic stimulus persists, and inhibitory signals are reduced, the sprout and network formation becomes less efficient and dysfunctional.

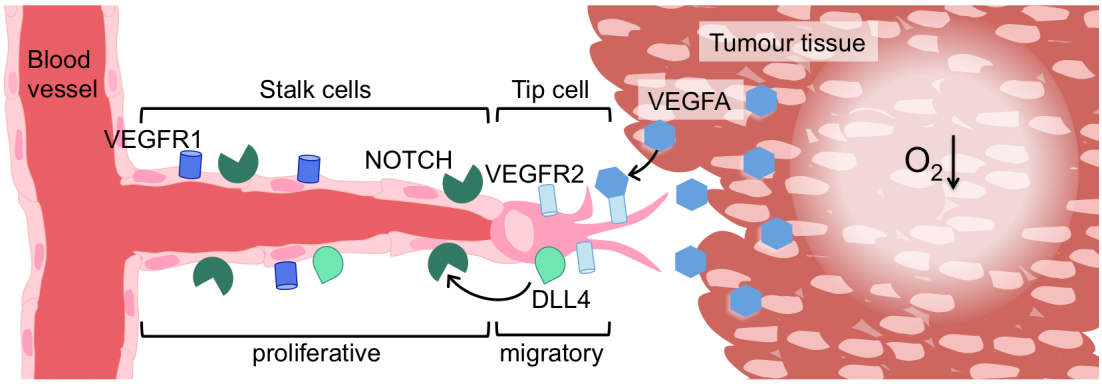


Figure 1.1. Angiogenic sprouting in tumour tissue. Tumour tissue at a distance from vessels has areas of dcreased vessel perfusion, leading to oxygen deprivation (hypoxia) and increased secretion of vascular endothelial growth factor A (VEGFA). VEGFA is a pro-angiogenic factor that recruits endothelial cells to improve blood perfusion. VEGFA binds to the VEGF receptor (VEGFR)2 on endothelial cells, leading to induction of angiogenic sprouting by promoting the tip cell phenotype, which is migratory and responds to the cue by breaking out of the endothelial cell layer and migrating towards the angiogenic signal. VEGFA signalling increases Delta-like ligand 4 (DLL4) expression on the tip cells, thereby promoting DLL4-NOTCH ligand-receptor interaction and transcription of NOTCH target genes in adjacent cells. Activation of NOTCH signalling instructs the stalk cell phenotype, with increased DLL4 and VEGFR1 expression. The stalk cells mainly compose the growing sprout and exhibit a more proliferative phenotype.

1.1.3 Tumour angiogenic factors – regulation of VEGA in tumour tissue and anti-VEGFA therapy

1.1.3.1 Angiogenic factors

Since Folkman's discovery of tumour angiogenic factor in the 1970s, a plethora of angiogenic factors has been discovered and characterized (Folkman, Merler *et al.* 1971). VEGFA is the most well-characterised pro-angiogenic factor. The VEGF family comprises a number of polypeptides, designated VEGFA, placental growth factor (PlGF), VEGFB, VEGFC, VEGFD, and VEGFE, all of which bind the receptor tyrosine kinase receptors VEGFR1, VEGFR2 and VEGFR3 with varying specificity and affinity. VEGFA preferentially binds to and signals via VEGFR2 on blood vessel endothelial cells and is a prototypical tumour angiogenesis promoting factor (reviewed by Veikkola and Alitalo 1999, and Ferrara, Gerber *et al.* 2003). VEGFR1 is a decoy receptor that binds VEGFA with high affinity but does not contribute to VEGFA function in endothelial cells due to its weak kinase activity (Hiratsuka, Minowa *et al.* 1998). Other pro-angiogenic factors are basic fibroblast growth factor (bFGF), platelet-derived growth factor PDGFB and C, Angiopoietin-1 and -2, and other hormones (e.g. oestrogen), and metabolites (e.g lactate) that promote endothelial cell proliferation and migration in the tumour tissue by direct or indirect mechanisms. Examples of anti-angiogenic factors are Thrombospondin-1 (a glycoprotein of the extracellular matrix), endostatin (a cleavage product of collagen IV), and angiostatin (cleavage product of plasmin) (Elkin, Orgel *et al.* 2004, partly reviewed by Potente, Gerhardt *et al.* 2011, Sonveaux, Copetti *et al.* 2012).

1.1.3.2 VEGFA expression in tumours

VEGFA is the most potent inducer of angiogenesis; it activates endothelial cell proliferation and migration and promotes survival pathways. VEGFA is expressed in many cancers and is upregulated as a direct or indirect consequence of oncogenic activation (e.g. *RAS*, *MYC*), tumour suppressor inhibition (e.g. p53), as well as indirectly by glucose deprivation, cellular acidosis, and oxygen deprivation (Rak, Mitsuhashi *et al.* 1995, Fukumura, Xu *et al.* 2001,

Baudino, McKay *et al.* 2002, Yun, Lee *et al.* 2005, Farhang Ghahremani, Goossens *et al.* 2013). Oxygen deprivation (hypoxia) leads to the induction of hypoxia-inducible factor (HIF)-1α, known to activate VEGFA transcription. HIF-1α is overexpressed in many cancer types, for example in head and neck cancer, ovarian cancer, and esophageal cancer (Forsythe, Jiang *et al.* 1996, Zhong, De Marzo *et al.* 1999, Talks, Turley *et al.* 2000). VEGFA is also upregulated in response to growth factors like PDGF, bFGF, and tumour necrosis factor, which are expressed by tumour cells and thereby potentiate VEGFA production in tumour and endothelial cells (Seghezzi, Patel *et al.* 1998, reviewed by Ferrara 2004). Some tumour cells express VEGFR2 and are responsive to VEGFA mitogenic stimulation, for example ovarian tumour cells (Masood, Cai *et al.* 2001). Thus in tumour tissue, VEGFA can act as a paracrine and autocrine signalling molecule, leading to the stimulation of tumour and endothelial cell growth. For these reasons, VEGFA is a valuable target for tumour therapy.

1.1.3.3 Targeting VEGFA for tumour therapy

There are currently a number of drugs targeting the VEGFA pathway, such as antibodies against VEGFA or VEGFR2, VEGFR mimics, and receptor-tyrosine kinase inhibitors that preferentially target VEGFR2. Bevacizumab (Bev) is an anti-VEGFA monoclonal antibody (known also as Avastin, Genentech), which shows clinical benefit in colorectal cancer and metastatic breast cancer when combined with chemotherapy (Hurwitz, Fehrenbacher *et al.* 2004, Miller, Wang *et al.* 2007). Additional agents targeting VEGFA, like selective receptor tyrosine kinase inhibitors have shown rates of success in phase III studies, either as single agents or in combination with chemotherapy in renal cell carcinoma and hepatocellular carcinoma (Sandler, Gray *et al.* 2006, Escudier, Eisen *et al.* 2007, Motzer, Hutson *et al.* 2007). Bev and the receptor tyrosine kinase inhibitors Sorafenib (known also as Nexavar, Bayer/ Onyx) and Sunitinib (known also as Sutent, Pfizer) have approval by the USA Food and Drug Administration for clinical use. The mechanisms of action of these drugs however are not fully defined and therapy benefit varies in patients, due to adverse effects and intrinsic or acquired resistance in the tumour vasculature (Casanovas, Hicklin *et al.* 2005, reviewed by

Jain, Duda *et al.* 2006). This resistance can be due to the selection of tumour cell clones that are resistant to hypoxia or upregulation of alternative angiogenic pathways, such as signalling by other VEGF family members, signalling via bFGF-FGFR, or signalling via DLL4-NOTCH (reviewed by Ferrara 2010).

1.1.4 The NOTCH signalling pathway

The NOTCH pathway is activated by receptor-ligand interaction. In mammals, four NOTCH receptors have been identified (NOTCH1-4) (Ellisen, Bird *et al.* 1991, Lardelli, Dahlstrand *et al.* 1994, Konerding, Fait *et al.* 2001, reviewed by Ferrara 2004). There are two different ligand families, which are the serrate family, comprised of Jagged1 and Jagged2, and the Delta family, comprised of Delta1, Delta3, and DLL4 (Bettenhausen and Gossler 1995, Lindsell, Shawber *et al.* 1995, Shawber, Nofziger *et al.* 1996, Dunwoodie, Henrique *et al.* 1997, Rao, Dorsch *et al.* 2000, Shutter, Scully *et al.* 2000).

1.1.4.1 The canonical NOTCH cascade

Upon ligand binding to the NOTCH receptors, a canonical signalling cascade is activated, leading to two proteolytic cleavages of the NOTCH receptor (Fig. 1.2). A disintegrin and metalloprotease domain (ADAM) 10 and ADAM17 cleave at the extracellular proteolysis site (site 2, S2), removing the extracellular domain, which is endocytosed by neighbouring cells. This allows presenilin/ γ-secretase complex-mediated cleavage at the transmembrane domain (site 3, S3), leading to release of the NOTCH intracellular domain (NICD). (Cleavage at site 1 allows NOTCH exocytosis and regulation of signalling activity upon synthesis. It is not directly involved in NOTCH downstream signalling). NICD translocates to the nucleus to regulate transcription as part of a multimer complex. Binding of NICD to the deoxyribonucleic acid (DNA)-binding protein Recombination Signal Binding Protein For Immunoglobulin Kappa J (RBPJk) leads to conversion of RBPJk from a transcriptional repressor into a transcriptional activator. Recruitment of the co-activator protein Mastermind-like protein 1 (MAML1) stabilises and completes the core of the complex leading to transcription of NOTCH target genes. NICD can be modified by ubiquitylation,

phosphorylation, hydroxylation, and acetylation events, thereby affecting activity and turnover of NICD. Primary target genes are HES (Hairy/Enhancer of Split) and HEY (HES-related with YRPW motif, also named HERP, HES-related repressor protein) genes (Fig. 1.2). This was reviewed by Gordon, Arnett *et al.* (2008), Herbert and Stainier (2011), and Kopan (2012). Further NOTCH targets include the VEGFR2 (downregulated), VEGFR1 (upregulated), and DLL4 (upregulated) (Holderfield, Henderson Anderson *et al.* 2006, Williams, Li *et al.* 2006, Harrington, Sainson *et al.* 2008).

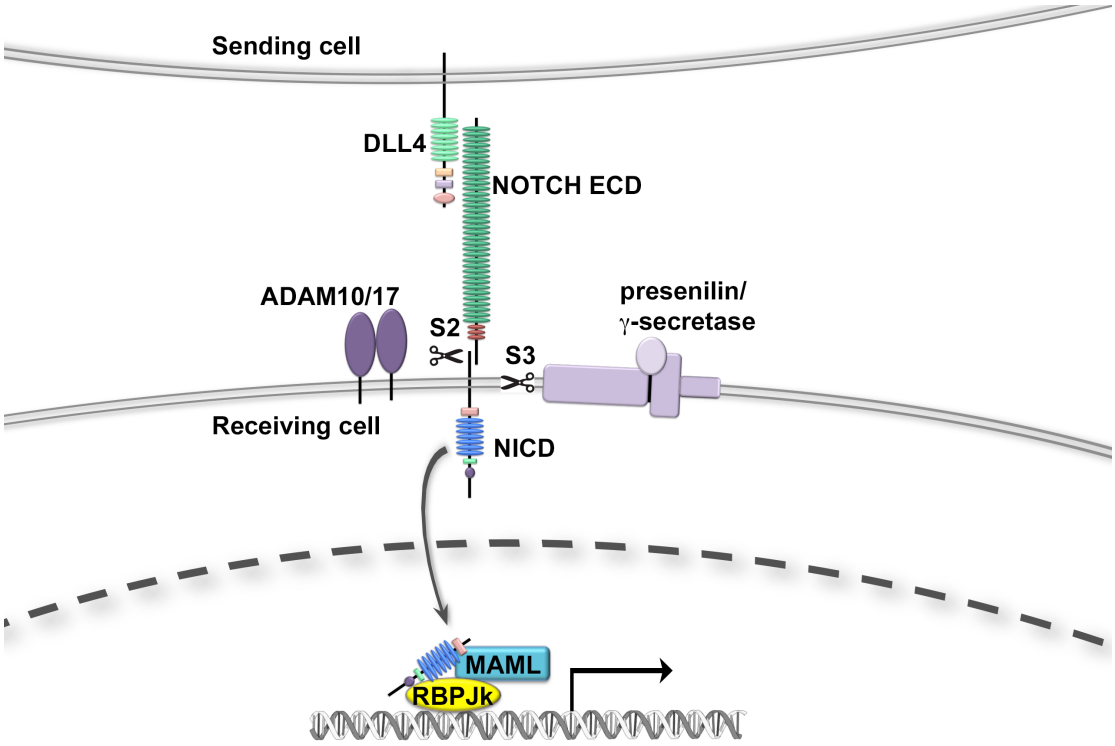


Figure 1.2 NOTCH signalling cascade activated by Delta-like ligand (DLL) 4. DLL4 is expressed on the cell surface of the signal-sending cell and binds to the extracellular domain (ECD) of the NOTCH receptor on adjacent cells (signal-receiving cell). Upon binding, the extracellular site undergoes cleavage by ADAM10/ ADAM17 ate site 2 (S2). ECD is released and endocytosed by neighbouring cells. This enables cleavage of the transmembrane domain at site 3 (S3) by the presenilin/ γ-secretase complex, leading to the release of NOTCH intracellular domain (NICD). NICD translocates to the nucleus and forms a complex with the DNA binding Recombination Signal Binding Protein For Immunoglobulin Kappa J (RBPJk), and the coactivator mastermind-like protein (MAML1). This results in the regulation of NOTCH target genes.

1.1.4.2 Expression and role of NOTCH and DLL4 in endothelial development

NOTCH receptors 1 and 4 are expressed in arterial endothelium, whereas NOTCH2 and 3 are expressed in smooth muscle cells, and all of the NOTCH ligands except for Delta 1 and 3 are expressed in arterial endothelium during mouse embryonic development (Villa, Walker *et al.* 2001). NOTCH1 is the primary functional receptor required for angiogenesis during mouse development, whereas NOTCH4 is dispensible. DLL4 is the only ligand that shows a gene expression pattern consistent with its function to activate NOTCH1 and NOTCH4 (Krebs, Xue *et al.* 2000). DLL4 is expressed only in large arteries during mouse development and is present in small arteries and capillary beds, as well as in tumour vessels in xenograft models of the adult mouse (Mailhos, Modlich *et al.* 2001). DLL4 haploinsufficency leads to early embryonic lethality, with severe defects in arterial development that are similar to the defects seen in NOTCH1 phenotypes (Duarte, Hirashima *et al.* 2004, Gale, Dominguez *et al.* 2004, Krebs, Shutter *et al.* 2004). From here on, NOTCH1 will be referred to as NOTCH.

1.1.5 The interplay between VEGFA and NOTCH signalling

During sprout formation, activation of NOTCH signalling enables controlled growth of the sprout, due to lateral inhibition of tip cell formation and promotion of stalk cell formation. VEGFA signalling activation via VEGFR2 leads to upregulation of DLL4 expression in endothelial cells. DLL4 expression positively correlates with VEGFA expression in tumours and inhibition of VEFGA signalling reduces DLL4 expression in tumour endothelial cells (Patel, Li *et al.* 2005, Patel, Dobbie *et al.* 2006, Thurston, Noguera-Troise *et al.* 2007). DLL4 overexpression in endothelial cells inhibits proliferation and migration in response to VEGFA, an effect, which is reversed by γ-secretase inhibition by the γ-secretase-specific inhibitor DBZ (dibenzazepine) and therefore dependent on activation of the NOTCH pathway (Williams, Li *et al.* 2006). In response to VEGFA, DLL4 is expressed on the cell surface and can activate NOTCH signalling on adjacent cells by interaction with the NOTCH receptor on these cells, thereby promoting stalk cell formation. Because DLL4 is a target gene of the NOTCH pathway, the stalk (anti-tip) cell signal is amplified across the endothelial cell layer

(Caolo, van den Akker *et al.* 2010). When NOTCH signalling is inhibited by DBZ or DLL4 binding blocked by a selective antibody, tip cell formation is favoured and hypersprouting occurs (Ridgway, Zhang *et al.* 2006, Scehnet, Jiang *et al.* 2007).

VEGFA signalling promotes the tip cell phenotype, whereas NOTCH signalling promotes the stalk cell phenotype. These phenotypes are dynamic and depend on differential expression of the VEGFR1 and VEGFR2. If the balance of VEGFA and NOTCH signalling tips, the phenotype changes. This is also why VEGFA-induced effects are inhibited by DLL4 overexpression, which leads to NOTCH signalling induction and changes in VEGFR expression (Fig. 1.1 - 1.3). Therefore, the signalling network that selects tip or stalk cells leads to a constant shuffling of tip and stalk cell positions due to changes in receptor expression and downstream signalling (Jakobsson, Franco *et al.* 2010).

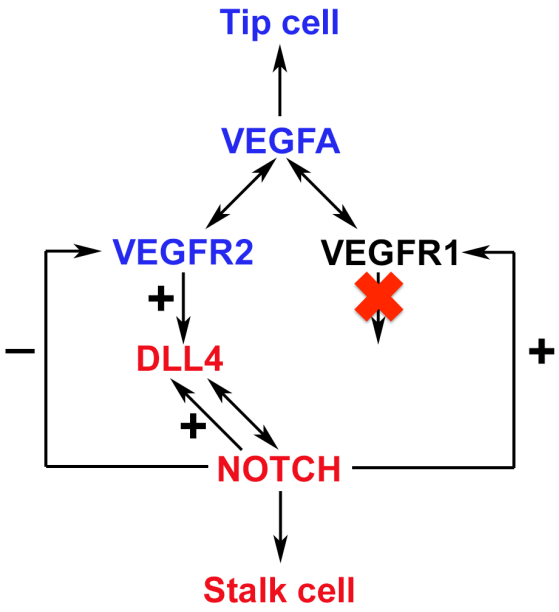


Figure 1.3 The vascular endothelial growth factor (VEGFA) and NOTCH regulatory network during tip and stalk cell phenotype formation. VEGFA signalling promotes tip cell formation via VEGF receptor (VEGFR) 2 mediated signal transduction (double-headed arrow, highlighted in blue), whereas Delta-like ligand (DLL) 4 mediated activation of NOTCH signalling (single-headed arrow) promotes stalk cell formation via mechanisms that include the upregulation of VEGFR1 (high affinity to VEGFA, but weak kinase activity, therefore considered being a VEGFA decoy), and downregulation of VEGFR2 (highlighted in red). VEGFA signal transduction via VEGFR2 leads to the upregulation of DLL4 expression, thereby promoting NOTCH activation and thereby stalk cell formation in cells adjacent to the tip cell (lateral inhibition) and controlled sprout formation.

1.1.6 DLL4-NOTCH signalling in tumour angiogenesis and implications for tumour therapy

1.1.6.1 Expression of DLL4 in tumours

Several studies link increased DLL4 expression in tumour and stromal cells to poor prognosis in cancer and depict the DLL4-NOTCH pathway as a valuable target in tumour therapy. DLL4 expression is strong in the vasculature of mouse breast and lung cancer xenograft models, human renal, colon, and bladder tumour vasculature, compared to normal tissue, and correlates with VEGFA expression (Mailhos, Modlich *et al.* 2001, Patel, Li *et al.* 2005, Noguera-Troise, Daly *et al.* 2006, Patel, Dobbie *et al.* 2006, Jubb, Turley *et al.* 2009). Upregulation of DLL4 expression in clear cell renal carcinoma correlates with distant metastasis and reduced overall survival (Hu, Liu *et al.* 2014). DLL4 expression is also upregulated in breast tumour vasculature and tumour cells, detected in the plasma, and correlates with nodal and distant metastasis (Kontomanolis, Panteliadou *et al.* 2014). DLL4 expression is also upregulated in gastric tumour vasculature and tumour cells and correlates with tumour size, and nodal and distant metastasis (Ishigami, Arigami *et al.* 2013).

1.1.6.2 Expression of NOTCH in tumours

NOTCH signalling is also known to act as an oncogenic pathway. In T cell-acute lymphocytic leukemia, NOTCH bears an activating mutation in >50% of the cases (Weng, Ferrando *et al.* 2004). Activation of NOTCH can drive breast cancer in the xenograft model and NOTCH and Jagged1 expression in human breast tumours correlate with poor prognosis (Reedijk, Odorcic *et al.* 2005). NOTCH is also implicated in melanoma, chronic lymphocyte leukemia, and non-small cell lung cancer (Liu, Xiao *et al.* 2006, Westhoff, Colaluca *et al.* 2009, Puente, Pinyol *et al.* 2011). However, NOTCH is also known to have a tumour suppressor function in some tumour types, such as in hepatocellular carcinoma and head and neck squamous cell carcinoma (HNSCC) (Stransky, Egloff *et al.* 2011, Viatour, Ehmer *et al.* 2011). Thus, the therapeutical disruption of the NOTCH pathway can be beneficial based on stromal as well as tumour-related anti-growth effects, but needs to be cautionary regarding the selectivity of the

treatment (targeting NOTCH signalling or ligand binding, tumour or stromal cells) and the NOTCH function in various tumour cell types.

1.1.7 DLL4-NOTCH and mechanism of resistance to anti-tumour therapy

A rat tumour model overexpressing DLL4 exhibits increased NOTCH signalling in the host stroma and decreased vessel density, with less sprouts and filopodia, compared to the control (Noguera-Troise, Daly *et al.* 2006). Vessels of these tumours are almost completely perfused, whereas those of control tumours show several non-perfused vessels with blind ends. Soluble DLL4 inhibits NOTCH signalling in the host stroma. Although increased in their density, vessels in soluble DLL4-overexpressing xenografts are not functional and tumours show increased hypoxia and decreased vascular perfusion. In tumour xenografts resistant to VEGFA blockade, NOTCH inhibition by soluble DLL4 or by DLL4 blocking antibodies leads to a decrease of tumour growth, and leads to a further increase of vessel density and increase of hypoxia (Noguera-Troise, Daly *et al.* 2006). The tumour growth inhibiting effect by soluble DLL4 or selective DLL4 blocking antibodies has been recapitulated in several different xenograft models, and combination of anti-VEGFA and anti-DLL4 treatment can further amplify the effect of growth inhibition (Ridgway, Zhang *et al.* 2006, Scehnet, Jiang *et al.* 2007). This shows that the hypersprouting phenotype that is observed *in vitro* when NOTCH or DLL4 are inhibited leads to non-productive vasculature *in vivo*. Blocking DLL4 *in vivo* decreases tumour growth due to increased vascular sprouting and defective maturation of the vessels.

DLL4-overexpressing human glioblastoma xenograft models, with enhanced NOTCH signalling in the host stroma, show improved function of the vasculature, with an increase of vessel diameter, better blood perfusion, and reduced hypoxia (Li, Sainson *et al.* 2011). The tumours grow faster and are less responsive to Bev than the control tumours, in which Bev leads to tumour hypoxia and disruption of vessels. Only DBZ or a combination of DBZ and Bev inhibits tumour growth in DLL4-overexpressing tumours and leads to a reduction of vessel size and increase of tumour hypoxia. Resistance to VEGFA therapy therefore is

dependent on downstream modifications of and cross-talk with other pathways and promoted by activation of the DLL4-NOTCH pathway. These mechanisms include differential VEGFR expression, activation of bFGF- FGFR signalling pathways, and EphB4-EphB2 signalling pathways (NOTCH and VEGFA induce EphB2, EphB2-EphB4 interaction inhibits sprouting, and VEGFA represses EphB4) (Li, Sainson *et al.* 2011).

Furthermore, DLL4-NOTCH signalling is implicated in response to radiotherapy and chemotherapy. As such, high DLL4 expression in tumour endothelium of HNSCC patients predicts a good response to radio/ chemotherapy, presumably due to decreased hypoxia and improved vasculature, leading to more effective radiation and better drug delivery (Koukourakis, Giatromanolaki *et al.* 2013). Demcizumab, an antibody targeting DLL4 and disrupting the NOTCH pathway, is currently in phase Ib trials as an agent to target the NOTCH pathway in cancer stem cells, non-small cell lung carcinoma, and pancreatic cancer. However, preclinical trials have shown its efficiency to be based on various effects, including disrupting angiogenesis, inhibiting cancer stem cell growth and promoting cell differentiation, and potentially immune activation (from OncoMed Pharmaceuticals).

1.2 Metabolism as a target for tumour therapy

1.2.1 Metabolic reprogramming in tumours - an emerging hallmark

Hanahan and Weinberg have summarised the complexity of cancer in 12 ‘hallmarks of cancer’, which are acquired capabilities that allow tumour cells to survive, proliferate, and disseminate. In recent years, the field of metabolic reprogramming in tumours has provided valuable insight into the capabilities of tumour cells to adapt, survive and proliferate, based on changes in their metabolism. This concept has been acknowledged as an ‘emerging hallmark’ (Hanahan and Weinberg 2000, Hanahan and Weinberg 2011). Please see figure 1.4 for an overview of metabolism pathways referred to in the following sections.

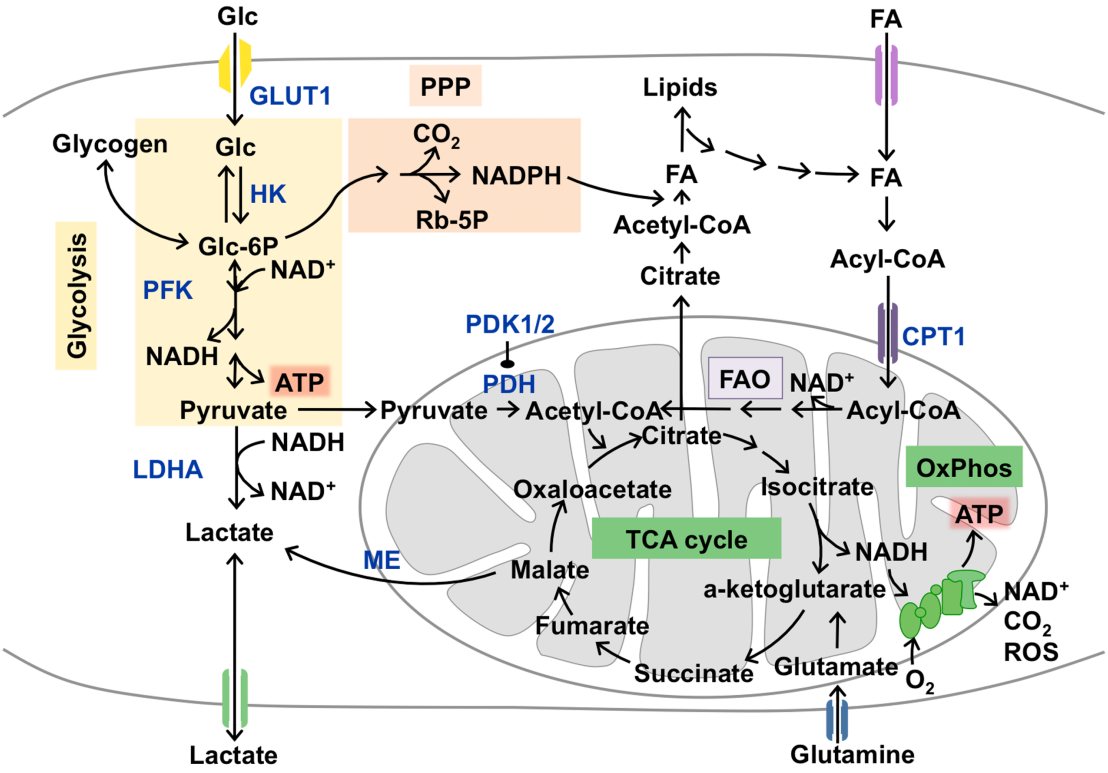


Figure 1.4 Overview of metabolic pathways important for tumour cell homeostasis. Cells derive their energy from glycolysis of extracellular glucose (Glc) (uptake: Glc transporter 1 (GLUT1)). Enzymes (blue) of glycolysis (yellow box) are for example hexokinase (HK), and Phosphofructokinase 1 (PFK1). Glycolysis is promoted by degradation of glycogen to Glc-6-phosphate (Glc-6-P). The glycolytic product pyruvate is converted to lactate (by lactate dehydrogenase A, LDHA) or fueled into the Krebs cycle by pyruvate dehydrogenase (PDH) (inhibited by pyruvate dehydrogenase kinase 1/2, PDK1/2). The pentose phosphate pathway (PPP, orange box, produces ribose-5-phosphate (Rb-5P) from Glc-6-P), contributes to the regeneration of nicotinamide adenine dinucleotide (NAD) phosphate hydrate (NADPH, essential for fatty acid (FA) synthesis). Acetyl-CoA production from citrate contributes to FA synthesis. NAD hydrate (NADH) derived from glycolysis, FA oxidation (FAO) and the tricarboxylic acid (TCA) cycle is an electron donor for oxidative phosphorylation (OxPhos, green). Cells can utilise FA (mitochondrial FA import through carnitine-palmitoyl transporter 1, CPT1), lactate and glutamine (conversion to α-ketoglutarate) to increase TCA cycle flux and OxPhos (green).

1.2.1.1 Aerobic glycolysis

Even though mitochondrial respiration is not affected in most tumour cells, they are highly glycolytic, even in oxygen-rich conditions, and secrete high levels of lactate (Warburg effect, (Warburg 1956)). Increased cell growth requires increased production of glycolytic and tricarboxylic acid (TCA) cycle intermediates to support synthesis of DNA, RNA, proteins and fatty acids (FA) during cell division. Although required for homeostasis, cell survival, and proliferation, adenosine triphosphate (ATP) production appears not to be the rate-limiting step for tumour growth. The contribution of glycolysis to ATP production is variable and varies depending on the type of tumour tissue and the environmental conditions (e.g. oxygen concentration). Glycolytic ATP production can range from 0.31% to 64%, with an average of 17% (reviewed by Zu and Guppy 2004). Glucose can provide precursors for the biosynthesis of molecules such as glucose-6-phosphate for nucleotide synthesis, dihydroxyacetone phosphate for FA synthesis, 3-phosphoglycerate and pyruvate derived from glycolysis for amino acid synthesis, acetyl-Coenzyme A (CoA) for FA synthesis, or α-ketoglutarate and oxaloacetate derived from the TCA cycle for amino acid synthesis (Fig. 1.4). Therefore it is thought that a main function of increased glycolysis in tumour cells is to provide biosynthetic precursors and thereby enable rapid proliferation (reviewed by Zu and Guppy 2004).

1.2.1.2 Glutamine addiction

Glutamine is the most abundant amino acid in the blood plasma. It can enter the TCA cycle through intracellular conversion to α-ketoglutarate (glutaminolysis). The glutamine addiction hypothesis states that tumour cells depend on exogenous glutamine for anabolic growth because glutamine starvation results in cell death (reviewed by Wise and Thompson 2010). The TCA cycle is replenished by pyruvate and various amino acids (anaplerosis). Glutamine carbons and glutamine-derived nitrogen can contribute to anaplerosis and are used in amino acid biosynthesis, FA synthesis (via citrate and acetyl-CoA) and nucleotide biosynthesis, as well as mitochondrial respiration and ATP production (Fig. 1.4). Glutamine-derived α-ketoglutarate can be converted to citrate through reverse TCA cycle reactions, mediated by

isocitrate dehydrogenase and aconitase (Wise, DeBerardinis *et al.* 2008, Metallo, Gameiro *et al.* 2012, Mullen, Wheaton *et al.* 2012). Citrate can then be injected into FA synthesis. A considerable part of glutamine metabolism contributes to lactate production too, via the activity of malic enzyme, which generates pyruvate, carbon dioxide, and Nicotinamide adenine dinucleotide phosphate hydroxide (NADPH, required for FA synthesis, regeneration of glutathione, and protection against reactive oxygen species (ROS)) (reviewed by DeBerardinis, Mancuso *et al.* 2007).

1.2.1.3 Lactate secretion in tumour tissue

Glucose consumption rates exceed their rates of incorporation into biomolecules because a considerable part (~93%) is secreted in the form of lactate or alanine (reviewed by DeBerardinis, Mancuso *et al.* 2007). Lactate is generated by lactate dehydrogenase A (LDHA) from pyruvate, regenerating Nicotinamide adenine dinucleotide (NAD^+) from NAD hydroxide (NADH) (Fig. 1.4). NAD^+ regeneration is required for a continuous flux through glycolysis and for nucleotide and amino acid biosynthesis, suggesting that increased lactate secretion is a mechanism of tumour cells to maintain the redox state and facilitate increased glucose and glutamine flux and incorporation into biomass. Additionally, lactate secretion may promote tumour growth by affecting the tumour microenvironment (see 1.2.2).

1.2.1.4 FA utilisation

The observation of increased FA synthesis in tumours has been made as early as the 1950s (Medes, Thomas *et al.* 1953) and is linked to the increased carbon produced through increased glycolysis and glutaminolysis in tumour cells. The key enzymatic complex for FA *de novo* synthesis, FA synthase (FASN), is upregulated in many tumour types, including ovarian, breast, colorectal, bladder, lung, and thyroid tumours (reviewed by Flavin, Peluso *et al.* 2010). FAs are required for the synthesis of membranes, can serve as signalling molecules, and can be used for energy production. Therefore, the increased availability of FAs in the cell through synthesis or uptake is beneficial for cell growth and survival in certain metabolic environments. FAs are either produced intracellularly, from acetyl-CoA or malonyl-CoA by

FASN, or derived extracellularly through FA uptake (via FA transport protein FAT/ CD36 or by passive diffusion ('flip-flop')). Before FAs can be utilised in the cell, they are activated by covalent modification by CoA (catalysed by Acyl-CoA synthetases (ACSL)) and become part of the bioactive FA pool. FA are transported by FA binding proteins (FABPs) to sites of utilisation, such as the endoplasmic reticulum (ER) or the mitochondria, once activated, and can be modified by desaturases or elongases. Acyl-CoA can be incorporated in phospholipids (PL), triglycerides (TG), or degraded via FA oxidation (FAO) in the mitochondria, thereby entering the TCA cycle (via acetyl-CoA) and contributing to mitochondrial energy production. However, the extent of FA utilisation in tumour cells is multifaceted and the implication for growth and survival has yet to be fully elucidated. In some tumours, FAO contributes to tumour cell survival and tumour growth (Pike, Smift *et al.* 2011, Zaugg, Yao *et al.* 2011) and the release of FAs from intracellular stores through hydrolysis of monoacylglycerols (MAG) by MAG lipase (MAGL) promotes tumour growth (Nomura, Long *et al.* 2010). Furthermore, hypoxic FA uptake and oxidation upon rexoygenation promote growth of glioblastoma xenografts (Bensaad, Favaro *et al.* 2014). The primary site of ovarian cancer metastasis is the omentum and ovarian cancer cells directly adjacent to fat tissue benefit from higher accumulation of lipids and higher rates of oxidation of FAs derived from adjacent adipocytes, which is dependent on the expression of FABP4 in both cell types (Nieman, Kenny *et al.* 2011). Tumour cells as potential FA users increase the secretion of lipoprotein lipase for extracellular lipolysis and expression of FA transporter FAT/CD36 for FA uptake, which promotes tumour cell proliferation *in vitro* (Kuemmerle, Rysman *et al.* 2011). Currie *et al* hypothesised that tumour cells generally have higher levels of intracellular FA based on increased *de novo* synthesis, and blocking intracellular availability of FAs by targeting several different aspects of FA metabolism is a therapeutic strategy worthy of investigation (reviewed by Currie, Schulze *et al.* 2013).

1.2.2 Mechanisms of metabolic reprogramming

1.2.2.1 Malignant transformation leads to a metabolic switch

The transcription factor MYC, commonly upregulated in cancer, induces genes involved in the regulation of glycolysis (glucose transporter GLUT1, phosphofructokinase 1 (PFK)), glutaminolysis (glutaminase), FA synthesis (FA synthase (FASN), stearoyl CoA-desaturase (SCD)), nucleotide biosynthesis, and mitochondrial biogenesis (reviewed by Dang 2013). The tumour suppressor p53 controls metabolism in response to stress and reduces glycolysis, while promoting oxidative phosphorylation (OxPhos) (reviewed by Gottlieb and Vousden 2010). Other pathways modulating the expression or activity of metabolic enzymes, which can be deregulated due to oncogenic activation or tumour suppressor repression, are phosphatidylinositol-4,5-bisphosphate 3-kinase (PI3K)-protein kinase B (AKT), involved in glucose homeostasis, mammalian target of rapamycin complex 1 (MTORC1), involved in protein synthesis, mitochondrial biogenesis, lipid synthesis, energy expenditure, and adenosine monophosphate (AMP)-activated kinase (AMPK), involved in mitochondrial biogenesis, glucose uptake, and FA oxidation (reviewed by Cairns, Harris *et al.* 2011). Fluctuating oxygen concentrations in tumour tissue below 150 mmHg (hypoxia) lead to stabilisation of HIF-1α, a master regulator of the cellular response to hypoxia and metabolism and commonly upregulated in cancer (reviewed by Harris 2002). Normoxic HIF-1α signalling is stabilised in response to oncogenic signals. For example, HIF-1α is stabilised by PI3K-AKT signalling, in response to growth factors like insulin growth factor (IGF)1, insulin, or heregulin, or through loss of PTEN, and oncogenic activation of RAS also results in HIF-1α stabilisation (Zundel, Schindler *et al.* 2000, Laughner, Taghavi *et al.* 2001, Fukuda, Hirota *et al.* 2002, Lim, Lee *et al.* 2004, Jiao and Nan 2012). Finally, NOTCH signalling is known to have oncogenic capabilities implicated in metabolism (Landor, Mutvei *et al.* 2011).

1.2.2.2 HIF-1α controls tumour cell metabolism

HIF-1α signalling controls the induction of a metabolic switch in tumours. HIF-1α activation turns on a program that is aimed at making the cells less dependent on oxygen and promoting survival in oxygen-deprived areas. For example, HIF-1α activation can result in the stimulation of tumour angiogenesis by VEGFA induction, activation of autophagy pathways, and regulation of pH (Forsythe, Jiang *et al.* 1996, Carmeliet, Dor *et al.* 1998, Swietach, Vaughan-Jones *et al.* 2007, Bellot, Garcia-Medina *et al.* 2009). Part of the program is a metabolic switch to glycolysis with a reduced flux through the TCA cycle and OxPhos, thereby promoting the already glycolytic phenotype of tumour cells. Key target genes for the metabolic switch are LDHA, the glucose transporter GLUT1, hexokinase (HK), PFK and pyruvate dehydrogenase kinase 1 (PDK)1 (Fig. 1.4) (reviewed by Harris 2002). Furthermore, HIF-1α induced transcription leads to an increase of reductive carboxylation of glutamine, to provide acetyl-CoA as a template for FA synthesis, which cells would otherwise lack due to TCA cycle flux reduction (Metallo, Gameiro *et al.* 2012). HIF-1α controls glycogen metabolism, by regulating glycogen synthase 1 (GYS1) and liver glycogen phosphorylase (PYGL), and thereby sustaining tumour cell proliferation by promoting glucose utilisation from glycogen stores (Favaro, Bensaad *et al.* 2012). HIF-1α upregulates the FA metabolism genes *FABP3* and *FABP7* and causes accumulation of lipid droplets (LD) (Bensaad, Favaro *et al.* 2014). LD are dynamic lipid storage organelles that consist of a monolayer of polar lipids (PL and cholesterol) coated by proteins of the PAT/ perilipin family, and surrounding a core of neutral lipids, TG and sterol esters (Bickel, Tansey *et al.* 2009). Upon reoxygenation, FAs can be released from storage to be utilised for rapid energy production and promote cell survival (Bensaad, Favaro *et al.* 2014).

1.2.2.3 NOTCH signalling –effects on breast cancer cell metabolism

NOTCH expression in breast cancer drives tumour growth (Reedijk, Odorcic *et al.* 2005). NOTCH signalling in breast cancer cell lines expressing low, medium or high levels of

NICD, has been linked to the regulation of metabolism and induction of the glycolytic switch (Landor, Mutvei *et al.* 2011). Landor *et al.* showed that high levels of NOTCH activity lead to increased glucose uptake and lactate secretion, via increased PI3K-AKT signalling compared to medium NOTCH activity, whereas low NOTCH signalling also increased glucose uptake and lactate secretion, but via a p53 dependent inhibition of mitochondrial function. Although exhibiting the same metabolic phenotype, only xenograft tumours of breast cancer cells with high NOTCH activity exhibited faster growth. High NOTCH activity was associated with a reversible glycolytic phenotype, whereas mitochondria in cells with low NOTCH activity were irreversibly damaged, therefore less flexible in terms of the metabolic response (Landor, Mutvei *et al.* 2011).

The metabolic regulation in tumours is highly diverse and extremely flexible, due to the multiple pathways potentially involved and potentially dysregulated throughout the course of tumour progression. Still, a few drugs targeting tumour metabolism are under clinical investigation and have shown favourable outcome in some cases. For example, 2-deoxyglucose (2DG) is metabolised by HK2 to 2DG-phosphate, which cannot enter the glycolytic pathway. 2DG inhibits cancer cell proliferation, however shows cytotoxicity when administered at high levels to glioblastoma patients and is still under investigation for the clinic, also in combination with other chemotherapeutic agents or radiotherapy (Landau, Laszlo *et al.* 1958, Mohanti, Rath *et al.* 1996, Dwarakanath and Jain 2009). PDK, which is increased in many cancers, is inhibited by the small molecule dichloroacetate (DCA). Inhibition of PDK increases PDH activity and oxidative decarboxylation of pyruvate to actetyl-CoA, thereby increasing the TCA cycle flux and decreasing lactate production. DCA, although a non-selective inhibitor, inhibits tumour growth in several models and is well-tolerated by patients (Michelakis, Sutendra *et al.* 2010). Notably, resistance to chemo- or radiotherapy may be overcome by adjusting the metabolic tumour phenotype to a less aggressive, quiescent phenotype. When considering the issue of drug selectivity, taking into account the tumour-associated stroma and changes in metabolism may help to predict

outcome and open new opportunities for targeting several aspects of tumour progression and problems of resistance based on their metabolic basis.

1.3 Endothelial cell metabolism

Activation of blood vasculature in the tumour involves phenotypic changes involving proliferation and migration and likely changes metabolism in endothelial cells. Advances in developing tumour metabolism as a therapeutic target have led to the increased investigation of endothelial cell metabolism in the context of tumour angiogenesis.

1.3.1 Perspectives of metabolic reprogramming in tumour angiogenesis

1.3.1.1 Aerobic glycolysis

Endothelial cells mainly utilise aerobic glycolysis in the quiescent and activated state (Krutzfeldt, Spahr *et al.* 1990, Tretyakov and Farber 1995, Parra-Bonilla, Alvarez *et al.* 2010). Upon activation in response to pro-angiogenic factors like VEGFA, glucose uptake increases via PI3K-AKT mediated induction of GLUT1 and the glycolytic rate merely doubles, showing that the baseline glycolytic rate in the quiescent state is high already (Yeh, Lin *et al.* 2008, De Bock, Georgiadou *et al.* 2013) (Fig. 1.5). Glycolysis is the main energy-producing pathway in endothelial cells, with >80% of ATP being produced by glucose conversion to pyruvate, and <1% of glucose being injected into the TCA cycle (Krutzfeldt, Spahr *et al.* 1990, De Bock, Georgiadou *et al.* 2013). Knockdown of LDHA in pulmonary endothelial cells reduces proliferation (Parra-Bonilla, Alvarez *et al.* 2010). Knockdown of 6-phosphofructo-2-kinase/fructose-2,6-bisphosphatase 3 (PFKFB3), which reduces synthesis of fructose-2,6-bisphosphate, an allosteric activator of PFK1 and stimulator of glycolysis, impairs endothelial proliferation, migration, sprouting, and functional network formation. The formation of filopodia and lamellipodia during directed migration is dependent on glycolytic ATP production and glycolytic enzymes are localised in protrusions through compartmentalization with F-actin (De Bock, Georgiadou *et al.* 2013).

It may seem paradoxical that cells most closely adjacent to oxygenated blood are not utilising oxygen for energy production. The preference for aerobic glycolysis may reduce oxidative damage and allow oxygen and glucose to diffuse into adjacent tissues. Furthermore, constitutively using glycolysis may prepare endothelial cells for rapid sprouting and migration into less oxygenated areas present in tumour tissue.

Glucose deprivation leads to increased oxidation of substrates like glutamine and palmitate, showing that although mitochondria are thought to act as a signalling organelle by using oxygen-derived species, there is a level of metabolic flexibility of endothelial cells to adapt to changes in the environment that includes TCA cycle activity and OxPhos (Krutzfeldt, Spahr *et al.* 1990, Therade-Matharan, Laemmel *et al.* 2004, Quintero, Colombo *et al.* 2006, De Bock, Georgiadou *et al.* 2013).

1.3.1.2 Lactate secretion in tumour tissue

Exogenous lactate, once taken up by neighbouring cells, can be channelled into the TCA cycle and fuel OxPhos in oxygenated cells (Fig. 1.4, 1.5). For example, a subpopulation of tumour cells readily takes up lactate via monocarboxylate transporter (MCT)1 and metabolises lactate via OxPhos (Sonveaux, Vegran *et al.* 2008). Endothelial cells show high MCT1 expression and readily oxidise lactate (Krutzfeldt, Spahr *et al.* 1990, Koukourakis, Giatromanolaki *et al.* 2006, Parra-Bonilla, Alvarez *et al.* 2010, Vegran, Boidot *et al.* 2011). Increased lactate influences endothelial cell signalling, by stimulating autocrine IL8/ NFκB signalling (Vegran, Boidot *et al.* 2011), as well as increasing VEGFA levels through stabilisation of HIF-1α (Hunt, Aslam *et al.* 2007) (Fig. 1.5). MCT1 blockade reduces lactate uptake and augments lactate-mediated HIF-1α stabilisation (Sonveaux, Copetti *et al.* 2012). Although MCT1 expression is low in tumour-associated vasculature in some cases (Koukourakis, Giatromanolaki *et al.* 2006), these data suggest that lactate in the tumour tissue presents a pro-angiogenic signalling molecule.

1.3.1.3 FA utilisation

FA activation and binding proteins carry out the intracellular activation and transport of FAs to sites of utilisation, as described in 1.2.1.4. Endothelial FABP4 production is upregulated in response to VEGFA (Elmasri, Karaaslan *et al.* 2009). Gene expression studies suggest that FABP4, in response to VEGFA, promotes integral signalling pathways such as p38, endothelial nitric oxide synthase and c-kit (Elmasri, Ghelfi *et al.* 2012). Downregulation of FABP4 reduces endothelial cell proliferation, migration and sprouting in response to VEGFA (Elmasri, Karaaslan *et al.* 2009, Elmasri, Ghelfi *et al.* 2012) (Fig. 1.5). Increased plasma levels of FABP4 are positively associated with atherosclerosis, diabetes and endothelial dysfunction (Holm, Ueland *et al.* 2011, Djousse and Gaziano 2012, Kralisch and Fasshauer 2013). For instance, exogenous FABP4 interferes with insulin-stimulated production of nitric oxide (NO) in endothelial cells, thereby interfering with their vasodilatory functions and demonstrating a causative role in the development of insulin resistance (Aragones, Saavedra *et al.* 2012).

VEGFB is expressed in colorectal cancer and breast cancer, although its role in tumour angiogenesis is not fully understood (Gunningham, Currie *et al.* 2001, Hanrahan, Currie *et al.* 2003). VEGFB induces endothelial FA transport, by inducing very long chain synthases/ FA transport proteins (FATP) 3 and 4. VEGFB homozygous deletion in mice causes a decrease of lipid accumulation in liver, muscle and heart (Hagberg, Falkevall *et al.* 2010). VEGFR1 is upregulated in response to NOTCH induction, drawing a link between VEGFB signalling and FA transport (Fig. 1.5).

Carnitine-palmitoyl transferase (CPT)1 is a mitochondrial FA translocase. CPT1 catalyses the transfer of the acyl group from Acyl-CoA to carnitine, forming acyl-carnitine, which is then translocated into the mitochondria and converted back to Acyl-CoA, to be fueled into the FA oxidation pathway. When starved for glucose, endothelial cells show increased AMPK, decreased acetyl-CoA carboxylase (ACC) activity, increased CPT1 expression (mitochondrial FA import, Fig. 1.4), and do not exhibit a drop of ATP levels. This suggests that FAO, in response to AMPK and increased mitochondrial FA import via CPT1 can act as a substitute

energy-producing pathway for endothelial cells to survive energy stress (Dagher, Ruderman *et al.* 2001). VEGFA and VEGFB signalling can increase endothelial AMPK activity without affecting FAO. Prolonged incubation of endothelial cells with VEGFA leads to an AMPK dependent increase of FA uptake (Reihill, Ewart *et al.* 2011), which might be related to an increased intracellular FA utilisation, for example in the TCA cycle, following AMPK activation.

1.3.2 Metabolism and endothelial cell plasticity

During angiogenic sprouting a dynamic shuffling between the tip and stalk cell phenotype is occurring. These phenotypes have different migratory and proliferative capabilities and are therefore likely to differ in their metabolism.

1.3.2.1 Glycolysis drives tip cell formation

VEGFA, which induces the tip cell phenotype, increases PFKFB3 expression and glycolysis. PFKFB3 knockdown reduces the number of angiogenic sprouts and reduces tip cell features like filopodia and lamellipodia formation. PFKFB3 knockdown also reduces stalk cell related features of angiogenesis like sprout length and proliferation. This suggests that the glycolytic pathway is active in tip and stalk cells. However, stalk cell promoting DLL4-NOTCH signalling reduces PFKFB3 expression and glycolysis, suggesting that the rate of glycolysis might be lower in stalk cells than in tip cells. Endothelial cells that overexpress PFKFB3 and have higher rates of glycolysis are more likely to take on the tip cell position, even when NOTCH signalling is promoted by overexpression of NICD (De Bock, Georgiadou *et al.* 2013). These data suggest that the glycolysis rate is a determinant of phenotype formation during sprouting.

1.3.2.2 Metabolic sensing and signalling response

NADH, the reduced form of NAD^+, is generated in glycolysis, FA oxidation, and the TCA cycle. NADH serves as an electron carrier in the electron transport chain and is reduced to NAD^+ during OxPhos. A change in the NAD^+/ NADH ratio affects energy production

because both molecules are required coenzymes for glycolysis, FAO, TCA cycle reactions, and OxPhos. A high level of NAD^+ leads to activation of the deacetylase Sirtuin1 (SIRT1). In endothelial cells, SIRT1 deacetylates and thereby destabilises NICD, thereby reducing NICD activity and limiting NOTCH signalling duration. SIRT1 also deacetylates and inactivates Forkhead box protein O1 (FOXO1), a transcription factor involved in glucose homeostasis and a negative modulator of angiogenesis (Fig. 1.5). SIRT1 is mainly expressed in endothelial stalk cells and its knockdown reduces endothelial sprouting and branching (Potente, Ghaeni *et al.* 2007, Guarani, Deflorian *et al.* 2011). FOXO1 is required for NOTCH mediated gene transcription in myoblasts and hepatic cells and may potentially play a role in the transcriptional induction of NOTCH target genes and formation of the stalk cell phenotype (Kitamura, Kitamura *et al.* 2007, Pajvani, Shawber *et al.* 2011, Harjes, Bridges *et al.* 2014). The counteracting activity of SIRT1 and FOXO1 and their responding to metabolic cues may therefore provide a fine-tuning mechanism for angiogenesis in nutrient-deprived tissue, such as tumour tissue and limit (by SIRT1) or favour (by FOXO1) the stalk cell phenotype.

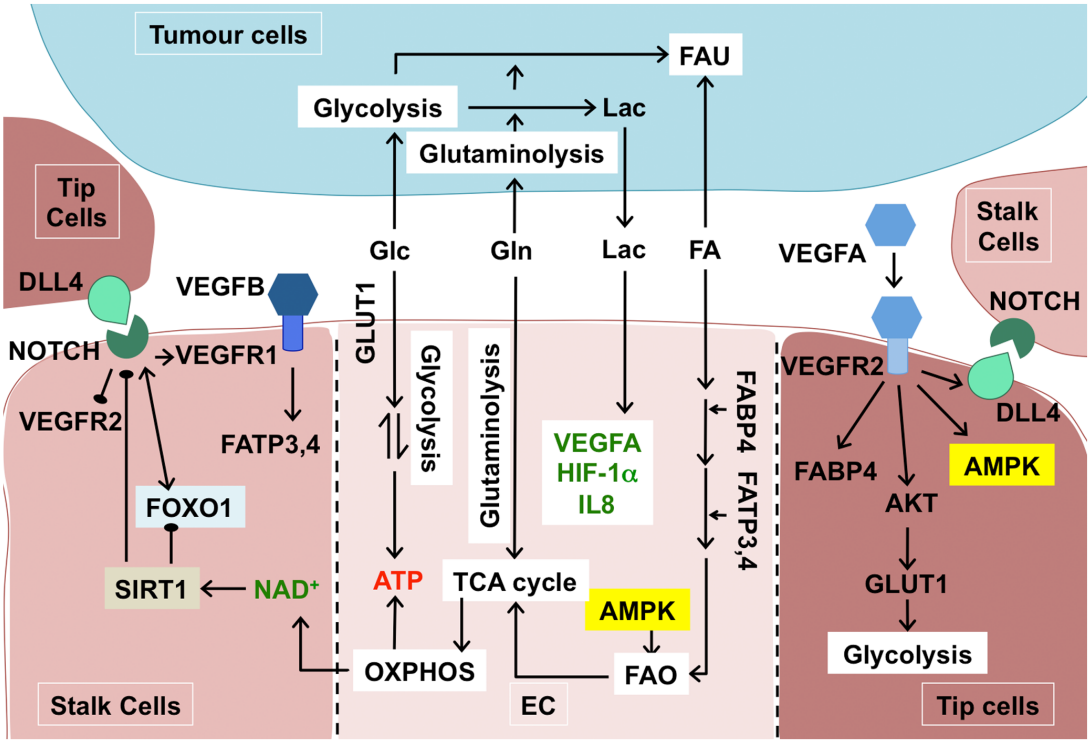


Figure 1.5 Endothelial cell metabolism in relation to the tumour metabolic environment. Tumour cells are highly glycolytic and glutaminolytic and have increased lactate secretion. Extracellular lactate can act as a signalling molecule and increase vascular endothelial growth factor (VEGF)A, hypoxia-inducible factor (HIF)-1α and Interleukin 8 (IL8) signalling in EC. Fatty acids (FAs) are utilised by TC for lipid synthesis, etc. In tumour tissue VEGFA secretion and binding to VEGF receptor (VEGFR) 2 on endothelial cells (EC) leads to tumour angiogenesis. VEGFA/VEGFR2 signalling induces Delta-like ligand 4 (DLL4), AKT and glucose transporter 1 (GLUT1), and FA binding protein 4 (FABP4). DLL4-NOTCH signalling regulates expression of VEGFR2 (inhibition) and VEGFR1 (activation). Increased oxidative phosphorylation (OxPhos) leads to increased NAD+ and activation of Sirtuin1 (SIRT1). SIRT1 mediated deacetylation limits FOXO1 and NOTCH activity. VEGFB binding to VEGFR1 activates AMPK and FA transport proteins (FATP) 3 and 4. VEGFA/VEGFR2 signalling is active in the endothelial tip cell and DLL4- NOTCH signalling in the stalk cell of the angiogenic sprout. Metabolism in endothelial cells depends on extracellular glucose (Glc) taken up through GLUT1, and processed through glycolysis to produce ATP. Endothelial cells can utilise glutamine (Gln) and FAs for energy production. FAs can be utilised (FAU) for the production of lipids (inhibited by AMPK), or fuelled into FA oxidation (FAO). FABP4 and FATP3/4 are involved in intracellular FAU.

1.4 Aims

Similar to tumour cells, endothelial cells also depend on the glycolytic pathway for proliferation and migration. In fact, glycolysis is a main driver for angiogenic sprouting and favours the formation of the tip cell phenotype, which is promoted during tumour angiogenesis. The number of tip cells formed is limited by activation of DLL4-NOTCH signalling during angiogenic sprouting. Activation of the DLL4-NOTCH signalling pathway in tumour vasculature results in larger, less leaky vessels and improved tissue perfusion, and promotes resistance to anti-angiogenic therapy. Targeting the DLL4-NOTCH pathway may improve chemo/ radiotherapy. The tumour vasculature, as a key player in tumour progression, may be a potential target of emerging therapies directed at metabolism in the tumour. Understanding the metabolic phenotype of enlarged, better perfused vessels induced by DLL4-NOTCH signalling in tumour tissue may open new avenues for therapeutic intervention.

The aims of this D.Phil. thesis are the

I. Characterisation of the metabolism in endothelial cells in response to the activation of the DLL4-NOTCH signalling pathway and the investigation of the effect of metabolic interference on angiogenesis
II. Development of an understanding of potential pathways involved and investigation of potential targets of NICD mediated transcription that may drive the observed metabolic phenotype
III. Analysis of the effect of DLL4-NOTCH and expression of DLL4-NOTCH targets during metabolism in relevant coculture models and human tumour tissues.

2 CHAPTER TWO

Material and Methods

2.1 Cell culture techniques

2.1.1 Cell growth conditions

Human umbilical vein endothelial cells (HUVEC) were obtained from Lonza, Switzerland as a pool of 3-5 donors and cultured in endothelial basal medium 2 with supplements (endothelial growth medium 2 (EGM2), Lonza, Switzerland) in sterile flasks at 37 °C and atmosphere of 5% CO_2 (Corning, NY, USA) in a humidified incubator.

2.1.2 Cell maintenance and passaging

Cells were passaged at 80-90% confluence. Cells were washed with phosphate buffered saline (PBS, composed of 10 mM sodium phosphate, 137 mM sodium chloride and 2.7 mM potassium chloride) and then incubated in 1x trypsin-(ethylenediaminetetraacetic acid) EDTA (Invitrogen, CA, USA) for 5 min at 37 °C. When the cells detached, the trypsin reaction was quenched by adding culture media containing fetal calf serum (FCS, Invitrogen, CA, USA). The cells were transferred into 15 ml conical bottom tubes (Corning, NY, USA) and centrifuged at 500 g for 5 min. The pellet was resuspended in media and cells were counted and seeded for an experiment or aliquotted into T175 flasks (Corning, NY, USA), at a ratio of 1 in 4, and in a total media volume of 25 ml for normal culture. The media was changed every two days.

2.1.3 Cell counting and seeding

The cells in the cell suspension were counted using the Cellometer Auto T4 cell counter (Nexcelom Bioscience LLC, MA, USA) according to the manufacturer's instructions. Briefly, 20 μl of the cell suspension was transferred into a Cellometer counting chamber (Nexcelom Bioscience LLC, MA, USA) and the chamber was inserted into the machine. Cells of a diameter of 4-14 μm were counted. The cell suspension was then diluted to the required

concentration for further experiments. Cells were seeded at a density of 10,500 cells per cm^2 unless otherwise stated.

2.1.4 Freezing and thawing cells

For long-term storage, cells were detached by exposure to trypsin, pelleted, and resuspended in FCS (Invitrogen, CA, USA) containing 10% dimethylsulfoxide (DMSO, Sigma-Aldrich, MO, USA). Per cryovial, 1 x 10^6 cells in 1 ml were aliquotted. The cryovials were transferred into a Mr. Frosty™ Freezing Container (Thermo Fisher Scientific, MA, USA) and moved to the -80 °C freezer. The next day, the vials were transferred into liquid-nitrogen storage. To thaw cells, the respective vials were taken from the liquid-nitrogen storage, and thawed by incubating the vials in a 37 °C water bath. The cell suspension was transferred immediately into 10 ml pre-warmed media and centrifuged for 5 min at 500 g for 5 min .The cell pellet was resuspended in 25 ml EGM2 media (Lonza, Switzerland), transferred into a T175 flask (Corning, NY, USA), and grown until 80-90% confluence. The cells were used for experiments after one passage.

2.1.5 Growth factor stimulation

To activate DLL4-NOTCH signalling by recombinant human DLL4 (rhDLL4, R&D systems, MN, USA), tissue culture ware was coated with 1 μg/ml rhDLL4 or 1 μg/ml bovine serum albumin (BSA) (Sigma-Aldrich, MO, USA) in 0.2% gelatine (Sigma-Aldrich, MO, USA) in PBS for 16 h at 4 °C. Then, HUVEC were seeded on pre-warmed coated tissue culture ware and grown for 16-48 h. To stimulate HUVEC with VEGFA, HUVEC were cultured in endothelial basal medium 2 (Lonza, Switzerland) with 2% FCS (Lonza, Switzerland), without supplements, for 16 h prior to addition of VEGFA. Recombinant human VEGFA (Invitrogen, CA, USA) or BSA was added at 50 ng/ml, and HUVEC were grown for 24-48 h.

2.1.6 Hypoxia incubation

For hypoxic incubation at 1% or 0.1% oxygen (5% CO_2), HUVEC were placed into an INVIVO$_2$ 400 Hypoxia workstation (Pro-Lab Diagnostics, ON, Canada).

2.1.7 Drugs

Drugs used were the γ-secretase inhibitor dibenzazepine (DBZ, Sigma-Aldrich, MO, USA), the ADAM17 inhibitor INCB004298 (Incyte, DE, USA), the ADAM17/10 inhibitor INCB003619 (Incyte, DE, USA), and the AKT inhibitor X (AKTiX, Sigma-Aldrich, MO, USA). The DLL4 blocking antibody was from Genentech, CA, USA. Rapamycin, Sunitinib, Etomoxir (EX) and carbonyl cyanide-4-(trifluoromethoxy)phenylhydrazone (FCCP) were purchased from Sigma-Aldrich, MO, USA. The FABP4 inhibitor BMS309403 was purchased from Cayman Chemical, MI, USA.

2.1.8 RNA interference (RNAi)

Reverse transfection of small interfering RNA (siRNA) duplexes (table 2) was performed using Lipofectamine RNAiMax (Invitrogen, CA, USA) according to the manufacturer's instructions. Briefly, siRNA diluted in serum-reduced Opti-MEM^{TM} (Invitrogen, CA, USA) and 0.1 μl/ml Lipofectamine RNAiMax (Invitrogen, CA, USA) were mixed and incubated for 10-20 min at RT. The cells were prepared in EGM2 free of antibiotics and heparan sulfate (Lonza, Switzerland). The cell suspension was added to the duplex mix, plated, and incubated for 16 h. Then, media was changed to full EGM2 containing antibiotics and heparin sulfate (Lonza, Switzerland), and incubated for the indicated time. ON-TARGETplus SMARTpool targeting *FOXO1,* or 4 different ON-TARGETplus siRNAs targeting *FABP4* (Dharmacon, CO, USA) were used (see table 1), and the ON-TARGETplus non-targeting pool (Dharmacon, CO, USA) was used as a control. siRNAs were used at a final concentration of 20 nM.

Table 1 Sequences of ON-TARGETplus siRNA targeting *FABP4*

ON-TARGETplus FABP4 siRNA	Target sequence (5'-3')
si1	CACGAGAGUUUAUGAGAGA
si2	AUACUGAGAUUUCCUUCAU
si3	GGUGGAAUGCGUCAUGAAA
si4	GAAAACGAGAGGAUGAUAA

2.2 Nucleic acid extraction and handling

2.2.1 RNA extraction

RNA extraction from cultured cells was performed using Trizol reagent (Invitrogen, CA, USA) and chloroform/ ethanol extraction according to the manufacturer's instructions. Briefly, cells were washed with ice-cold PBS and lysed in 1 ml Trizol per 10-cm dish. Per 1 ml Trizol (Invitrogen, CA, USA), 200 µl chloroform (Sigma-Aldrich, MO, USA) were added. The samples were shaken for 15 sec and incubated for 10 min at room temperature, followed by a centrifugation at 12,000 g for 10 min, leading to a phase separation. The aqueous phase was transferred into a fresh RNAse-free 1.5 ml tube and 500 µl isopropanol (Sigma-Aldrich, MO, USA) were added. The samples were shaken and incubated for 10 min at room temperature, followed by a centrifugation at 20,000 g for 10 min. The supernatant was removed and 1 ml 75% ethanol (VWR, PA, USA) was added to the pellet, followed by a centrifugation at 12,000 g for 10 min. The supernatant was removed and the pellet air-dried. The pellet was dissolved in 50 µl diethyl pyrocarbonate (DEPC)-treated water (RNAse and DNAse free water, Life technologies, CA, USA). The RNA was stored at -80 °C.

2.2.2 RNA quantification

RNA quantification was performed using the NanoDrop 1000 Spectrophotometer (NanoDrop Technologies, DE, USA), by measuring absorbance at 260 nm. The absorbance of 1 is approximately equivalent to 40 µg/ml of RNA.

2.2.3 cDNA synthesis by reverse transcription

Reverse transcription (RT) was performed using the High Capacity cDNA RT kit (Applied Biosystems, United Kingdom) according to the manufacturer's instructions. Briefly, 2 µg of RNA per reaction were transcribed by adding RT buffer (1x), random primers (1x), 4 mM deoxyribonucleotide triphosphate (dNTP)s, 5 units of multiscribe, and DEPC-treated water to

a final volume of 20 µl. RT was performed on a thermal cycler (PTC-2000, MJ systems, UK) for 10 minutes at 25 °C followed by 120 min at 37 °C and 85 °C for 5 sec.

2.3 Real-time quantitative polymerase chain reaction (qrtPCR)

QrtPCR was performed using the 7900HT Fast Real-Time PCR system in a 384 well format, and the SensiFAST™ SYBR No-ROX Kit (Bioline, UK) according to the manufacturer's instructions. Briefly, 2 µl cDNA were mixed with 1x SensiFAST™ SYBR No-ROX mastermix (Bioline, UK), and the respective gene-specific primers (Invitrogen, CA, USA, see table 2) to a final volume of 10 µl. Forward and reverse primers were used at a final concentration of 600 nM. Conditions for the PCR reaction were as follows: 2 minutes at 50 °C, 10 minutes at 10 °C after which there were 50 cycles, each consisting of 15 seconds at 95 °C and 1 minute at 60 °C. Raw ct values were analysed using the 2(-Delta Delta ct), using *ACTB* as a housekeeping gene to obtain fold changes. Primer sequences used for analysis of messenger ribonucleic acid (mRNA) expression or for detection of immunoprecipitated DNA sequences were synthesized by Invitrogen, CA, USA and are listed in table 2.

Table 2 Sequences of primers used for detection of mRNA or for detection of immunoprecipitated (IP) DNA sequences

Gene name	forward primer (5'-3')	reverse primer (5'-3')
ACACA	AACGTGAAGACGGATAAGCAG	CTTCTTCGGAGAATCTGACCA
ACACB	CAGTTCGCCGACTTCCAT	TCTTCCACTCCAGGATGTCA
ACLY	CCAGCAGGACAGCATCTTTT	GGATCTTGGACTTGGGACTG
ACSL1	GGAGTGGGCTGCAGTGAC	GGGCTTGCATTGTCCTGT
ACSL3	TCAGGGATACGGGCTCACT	TGCCAGTATTGTAGTCCCACAC
ACSL4	TGTACTGTACTGAAGCCCACACTT	TTCATCTCTTGGACTTTGCTCA
ACSL5	GCGTCATCTGCTTCACCA	AGCATGCTCCACACATTTGA
ACSL6	TATGTCCATGGGGACAGCTT	TCCTTCAATTCCTCTCTTCTGG
ACTB	GAGGAGGCACCGGTAAATG	GTCACTCACTGGGACATAGGC

CD36	GTGCCTATTCTTTGGCTTAATGA	TTACTTGACTTCTGAACATGTTTGC
CPT1A	CAATCGGACTCTGGAAACG	CCGCTGACCACGTTCTTC
CPT1B	GAGCAGCACCCCAATCAC	AACTCCATAGCCATCATCTGCT
CPT1C	CCACTGCTCCGAATGGAC	TTGCGCTGTACATCGTGTC
DLL4	CCCTGGCAATGTACTTGTGAT	TGGTGGGTGCAGTAGTTGAG
FABP1	TTTCTCCGGCAAGTACCAAC	CCAGAGAGTTGATCTTCCAAGC
FABP2	TTTGAACTTGGTGTCACCTTTAAT	TCCATTGTCTGTCCGTTTGA
FABP3	CTGGGCACCTGGAAGCTA	TGGTAGCAAAACCCACACC
FABP6	TGAAGGGACTAGAAGGAGGGACA	GAGCCAGAGAGGTGCAAAGTCT
FABP7	TGAAACCACTGCAGATGATATAA	TGTTTGCTTTGCCATCCCATT
FABP8	AGTGAGAACTTTGACGATTACATGA	GCTGATGATCACAGTGGGTTT
FABP9	GTTGAGCCCTTCTTGGGAAC	GGCTGGCGAAATTCACTCC
FASN	CAGGCACACACAGGATGGAC	CGGAGTGAATCTGGGTTGAT
FOXO1	TGGACATGCTCAGCAGACATC	CTTGGGTCAGGCGGTTCA
GPIHBP1	GGAAGAGGAGGAGACCAACA	AGGGACTTGCAGGTGTAGCA
HEY1	CGAGCTGGACGAGCCCAT	GGAACCTAGAGCCGAACTCA
FABP4	ACGAGAGGATGATAAACTGGTGG	GCGAACTTCAGTCCAGGTCAAC
PPARA	TTTAGAAGGCCAGGACGATCT	GCACTGGAACTGGATGACAG
PPARG	GGGGTGATGTGTTTGAACTTG	GACAGGAAAGACAACAGACAAATC
SLC27A1	AGGTGCTGGCACCCTATG	GCAGCCTCGTCTTCTGGAT
SLC27A2	GCTGCACTACTGATTGGCATT	ATTTAGTCCGCAAGGCAAGGCAAGA
SLC27A3	CTCCCACTCTACCACATGTCC	CTTGGATTTCAGCACCACTG
SLC27A4	CTCCCACTCTACCACATGTCC	CCGAATCACCACCGTCAT
SLC27A5	GACAATCAGGGCTTCTGCAT	GTTGCTGGCTTACCACCTTG
SLC27A6	TTACATTTTTACCTCTGGAACAACA	CATGAGCAGTACAACCAAAAGC
PPARD	GGGAAAAGTTTTGGCAGGAG	TGCCCAAAACACTGTACAACA
PPARGC1A	TGAGAGGGCCAAGCAAAG	ATAAATCACACGGCGCTCTT
PPRC	CCTCCCTTATCTCCCTCATTG	TGAGCAGCGACACTTCATTC
LPL	ATGTGGCCCGGTTTATCA	CTGTATCCCAAGAGATGGACATT
LIPG	AAACCAGTGCTCGGAATCAC	CAGGTCCATGTTGTGGATGA
PLIN	ACATTAAAGGGAAGAAGTTGAAGC	TTCTCCTGCTCAGGGAGGT
LDHA	CAGAAGGCTCGAGAAGGTATATTGCTGT	CCTAAAGTAGCCCCTTGAATTCCGAGG

	TGACAGTGAGCG	CAGTAGGCA
ASCT2	GTGCGCAGACCCTTCAGT	GGAGGGAAACAGGTTTCTGG
HEY1 (IP)	AATTCAGCGGCGCGAGA	CTCACGCTTTGCCTCTGGTTA
DLL4 (IP)	GACGCTTAGCTTGGCCTGGAGCTG	TGTGTAAAATACAGGAAGGGGCCCGTCAGT
UBC (IP)	TTGCTGGCAAATATCAGACG	GCAAGACCATCACCCTTGAG
FABP4 R-F1 (IP)	TTTTGCAGCAACATAGGTGAA	ACCTTCCCACCTTTTGGAGT
FABP4 R-2 (IP)	GAGACTCCAAAAGGTGGGAAG	CTCCCAAAGTGCTGGGATTA

2.4 Chromatin-Immunoprecipitation (ChIP) assay

ChIP was performed using the EZ-ChIP™ - Chromatin Immunoprecipitation Kit (Millipore, MA, USA) according to the manufacturer's protocol, and using buffers and reagents provided with the kit. Briefly, 2.5x10^6 cells were plated on BSA- or rhDLL4-coated 150 mm-dishes, using two dishes per condition to obtain sufficient cell numbers, while remaining at 50-70% cell confluence to reduce cell-cell contact-induced NOTCH signalling. After 16 h in media with or without DBZ, cells were detached by exposure to trypsin and counted. Per condition, 5x10^6 cells were cross-linked in 1% paraformaldehyde (PFA) for 10 min. Glycine was added to quench unreacted PFA. Cells were washed in ice-cold PBS containing protease inhibitors, and lysed in the supplied SDS-lysis buffer at 1x10^7 cells per ml. To shear cellular DNA into 200-1,000 bp, samples were sonicated in 100 µl aliquots containing 1x10^6 cells, for 12 cycles of 30 sec pulses at high power, using the Bioruptor Plus (Diagenode, PA, USA). An aliquot of each of the samples was taken and used as input for normalisation purposes. Immunoprecipitation was performed overnight at 4 °C, using a NOTCH1 (D1E11) antibody (Cell Signalling technology, MA, USA) dilution of 1:100, or rabbit IgG (Cell Signalling technology, MA, USA) as a negative control. Antibody-antigen-DNA complexes were

collected with Protein G-agarose, and eluted using appropriate buffers as provided. After crosslink reversal and DNA purification, the samples were analysed by qrtPCR using the primers indicated in table 2. Raw ct values were analysed using the Percent Input method. Ct values obtained from the ChIP samples were divided by ct values obtained from the appropriate input samples (1% of the starting chromatin), using the formula 100x2^((ct input-log2(100))-ct IP) to obtain percent input values (% input). The obtained % input values were then divided by the % input values of the control condition (BSAc with DMSO as vehicle control) of the respective gene promoter region to obtain fold changes.

2.5 Protein analysis

2.5.1 Preparation of cell lysate

Cells were put on wet ice and media was taken off. Cells were washed with ice-cold PBS. Per 6-well dish, 100 µl of lysis buffer (10% (v/v) glycerol (Sigma-Aldrich, MO, USA), 10 mM Tris-HCl pH 6.8 (Sigma-Aldrich, MO, USA), 5 mM dithiothreitol (Sigma-Aldrich, MO, USA), 1% (v/v) sodium dodecyl sulphate (SDS, Sigma-Aldrich, MO, USA), 6.25 M urea (Sigma-Aldrich, MO, USA), protease inhibitor (Roche, Switzerland), phosphatase inhibitor (Roche, Switzerland) were added, and cells were scraped into a 1.5 ml tube. The lysate was centrifuged at 5,000 g for 5 min, and the supernatant was saved and transferred into a fresh tube. Protein concentrations were determined with the NanoDrop 1000 Spectrophotometer (NanoDrop Technologies, DE, USA) or the Bio-Rad protein assay (Bio-Rad, CA, USA). For the Bio-Rad protein assay, briefly, 20 µl of reagent S were added per 1 ml of reagent A (reagent A*). Into each well of a microplate, 5 µl protein sample and 25 µl of reagent A* were added. 200 µl of reagent B were added, mixed, and incubated for 15-60 min. Absorbance was read at 750 nm. The protein concentration was calculated based on a standard curve, which was prepared for each assay, a standard curve using a serial dilution of 2 mg/ml BSA (Sigma-Aldrich, MO, USA). Samples were kept at -20 °C.

2.5.2 Western blot analysis

Western blot analysis was performed using the Novex® NuPAGE® SDS-polyacrylamide gel electrophoresis (PAGE) Gel System and Semi-dry blotter (Invitrogen, CA, USA), according to the manufacturer's instructions. Briefly, 30 μg of protein sample was diluted in NuPAGE® sample buffer (Invitrogen, CA, USA) (1:4) and the samples denatured at 95 ^{o}C for 5 minutes. Proteins were separated by SDS-gel electrophoresis on precast NuPAGE® Bis-Tris gels (Invitrogen, CA, USA) by electrophoresis at 100 V for 2 h in 1x NuPAGE® 2-(N-morpholino)ethanesulfonic acid (MES) running buffer (Invitrogen, CA, USA). Then, the SDS-gel, 6 filter papers (Whatman, UK) and a polyvinylidene difluoride (PVDF) membrane (hydrated in methanol and rinsed in water prior to use, pore size 0.2 μm, Immobilon, Sigma-Aldrich, MO, USA) were incubated in 1x NuPAGE® transfer buffer (Invitrogen, CA, USA) with 20% methanol (VWR, PA, USA) prior to assembling the transfer sandwich consisting of the gel on top of the membrane, and three filter papers on each side. Then, the protein was transferred by semi-dry transfer for 60 min at 20 V. After the transfer the membrane was blocked in 5% milk or 5% BSA in TBST buffer (Tris buffered saline – Tween 20, composed of 25 mM Tris, 150 mM sodium chloride, 2.8 mM potassium chloride and 0.1% Tween-20) for 1 h. The membrane was incubated in the respective primary antibody diluted as indicated in 2.5.3 in 5% milk-TBST or 5% BSA-TBST overnight. Then the membrane was washed for 3 times for 5 min in TBST and the appropriate species-specific horseradish peroxidase (HRP)-conjugated secondary antibody (Sigma-Aldrich, MO, USA) in 5% milk-TBST or 5% BSA-TBST was added at 1:10,000 and incubated for 1 h at room temperature. The membrane was washed 3 times for 10 min, before immunoreactivity was detected using the ECL™ chemiluminescent reagent (Amersham, GE Healthcare, UK) and visualised using the ImageQuant LAS 4000 digital imaging system (GE Healthcare, UK). Band densitometry analysis was performed using the ImageQuant TL software (GE Healthcare, UK).

2.5.3 Antibodies for Western blot

Anti-DLL4 (1:1000 in 5% milk-TBST, rabbit), anti-phosphorylated AKT (serine 473, 1:500 in 5% milk-TBST, rabbit), anti-total AKT (1:1000 in 5% milk-TBST, rabbit), and anti-FOXO1 (1:1000 in 5% milk-TBST, rabbit) were purchased from Cell Signalling Technology, MA, USA. Anti-FABP4 (1:500 in 5% BSA-TBST, rabbit) was purchased from Sigma-Aldrich, MO, USA. Anti-ADAM17 (1:1000 in 5% milk-TBST, rabbit) and anti-ADAM10 (1:1000 in 5% milk-TBST, rabbit) were purchased from ProSci Inc., CA, USA and Abcam, UK respectively. Monoclonal anti-β-ACTIN-Peroxidase (1:10,000 in 5% milk-TBST, Sigma-Aldrich, MO, USA) was used to control for protein loading. Anti-rabbit-HRP (1:10,000 in 5% milk-TBST, Dako, Denmark) was used as a secondary antibody.

2.6 Cell-based assays

2.6.1 Fluorescence- or luminescence-based assays

2.6.1.1 CyQuant NF cell proliferation assay (Invitrogen, LCA, USA)

5,000 cells were seeded per well on a 96-well plate (Corning, NY, USA) pre-coated with BSA or rhDLL4 and allowed to settle down for 16 h. Where indicated, the media was changed to drug containing media prior to starting the incubation of 24-120 h. The CyQuant reaction mix was prepared using 8.8 ml deionised water, 2.2 ml of 5x Hank's balanced salt solution (HBSS) and 22 µl Cyquant NF dye. After the indicated incubation time, media was removed and saved at -20 °C for analysis of lactate and glucose concentration as appropriate (see 2.7.2). 50 µl of the Cyquant reaction mix was added, and incubated for 30 min. The fluorescence intensity was measured using a FLUOstar OPTIMA microplate reader (BMG Labtech Inc., NC, USA) with excitation at 485 nm and emission detection at 530 nm.

2.6.1.2 Luxcel Oxygen consumption assay

The cells were seeded 48 h prior to the assay. Cells were seeded at a density of 4,000,000 cells in a BSA or rhDLL4 pre-coated T175 flask (Corning, NY, USA) and incubated for 48 h

in EGM2 (Lonza, Switzerland). Drugs were added after 3-5 h, when the cells had been allowed to settle down and started adhering to the plate. On the day of the assay, the media was removed and cells were detached by exposure to trypsin. The cell pellets were resuspended and cell concentration determined. Per assay condition, at least 5 technical replicates were performed. Assay media was substrate-depleted EBM2 (Promocell, Germany) containing 2% FCS and 5 mM glucose, 10 mM glutamine or 100 μM BSA-conjugated OA (OA-BSA) (Sigma-Aldrich, MO, USA), or substrate-depleted EBM2 (Promocell, Germany) containing 50 μM Carnitine (Sigma-Aldrich, MO, USA), and 100 μM OA-BSA or FA-free BSA, with or without 5 mM glucose and with or without the indicated drugs. Per replicate, 150,000 cells were seeded in 150 μl assay media, in a black-walled 96-well plate, pre-coated with BSA or rhDll4. Before seeding the cells, 10 μl MitoXpress-Xtra-HS Probe (Luxcel Biosciences, Ireland) were added in each well. Control wells without cells were included. Then, 150 μl of the appropriate cell suspension or media without cells were added per well (5 replicates per condition). To seal it, the suspension was then carefully covered with 100 μl High-sensitivity Oil (Luxcel, Biosciences, Ireland) and the change of fluorescence over time was measured with the FLUOstar OMEGA microplate reader (BMG Labtech Inc., NC, USA). The data was analysed with the OMEGA Mars data analysis tool (BMG Labtech Inc., NC, USA).

2.6.1.3 Lipid droplet (LD540) staining and FACS (fluorescence-activated cell sorting) analysis

Cells were grown on BSA- or rhDLL4-coated dishes for 48 h. After washing the cells with PBS, cells were detached by exposure to trypsin, pelleted and fixed with 4% PFA for 10 min, and then resuspended in PBS. Neutral and polar lipids were stained with the fluorescent LD dye LD540 (kindly supplied by Dr C Thiele, LIMES Life and Medical Sciences Institute, University of Bonn, Germany), diluted in PBS (1:50,000) for 5 min. The fluorescent signal in the fluorescein isothiocyanate (FITC) channel was measured using a FACSCalibur flow cytometer (BD Biosciences, NJ, USA) and Cellquest software (BD Biosciences, NJ, USA).

2.6.1.4 Lipid droplet (LD540) staining and analysis by confocal microscopy

Cells were grown on BSA- or rhDLL4-coated glass slides for 48 h. Cells were fixed with 4% PFA for 10 min. Neutral and polar lipids were stained with the fluorescent LD dye LD540 (kindly supplied by Dr C Thiele, LIMES Life and Medical Sciences Institute, University of Bonn, Germany), diluted in PBS (1:50,000) for 15 min. Samples were washed in PBS 3 times, and mounted in Vectashield Mounting Medium (Vector Laboratories, UK). The fluorescence was visualised using the Zeiss Laser Scanning Microscope (LSM) 510 META (Zeiss, Germany).

2.6.2 Luminescence-based assays

2.6.2.1 CellTiter-Glo® (Promega, WI, USA)

With the CellTiter-Glo® assay (Promega, WI, USA) the intracellular content of ATP was measured. 5,000 cells were seeded per well on BSA or rhDLL4 pre-coated opaque-walled 96 well plates (Corning, NY, USA) and allowed to settle down for 16 h. Where appropriate, the media was changed to drug containing media prior to starting the incubation of 24-120 h. After the indicated incubation time, the CellTiter-Glo® assay (Promega, WI, USA) was performed according to the manufacturer's instructions with minor adaptations. Briefly, the media was removed from the cells and replaced with 50 µl EGM2 (Lonza, Switzerland) equilibrated to room temperature. 50 µl of CellTiter-Glo® Reagent (Promega, WI, USA), prepared from the reagents provided in the kit, were added to each sample well and empty control wells. After mixing during which cell lysis occurred, the samples were incubated for 10 min and luminescence was read. The readings were normalised to cell growth measured with the CyQuant NF cell proliferation assay (Invitrogen, LCA, USA) in replicate plates.

2.6.3 Absorbance-based assays

2.6.3.1 Glucose assay (Instruchemie, Netherlands)

5,000 cells were seeded per well on a 96-well plate (Corning, NY, USA) pre-coated with BSA or rhDLL4 and allowed to settle down for 16 h, then incubated for 24-120 h. Glucose

concentration in the media was determined every 24 h using the glucose assay (Instruchemie, Netherlands), based on the NADH-producing conversion of glucose to glucose-6-phosphate by HK. The assay was used according to the manufacturer's instructions but downscaled to a 96-well format. Briefly, the sample media was centrifuged for 5 min at 10,000 g to pellet cell debris and the supernatant was used for analysis. 20 μl of the sample media were mixed with 150 μl of supplier-provided glucose reagent, incubated for 60 sec, and absorbance was measured at 340 nm (background measurement). Then, 30 μl of the supplier-provided glucose start reagent were added, mixed and incubated for 2 min. A standard curve was obtained from measurements of serial dilutions of fresh EGM2 media (5 mM glucose, Lonza, Switzerland). The absorbance was measured at 340 nm and glucose concentrations determined based on the standard curve. Each sample was measured in triplicate, and a blank measurement of water was done. Glucose consumption was calculated on values normalised to cell growth measured with the CyQuant NF cell proliferation assay (Invitrogen, LCA, USA) by using the formula

$$Glc_{consumed\ at\ tx} = \frac{Glc_{t0}}{Cy_{t0}} - \frac{Glc_{tx}}{Cy_{tx}}.$$

Equation 1. Glucose consumption (cell viability=Cy, t=time)

2.6.3.2 Lactate assay (Instruchemie, Netherlands)

5,000 cells were seeded per well on a 96-well plate (Corning, NY, USA) pre-coated with BSA or rhDLL4 and allowed to settle down for 16 h, then incubated for 24-120 h. Lactate concentration in the media was determined every 24 h using the lactate assay (Instruchemie, Netherlands), based on the NADH-producing conversion of lactate to pyruvate by LDHA. The assay was used according to the manufacturer's instruction but downscaled to a 96-well format. Briefly, the sample media was centrifuged for 5 min at 10,000 g to pellet cell debris and the supernatant was used for analysis. The NAD mixture was made up of 2 ml supplier-provided lactate buffer, 0.1 ml supplier provided lactate LDHA reagent and 4 ml deionized water. 10 μl of the sample media were mixed with 290 μl of the NAD mixture and incubated

for 15 min at 37 °C. A standard curve was obtained from measurements of serial dilutions of the supplier-provided lactate standard (4.44 mM). The absorbance was measured at 340 nm and lactate concentrations determined based on the standard curve. Each sample was measured in triplicate, and a blank measurement of water was done. Lactate secretion was calculated on values normalised to cell growth measured with the CyQuant NF cell proliferation assay (Invitrogen, LCA, USA) by using the formula

$$Lactate_{sereted\ at\ tx} = \frac{Lact_{tx}}{Cy_{tx}} - \frac{Lact_{t0}}{Cy_{t0}}.$$

Equation 2. Lactate secretion (cell growth=Cy, t=time)

2.6.3.3 Non-esterified FA (NEFA) assay (Randox, UK)

Adipocytes prepared for a lipolytic capacity test were switched to basal media without insulin and FAs 24 h prior to measuring NEFAs. The media was changed to 400 μl EGM2 without FCS (Lonza, Switzerland) containing 100 nM insulin (Sigma-Aldrich, MO, USA), 1 μM isoprenaline (Sigma-Aldrich, MO, USA) or vehicle control, and incubated for 2 h. The media was collected, centrifuged for 5 min at 10,000 rpm and NEFA assessed using the NEFA assay (Randox, UK) according to the manufacturer's instructions. The assay is based on the 3 step conversion of NEFA to a purple adduct, the amount of which can be determined by measuring absorbance. The following reactions occur during the assay

$$NEFA + ATP + CoA \xrightarrow{Acyl-CoA\ synthetase} Acyl - CoA + AMP + PPi$$

$$Acyl - CoA + O_2 \xrightarrow{Acyl-CoA\ oxidase} 2,3,-trans - enoyl - CoA + H_2O_2$$

$$2H_2O_2 + N - ethyl - N - (2hydroxy - 3 - sulphopropyl)m - toludine \xrightarrow{Peroxidase} purple\ adduct + 4H_2O$$

Equation 3 Non-esterified FA (NEFA) detection method

Briefly, the sample media was centrifuged for 5 min at 10,000 g to pellet cell debris, and the supernatant was used for analysis. The required enzyme-containing reagents 1 and 2 were prepared according to the manufacturer's instructions, using the buffers and enzyme tablets

provided. 10 µl of the sample media were mixed with 100 µl of Reagent 1 and incubated for 5 min at 37 °C. Then, 200 µl of Reagent 2 were added, mixed, and incubated for 5 min at 37 °C. A standard curve was obtained from measurements of serial dilutions of the supplier-provided NEFA standard (1 mM). The absorbance was measured at 550 nm. Each sample was measured in triplicate, and a blank measurement of water was done. NEFA concentrations were determined based on the standard curve.

2.6.4 MitoStress test, Seahorse Bioscience, Denmark

The Seahorse XFe analyser (Seahorse Bioscience, Denmark) was utilized to measure the extracellular oxygen concentration in a 96-well format. The Mito Stress Test (Seahorse Bioscience, Denmark) was performed according to the manufacturer's instructions, with slight adaptations. Briefly, 16 h prior to the assay, 60,000 cells per well in 80 µl EGM2 (Lonza, Switzerland) were seeded in a XF96 cell culture microplate (Seahorse Bioscience, Denmark) and incubated at 37 °C and atmosphere of 5% CO_2 in a humidified incubator. Also 16 h prior to the assay, a XF96 sensor cartridge (Seahorse Bioscience, Denmark) was transferred in XF calibration buffer (Seahorse Bioscience, Denmark) and placed into an incubator at 37 °C. Just before the assay, the drug dilutions were prepared at the appropriate concentrations as determined during optimisation experiments (see Appendix I, Fig. 0.1) and taking into account the change of volume after pneumatical sequential addition of the drugs into each well. Drugs used were oligomycin (0.5 µM, inhibits ATP synthase), FCCP (10 µM, uncouples OxPhos), and antimycin A (AA, 0.5 µM, inhibits OxPhos) and rotenone (0.75 µM, inhibits OxPhos). Indicated are final concentrations. For more information on the effect of the drugs please see section 3.2.2. 25 µl of the drug dilutions were added into the injection ports of the XF96 sensor cartridge, prior to transferring the cartridge into the Seahorse XFe analyser to start calibration of the sensors. Then, the media of the cells was removed, the cells were washed, and 175 µl assay media (customised EBM2 (Promocell), free of glucose, glutamine or pyruvate, with appropriate supplements as indicated in section 3.2) was added. The cell plate was placed into the machine, and the calibrated sensor cartridge automatically

placed above it. The assay was started and measurements of oxygen levels were taken every 5 min and media was mixed each time before the measurements were taken. This first cycle of measurements determines the basal oxygen consumption (rate 0). After this first cycle, oligomycin was added through injection port A, and the measurements were taken again for three times (rate A). Then, the cycle was repeated after injection of FCCP through injection port B (rate B). AA and rotenone were then injected through port C, and the measurement cycle repeated (rate C). The difference between the basal oxygen consumption and oxygen consumption after oligomycin injection is the ATP production-linked oxygen consumption rate (Rate 0 minus rate A). The maximal oxygen consumption rate was determined after FCCP addition as the difference of rate A and rate B. The spare capacity was determined by addition of AA and rotenone, by subtracting rate C from rate B. The proton leak is determined by subtracting rate C from rate A. All measurements were normalised to cell growth as determined by the CyQuant NF cell proliferation assay (Invitrogen, LCA, USA).

2.6.5 ^{14}C-oleic acid utilisation assays

The assay media was based on customised EBM2 (Promocell, Germany), which was free of glucose, glutamine or pyruvate. It was supplemented with 50 μM carnitine (Sigma-Aldrich, MO, USA), 500 μM oleic acid (OA) conjugated to FA-free BSA (Sigma-Aldrich, MO, USA), and 0.5 μCi/ml [1-^{14}C]-OA (Perkin Elmer, MA, USA). Drugs and/ or metabolic substrates were added as indicated.

2.6.5.1 ^{14}C-OA uptake assay

The assay was performed with cells seeded in 6-well plates (Corning, NY, USA) that were incubated for 16-48 h in the indicated media. Prior to the assay, the cells were washed with PBS. The cells were then incubated in the assay media for 3 h at 37 °C and 5% CO_2 in a humidified incubator. The cells were then washed twice in ice-cold PBS, and lysed in 0.1 M NaOH for 1 h. The lysate was collected in scintillation vials (Fisher Scientific, UK) containing 9 ml of OptiPhase 'HighSafe' 3 scintillation fluid (Perkin Elmer, MA, USA).

Radiation in the lysate was determined by liquid scintillation counting using a Beckman LS6500 scintillation counter (Beckman Coulter, CA, USA). Raw data was normalised to cell number determined from a replicate well.

2.6.5.2 ^{14}C-OA oxidation assay

The assay was performed with cells seeded in T75 flasks (Corning, NY, USA) and incubated for 48 h in the indicated media. Prior to the assay, the cells were washed with PBS. The cells were then incubated in the assay media for 1 h at 37 °C and 5% CO_2 in a humidified incubator. Then, glass "boats" containing 1 ml of KOH (3 mol/l) were inserted inside the flasks to trap CO_2 and the caps were sealed with parafilm. Cells were incubated at 37 °C. After 2 h, 1 ml of 60% perchloric acid (Sigma-Aldrich, MO, USA) was injected through the cap of the flask using a syringe, to liberate CO_2 trapped in the media and intracellularly. The caps were resealed and the flasks were placed on a shaker for 2 h at room temperature. Then, the boats were removed and the KOH was collected and added to scintillation vials (Fisher Scientific, UK) containing 9 ml of OptiPhase 'HighSafe' 3 scintillation fluid (Perkin Elmer, MA, USA). ^{14}C was determined by liquid scintillation counting using a Beckman LS6500 scintillation counter (Beckman Coulter, CA, USA). Raw data was normalised to cell number determined from a replicate flask.

2.6.5.3 ^{14}C-OA transfer assay

This experiment was based on a coculture of primary human adipocytes with HUVEC. The adipocytes were obtained by differentiating pre-adipocytes isolated from fresh fat tissue biopsies. The fat biopsies were obtained by a research nurse in the Clinical Research Unit at the Oxford Centre for Diabetes, Endocrinology and Metabolism, University of Oxford. This procedure received ethical approval from the Oxfordshire Clinical Research Ethics Committee and all participants gave written, informed consent. The fat biopsies were taken from the abdominal subcutaneous adipose tissue of five healthy female volunteers (body mass index 18.5-24.9) registered in the Oxford BioBank. Immediately upon the performance of the biopsy, the tissue was kept on ice. The biopsy was transferred from the biopsy syringe into a

50 ml conical bottom tube (Corning, NY, USA) containing 10 ml of HBSS (Sigma-Aldrich, MO, USA) and minced using sterile scissors. After a gentle wash, the biopsy was transferred to a fresh 50 ml conical bottom tube (Corning, NY, USA) containing 10 ml HBSS and washed gently. After repeating this procedure another time, the biopsy was transferred into a 50 ml conical bottom tube (Corning, NY, USA) containing HBSS with 1 mg/ml collagenase (Roche, Switzerland) and incubated for 60 min in a waterbath at 37 °C, shaking at 90 rpm, until the tissue was fully digested and the solution appeared milky. The solution was centrifuged for 5 min at 500 g at 4 °C. The supernatant was discarded and the cell pellet resuspended in 5 ml HBSS. The cell suspension was filtered through a 250 μm and a 100 μm pore mesh (Sefar, Switzerland) and centrifuged for 5 min at 500 g and 4 °C. The cell pellet was resuspended in pre-adipocyte growth media (Dulbecco's Modified Eagle's Medium/Nutrient Mixture F-12 Ham with 15 mM HEPES and sodium bicarbonate, without L-glutamine (Sigma-Aldrich, MO, USA), 10% FCS (Invitrogen, CA, USA), 1000 U/ml penicillin and 100 μg/ml streptomycin (Invitrogen, CA, USA), 2 mM glutamine (Invitrogen, CA, USA), 0.25 ng/ml human bFGF (Sigma-Aldrich, MO, USA)), and seeded into a T25 flask. The following day the media was replaced with fresh media to remove any red blood cells. Cells were grown in pre-adipocyte growth media and transferred to larger tissue culture ware when they reached confluence, and expanded until the right amount of cell number (6.6x10^6 cells) was reached.

All conditions were prepared in duplicate and a replicate set was prepared for control and normalisation purposes. 1x10^5 pre-adipocytes were seeded on Thincert™ 6-well culture inserts (Greiner Bio-one, Austria) and were kept still for 30 min in the tissue culture hood to allow even cell attachment. Cells were grown to confluency. Then growth media was replaced by differentiation media (Dulbecco's Modified Eagle's Medium/Nutrient Mixture F-12 Ham with 15 mM HEPES and sodium bicarbonate, without L-glutamine (Sigma-Aldrich, MO, USA), 1000 U/ml penicillin and 100 μg/ml streptomycin (Invitrogen, CA, USA), 2 mM glutamine (Invitrogen, CA, USA), 17 μM pantothenate (Sigma-Aldrich, MO, USA), 100 nM

human insulin (Invitrogen, CA, USA), 10 nM 3,3,5-triiodo-L-thyronine sodium salt (Sigma-Aldrich, MO, USA), 33 μM biotin (Sigma-Aldrich, MO, USA), 130 nM transferrin (Sigma-Aldrich, MO, USA), 1 μM dexamethasone (Sigma-Aldrich, MO, USA), 250 μM IBMX (only from day 1-4, Sigma-Aldrich, MO, USA) and 4 μM troglitazone (only from day 1-4, Sigma-Aldrich, MO, USA)). The media was changed every two days (3 ml media per well).

On day 7, the differentiation media was supplemented with a mix of FAs (final concentration 100 μM), with or without ^{14}C-oleate. The FA mix consisted of 45% OA (Sigma-Aldrich, MO, USA), 30% palmitic acid (Sigma-Aldrich, MO, USA), and 25% linoleic acid (Sigma-Aldrich, MO, USA) in 10% FA-free BSA (Sigma-Aldrich, MO, USA), with or without 0.05 μCi [1-^{14}C]-OA per ml media. The media was changed every two days for 7 days (day 7, day 9, and day 11).

On day 13, 1x10^5 HUVEC were seeded on BSA or rhDll4 coated 6-well plates, intended to use for co-culture. Per time point, 4 wells in a 6-well plate (duplicate for w/o ^{14}C-oleate), and 2 wells in a separate plate were seeded for single culture. Furthermore, adipocyte media was changed to ^{14}C-oleate free differentiation media after a PBS wash. On day 14, adipocytes were photographed, washed with 1 ml PBS once, and Thincerts^{TM} were transferred to the prepared co-culture plates. Cells were grown in 3 ml EGM2 (Lonza, Switzerland) for 24 h, 48 h or 72 h.

After each time point, the media was collected and adipocytes and endothelial cells were washed with 1 ml ice-cold PBS, then lysed in 1 ml of 0.5 M NaOH (^{14}C) for 1 h at 37 °C or in protein lysis buffer (control) and placed on ice. Media was collected, centrifuged for 5 min at 10,000 rpm, and the supernatant stored on ice. Media or samples containing radioactivity were processed in the radiation suite or in RA-dedicated areas. ^{14}C in samples were measured in 9 ml of scintillation fluid using a Beckman LS6500 scintillation counter (Beckman Coulter, CA, USA). Raw data was normalized to protein concentrations.

2.6.6 Gas chromatography/ mass spectrometry (GC/MS) techniques

2.6.6.1 Triglyceride (TG) composition

This method was carried out by Dr Jennifer Collins, Oxford Centre for Diabetes, Endocrinology and Metabolism, University of Oxford. FA methyl esters were prepared from cells based on a standard laboratory protocol and described in Burdge, Wright *et al.* (2000). Briefly, cellular total lipids were extracted using the Folch method (Folch, Lees *et al.* 1957), using chloroform-methanol (2:1, v/v) containing 0.1mg/ml butylated hydroxytoluene, as an antioxidant and internal standards. The total lipid fraction in the solvent phase was evaporated to dryness under nitrogen. The dry lipid extract was resolved in 1 ml chloroform.

Separation of the TG and PL fractions of the lipid extract was done using solid phase extraction aminopropyl columns (Varian Ltd, Oxford, UK). The third elute with 1 ml chloroform contained TG FAs and cholesteryl esters. The elute was evaporated to dryness under nitrogen. The TG FA/cholesteryl ester fraction was resolved in 1 ml hexane and passed through a solid phase extraction column into a collection tube. The column was washed twice with 1 ml hexane, which eluted cholesteryl esters, The TG FA fraction was eluted with 2 x 1ml hexane:chloroform; ethyl acetate (100:5:5) under vacuum. The elute was evaporated to dryness under nitrogen.

Methylation of the TG fraction was carried out next. 400 µl of toluene was added to each dried fraction, the sample was vortexed, and 800 µl of 1.5% H_2SO_4 in methanol was added Samples were then placed in a waterbath at 80°C for 1 h. Then 2 ml of neutralising solution (0.025 M potassium hydrogen carbonate and 0.025 M potassium), and 2 ml cyclohexane were added to each sample, mixed and centrifuged. The upper solvent phase was transferred into a new glass tube and evaporated to dryness under nitrogen. FA methyl esters (FAME) of the isolated TG FA were prepared by incubating the samples for 1 h at 80 ^{o}C with methanolic sulphuric acid. In order to allow quantification of FAs a 50 µg internal standard (C15:0 TAG) was added to each sample prior to Folch extraction whilst an external standard (50 µg, C23:0 FAME) was added to each sample just before GC analysis. GC analysis was carried out using

the Agilent 6890 system and individual FA peaks identified by reference to known FAMEs from the internal standard. The addition of both an internal and external standard allowed the calculation of the percentage recovery of FAs (i.e. estimation of the loss of FA during extraction.) The amount of FA for each sample was then expressed in µg per 4x 10^6 cells based on the cell count prior to extraction.

2.6.6.2 Phospholipid (PL) composition

This method was performed by Ms Katherine Kearney, University of Surrey. FA methyl esters were prepared from cells based on a standard laboratory protocol and described in Burdge *et al.* except that thin layer chromatography (TLC) was used to separate PL from the other lipid fractions (Burdge, Wright *et al.* 2000). Briefly, cellular total lipids were extracted using the Folch method (Folch, Lees *et al.* 1957), using chloroform-methanol (2:1, v/v) containing 10 mg of butylated hydroxytoluene to each 100 ml, as an antioxidant and 1,2-diheptadecanoyl-*sn*-glycero-3-phosphocholine (50 µg per sample) from 'Avanti Polar Lipids' as an internal standard. The total lipid fraction was evaporated to dryness under nitrogen, reconstituted in 50 µl chloroform and applied to silica gel TLC plates 20x20 cm, 250 µm thick. The plates were placed in a TLC tank containing 70 ml hexane, 30 ml diethyl ether and 1.8 ml glacial acetic acid. After developing for approximately 35-40 min, the plates were dried and sprayed with 0.1% ANS (8-anilino-1-napthalene-sulfonic acid) in de-ionised water, 0.1 g in 100 ml. The PL spots (identified with reference to a PL standard) remained on the origin and were scraped off and methylated with methanolic sulphuric acid. FA methyl esters were analysed using a gas-chromatograph (6890N, Agilent, Stockport, Cheshire UK) linked to a mass spectrometer (5973 Network MSD, Agilent, UK) equipped with a Supelco capillary column (75 m x 0·18 mm with 0·14 mm film thickness; Supelco, Bellefonte, PA, USA). The injector was set at 250 °C and the oven was programmed from 120 to 240 °C. Individual FAs were identified by comparison with a known standard (37FAMES, Sigma-Aldrich, UK). Individual FAs were calculated according to the peak area relative to the total area and

expressed as the percentage of total FAs, or as μg per sample calculated using the internal standard.

2.6.6.3 Calculation of desaturation and elongation indexes as indicators of desaturase and elongase activities

The obtained levels of FA were used to estimate the activity of desaturases, by dividing the levels of desaturated FA through the levels of their unsaturated form. The desaturation indexes were the ratio of the levels of palmitoleic acid (C16:1n-7) and the levels of palmitic acid (C16:0), or the level of oleic acid (C18:1n-9) and the levels of stearic aicd (C18:0). Palmitoleic acid can be lengthened to vaccenic acid (C18:1n-7). The elongation index, indicating elongase activity, is formed by the ratio of vaccenic acid and palmitoleic acid.

2.6.7 Angiogenic assays

2.6.7.1 Scratch wound assay for measuring endothelial cell migration

30,000 HUVEC were seeded on ImageLock 24-well plates (Essen BioScience, MI, USA) and grown to confluence. The scratch was introduced by using a 24-pin woundmaking tool (WoundMaker^{TM}, Essen BioScience, MI, USA). The media was changed to the appropriate media with or without drugs as indicated and the plate placed into a live cell imaging incubator (Incucyte, Essen BioScience, MI, USA), which enables automatic photographing of the same scratch area at a given time interval. The assay was stopped when the control scratch reached 100% confluence. For analysis, the percentage of scratch or wound closure in the test conditions at the time that the control scratch reached 80% confluence were used.

2.6.7.2 Sprouting assay

In this assay, HUVEC are seeded in drops containing methylcellulose, and incubated upside down. The cells would assemble in the bottom of the drop and form a spheroid. These spheroids were then embedded into a matrix. Cells would bud from the spheroid, migrate towards the angiogenic cue, and trailing cells would start proliferating and form a sprout. For the sprouting assay, drops of 500 cells per 20 μl EGM2 (Lonza, Switzerland) containing 2.5

mg/ml methylcellulose (Sigma-Aldrich, MO, USA) were pipetted on a non-coated dish. The dish was inverted, and incubated for 16 h, during which time the cells accumulated in the bottom of the hanging drops and formed spheroids. The spheroids were embedded in Gibco® Geltrex™ lactose dehydrogenase elevating virus-free Reduced Growth Factor Basement Membrane Matrix (Life technologies, CA, USA). This matrix is extracted from murine Engelbreth-Holm-Swarm tumours, and is used as a model matrix that resembles the extracellular matrix of the tumour microenvironment. In some experiments, fibrin gel (2.5 mg/ml fibrin (Sigma-Aldrich, MO, USA) in PBS, polymerised with 0.2 U/ml thrombin (Sigma-Aldrich, MO, USA), an inert matrix, was used to embed the spheroids. The spheroids were incubated in the indicated conditions for >24 h to enable sprout formation. The sprouts were photographed using the EVOS® XL Cell Imaging System (Life technologies, CA, USA) and sprout length, sprout number, or sprout area were determined using the ImageJ analysis software.

2.6.8 Zebrafish angiogenesis assay

This method was performed by Dr. Tessa Peterkin, Weatherall Institute of Molecular Medicine, University of Oxford. Briefly, embryos were treated with various concentrations of EX diluted in zebrafish E3 medium and collected at 48 h post fertilisation (hpf). Tg(kdrl:GFP) (transgenic product, Kinase Insert Domain Receptor (A Type III Receptor Tyrosine Kinase) tagged with green fluorescent protein) transgenic embryos were imaged for GFP under a Zeiss fluorescent microscope. The embryos were observed for morphological phenotypes, heart rate, intersegmental vessel (ISV), and caudal vein plexus (CVP) abnormalities.

2.7 Immunohistochemical (IHC) staining

2.7.1 IHC staining of in vitro cell pellets for antibody validation

The cells were transfected with siRNA targeting *FABP4* and grown for 48 h. The cells were detached by exposure to trypsin and centrifuged for 5 min at 500 g. The cell pellet was fixed

overnight in 10% neutral buffered formalin solution (Sigma-Aldrich, MO, USA), and placed in 70% ethanol (VWR, PA, USA). The pellet was embedded in paraffin, sectioned, and FABP4 was stained according to the conditions listed in table 3, and according to the protocol described in 2.8.2.

2.7.2 IHC staining of patient samples

Patient samples were selected, reviewed and scored by Dr Ioannis Roxannis, Dept. of Cellular Pathology, Oxford University Hospitals and obtained from the Oxford Centre for Histopathology Research (OCHRe), under the ethical approval license of Prof Ahmed Ahmed, Dept. Oncology, University of Oxford. Of low-grade serous carcinomas, there were 8 serous borderline tumours (SBT), 5 non-invasive implants (NII) and 3 invasive implants (II), and there were 3 high-grade serous carcinomas (HGSC), and 5 omental deposits of high-grade serous carcinomas (HGSC-D). The sections were scored for intensity and extent with 0 for weak/no staining, 3 for strong staining, or percentage of cells positively stained (extent). The scoring was performed in the epithelial, the stromal, and the vascular department. The scores in SBT were compared to NII and II and the scores of HGSC were compared to HGSC-D.

The formalin-fixed and paraffinembedded tissue sections were retrieved, dewaxed, and rehydrated. Briefly, slides were heated to 65 °C for 10 min. Then, they were dewaxed in Citroclear (HD, supplies, UK) twice for 5 min and rehydrated in graded industrial methylated spirit solutions of 100% (twice, 5 min each), followed by 50% (once, 5 min), before placing the slides into PBS. The antigen retrieval was performed in the appropriate buffer (see table 3) using a decloaking chamber (Biocare Medical, CA, USA). The slides were placed in PBS to cool down. The sections were then blocked in 10% normal horse serum (Vector Laboratories, UK) for 30 min. The primary antibody incubation was performed as listed in table 3. Following the primary antibody incubation, the slides were washed in PBS, and the secondary antibody was applied (table 3). Visualisation was performed by using the DAB (3, 3'-diaminobenzidine) Peroxidase (HRP) Substrate Kit (Vector Laboratories, UK) for 5-8 min.

The slides were washed in tap water, before immersing them in heamatoxylin solution (Gill No3, Sigma-Aldrich, MO, USA) for 5 sec, and rinsing them in tap water. The slides were mounted with Aquamount (Fisher Scientific, UK) and visualized and photographed on a BX51 microscope (Olympus, Japan) attached to a DP40 digital camera (Olympus, Japan). Images of human ovarian cancer sections were analysed and scored by Dr Ioannis Roxannis, Dept. of Cellular Pathology, Oxford University Hospitals.

Table 3 Antibodies and conditions used for IHC staining of human tissues

Antigen	Supplier	Species	Antigen retrieval	Dilution in RPMI (Lonza, Switzerland)	Incubation	Secondary antibody
FABP4	Sigma-Aldrich, MO, USA	rabbit, poly-clonal	Dako R1669 buffer	1 in 500	16 h at 4 °C	ImmPRESS HRP Universal Antibody Polymer Detection Kit (Vector Laboratories, UK)
DLL4	Regeneron NY, USA,	mouse, mono-clonal	Dako R1669 buffer	1 mg/ml	16 h at 4 °C	Novocastra Novolink immunostaining kit (Leica, Germany)
NICD	Abcam, UK	rabbit, mono-clonal	Dako R1669 buffer	1 in 130	16 h at 4 °C	ImmPRESS HRP Universal Antibody Polymer Detection Kit (Vector Laboratories, UK)
VEGFR2	Cell Signalling Technology, MA, USA	mouse, mono-clonal	Dako R1669 buffer	1 in 300	1 h at room temperature	ImmPRESS HRP Universal Antibody Polymer Detection Kit (Vector Laboratories, UK)

2.8 Statistical analysis

Results are expressed as the mean ± standard deviation (S.D.) of at least three independent experiments. The Graphpad PRISM^{TM} Software package was used for statistical analyses. Statistical analysis was performed by analysis of variance (ANOVA) with the Bonferroni post-hoc test unless stated otherwise. $p<0.05$ was considered statistically significant.

3 CHAPTER THREE

DLL4-NOTCH signalling increases fatty acid utilisation

3.1 Introduction

Highly proliferative cells tend to be mainly glycolytic, which is the case with most tumour cell lines. However, in the tissue, a metabolic adaptation can occur, depending on the anatomical location and the microenvironment. An example of this adaptation has been demonstrated by Nieman *et al.*, who showed that ovarian cancer cells adjacent to the omentum increasingly metabolise adipocyte-derived FA (Nieman, Kenny *et al.* 2011). Recent studies have shown that glycolysis is a major angiogenic pathway that drives proliferation, migration, and sprouting of endothelial cells in physiological conditions and is driven by VEGFA (De Bock, Georgiadou *et al.* 2013). DLL4-NOTCH signalling has been shown to limit angiogenesis, slow proliferation of endothelial cells, and control tip cell formation during angiogenic sprouting. DLL4-NOTCH signalling is implicated in tumour angiogenesis and its overexpression is a potential mechanism of resistance to anti-VEGFA therapy (Li, Sainson *et al.* 2011). Endothelial cells in tumour tissue are exposed to varying concentrations of glucose, lactate, amino acids, and FAs. Signalling pathways that drive a certain metabolic 'configuration' might therefore give the cells a selective advantage in certain environments. So far, studies investigating angiogenic drivers of metabolic pathways in endothelial cells are scarce, but have the potential to give great insight into the basic mechanism of angiogenic sprouting and the mechanism of tumour angiogenesis and resistance.

In the following chapter, the effect of the DLL4-NOTCH signalling pathway on the metabolism of HUVEC was investigated. Metabolic parameters measured were glucose consumption and lactate secretion as indicators of the glycolytic rate and oxygen consumption to assess mitochondrial respiration in response to different metabolites. Through the course of this chapter, investigations were focused on the aspect of the DLL4-NOTCH effect on FA metabolism in HUVEC. Assays with radiolabelled tracer molecules, fluorescent labeling of lipid stores, and GC/MS analysis of TG and PL were used. Finally, the effect of inhibition of FA oxidation on angiogenesis and metabolism in response to DLL4-NOTCH was assessed.

3.2 Results

3.2.1 DLL4-NOTCH signalling decreases glycolysis

To profile metabolic parameters in proliferating endothelial cells in which DLL4-NOTCH signalling is activated, HUVEC were grown on BSA- or DLL4-coated plates (BSAc or DLL4c) over a time course of five days. Cellular DNA measured by the CyQuant NF Cell Proliferation Assay was used as an indicator of cell growth, total ATP levels as an indicator of metabolic activity (all ATP-producing and consuming processes), and glucose consumption and lactate secretion as indicators of glycolytic activity. These parameters were measured every 24 h, over a time course of 5 days. Proliferation was significantly decreased in HUVEC with activated DLL4-NOTCH signalling and the growth of DLL4c versus BSAc-stimulated cells diverged after 48 h (Fig. 3.1 A). ATP levels and glucose consumption were not significantly changed in DLL4c compared to BSAc-stimulated cells (Fig. 3.1 B and C). Lactate secretion was consistently downregulated in HUVEC with activated DLL4-NOTCH signalling, which was significant at 48 h, 96 h, and 120 h (Fig. 3.1 D). These results showed that DLL4-NOTCH signalling activation inhibited proliferation of HUVEC, which was paralleled by a decrease in lactate secretion as a main indicator for the glycolytic rate. Given that ATP levels remained unchanged, this indicated that although the glycolytic rate was decreased in response to DLL4-NOTCH, the cells were able to maintain their energy levels.

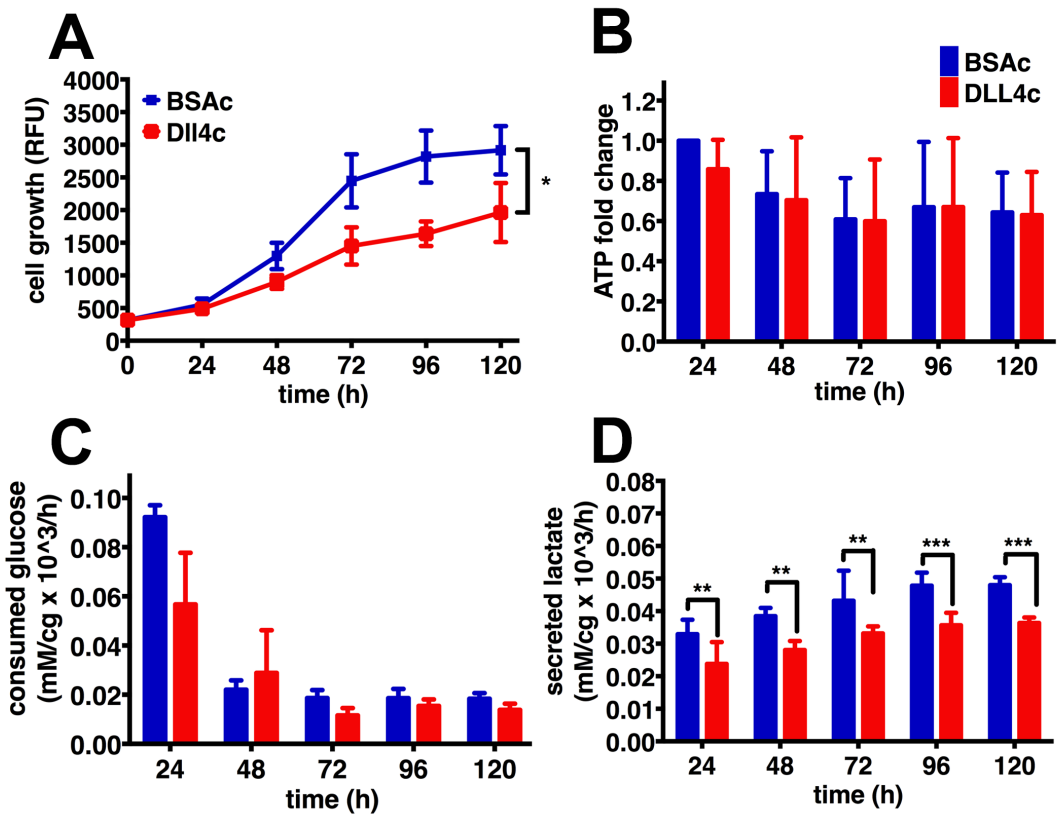


Figure 3.1 DLL4-NOTCH signalling decreases glycolysis. HUVEC were grown on BSA- or DLL4-coated (BSAc or DLL4c) dishes over five days. Every 24 h, cells were harvested and analysed for cell growth (cg, A) and ATP production (B). The supernatants were collected and glucose consumption (C) and lactate secretion (D) were measured. Values are expressed as mean +/- S.D., *p<0.05, **p<0.01, ***p<0.001 (n=3, Two-way ANOVA, Bonferroni post-hoc test).

3.2.2 DLL4-NOTCH signalling decreases mitochondrial respiration

Quiescent cells, and slow proliferating cell types are known to rely on energy production via mitochondrial respiration, which can be measured indirectly by monitoring the levels of extracellular oxygen. The Seahorse XFe analyser was utilised to measure the extracellular oxygen concentration in a 96-well format, by a solid-state sensor probe that is placed 200 μm above the cell monolayer, thereby isolating a very small volume of media above the cells. In this transient microchamber, rapid changes of oxygen over time could be monitored. The measurements took place 3 times every 3 minutes. After each measurement, the probe lifts, releasing the transient microchamber and allowing the media to mix. To investigate the effect of DLL4-NOTCH signalling on mitochondrial fitness, the Seahorse XFe MitoStress test was performed. The MitoStress test is based on the respiratory changes after sequential addition of the mitochondrial drugs oligomycin (inhibits ATP synthase), FCCP (uncouples OxPhos), and antimycin A and rotenone (inhibits OxPhos) into the wells via injection ports, during real-time monitoring of oxygen consumption. The respiratory changes after the addition of each drug were used to calculate several key mitochondrial parameters: basal respiration, respiration linked to ATP production, maximal respiration, spare capacity and proton leak. Please refer to section 2.6.4 for further details. For optimisation experiments to determine optimal cell density and drug concentrations please refer to the Appendix, Fig. 7.1.

The cells were incubated on BSAc or DLL4c for 16 h. The media was changed to customised, substrate free endothelial cell media supplemented with 2% FCS, 5 mM glucose, 2 mM Glutamax and 1 mM pyruvate, and the MitoStress test was performed. Fig. 3.2 A shows the oxygen consumption or respiration profile of HUVEC grown on BSAc or DLL4c. Basal respiration rate in both conditions was at 60-80 pmol/min and was reduced to 40 pmol/min by oligomycin. Addition of FCCP led to an increase of respiration to 120 pmol/min or 80 pmol/min in BSAc- or DLL4c-stimulated HUVEC, respectively. Antimycin A/rotenone reduced the rate in both conditions to 30-40 pmol/min. Basal respiration (Fig. 3.2 B, upper left panel) was not significantly changed by DLL4-NOTCH activation. ATP-linked respiration

and maximal respiration (Fig. 3.2 B, upper middle, and upper right panels) were significantly downregulated by 50% by DLL4-NOTCH activation. Spare capacity and proton leak were not significantly changed by DLL4-NOTCH signalling. The observed changes were indicative of a reduced mitochondrial metabolic rate, as the respiration rate linked to mitochondrial ATP production was reduced by DLL4-NOTCH. Maximal respiration was indicative of how well the cells can respond to increased ATP demand and its decrease in cells with DLL4-NOTCH signalling showed that they were more likely to undergo an energetic crisis in the observed substrate conditions.

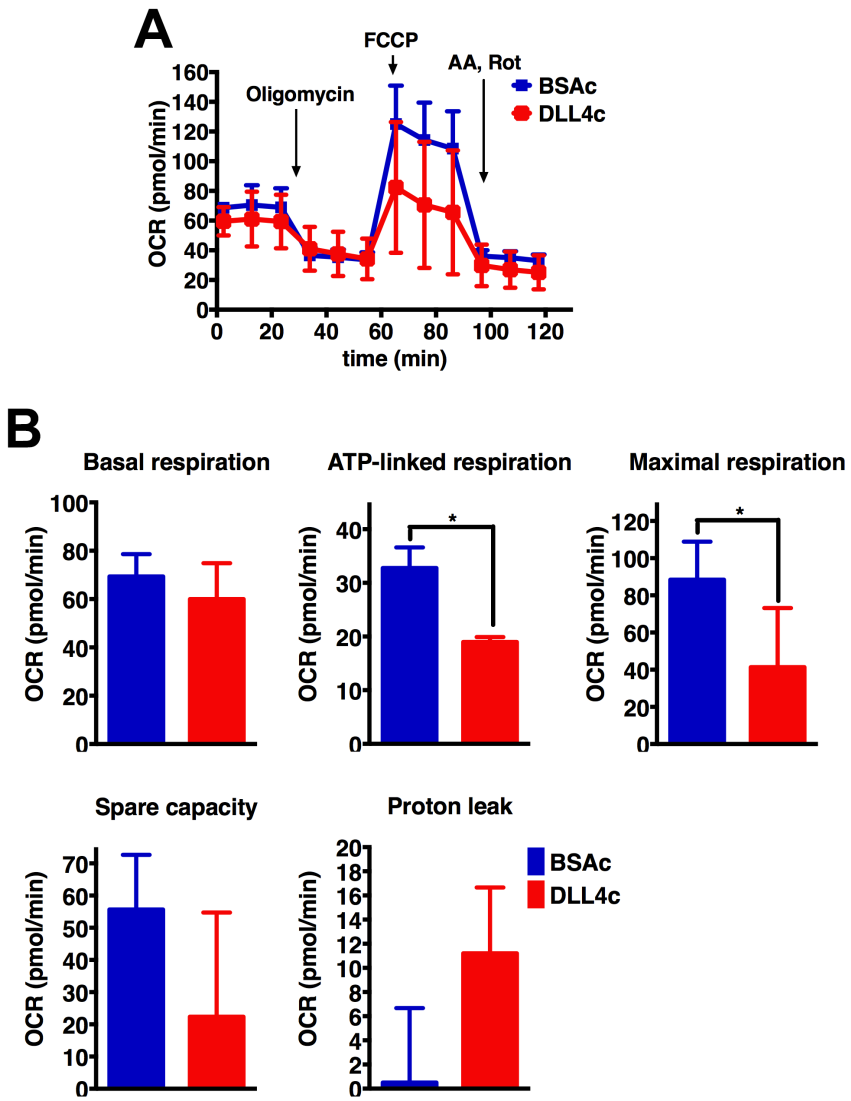


Figure 3.2 DLL4-NOTCH signalling decreases mitochondrial respiration at 5 mM glucose. HUVEC were seeded on BSA- or DLL4-coated (BSAc or DLL4c) XF96 Cell Culture microplates overnight. Oxygen consumption rates (OCR) were measured with the XFe Seahorse Bioanalyzer. The MitoStress test was performed, by sequential addition of oligomycin (0.5 μM) FCCP (10 μM) and antimycin A (AA) (0.5 μM), and rotenone (Rot) (0.75 μM), (A). The mitochondrial parameters basal respiration (B, upper left panel), ATP-linked respiration (upper middle panel), maximal respiration (upper right panel), spare capacity (lower left panel) and proton leak (lower right panel) were assessed based on changes in OCR after inhibitor addition. Raw values were normalised to cell growth. Values are expressed as mean +/- S.D., *p<0.05 (n=3, paired student's t test).

3.2.3 DLL4-NOTCH signalling leads to a substrate-dependent increase of oxygen consumption

In the previous experiment, the cells were assessed in media containing glucose and glutamine as main substrates. Nutrients that are used for mitochondrial respiration are mainly glucose, amino acids, and FAs, all of which can participate in TCA cycle via different pathways. To assess the ability of HUVEC to respire on different substrates, the Luxcel MitoXpress Xtra Oxygen consumption assay was used. This assay is based on a fluorescent probe that is added to the media before the assay, and is quenched by the presence of oxygen. The increased intensity of fluorescence is directly related to a decrease in extracellular oxygen concentration. The cells were grown on BSAc or DLL4c for 48 h. Qxygen consumption was then measured in a highly concentrated cell suspension in the respective assay media for up to 4 h. The high number of cells increases the cell surface directly exposed to the assay media and provides a very sensitive system to measure changes in oxygen concentration.

In this experiment, the ability of cells to respire on glucose, glutamine, and oleic acid (OA) was investigated, with or without DBZ to inhibit DLL4-NOTCH signalling (Fig. 3.3). There was no change of oxygen consumption when cells were exposed to glucose in either experimental condition and the rate of oxygen consumption was also very low (Fig. 3.3 A, left panel). When the cells were exposed to glutamine, there was a marked increase in oxygen consumption by DLL4-NOTCH signalling activation, which was prevented in cells following DBZ treatment (Fig. 3.3 A, middle panel). When the cells were exposed to OA, cells with activated DLL4-NOTCH signalling responded with higher rates of oxygen consumption, which was not observed in cells also treated with DBZ (Fig. 3.3 A, right panel).

The increased oxygen consumption in media with OA indicated increased FA oxidation in response to DLL4-NOTCH. Next, HUVEC were treated with the FA oxidation inhibitor etomoxir (EX, 50 μM), which inhibits mitochondrial import of Acyl-CoA via inhibition of the mitochondrial FA transferase CPT1, for 48 h. Cellular oxygen consumption was measured, in

media with glucose, OA, or glutamine, with or without EX. Cells in media with glucose did not show a change in response to any of the treatments (Fig. 3.3 B, left panel). Cells in media with OA showed a significant increase of oxygen consumption when DLL4-NOTCH signalling was active (Fig. 3.3 B, middle panel). EX treatment led to a significant reduction of oxygen consumption in response to OA, in DLL4c-stimulated cells (Fig. 3.3 B middle panel). Cells in media with glutamine showed no significant change in oxygen consumption when DLL4-NOTCH signalling was active. EX treatment led to a significant reduction of oxygen consumption in BSAc- or DLL4c-stimulated cells in media with glutamine (Fig. 3.3 B, right panel). These results showed that HUVEC with DLL4-NOTCH signalling increased respiration when exposed to glutamine and FAs. This effect was dependent on FA oxidation.

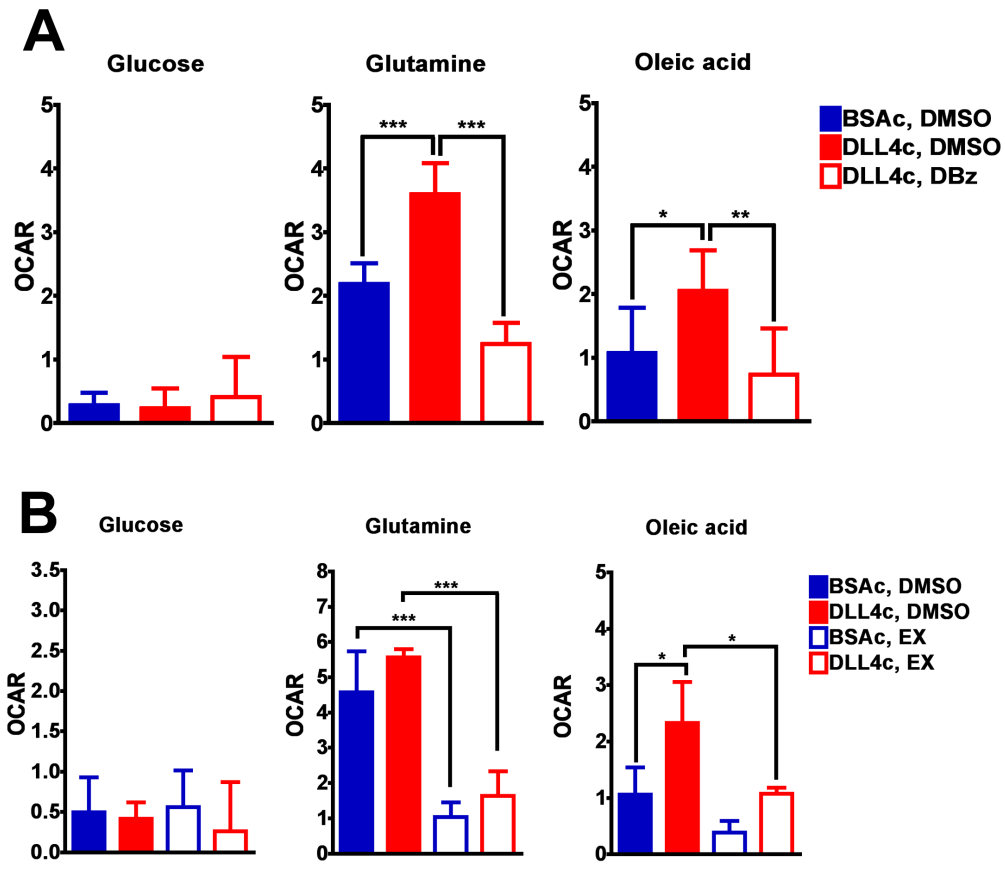


Figure 3.3 DLL4-NOTCH signalling leads to a substrate-dependent increase of oxygen consumption. HUVEC were grown on BSA- or DLL4-coated (BSAc or DLL4c) dishes for 48 h with or without dibenzazepine (DBZ) to inhibit NOTCH cleavage (A), etomoxir (EX, 50 μM) to inhibit fatty acid oxidation, (B), or DMSO as a vehicle control. Cells were detached by exposure to trypsin and reseeded in the respective assay media, containing DMSO, DBZ or EX, and 5 mM glucose, 10 mM glutamine, or 100 μM BSA-conjugated oleic acid. Oxygen consumption arbitrary rate (OCAR) was measured by addition of the fluorescent MitoXPress HS probe, and monitoring the change of fluorescence over time. Values are expressed as mean +/- S.D., *p<0.05, **p<0.01, ***p<0.001 (n=3, One-way ANOVA, Bonferroni post-hoc test).

3.2.4 Increased oxygen consumption in FA-enriched media is dependent on DLL4-NOTCH signalling, mitochondrial FA import, and glucose availability

The previous results showed increased FA utilisation in response to DLL4-NOTCH signalling that was sensitive to EX. Next, HUVEC grown on BSAc or DLL4c were treated with DBZ to inhibit NOTCH signalling for 48 h (chronic treatment) and exposed to EX only for the time of the assay, to avoid secondary effects (acute treatment). The cells were assayed for oxygen consumption in media containing 50 μM carnitine, OA, or FA-free BSA as a control, with or without DBZ or 50 μM EX (Fig. 3.4 A). HUVEC with activated DLL4-NOTCH signalling showed a significant increase of oxygen consumption in media with OA, which was downregulated to base-line levels by DBZ treatment (see section 3.2.3). Acute addition of EX for the time of the assay (3 h) led to a significant inhibition of oxygen consumption in media with OA, when DLL4-NOTCH signalling was active. This was further reduced by DBZ treatment. This indicates that the increase of cellular oxygen consumption in media with OA following DLL4-NOTCH stimulation was dependent on DLL4-NOTCH activity and sensitive to EX treatment, even during acute treatments.

To investigate the effect of glucose in the media, HUVEC, grown on BSAc or DLL4c for 48 h, were assayed for oxygen consumption in media containing OA or FA-free BSA, with or without 5 mM glucose. Addition of glucose led to a significant downregulation of oxygen consumption in response to OA, in cells stimulated with BSAc or DLL4c (Fig. 3.4 B), similar to the trend observed in 3.2.3. Overall, these results indicated that oxygen consumption in media with OA, as an indirect measurement of mitochondrial respiration, was induced by DLL4-NOTCH signalling and sensitive to inhibition of FA oxidation. This effect was reduced when glucose was added to the media, possibly reflecting a shift to glycolysis that overrides mitochondrial respiration.

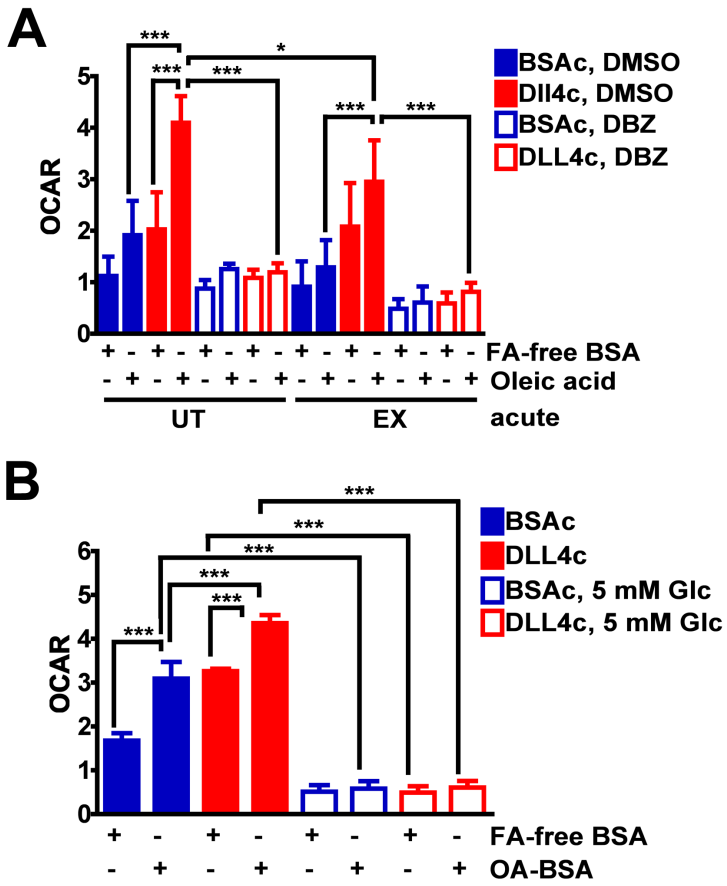


Figure 3.4 Increased oxygen consumption in media with oleic acid (OA) is dependent on DLL4-NOTCH signalling, mitochondrial fatty acid (FA) import, and glucose availability. HUVEC were grown on BSA- or DLL4-coated (BSAc or DLL4c) dishes for 48 h with or without dibenzazepine (DBZ) to inhibit NOTCH cleavage or DMSO as a vehicle control (A), or without addition of any drug or vehicle (B). Cells were detached by exposure to trypsin and reseeded at equal cell density in the respective assay media, containing DMSO or DBZ with or without etomoxir (EX) to inhibit fatty acid oxidation only for the time of the assay (acute), (A), and fatty acid (FA)-free BSA, BSA-conjugated oleic acid (OA-BSA) (A, B), with or without 5 mM glucose (B). Oxygen consumption arbitrary rates (OCAR) were measured by addition of the fluorescent MitoXPress HS probe, and monitoring the change of fluorescence over time. Values are expressed as mean +/- S.D., *p<0.05, ***p<0.001 (n=5 (A), n=3 (B), One-way ANOVA, Bonferroni post-hoc test).

3.2.5 Metabolism of ^{14}C-OA is increased by DLL4-NOTCH signalling

Next, the effect of DLL4-NOTCH on FA oxidation in HUVEC was investigated by monitoring the intracellular production of CO_2 from extracellular, radioisotope-labelled ^{14}C-OA. Intracellular ^{14}C and production of $^{14}CO_2$ were measured. HUVEC were grown in media containing 5 mM glucose (normal glucose), 0.75 mM glucose (low glucose), or 5 mM glucose with 10 mM lactate (lactate) for 48 h, to mimic the tumour microenvironment, in which glucose concentrations reach very low levels and extracellular lactate concentrations can peak due to high levels of glycolysis in tumour cells (Vegran, Boidot *et al.* 2011). The assay was performed in media containing the indicated substrate concentrations, 50 μM carnitine and 500 μM OA conjugated to FA-free BSA, and 0.05 μCi/ml ^{14}C-OA. FA oxidation rates were assessed by KOH capture of CO_2 and scintillation counting. A replicate of cells were lysed to assess intracellular ^{14}C. Intracellular ^{14}C did not show any significant change in any of the conditions (Fig. 3.5 A) and only 0.2-1% of intracellular ^{14}C was oxidised to CO_2 (Fig. 3.5 B). Cells with active DLL4-NOTCH signalling had significantly higher ^{14}C-oxidation rates in 5 mM glucose or 10 mM lactate media, compared to the BSAc-stimulated control in the respective condition (Fig. 3.5 B). In 0.75 mM glucose, ^{14}C-OA oxidation rates showed the tendency to increase compared to normal glucose or lactate media and DLL4-NOTCH activation resulted in a tendency to increased FA oxidation rates compared to the BSAc control in low glucose. These results showed that cells with active DLL4-NOTCH signalling have consistently higher FA oxidation rates under varying glucose and lactate concentrations.

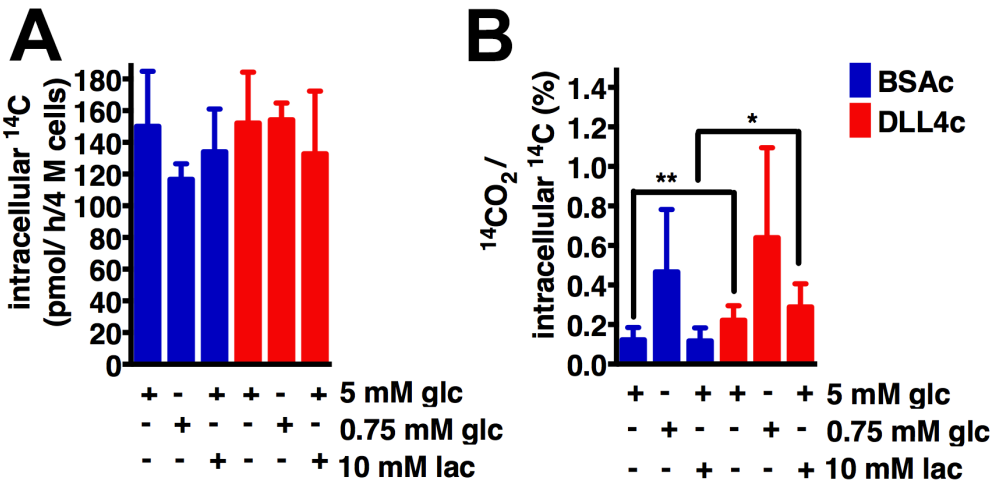


Figure 3.5 Metabolism of ^{14}C-oleic acid is increased by DLL4-NOTCH signalling. HUVEC were grown on BSA- or DLL4-coated (BSAc or DLL4c) dishes for 48 h, in media containing 5 mM glucose, 0.75 mM glucose, or 5 mM glucose and 10 mM lactate. ^{14}C-uptake (A) or oxidation assays (B) were performed in assay media containing 50 μM carnitine and 500 μM oleic acid conjugated to FA-free BSA, and 0.05 μCi/ml ^{14}C-oleic acid and the indicated substrate concentrations. Raw values were normalised to cell number. Values are expressed as mean +/- S.D., *p<0.05, **p<0.01. (n=5, One-way ANOVA, Holm-Sidak post-hoc test).

3.2.6 Accumulation of intracellular ^{14}C from exogenous ^{14}C-OA is increased by DLL4-NOTCH signalling

The data in the previous experiment suggested higher FA oxidation rates in cells with active DLL4-NOTCH signalling. Increased FA utilisation can lead to increased FA uptake (Mashek and Coleman 2006). Therefore, the accumulation of ^{14}C from ^{14}C-OA in HUVEC with activated DLL4-NOTCH signalling was investigated. HUVEC were grown on BSAc- or DLL4c for 16, 24 or 48 h to stimulate NOTCH signalling (time of NOTCH pre-stimulation). The cells were grown in normal glucose and then switched to assay media containing 50 μM carnitine, 500 μM OA conjugated to FA-free BSA, and 0.05 μCi/ml ^{14}C-OA. Stimulation of DLL4-NOTCH signalling led to a significant increase of intracellular ^{14}C levels at each time point (Fig. 3.6 A). Next, HUVEC were grown on BSAc or DLL4c plates for 24 h, with or without DBZ to inhibit NOTCH signalling, or DMSO as a vehicle control. DBZ treatment led to a significant decrease of intracellular ^{14}C levels in response to DLL4c, compared to BSAc (Fig. 3.6 B). These results showed that cells with DLL4-NOTCH activation and exposed to glucose-depleted media, have increased intracellular levels of ^{14}C derived from extracellular ^{14}C-OA. This indicates increased intracellular utilisation of FAs in HUVEC when DLL4-NOTCH signalling is active.

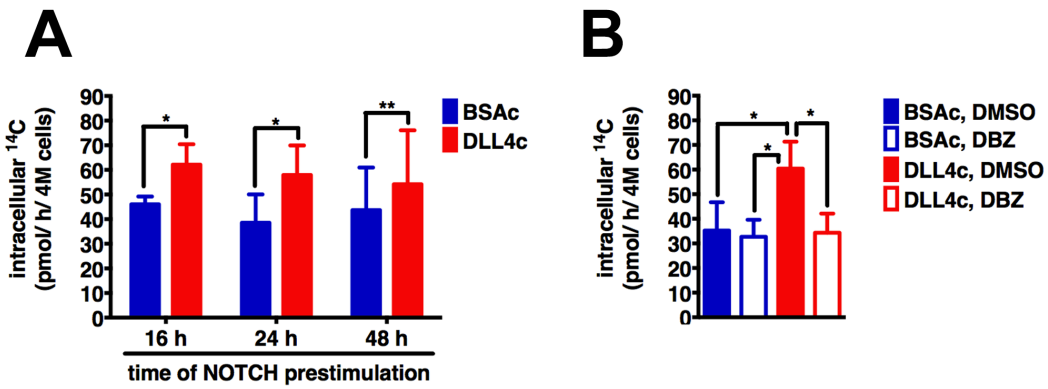


Figure 3.6 Accumulation of intracellular ^{14}C from exogenous ^{14}C-oleic acid is increased by DLL4-NOTCH signalling. HUVEC were grown on BSA- or DLL4-coated (BSAc or DLL4c) dishes for 16, 24 or 48 h, (A), or with or without dibenzazepine (DBZ) to inhibit NOTCH signalling or DMSO as a vehicle control for 24 h (B). ^{14}C-uptake assays were performed in assay media containing 50 μM carnitine and 500 μM oleic acid conjugated to FA-free BSA, and 0.05 μCi/ml ^{14}C-oleic acid. Raw values were normalised to cell number. Values are expressed as mean +/- S.D., *p<0.05, **p<0.01 (n=4, Two-way ANOVA (A), One-way ANOVA (B), Bonferroni post-hoc test).

3.2.7 DLL4-NOTCH signalling activation leads to an increase of lipid droplet accumulation

Since intracellular ^{14}C levels derived from ^{14}C-OA in the media were significantly increased by DLL4-NOTCH, but only a small fraction of 0.2-1% was oxidised, the ability of HUVEC to store FAs in the form of LD was investigated. The LD dye LD540 binds to non-polar lipids inside the cell and enables the measurement of intracellular LD quantitatively by FACS analysis. HUVEC were grown on BSAc or DLL4c for 48 h. The media was supplemented with OA-BSA, as a control to promote LD formation, or FA-free BSA (vehicle control). Cells were PFA-fixed, and LD were stained with LD540 and quantified by FACS (Fig. 3.7 A). Supplementation of OA led to a significant increase of LD formation in BSAc- or DLL4c-stimulated cells versus vehicle control (Fig. 3.7 A). There was a significant increase of LD540 signal intensity in cells with active DLL4-NOTCH signalling compared to BSAc, in media with vehicle control. Fluorescent microscopy showed that LD levels were very low in cells grown in media without OA. In media with OA, LD were visible and DLL4-NOTCH signalling led to a slight but noticeable increase of LD levels (Fig. 3.7 B lower panel). This indicated that DLL4-NOTCH upregulation led to increased lipid stores.

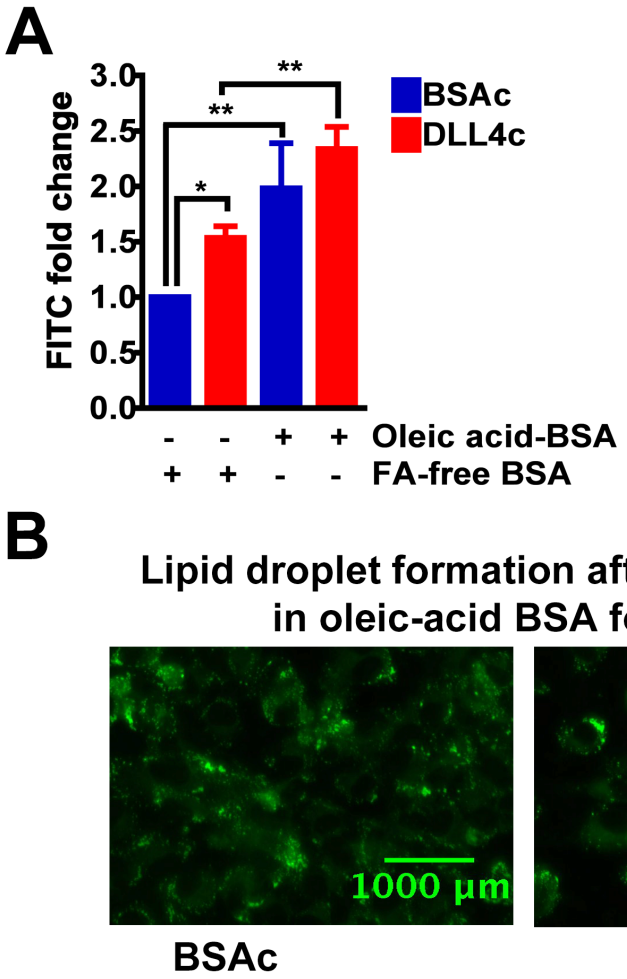


Figure 3.7 DLL4-NOTCH signalling activation leads to an increase of lipid droplet accumulation. HUVEC were grown on BSA- or DLL4-coated (BSAc or DLL4c) dishes for 48 h, with or without fatty acid (FA)-free BSA or BSA-conjugated oleic acid (Oleic acid-BSA). Cells were PFA-fixed and stained with LD50, and analysed by FACS (A) or fluorescent microscopy (B). Values are expressed as mean +/- S.D., *p<0.05, **p<0.01, ***p<0.001 (n=3, One-way ANOVA (A), Bonferroni post-hoc test)..

3.2.8 DLL4-NOTCH activation leads to upregulation of intracellular triglyceride stores

The previous experiment indicated higher levels of FA influx in cells with activated DLL4-NOTCH signalling. Next, intracellular TG stores in HUVEC were assessed by GC/MS analysis. HUVEC were grown on BSAc or DLL4c in normal glucose for 48 h, with or without DBZ to inhibit NOTCH signalling and subjected to GC/MS analysis to assess total TG levels and FA composition. The levels of most long chain FAs (more than 18 carbons) were below the detection level. FAs of 14-18 carbons did not show any significant change in response to DLL4-NOTCH signalling. Total TG however were significantly increased in HUVEC with activated DLL4-NOTCH signalling (Fig. 3.7 A). Furthermore, the desaturation index, indicating the activity of FA desaturases, and elongation index, indicating the activity of FA elongases were calculated. The desaturation indexes of palmitic acid (C16) or stearic acid (C18) were significantly reduced in response to DLL4-NOTCH signalling. The elongation index was not significantly changed (Fig. 3.7 B). Overall these results indicated that there was an increase of total TG in HUVEC with DLL4-NOTCH signalling and a slight decrease of desaturation of FAs.

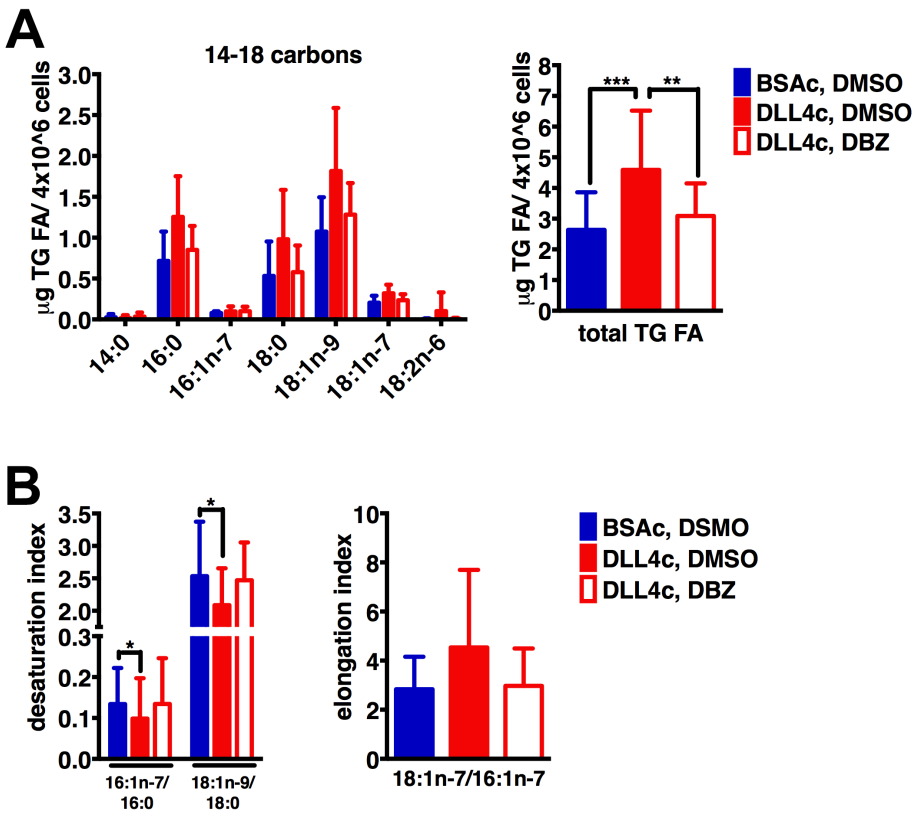


Figure 3.8 DLL4-NOTCH activation leads to upregulation of intracellular triglyceride stores. HUVEC were grown on BSA- or DLL4-coated (BSAc or DLL4c) dishes for 48 h with or without dibenzazepine (DBZ) to inhibit NOTCH cleavage or DMSO as a vehicle control. Cells were collected for GC analysis of triglyceride-associated fatty acids (TG FA), (A, left panel), and total triglycerides (TG), (A, right panel)). Desaturation or elongation indexes were calculated as indicated on the x-axis of the respective graphs (B). Values are expressed as mean +/- S.D., *p<0.05, **p<0.01, ***p<0.001 (n=5, One-way ANOVA, Bonferroni post-hoc test).

3.2.9 PL-FA composition does not change in response to DLL4-NOTCH activation

FAs can be incorporated into PL and contribute to membrane formation. Total levels of PL and a change in the saturation state of FAs in PL can impact on the total amount of membrane and membrane fluidity (higher when PL FA are less saturated). This can indirectly affect the ability of the cells to move and migrate. Since an increase in FA uptake and storage and a decreased desaturation index were observed, the levels of PL and the FA composition were investigated in the context of activated DLL4-NOTCH signalling and its inhibition by DBZ. HUVEC were grown on BSAc or DLL4c for 48 h and PL were analysed by GC/MS. The levels of FAs in PL did not show any significant changes in response to any treatment (Fig. 3.9 A). The levels of total PL were not changed in response to DLL4-NOTCH signalling (Fig. 3.9 B, upper left panel). Also, the percentages of saturated, monounsaturated, or polyunsaturated FAs relative to the total of PL FAs remained unchanged in response to any treatment (Fig. 3.9 B, upper right panel). Finally, the desaturation indexes were unchanged, whereas the elongation index was slightly, but significantly increased in response to the treatment (Fig. 3.9 B, lower panels). These results indicated that the DLL4-NOTCH signalling pathway does not play a major role in regulating the total levels or the FA composition of PL.

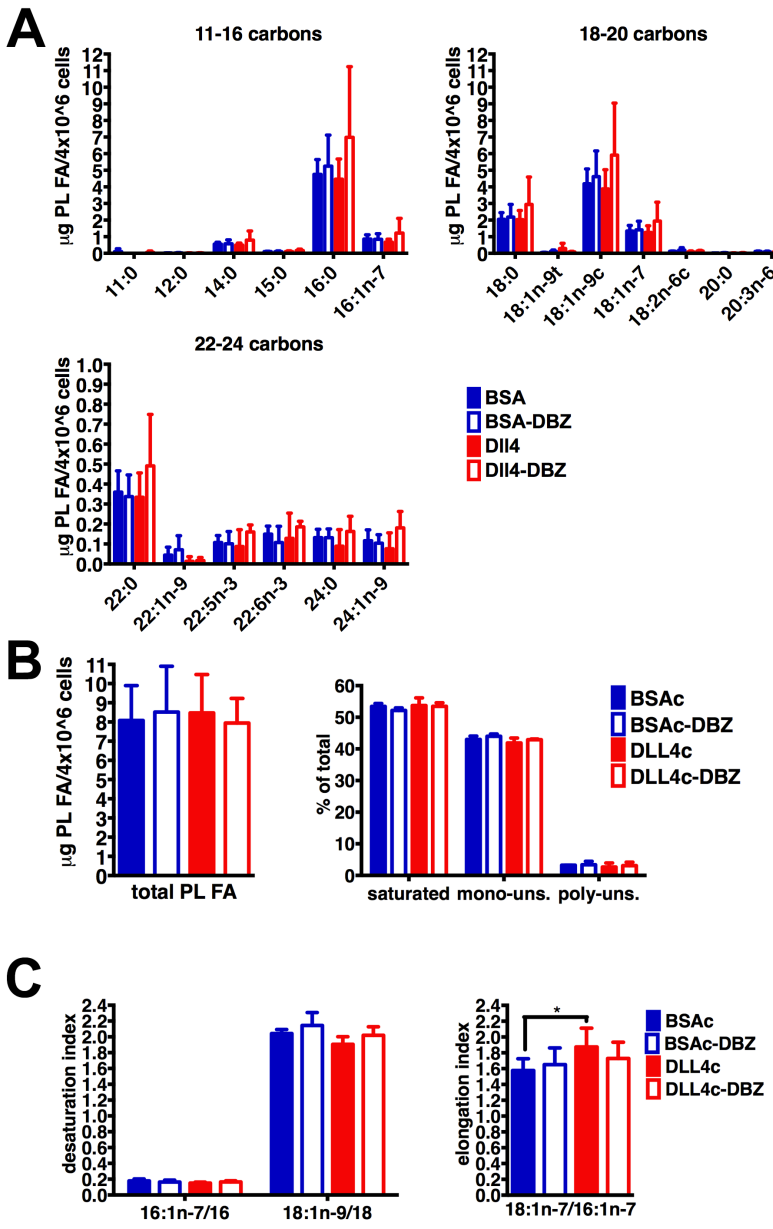


Figure 3.9 Phospholipid-fatty acid composition does not change in response to DLL4-NOTCH. HUVEC were grown on BSA- or DLL4-coated (BSAc or DLL4c) dishes for 48 h with or without dibenzazepine (DBZ) to inhibit NOTCH cleavage or DMSO as a vehicle control. Cells were collected for GC/MS analysis of phospholipid-associated fatty acids (PL FA), (A), and total PL (PL), (B, left panel). The percentages of unsaturated, mono-unsaturated, and polyunsaturated PL FA relative to total PL FA were calculated (A). Desaturation or elongation indexes were calculated as indicated on the x-axis of the respective graphs (B, right panel). Desaturation or elongation ratios were calculated (C). Values are expressed as mean +/- S.D., *p<0.05 (n=3, One-way ANOVA, Bonferroni post-hoc test).

3.2.10 Inhibition of FA oxidation by EX affects HUVEC proliferation but not migration

In the previous experiments, it was shown that DLL4-NOTCH increases FA influx, FA oxidation, and intracellular TG stores, without affecting the amount of PL produced. Therefore, it was hypothesised that intracellular lipid stores in HUVEC were used for energy production by FA oxidation during migration or proliferation of HUVEC, both of which are processes activated during angiogenic sprouting: sprout elongation occurs through proliferation of stalk cells, or migration/ elongation by tip and/or stalk cells.

Scratch wound and proliferation assays were performed with or without EX to inhibit FA oxidation to assess which of these processes are driven by FA oxidation. The scratch wound assay was used to measure migration of HUVEC, treated with or without EX at two concentrations. Additionally, the media was supplemented with OA-BSA or FA-free BSA to investigate if addition of OA leads to higher migratory abilities and if this was dependent on FA oxidation (Fig. 3.10 A). Media supplemented with OA-BSA led to increased migration and faster wound closure than in the untreated control. EX treatment did not reduce HUVEC migration at any concentration examined and did not reduce migration in OA-BSA supplemented media (Fig. 3.10 A). Proliferation was measured by using the CyQuant NF Cell Proliferation Assay, based on total cellular DNA. HUVEC were grown on BSAc or DLL4c over five days and treated with increasing concentrations of EX. EX in BSAc- or DLL4c-stimulated cells significantly reduced proliferation in a concentration-dependent manner. DLL4c-stimulated cells were not more sensitive to EX treatment in this experiment (Fig. 3.10 B). These results showed that OA-BSA increases migration of HUVEC. Inhibition of FA oxidation caused reduced HUVEC proliferation and no change in migration. Thus, FA oxidation is important for proliferation of HUVEC.

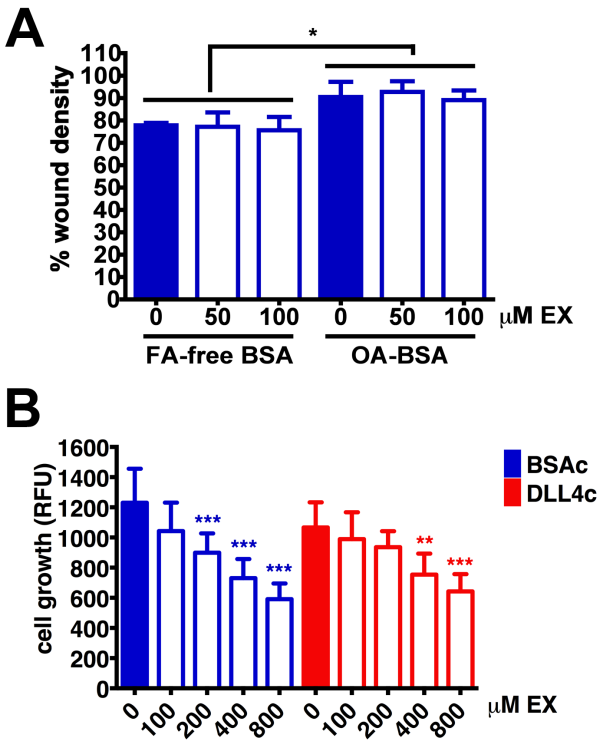


Figure 3.10 Inhibition of fatty acid oxidation by etomoxir does not affect HUVEC migration but does affect proliferation. HUVEC were grown to a confluent monolayer for 24 h. The media was changed to media with or without etomoxir (EX) to inhibit fatty acid oxidation, and DMSO as a vehicle control, and with fatty acid (FA)-free BSA or BSA-conjugated oleic acid (OA-BSA). The scratch wound assay was performed, and the percentage of wound density was determined, relative to the control at the time of confluence after 7-8 h (0 μM EX, FA-free BSA), (A). HUVEC were grown on BSA- or DLL4-coated (BSAc or DLL4c) dishes in media with varying concentrations of etomoxir (EX, 50 μM) to inhibit fatty acid oxidation, and DMSO as a vehicle control, for 96 h. Cell viability was determined by using the fluorescence-based CyQuant NF Cell Proliferation Assay (B). Values are expressed as mean +/- S.D., *p<0.05, **p<0.01, ***p<0.001 (n=3, One-way ANOVA, Bonferroni post-hoc test).

3.2.11 EX treatment depletes endothelial ATP levels at high concentrations

An increase in FA oxidation was observed in response to DLL4-NOTCH, which might contribute to ATP production and thus to proliferation and sprouting. Next, it was investigated whether ATP levels in BSAc- or DLL4c-stimulated HUVEC were sensitive to EX treatment. HUVEC were grown on BSAc or DLL4c over 5 days and treated with increasing concentrations of EX. ATP levels were determined after 5 days. EX treatment led to a dose-dependent decrease of cellular ATP levels. In BSAc- and DLL4c-stimulated cells, ATP levels were significantly decreased in cells treated with 200-400 μM EX (Fig. 3.11). There was no difference in EX sensitivity when BSAc was compared to DLL4c. These data showed that ATP levels were reduced by EX at high concentrations, which were 2 fold higher than the concentrations that showed an effect in the oxygen consumption and proliferation assays.

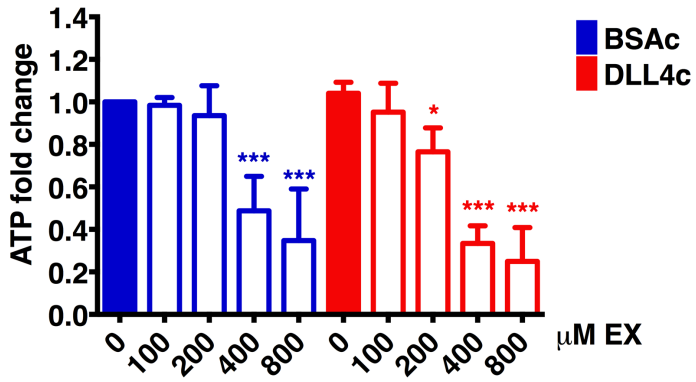


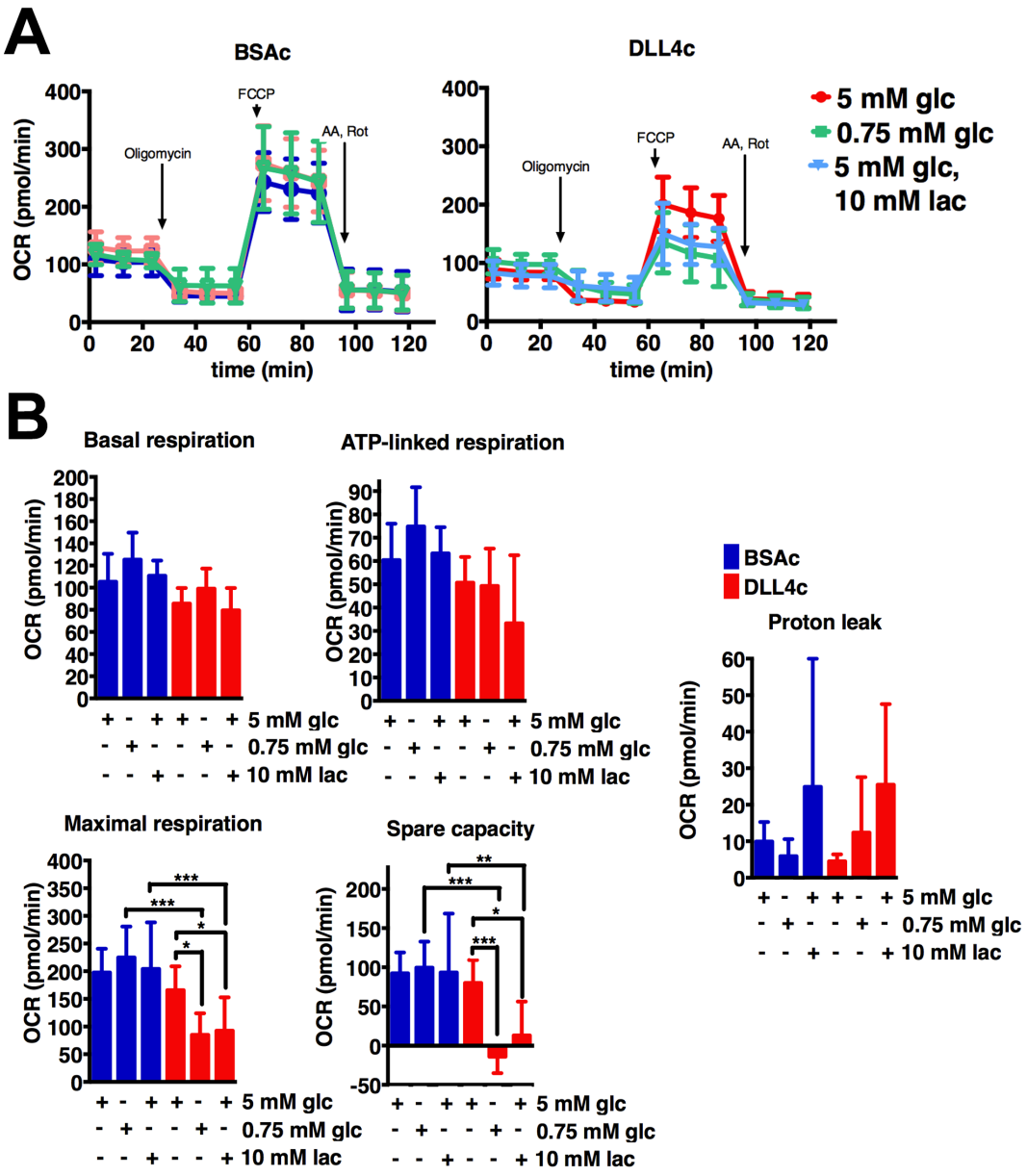
Figure 3.11 Etomoxir treatment depletes intracellular ATP levels at high concentrations. HUVEC were grown on BSA- or DLL4-coated (BSAc or DLL4c) dishes in media with varying concentrations of etomoxir (EX) to inhibit fatty acid oxidation, and DMSO as a vehicle control, for 96 h. ATP levels were determined by using the luminescence-based Cell-titerGlo assay. Raw values were normalised to cell growth. Values are expressed as mean +/- S.D., *p<0.05, **p<0.01, ***p<0.001 (n=3, One-way ANOVA, Bonferroni post-hoc test).

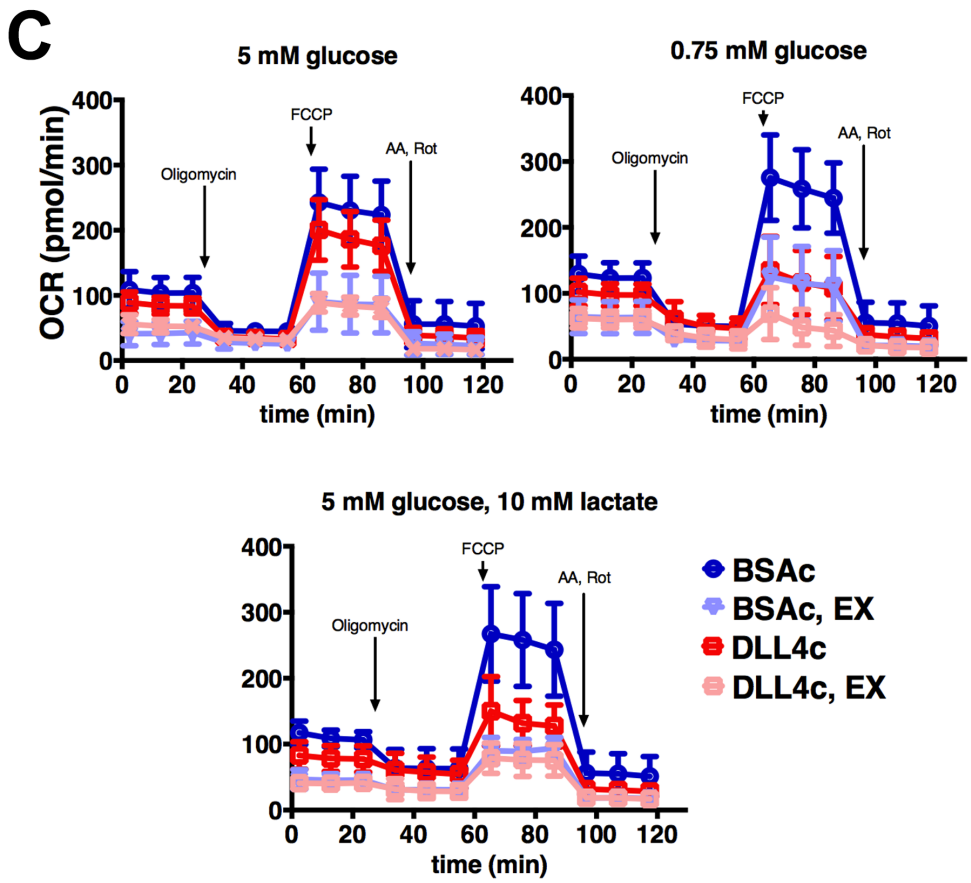
3.2.12 EX treatment affects mitochondrial respiration

EX inhibits FA oxidation and therefore depletes the cells of FA-derived acetyl-CoA that would enter the TCA cycle. The TCA cycle is crucial for mitochondrial respiration and metabolism. If FAs are major contributors to the TCA cycle, EX treatment will affect parameters of mitochondrial respiration measured in the MitoStress Test. To test this hypothesis, cells grown on BSAc or DLL4c in 5 mM glucose, 0.75 mM glucose, or 5 mM glucose and 10 mM lactate (because lactate concentration in the tumour microenvironment is high), were treated with or without 50 μM EX for 48 h and subjected to the MitoStress Test as described previously (Section 3.2.2).

First, mitochondrial stress parameters in the different media in BSAc- or DLL4c- stimulated cells were compared (Fig. 3.12 A). There were no significant changes in basal respiration or ATP-linked respiration in any of the conditions (Fig. 3.12 A, upper panels). Maximal respiration and spare capacity were significantly downregulated in DLL4c-stimulated cells in media with low glucose or lactate, compared to the respective condition in BSAc-stimulated cells or compared to DLL4c-stimulated cells in 5 mM glucose (Fig. 3.12 B, middle panels). The proton leak was not significantly changed in any of the conditions (Fig. 3.12 B, lower panel). Second, the mitochondrial stress parameters in EX treated cells in normal glucose, low glucose, or lactate media were compared to untreated cells. In BSAc-stimulated cells, EX treatment led to a significant 50% downregulation of basal respiration, ATP-linked respiration, maximal respiration, and spare capacity, in 5 mM glucose, 0.75 mM glucose, and 5 mM glucose, and 10 mM lactate media. In DLL4c-stimulated cells, EX treatment led to significant downregulation by 30-40% of basal respiration, in normal glucose, low glucose, and lactate media. ATP-linked respiration in DLL4c-stimulated cells showed a tendency to decrease in response to EX (not significant). Maximal respiration and spare capacity were significantly downregulated by EX in normal glucose media, but not in low glucose or lactate media. There were no significant changes of proton leak in any of the conditions.

These results indicated that cells with activated DLL4-NOTCH signalling grown in low glucose or lactate with no additional substrate were significantly impaired in their capacity to respond to mitochondrial stress, as maximal respiration and spare capacity were decreased. EX sensitised the cells to mitochondrial stress in normal glucose, low glucose, or lactate media, in BSAc- or DLL4c-stimulated cells, showing that mitochondrial FA import and the entrance of FA derived acetyl-CoA into the TCA cycle is crucial for mitochondrial function in cells with basal NOTCH or activated DLL4-NOTCH signalling.


A
BSAc
DLL4c
OCR (pmol/min)
time (min)
Oligomycin
FCCP
AA, Rot
5 mM glc
0.75 mM glc
5 mM glc,
10 mM lac
B
Basal respiration
ATP-linked respiration
Proton leak
Maximal respiration
Spare capacity
BSAc
DLL4c
5 mM glc
0.75 mM glc
10 mM lac


C
5 mM glucose
0.75 mM glucose
5 mM glucose, 10 mM lactate
OCR (pmol/min)
time (min)
Oligomycin
FCCP
AA, Rot
BSAc
BSAc, EX
DLL4c
DLL4c, EX

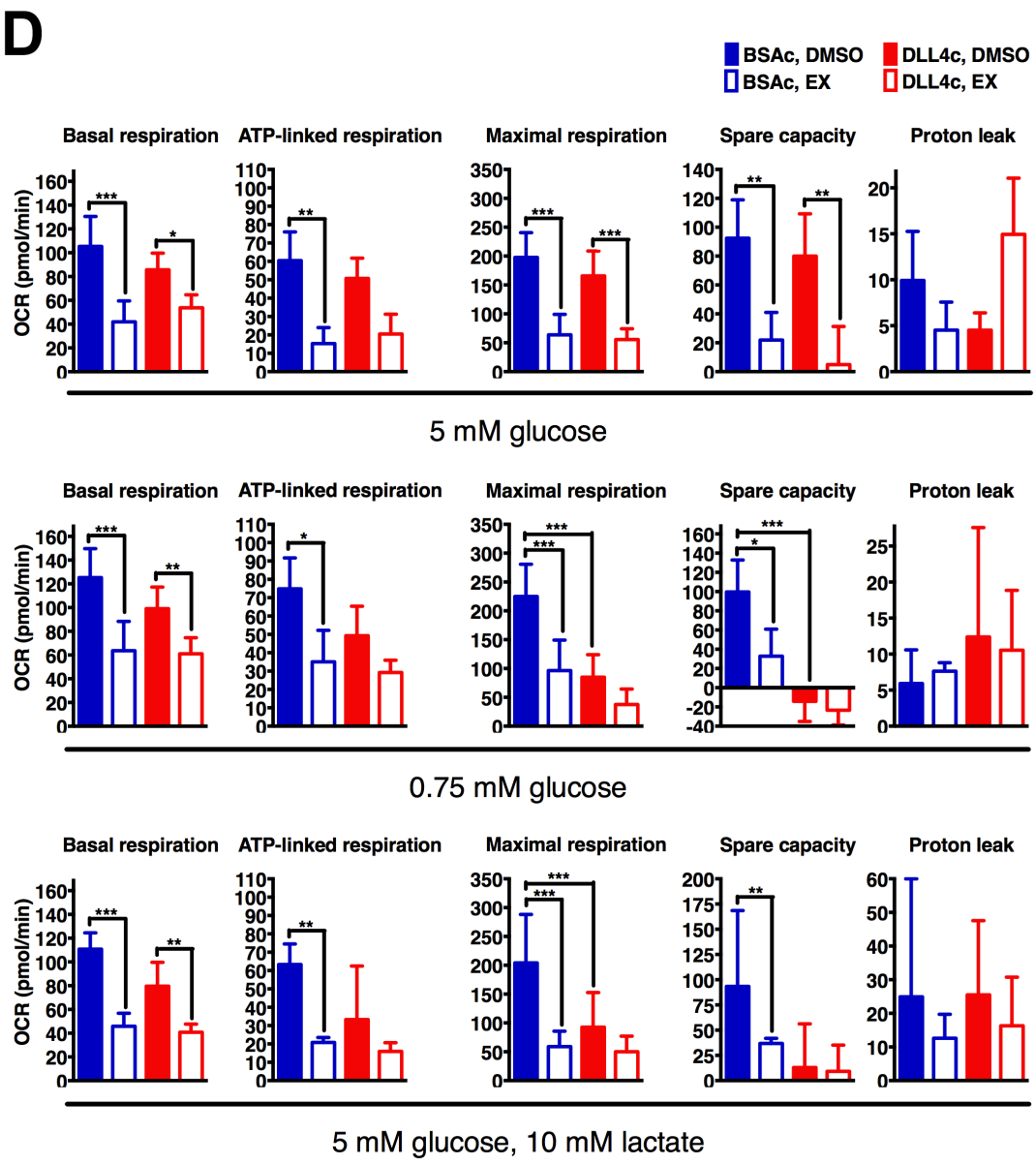


Figure 3.12 Etomoxir treatment affects mitochondrial respiration. HUVEC were grown on BSA- or DLL4-coated (BSAc or DLL4c) dishes in media with or without etomoxir (EX) to inhibit fatty acid oxidation, and DMSO as a vehicle control, for 48 h, in media containing 5 mM glucose, 0.75 mM glucose, or 5 mM glucose and 10 mM lactate. The cells were detached by exposure to trypsin, and reseeded on BSA- or DLL4-coated (BSAc or DLL4c) Seahorse plates at equal cell densities, and incubated overnight, in the respective media conditions. Oxygen consumption rates (OCR) were measured with the XFe Seahorse Bioanalyzer. The Mito Stress test was performed, in the respective media conditions, by sequential addition of oligomycin, FCCP, and antimycin A (AA) and rotenone (Rot), (A, C). The mitochondrial parameters basal respiration, ATP-linked respiration, maximal respiration, spare capacity and proton leak were assessed based on changes in OCR after inhibitor addition (B, D). Raw values were normalised to cell viability. Values are expressed as mean +/- S.D., *p<0.05, **p<0.01, ***p<0.001 (n=3, paired student's t test).

3.2.13 Lipid droplets in sprouting HUVEC

DLL4-NOTCH signalling activation limits angiogenic sprouting and promotes stalk cell formation. The process of angiogenic sprouting can be mimicked *in vitro* by using the sprouting assay. In this assay, HUVEC bud from an embedded, previously grown spheroid, migrate towards the angiogenic cue, and trailing cells would start proliferating and form a sprout.

Because of the previous findings showing a change in FA metabolism upon activation of DLL4-NOTCH, angiogenic sprouts grown in fibrin gel were stained with LD540 to visualise lipid droplets (LD) in sprouting HUVEC. The growth media was supplemented with OA-BSA to promote LD formation or FA-free BSA (vehicle control). Sprouts were grown in 5 mM glucose for 48 h, then fixed and stained with LD540. LD were present in the leading tip cells and trailing stalk cells (Fig. 3.13 A). LD were peri-nuclear or at the migrating front (indicated by red arrows in tip cells, yellow arrows in stalk cells). It was noted that HUVEC sprouts grown in OA-BSA supplemented media had an altered morphology. Quantification of sprout number and length showed that OA-BSA supplementation led to a significant increase in sprout length, but no change in sprout number (Fig. 3.13 B). These results showed that LD were present in HUVEC sprouts and that an increase of FA availability modifies sprout length morphology.

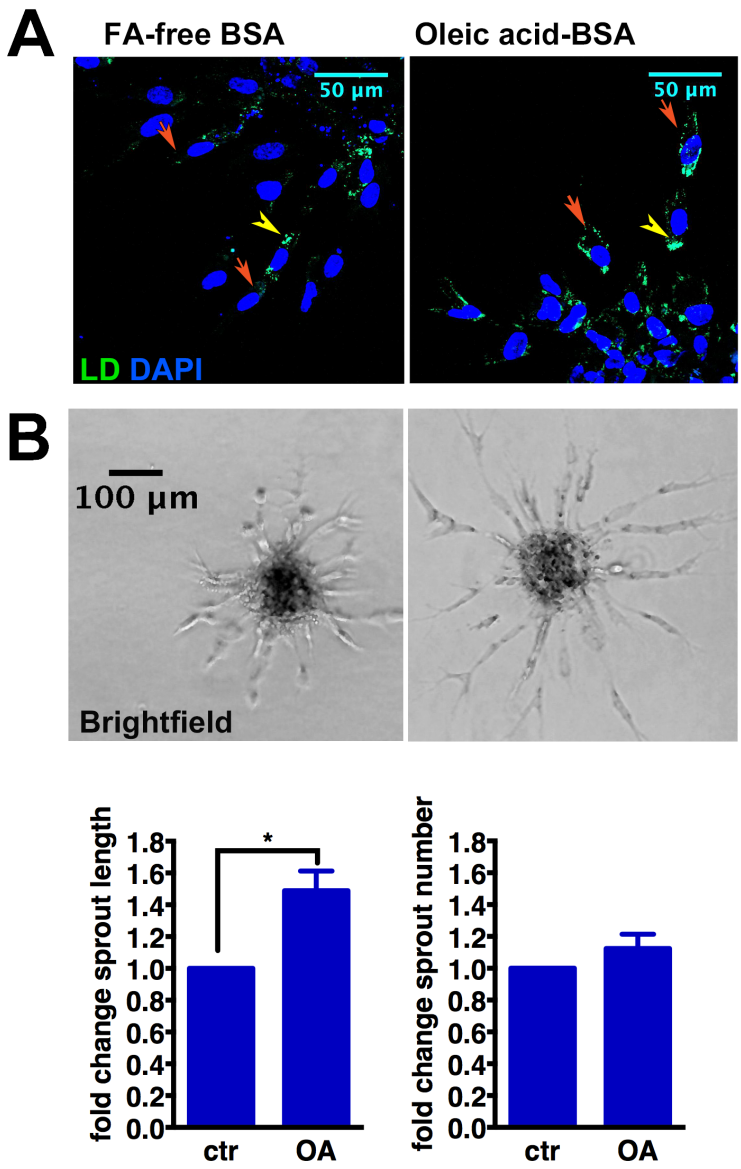


Figure 3.13 Lipid droplets in sprouting HUVEC. HUVEC spheroids were grown overnight and then embedded in fibrin gel and grown in media supplemented with fatty acid (FA)-free BSA (ctr) or BSA-conjugated oleic acid (OA-BSA, A; OA, B) for 48 h. Cells were PFA-fixed, and stained with LD540 and DAPI, and analysed by fluorescence microscopy (A), or analysed by brightfield microscopy and sprout number and length were quantified (B). Red arrows indicate lipid droplets (LD) in tip cells; yellow arrows indicate LD in stalk cells (A). Values are expressed as mean +/- S.D., *$p<0.05$ (n=3, paired t-test).

3.2.14 Sprouting angiogenesis is decreased by EX

Since DLL4-NOTCH signalling led to increased oxidation of FAs, the contribution of FA oxidation to sprouting of HUVEC was investigated. To promote stalk cell formation and limit tip cell formation during sprouting, the cells were pre-stimulated with DLL4c for 48 h before the assay. Spheroids were embedded in growth factor-reduced matrigel (composed of tumour-derived extracellular matrix) and grown in media with or without 50 μM EX. Moreover, because FA oxidation was increased in low glucose, the cells were incubated in 5 mM or 0.75 mM glucose during sprout formation.

Sprouts are shown in Fig. 3.14 A. Sprout number and length was quantified in the respective conditions (Fig. 3.14 B). There was no significant change of sprout number in any of the conditions. Pre-DLL4c treatment did not lead to significantly longer sprouts. Sprouts grown in low glucose were not significantly changed in length compared to normal glucose. Sprouts treated with EX were significantly shorter than control sprouts, in 5 mM or 0.75 mM glucose and in pre-BSAc or pre-DLL4c stimulated cells. These results showed that FA oxidation inhibition impaired angiogenic sprout formation by reducing sprout length.

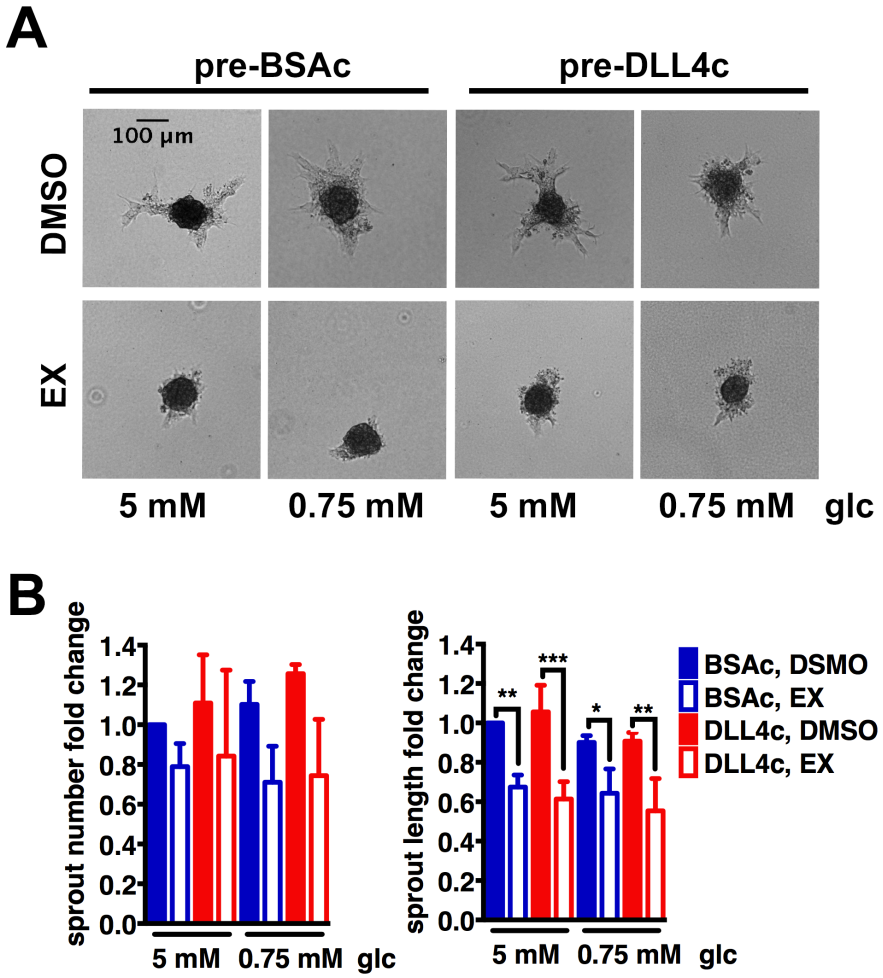


Figure 3.14 Sprouting angiogenesis is decreased by EX in growth factor-reduced matrigel. HUVEC were grown on BSA- or DLL4-coated (BSAc or DLL4c) dishes for 48 h, in media containing 5 mM or 0.75 mM glucose (glc), with or without etomoxir (50 µM, EX) to inhibit fatty acid oxidation, and DMSO as a vehicle control, for 48 h. The cells were detached by exposure to trypsin, grown as spheroids overnight and then embedded in matrigel and grown in the respective media containing 5 mM or 0.75 mM glc, and EX or DMSO for 48 h. Then the cells were analysed by brightfield microscopy and sprout number and length were quantified. Values are expressed as mean +/- S.D., *p<0.05, **p<0.01, ***p<0.001 (n=3, One-way ANOVA, Bonferroni post-hoc test).

3.2.15 Inhibition of FA oxidation in zebrafish affects vascular plexus formation

The zebrafish is a vertebrate model system to study blood vascular development, as underlying mechanisms of angiogenesis are very similar to those in humans. Angiogenic sprouting is recapitulated during the formation of ISVs, following the formation of the primitive vasculature by vasculogenesis. Intersegmental vessels are formed by sprouts that project dorsally from the dorsal aorta. The caudal vein plexus is a honeycomb-like network, formed by sprouts that project ventrally from the posterior axial vein. Sprout formation contributing to intersegmental vessel or caudal vein plexus development is regulated by distinct signalling programs. Intersegmental vessel development is governed by VEGFA signalling and limited by NOTCH, whereas caudal vein plexus development is governed by bone-morphogenic protein (BMP) signalling (Wiley, Kim *et al.* 2011).

In this experiment, a zebrafish model with green fluorescent protein (GFP)-tagged vasculature was used to identify the effect of FA oxidation inhibition on intersegmental vessel and caudal vein plexus formation. Tg(kdrl:GFP) transgenic embryos were treated with 0, 3, or 5 μM EX for 48 hpf (Fig. 3.15 A). Quantification is shown in Fig. 3.15 B. The CVP was reduced in 47% (46 out of 98) or 58% (42 out of 74) of the cases in zebrafish treated with 3 or 5 μM EX, respectively (Fig. 3.15 A, marked in red line). In zebrafish with reduced CVP, 95% (44 out of 46) or 85% (36 out of 42) had a reduced heart rate, and 13% (6 out of 46) or 24% (10 out of 42) had up to two intersegmental vessels missing, at 3 or 5 μM EX, respectively (Fig. 3.15 A, marked in red arrow). This showed that EX affected caudal vein plexus formation, heart rate and intersegmental vessel number in developing zebrafish.

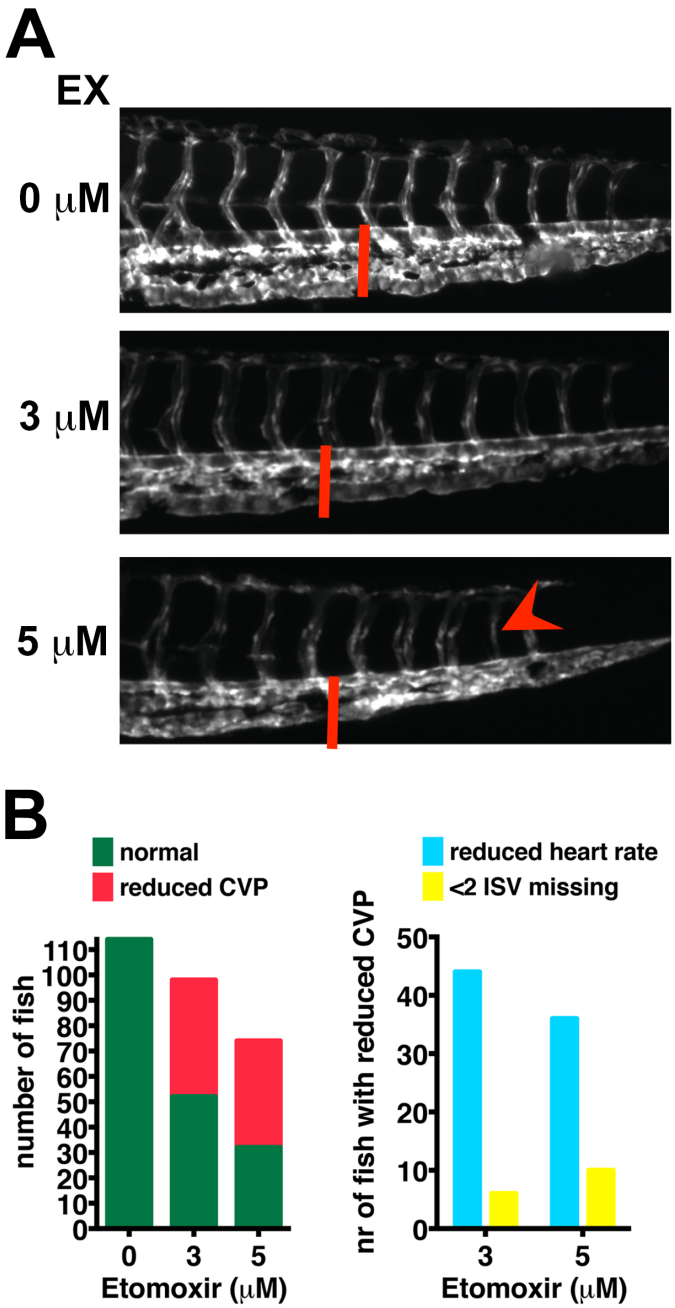


Figure 3.15 EX treatment affects caudal vein plexus (CVP) development and intersegmental vessel (ISV) number in zebrafish. Tg(kdrl:GFP) transgenic embryos were treated with 0, 3, or 5 μM etomoxir (EX) for 48 h post fertilization (hpf). Embryos were fixed and analysed by fluorescent microscopy (A, red line indicates the width of the caudal vein plexus (CVP) in untreated control, red arrow shows missing intersegmental vessels (ISV)).

3.3 Discussion

Taken together, this chapter showed that activation of DLL4-NOTCH signalling caused a decrease of glycolysis and mitochondrial respiration, but increased metabolism of extracellularly derived FAs (Fig. 3.16). HUVEC proliferation and sprouting, as well as zebrafish CVP formation and ISV number were decreased when FA oxidation was inhibited by EX. The results suggested that FA oxidation contributes to the angiogenic process and that DLL4-NOTCH signalling increases intracellular FA utilisation and promotes oxidation.

DLL4-NOTCH activation in endothelial cells led to decreased rates of glycolysis and downregulation of mitochondrial respiration when glucose was the limiting substrate. It has previously been demonstrated that glycolysis is a main driving force of tip cell formation, which can even override the limiting effects of NOTCH on sprout formation (De Bock, Georgiadou *et al.* 2013). Cells overexpressing PFKFB3, with higher glycolytic rates, were more likely to take on the tip cell position, even when NICD was overexpressed simultaneously. Our study is in line with already published data that DLL4 reduces glycolysis (De Bock, Georgiadou *et al.* 2013). Furthermore, in the present study it was observed that a key glycolytic gene, LDHA, was downregulated 0.5 fold by DLL4-NOTCH activation (see Appendix I Fig. 0.3). Therefore it is a possibility that the mechanism by which DLL4-NOTCH limits tip cell formation includes a reduction of glycolysis, which adds to the complex fine-tuning of angiogenic tip and stalk cell formation.

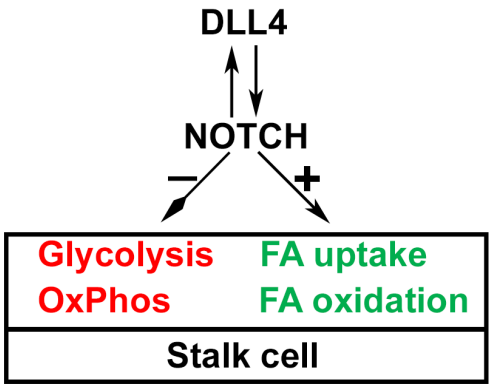


Figure 3.16 Schematic of effects of DLL4-NOTCH signalling on metabolism in endothelial stalk cells. DLL4 activates NOTCH signalling by receptor-ligand interaction, leading to induction of the stalk cell phenotype, and amplification of the signal by induction of DLL4. Effects on metabolism are reduction of glycolysis and oxidative phosphorylation (OxPhos, highlighted in red), and upregulation of uptake and oxidation of extracellular fatty acids (FA, highlighted in green). These changes in metabolism may contribute to the induction and maintenance of the stalk cell phenotype.

Part of this study investigated rates of oxygen consumption in cells incubated with OA-BSA or glutamine. OA-BSA incubation led to a significant increase of oxygen consumption arbitrary rate (OCAR) in cells with active DLL4-NOTCH that was downregulated by DBZ or/and EX, which directly links DLL4-NOTCH signalling to an increase of FA oxidation. Glutamine led to an increase of OCAR, which was sensitive to DBZ treatment and FA oxidation inhibition. Since glutamine can serve as a precursor for FA synthesis via conversion to α-ketoglutarate and reductive metabolism to acetyl-CoA in the cytoplasm, glutamine might have indirectly contributed to the intracellular FA pool (Metallo, Gameiro *et al.* 2012). Interestingly, DLL4-NOTCH activation led to upregulation of the gene expression of the glutamine transporter SLC1A4 (see Appendix I Fig. 0.3). The DLL4-NOTCH regulation of glutamine uptake and its channeling into FA oxidation might be another mechanism of the observed effects.

This study identified extracellular FAs as main substrates for HUVEC during sprouting, with influx regulated by DLL4-NOTCH. The uptake of FAs across the cell membrane can occur via specific transport proteins called FA binding proteins (FABP) or via rapid diffusion of FA across the membrane, promoted by an inwardly directed gradient (flip-flop) and dissociation from the membrane into the aqueous cytoplasm. The concentration of free FAs inside the cell is a main determinant of the rate of uptake. A change of the concentration gradient affects the influx of FAs. A block of FA activation by triacsin C and thus a block of FA utilisation decreases uptake of ^{14}C-OA, which is reversed by overexpressing a resistant Acyl-CoA synthetase, ACSL5 (reviewed by Mashek, McKenzie *et al.* 2006). Similarly, FABP may deliver non-esterified FAs (NEFA) from the site of influx or lipolysis to sites of activation inside the cell, thereby affecting the intracellular pool of NEFA. It has been shown previously that FA uptake rates in FABP1 -/- mice are decreased (Prows, Murphy *et al.* 1995). FAs in the cell that are bound to FABP or have been activated by ACSL do not contribute to the free FA

pool anymore. Therefore, increased FA utilisation can contribute to increased FA influx by depletion of the intracellular free FA pool (reviewed by Mashek, McKenzie *et al.* 2006).

In the experiments performed to determine oxidation of ^{14}C-OA and intracellular accumulation of ^{14}C derived from ^{14}C-OA, studies in a time frame of 3 h were performed. A small percentage of ^{14}C derived from ^{14}C-OA was detected in the form of CO_2 in 0.75 mM and 5 mM glucose conditions that was increased by DLL4-NOTCH activation. An increase of intracellular ^{14}C in response to DLL4-NOTCH activation was only observed in low glucose, when FA oxidation and mitochondrial respiration rates were higher compared to normal glucose. Intracellular ^{14}C represented any ^{14}C-label derived from ^{14}C-OA inside the cell and hence included ^{14}C in protein-bound form or downstream metabolites (FAs bound to FABP/ activated FAs/TG/FA oxidation products/TCA cycle intermediates). Activated FAs (Acyl-CoA) are metabolised by incorporation into PL, TG or by FA oxidation. For example, the mitochondrial import of Acyl-CoA for FA oxidation occurs via the mitochondrial transporter CPT1. CPT1 overexpression in myotubes leads to an increase of FA oxidation and an increase of FA uptake, without a change of cellular diacylglycerol or triacylglycerol levels, indicating that it is increased flux of Acyl-CoA through mitochondrial oxidation that leads to increased uptake of FAs (Perdomo, Commerford *et al.* 2004). Hence increasing metabolism of FAs and thereby decreasing the free FA pool in the cytoplasm can upregulate FA influx.

In this study, oxygen consumption as an indicator of mitochondrial respiration was significantly increased by DLL4-NOTCH activation when the cells were incubated in OA. The oxidation of ^{14}C-OA was increased in response to DLL4-NOTCH. However, the most part of ^{14}C-OA taken up by the cells was trapped intracellularly, since only 0.2-1% of total ^{14}C was detected in the form of CO_2. In cells cultured in normal glucose over a time of 48 h, we found that DLL4-NOTCH signalling caused an accumulation of LD and TG.

These observations led to the hypothesis that upregulation of DLL4-NOTCH signalling results in increased utilisation of FAs that is shifted to storage or degradation pathways in response to environmental cues, for example glucose availability. This hypothesis would be

strengthened by a metabolic flux analysis, to determine the metabolic destination of FA derived carbons in response to DLL4-NOTCH activation. However, the existence of the variable 'outputs' (increased ^{14}C accumulation, increased ^{14}C oxidation, increased TG levels) indicates that the DLL4-NOTCH regulatory 'input' might occur on the level of FA activation by ACSL or binding to FABP, that is then modulated by environmental cues.

Stromal cells that do not depend on glucose for growth and maintenance may be in an advantageous position in tumour tissue, where glucose concentrations fluctuate. Since FAs are readily available from the plasma and possibly from the surrounding tissues (for example hypoxic tumour cells that have lipid accumulation, or breast cancer or ovarian cancer metastasis that is adjacent to adipose tissue), the breakdown of FAs might represent an advantage to secure supply of metabolites for growth and proliferation, and vessel development.

This study showed that HUVEC sprouts had LD present in tip and stalk cells, which dynamically fused and changed position. FA oxidation significantly contributed to HUVEC proliferation and sprout elongation in matrigel, as investigated by treatment of the cells with EX.

The sprouting experiment in response to EX was also performed in fibrin gel instead of matrigel (see Appendix I Fig. 0.2). Here, EX treatment did not lead to a measurable decrease in sprouting. This may be due to the different composition of the matrices and the adhesion molecules present in these matrices. Fibrin gel is an inert matrix that does not contain any adhesion molecules. Therefore, the cells are not inhibited by increased adhesion and are more motile, leading to longer sprouts even when proliferation is inhibited. Growth factor-reduced matrigel contains a mix of adhesion molecules that resembles the extracellular matrix, leading to increased adhesion of the cells to the matrix and less motility.

EX inhibits Acyl-CoA translocation from the cytoplasm into mitochondria, where oxidation takes place. Upon mitochondrial import of Acyl-CoA, it is converted to Acetyl-CoA and injected into the TCA cycle. TCA cycle intermediates serve as precursor molecules for purins

and pyrimidines (DNA and RNA synthesis), porphyrin (heme production), and amino acids and are crucial for maintaining cell growth and proliferation (Berg, Tymoczko *et al.* 2002). EX treatment leads to increased levels of reactive oxygen species (ROS) by depleting NADPH levels and affecting energy charge (Pike, Smift *et al.* 2011). Since EX treatment affected ATP levels only to a minor extent and at higher concentrations, it is possible that the observed effects on sprouting and proliferation can be attributed to the lack of TCA cycle intermediates derived from Acyl-CoA. This is supported by the decrease of mitochondrial respiration parameters in response to EX in the present study. A lack of ATP might be counteracted by an increase of glycolysis; therefore masking decreased respiration-linked ATP production. Therefore, when glucose supply is limited or glucose-fuelled metabolic pathways like the TCA cycle are decreased by DLL4-NOTCH activation, an increase of FA oxidation may counteract a lack of TCA intermediate supply. This would help maintaining proliferation in the DLL4-NOTCH-governed stalk cell phenotype and promote sprout elongation (Fig. 3.17). Here, it is shown that NOTCH promotes a pro-proliferative metabolic pathway, inhibition of which reduces sprout length. Activation of glycolysis promotes the tip cell phenotype and is decreased by NOTCH. The results presented here indicate for the first time that activation of NOTCH signalling may maintain stalk cell proliferation by inducing FA oxidation as a biomass producing pathway and thereby weigh in on stalk cell over tip cell formation. Since NOTCH slows down endothelial cell proliferation, a signal, which during sprouting, is thought to be overturned by activation of the pro-proliferative WNT pathway (Phng, Potente *et al.* 2009), this pathway might play a role in promoting FA oxidation in the stalk cells further.

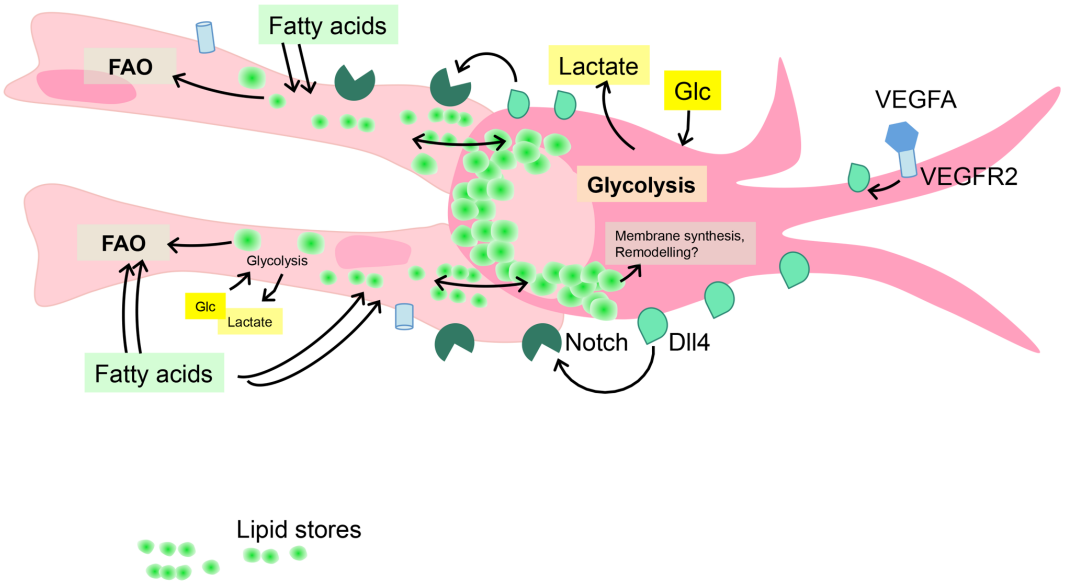


Figure 3.17 Model of DLL4-NOTCH effect on metabolism in sprouting endothelial cells. The tip cell phenotype is induced by vascular endothelial growth factor A (VEGFA) signalling transduction via VEGF receptor 2 (VEGFR2). The tip cell phenotype is driven by glycolysis and has therefore high glucose consumption and lactate secretion rates. Lipid droplet accumulation was observed mainly perinuclear, where triglycerides and phospholipids are produced at the endoplasmic reticulum. Fatty acids might be transported across membranes and enter the trailing stalk cells. VEGFA signalling induces DLL4 expression, leading to NOTCH signalling induction in adjacent cells, and stalk cell phenotype formation. This cell type is proliferative and depends on fatty acid oxidation (FAO). DLL4-NOTCH activation increases FA flux, and enables the production of fatty acid derived precursors for nucleotide and protein production. Fatty acids are derived extracellularly or might be imported transcellularly and partly stored in triglycerides. Reduction of the glycolytic rate in the stalk cell phenotype might be required for maintaining this phenotype.

In the zebrafish model, a defect in caudal vein plexus formation was observed in response to EX treatment. Intersegmental vessels were affected only in number and only in those embryos that showed defects in caudal vein plexus. Caudal vein plexus and intersegmental vessel formation represent distinct angiogenic signalling programs and are governed by Bmp (Bmp2) and Vegf-A signalling pathways, respectively (Wiley, Kim *et al.* 2011). Bmp signalling leads to activation of downstream effectors Smad1/5/8 and Erk. In bmp receptor type II morpholinos, *vegfa-A* or *dll4* levels were not or marginally affected. However, there is some evidence for BMP/NOTCH cross-signalling in endothelial cells, involving SMAD1/5, that orchestrates tip and stalk cell priming/ formation ((Moya, Umans *et al.* 2012); reviewed in (Beets, Huylebroeck *et al.* 2013)). Furthermore, metabolome studies in human pulmonary endothelium with dysfunctional *BMPR2* have shown suppression of carnitine and FA oxidation metabolites and genes, along with decreases in TCA cycle intermediates (Fessel, Hamid *et al.* 2012). The present findings support a functional role of FA oxidation in axial vein sprouting and are in line with a possible bmpr2-mediated regulation of this pathway during caudal vein plexus formation in zebrafish. The defects in caudal vein plexus formation might indirectly have affected proper intersegmental vessel formation.

Collectively, the work in this chapter shows that FA metabolism is a major contributor to the angiogenic process and is regulated by the DLL4-NOTCH signalling pathway. Glycolytic inhibition by DLL4-NOTCH might serve as an additional mechanism to limit tip and promote stalk cell formation. It suggests that FA oxidation is indirectly promoted by DLL4-NOTCH and is a DLL4-NOTCH-dependent metabolic pathway that promotes stalk cell proliferation during sprouting.

4 CHAPTER FOUR

The regulation of FABP4 by DLL4-NOTCH

*Significant portions of the results and text of this chapter have been published in Harjes, U., *et al.* (2014). "Fatty Acid-binding Protein 4, a Point of Convergence for Angiogenic and Metabolic Signalling Pathways in Endothelial Cells." J Biol Chem **289**(33): 23168-23176.

4.1 Introduction

The results in the previous chapter led to the hypothesis that increased intracellular utilisation of FAs was driving FA influx in response to DLL4-NOTCH signalling activation. DLL4-NOTCH binding induces intracellular proteolytic cleavages of the NOTCH receptor by ADAM10 and ADAM17 and by presenillin/γ-secretase. NICD is released and translocates to the nucleus to regulate gene transcription in a complex with other transcription factors such as the DNA binding and NOTCH responsive Recombination Signal Binding Protein For Immunoglobulin Kappa J Region (RBPJκ). Target genes are for example *DLL4*, *HEY1*, *HES1,* and *VEGFR2.*

DLL4-NOTCH might promote increased FA flux by regulation of gene expression. The rate of FA influx is mainly driven by FA import, intracellular FA activation, binding to cytosolic proteins, and intracellular metabolism (Fig. 4.1 for a summary). Candidate FA metabolism genes potentially involved in the metabolism effects in response to DLL4-NOTCH signalling are FA transporters, the members of the family of long-chain acyl-CoA synthetases (ACSL1-6), which activate FAs, the solute carrier family 27/FA transport proteins/family of very long chain acyl-CoA synthetases (SLC27A1-6/FATP1-6/ACSVL1-6), which activate and/or transport FAs, the family of FA binding proteins (FABP1-9), which bind and transport FAs, and genes involved in catabolic and anabolic FA metabolism pathways.

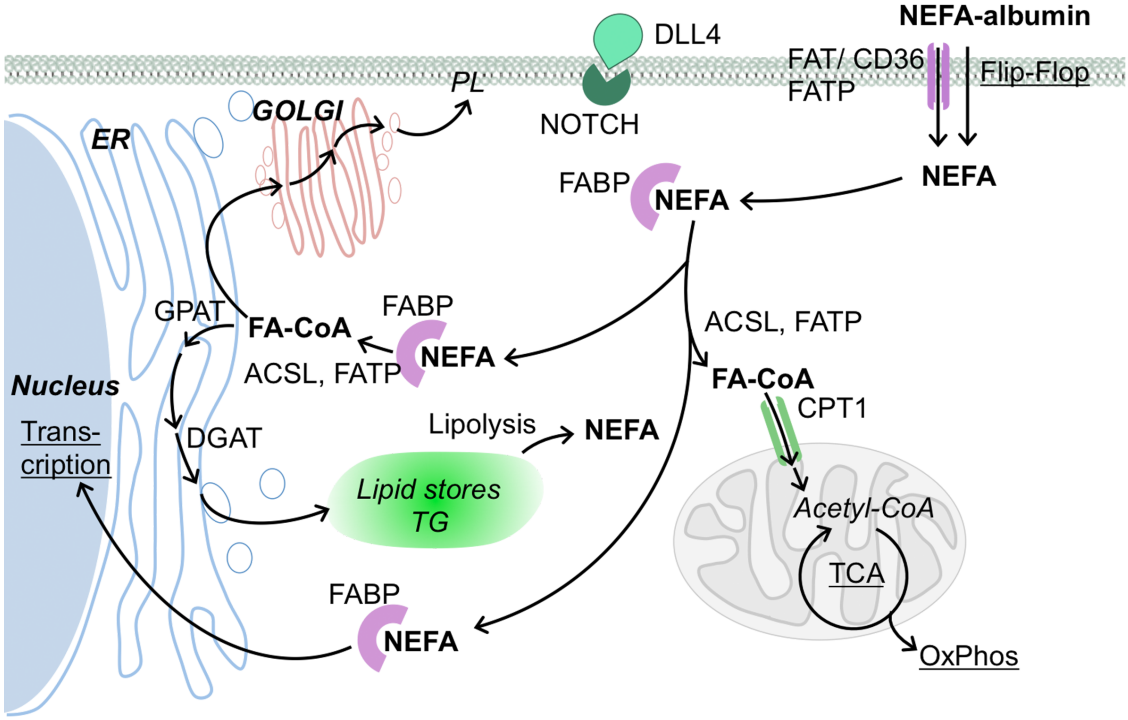


Figure 4.1 Mechanisms of fatty acid uptake and utilisation. The majority of non-esterified fatty acids (NEFA) in the plasma are bound to albumin. Uptake into the cell occurs via transport proteins, for example fatty acid (FA) translocase (FAT)/ cluster of differentiation 36 (CD36) or via the flip-flop mechanism. NEFA enter the cytoplasm and are delivered to sites of activation or utilisation by fatty acid binding proteins (FABP), where they are first activated by acyl-CoA synthetases (ACSL) or very long chain acyl-CoA synthetases/ fatty acid transport proteins (FAT) to form FA-CoA. FABPs bind NEFA and deliver them to the endoplasmic reticulum (ER) (blue layers) for production of phospholipids (PL) or triglycerides (TG), to the nucleus where FA can activate transcription factors and regulate gene transcription, or to the mitochondria. Glycerol-3-phosphate acyltransferases (GPAT) and Diglyceride acyltransferase (DGAT) are involved in PL and/ or TG synthesis. TG are stored in lipid droplets (green). Through lipolysis, NEFA can be released from lipid stores for further utilization. PL production involves the GOLGI apparatus (red layers) and transport to the membrane via vesicles. FA-CoA might also be destined for FA oxidation and be transported to the mitochondria. They enter mitochondria via carnitine palmitoyl transferase 1 (CPT1), undergo oxidation to acetyl-CoA and enter the TCA cycle, and eventually oxidative phosphorylation (OxPhos). Intracellular FA, TG stores, and FA oxidation were increased in cells with active DLL4-NOTCH signalling.

In the following chapter, the effect of DLL4-NOTCH activation on expression of a selection of FA metabolism genes was investigated. FABP4 was found to be significantly induced following DLL4-NOTCH activation. Since FABP4 has been reported to be a VEGFA target and pro-angiogenic (Elmasri, Karaaslan *et al.* 2009), it was then focused on elucidating the mechanism of FABP4 induction in HUVEC in response to VEGFA or DLL4-NOTCH stimulation. This was done by using gene and protein expression analysis, as well as DNA-protein interaction analysis in response to inhibitor treatment or RNA interference.

4.2 Results

4.2.1 DLL4-NOTCH signalling regulates FABP4

The expression of genes involved in FA metabolism pathways was investigated in HUVEC grown on BSAc or DLL4c for 16 h. Genes investigated were long-chain acyl-CoA synthetases (ACSL1-6), which convert free long-chain FAs into Acyl-CoA esters, members of the solute carrier family 27 (*SLC27A1-6*), involved in FA uptake, transport, and activation, FA binding protein isoforms (*FABP1-9*), involved in FA uptake and intracellular distribution, ATP citrate lyase (*ACLY*), which catalyse the synthesis of cytosolic acetyl-CoA, FA translocase (*FAT/CD36*), involved in import of FAs, carnitine palmitoyltransferase 1 isoforms (*CPT1A-C*), which regulate mitochondrial FA import, acetyl-CoA carboxylase α and β (*ACACA*, *ACACB*), which catalyse the carboxylation of acetyl-CoA to malonyl-CoA, thereby inhibiting mitochondrial FA import and promoting synthesis, and FA synthase (*FASN*) (Fig. 4.2 A). *ACSL1,3,4,5* expression was not significantly changed in DLL4c-treated HUVEC. *ACSL6* was expressed at very low levels and not significantly changed (labeled with §). *SLC27A1-6* expression was not significantly changed. *FABP1*, *FABP2*, and *FABP8* were expressed at very low levels or not detected after 16 h (labeled with §). *FABP4* was significantly upregulated 2-8 fold in DLL4c-treated HUVEC compared to BSAc after 16 h. *FABP3*, *FABP5*, *FABP6*, *FABP7* or *FABP9*, *ACLY*, *CD36*, or *CPT1A-C* expression, and *ACACA*, *ACACB*, or *FASN* expression were not significantly changed in DLL4c-treated HUVEC compared to BSAc at 16 h. These results showed that DLL4-NOTCH activation did not lead to significant changes of several FA metabolism genes under the investigated conditions. The only gene significantly induced in DLL4c-treated HUVEC was *FABP4*.

In accordance with this, preliminary analysis of mRNA expression arrays of immortalised human endothelial microvascular endothelial cells overexpressing DLL4 showed a 1.6-fold upregulation of *FABP4*. Therefore, FABP4 mRNA and protein expression were investigated in HUVEC grown on BSAc or DLL4c for 16, 24, or 48 h. *FABP4* mRNA expression was

significantly induced by DLL4c stimulation after 16 h (Fig. 4.2 B). FABP4 protein expression was significantly induced after 48 h (Fig. 4.2 C, band densitometry analysis in Fig. 4.2 D).

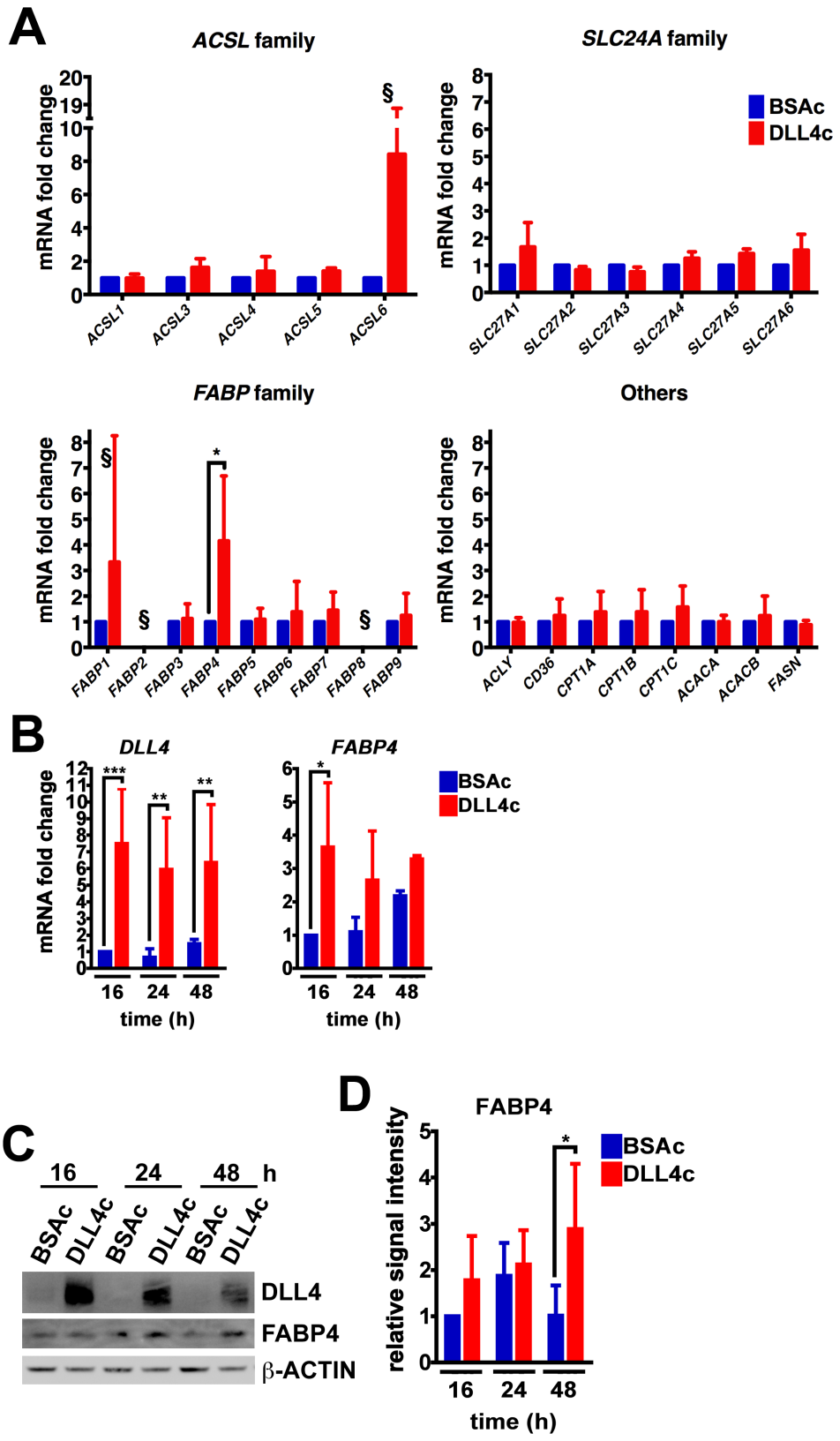


Figure 4.2 DLL4-NOTCH signalling regulates fatty acid binding protein 4 (FABP4). HUVEC were grown on BSA- or DLL4-coated (BSAc or DLL4c) dishes for the indicated time points. Cells were harvested and analysed for mRNA expression of fatty acid metabolism genes (A), *DLL4* and *FABP4* (B) or protein expression of DLL4 and FABP4 (C),

and band densitometry analysis of FABP4 expression relative to the loading control in three independent experiments was performed (D). mRNA expressed at very low levels or not detected after 16 h is labeled with § (A). Values are expressed as mean +/- S.D., *$p<0.05$, **$p<0.01$, ***$p<0.001$ (A, B, D). (n=3, One-way ANOVA (A), Two-way ANOVA (B, D), Bonferroni post-hoc test). β-ACTIN was used as a loading control (C).

4.2.2 FABP4 expression in response to DLL4-NOTCH is downregulated by γ-secretase inhibition and oxygen deprivation

FABP4 was previously shown to be regulated by VEGFA and to promote angiogenesis (Elmasri, Karaaslan *et al.* 2009). Since oxygen deprivation strongly induces VEGFA signalling and angiogenesis, FABP4 expression was assessed in HUVEC at 21%, 1% or 0.1% oxygen. Additionally, to assess NOTCH-dependent regulation, HUVEC were grown on BSAc or DLL4c and treated with the γ-secretase inhibitor DBZ. Protein expression of DLL4, and FABP4 are shown in Fig. 4.3 A. Band densitometry analysis of FABP4 relative to the loading control is shown in Fig. 4.3 B. DLL4-NOTCH signalling in HUVEC stimulated with DLL4c upregulated FABP4 at 21%, and 1% oxygen. FABP4 in response to DLL4-NOTCH signalling was reduced at 1% oxygen, and further reduced at 0.1% oxygen, compared to 21% oxygen (Fig. 4.3 A and B). DBZ reduced FABP4 induction in response to DLL4-NOTCH at 21% and 1%, indicating a DLL4-NOTCH-dependent regulation of FABP4 in normoxic and hypoxic conditions (Fig. 4.3 A and B).

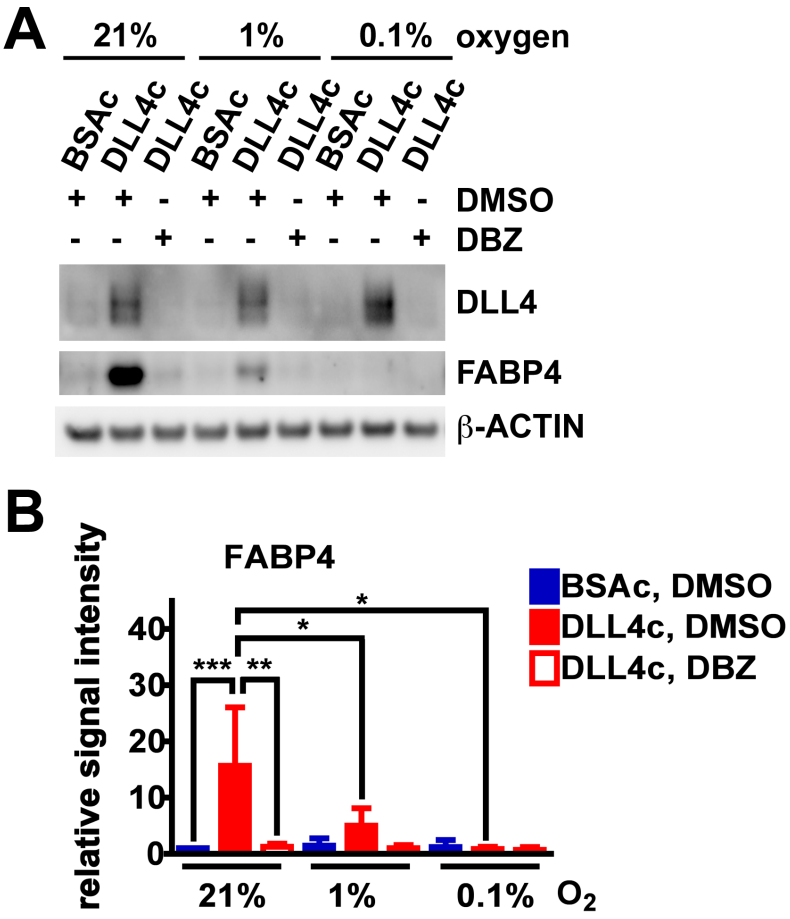


Figure 4.3 Fatty acid binding protein 4 (FABP4) in response to DLL4-NOTCH is downregulated by γ-secretase inhibition and by oxygen deprivation. HUVEC were grown on BSA- or DLL4-coated (BSAc or DLL4c) dishes in 21% oxygen, 1% oxygen, or 0.1% oxygen. Cells were treated with dibenzazepine (DBZ, 10 nM) to inhibit NOTCH cleavage or vehicle control (DMSO). Cells were harvested and analysed for protein expression of DLL4 and FABP4 (A), and band densitometry analysis of FABP4 protein expression relative to the loading control in three independent experiments was performed (B). β-ACTIN was used as a loading control. Values are expressed as mean +/- S.D., *p<0.05, ***p<0.001 (B) (n=3, One-way ANOVA, Bonferroni post-hoc test).

4.2.3 FABP4 expression does not follow peroxisome proliferator-activated receptor expression in hypoxia

FABP4 is a target gene of the peroxisome proliferator-activated receptor gamma (PPARγ) pathway, which has been indicated to be responsible for DLL4-NOTCH-mediated induction of FABP4 (Abstract A11257, Circulation Research 2012). There are studies showing that PPARγ is regulated in hypoxia, but it is cell type-dependent. In HepG2 cells, PPARγ is induced in hypoxia, whereas in glioblastoma, PPARγ is downregulated in hypoxia (Galzio, Cristiano *et al.* 2012, Zhao, Liu *et al.* 2014). There are three PPAR isoforms, all of which are implicated in lipid metabolism regulation. Therefore, the gene expression of *PPARγ*, the isoforms *PPARα* and *PPARδ*, and PPARγ co-activator or target genes were investigated in HUVEC grown on BSAc or DLL4c, treated with a DLL4 blocking antibody (anti-DLL4) to inhibit DLL4-NOTCH signal transduction, and exposed to 21% oxygen (normoxia) or 0.1% oxygen (hypoxia). Gene expression of *DLL4, VEGFA*, *PPARα*, *PPARγ*, *PPARδ*, *FABP4*, peroxisome proliferator-activated receptor gamma co-activator 1 α (*PPARGC1A,* PGC1-α), Glycosylphosphatidylinositol anchored high density lipoprotein binding protein 1 (*GPIHBP1*), perilipin (*PLIN*), and endothelial lipase (*LIPG*) were investigated (Fig. 4.4). *DLL4* was significantly induced by DLL4c and reduced by anti-DLL4 in normoxia and hypoxia. *VEGFA* was significantly induced in hypoxia and not changed in response to DLL4c or anti-DLL4 treatment. *PPARα* was not significantly changed in any of the conditions. *PPARγ* was significantly upregulated by 10 fold in hypoxia compared to normoxia and was significantly upregulated by 10 fold in DLL4c in hypoxia compared to BSAc in hypoxia, which was reduced by anti-DLL4 treatment. *PPARδ* was not significantly changed in any of the conditions. *FABP4* was significantly upregulated in DLL4c in normoxia, which was reversed by anti-DLL4 treatment. *FABP4* was significantly downregulated in hypoxia compared to normoxia in DLL4c-treated HUVEC. *PPARGC1A, GPIHBP1*, *PLIN*, or *LIPG* did not show significant changes in any of the conditions. These results showed that the induction of *FABP4* in response to DLL4c was not following the same pattern as *PPARγ* or

other PPAR family members and target genes and rather showed an inverse pattern in regards to hypoxic expression of *PPARγ*. Furthermore, *FABP4* induction was dependent on DLL4-NOTCH signalling initiation and modulated by hypoxia.

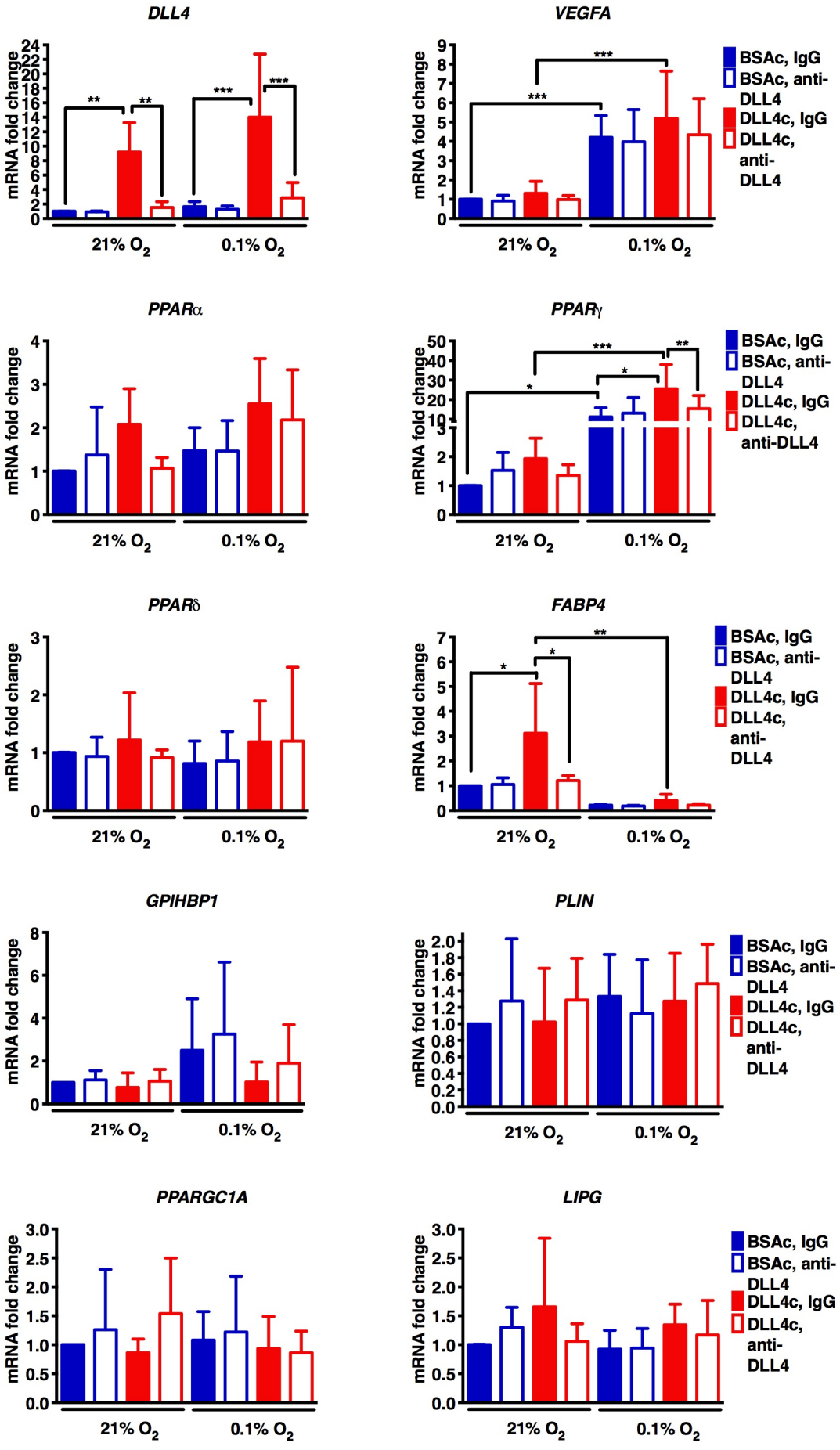

DLL4
VEGFA
PPARα
PPARγ
PPARδ
FABP4
GPIHBP1
PLIN
PPARGC1A
LIPG
mRNA fold change
21% O2
0.1% O2
BSAc, IgG
BSAc, anti-DLL4
DLL4c, IgG
DLL4c, anti-DLL4

Figure 4.4 Fatty acid binding protein 4 (FABP4) expression does not follow peroxisome proliferator-activated receptor (PPAR) expression in hypoxia. HUVEC were grown on BSA- or DLL4-coated (BSAc or DLL4c) dishes in 21% oxygen (normoxia), or 0.1% oxygen (hypoxia) for 48 h, and treated with a DLL4 blocking antibody (anti-DLL4) or IgG control. Cells were harvested and analysed for mRNA expression of the indicated genes. Values are expressed as mean +/- S.D., *p<0.05, **p<0.01, ***p<0.001 (n=3, One-way ANOVA, Bonferroni post-hoc test).

4.2.4 FABP4 expression in hypoxia is dependent on HIF-1α

Next, the mechanism of hypoxic FABP4 downregulation was investigated. HIF1-α and HIF2-α are transcription factors that, under normoxic conditions, are subject to hydroxylation by prolyl-hydroxylases, ubiquitination, and degradation via the proteasome. Under hypoxic conditions, prolyl-hydroxylases are inactive and HIF1-α and HIF2-α expression is stabilised. This leads to activation of target gene transcription and induction of the hypoxic response including upregulation of VEGFA, LDHA, carbonic anhydrase 9 or adenylate kinase 4, and subsequent phenotypic changes that enable the cells to survive in hypoxia and induce angiogenesis in surrounding tissue (Harris 2002).

The regulation of *FABP4* and *PPARγ* by HIF1-α and HIF2-α was investigated. HUVEC were transfected with siRNA targeting *HIF1-α* or *HIF2-α* and grown for 48 h (Fig. 4.5). *HIF1-α* mRNA and *HIF2-α* mRNA were significantly downregulated by the respective siRNAs. *FABP4* mRNA was significantly downregulated in hypoxia compared to normoxia. *HIF1-α* knockdown led to a significant upregulation of *FABP4* by 6 fold compared to the control in hypoxia. *HIF2-α* knockdown did not lead to a change of *FABP4* expression. *PPARγ* mRNA was significantly upregulated in hypoxia compared to normoxia. *HIF1-α* knockdown did not lead to a change of *PPARγ* expression. *HIF2-α* knockdown led to a significant downregulation of *PPARγ* mRNA.

Overall, these results indicated that *FABP4* was regulated in hypoxia by a HIF1-α dependent mechanism, whereas *PPARγ* was regulated by a HIF2-α dependent mechanism in HUVEC.

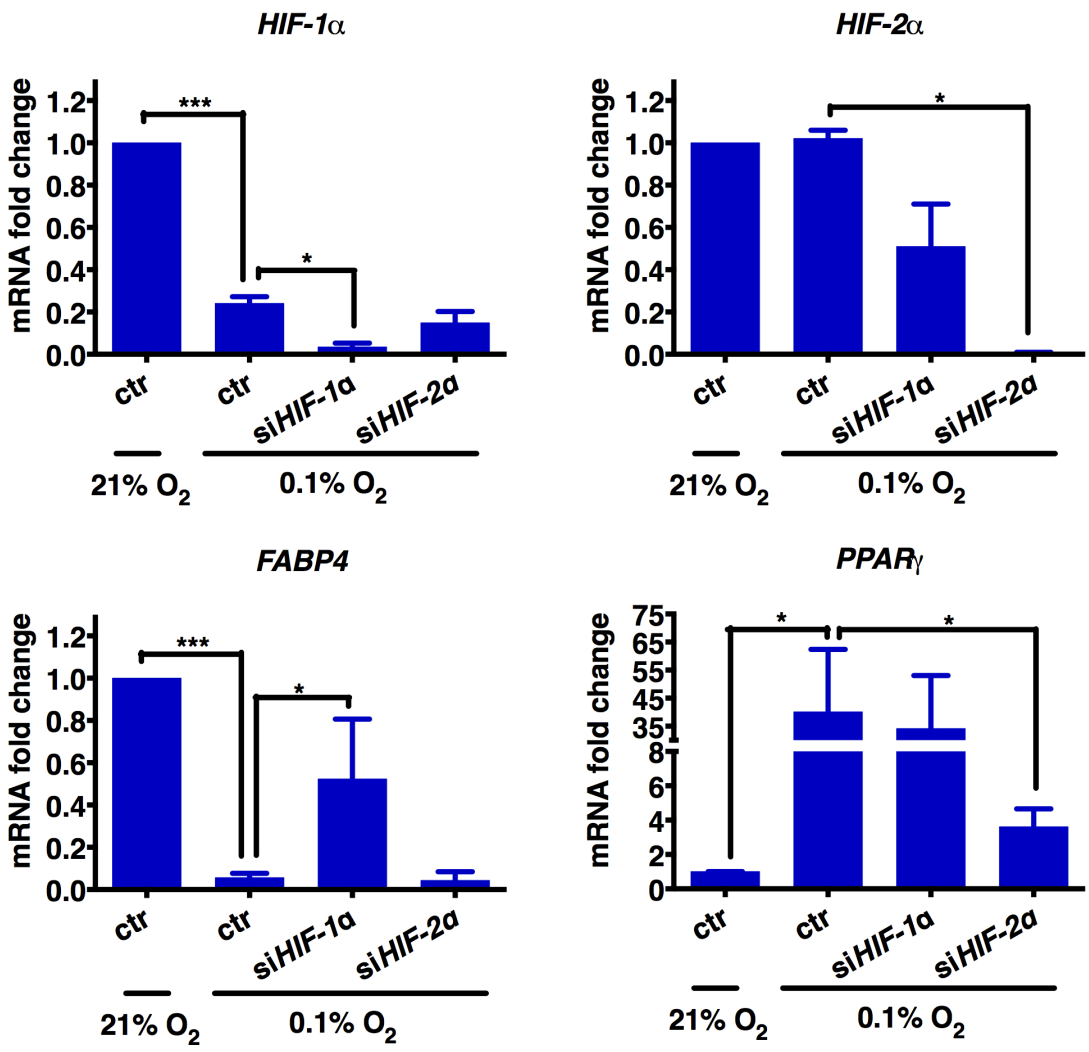


Figure 4.5 Fatty acid binding protein 4 (FABP4) expression in hypoxia is dependent on hypoxia-inducible factor 1 alpha (*HIF-1α*). HUVEC were transfected with siRNA targeting *HIF-1α* (si*HIF-1α*) or non-targeting siRNA (control=ctr) and grown on BSA- or DLL4-coated (BSAc or DLL4c) dishes in 21% oxygen (normoxia), or 0.1% oxygen (hypoxia) for 48 h. Cells were harvested and analysed for mRNA expression of the indicated genes. Values are expressed as mean +/- S.D., *p<0.05, ***p<0.001 (n=3, One-way ANOVA, Bonferroni post-hoc test).

4.2.5 Inhibition of DLL4-NOTCH binding by a DLL4 blocking antibody reduces FABP4 induction by VEGFA

Next, the contribution of DLL4-NOTCH signalling to normoxic FABP4 induction in response to VEGFA was assessed. To investigate the requirement of DLL4 binding to NOTCH as the first step of NOTCH signal transduction, HUVEC were treated with anti-DLL4 to prevent DLL4 from binding to the NOTCH receptor, in the presence of VEGFA or BSA. *DLL4* and *FABP4* mRNA induction in response to VEGFA was significantly downregulated by treatment with anti-DLL4 (Fig. 4.6).

These results indicated that induction of NOTCH signalling in response to VEGFA was dependent on DLL4-NOTCH binding and signal transduction and that FABP4 induction in response to VEGFA was dependent on the initial step of NOTCH pathway activation.

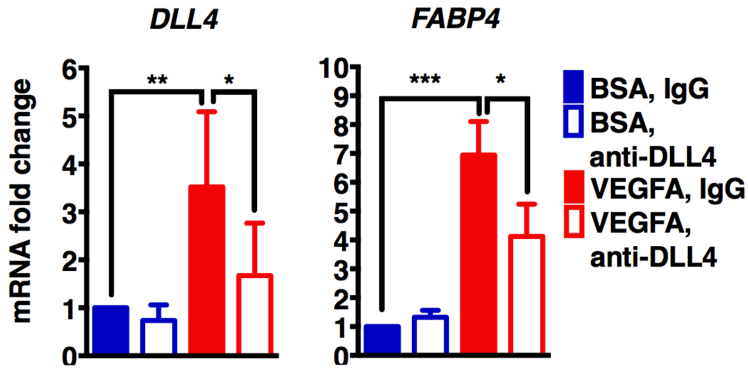


Figure 4.6 Inhibition of DLL4-NOTCH binding by a DLL4 blocking antibody reduces fatty acid binding protein 4 (FABP4) induction by VEGFA. HUVEC were growth factor-starved and stimulated with BSA or VEGFA (50 ng/ml) and treated with DLL4 blocking antibody (anti-DLL4) or IgG control. Cells were harvested and analysed for mRNA expression of *DLL4* and *FABP4*. Values are expressed as mean +/- S.D., *p<0.05, **p<0.01, ***p<0.001 (n=3, One-way ANOVA, Bonferroni post-hoc test).

4.2.6 VEGFA induced FABP4 is downregulated by γ-secretase inhibition.

The previous results indicated that FABP4 in response to VEGFA was dependent on the interaction between DLL4 and NOTCH. Next, VEGFA-stimulated HUVEC were treated with DBZ to inhibit NOTCH cleavage, the next step during NOTCH signal transduction. Canonical NOTCH target gene expression was investigated to control for selectivity of NOTCH signal transduction inhibition. FABP4 protein and mRNA were upregulated by VEGFA. This upregulation was significantly reduced by DBZ treatment, indicating that VEGFA-mediated FABP4 induction was through activation of DLL4-NOTCH signalling (Fig. 4.7 A and B). DLL4 protein expression in response to VEGFA was downregulated by DBZ (Fig. 4.7 B) and VEGFA-mediated upregulation of *DLL4* and *HEY1* mRNA was sensitive to DBZ treatment (Fig. 4.7 C). The previously reported DLL4-NOTCH target *PPARγ*, an inducer of *FABP4*, was not significantly upregulated by VEGFA (Fig. 4.7 C). Taken together, VEGFA led to DBZ sensitive induction of canonical NOTCH targets and FABP4 mRNA and protein, indicating that FABP4 expression was dependent on NOTCH cleavage by γ-secretase and further signal transduction.

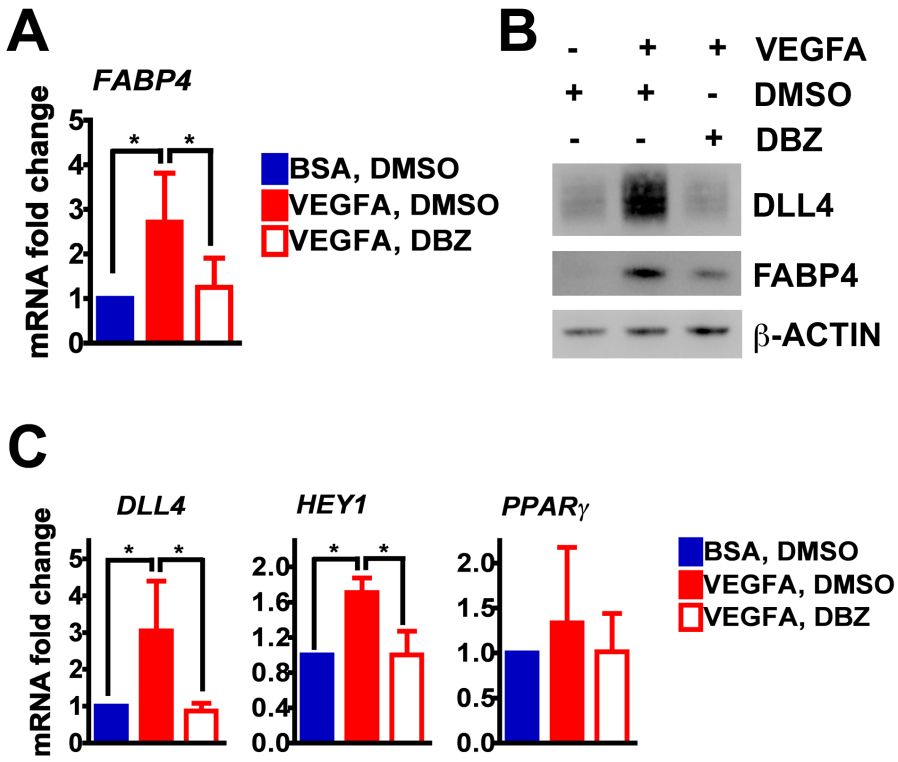


Figure 4.7 VEGFA-induced fatty acid binding protein 4 (FABP4) is downregulated by γ-secretase inhibition. HUVEC were growth factor-starved and stimulated with BSA or VEGFA (50 ng/ml) and treated with dibenzazepine (DBZ, 10 nM) or vehicle control (DMSO). Cells were harvested and analysed for mRNA expression of *FABP4* (A), protein expression of DLL4 and FABP4 (B), or mRNA expression of *DLL4*, *HEY1* and *PPARγ* (C). β-ACTIN was used as a loading control (B). Values are expressed as mean +/- S.D., *p<0.05 (A,C) (n=3, One-way ANOVA, Bonferroni post-hoc test).

4.2.7 Inhibition of ADAM 10 and ADAM 17 reduces FABP4 induction by VEGFA.

VEGFA has been reported to induce activation of ADAM10 and ADAM17 and thereby regulate the shedding of VEGFR2, neuropilin 1, and several other receptors (Swendeman, Mendelson *et al.* 2008). ADAM10 and ADAM17, required for NICD release following DLL4-Notch binding, are expressed as inactive enzyme precursors (pre-mature form) and removal of the pro-domains result in maturation or activation of the enzymes (Endres, Anders *et al.* 2003). To investigate if the mechanism of VEGFA-mediated NOTCH signalling induction is related to increased activation of ADAM10 and/or ADAM17 and thus increased NOTCH cleavage, the pre-mature versus mature forms of ADAM10 or ADAM17 were analysed in HUVEC treated with VEGFA. VEGFA treatment did not lead to increased maturation of ADAM10 or ADAM17 (Fig. 4.8 A) and band densitometry analysis did not show a significant change in the ratio of the pre-mature (pADAM) and mature form (mADAM) of ADAM 10 or ADAM17 (Fig. 4.8 B). This indicated that increased activity of ADAM10 or ADAM17 is not responsible for increased NOTCH signalling in response to VEGFA.

Since basal activities of ADAM17 and ADAM10 are required for NICD release and transduction of NOTCH signalling, it was tested whether VEGFA induced FABP4 was dependent on ADAM17 and ADAM10 activity. VEGFA stimulated HUVEC were treated with the ADAM17 inhibitor INCB4298 or the ADAM17/10 inhibitor INCB3619. *DLL4, HEY1* and *FABP4* mRNA expression in response to VEGFA were significantly downregulated by ADAM17 or ADAM17/10 inhibitor treatment (Fig. 4.8 B). This showed that basal activities of ADAM10 and especially ADAM17 were required for NOTCH signalling and *FABP4* induction in response to VEGFA, showing that NOTCH cleavage by ADAM17, which is part of the canonical NOTCH signal transduction, was required for FABP4 expression.

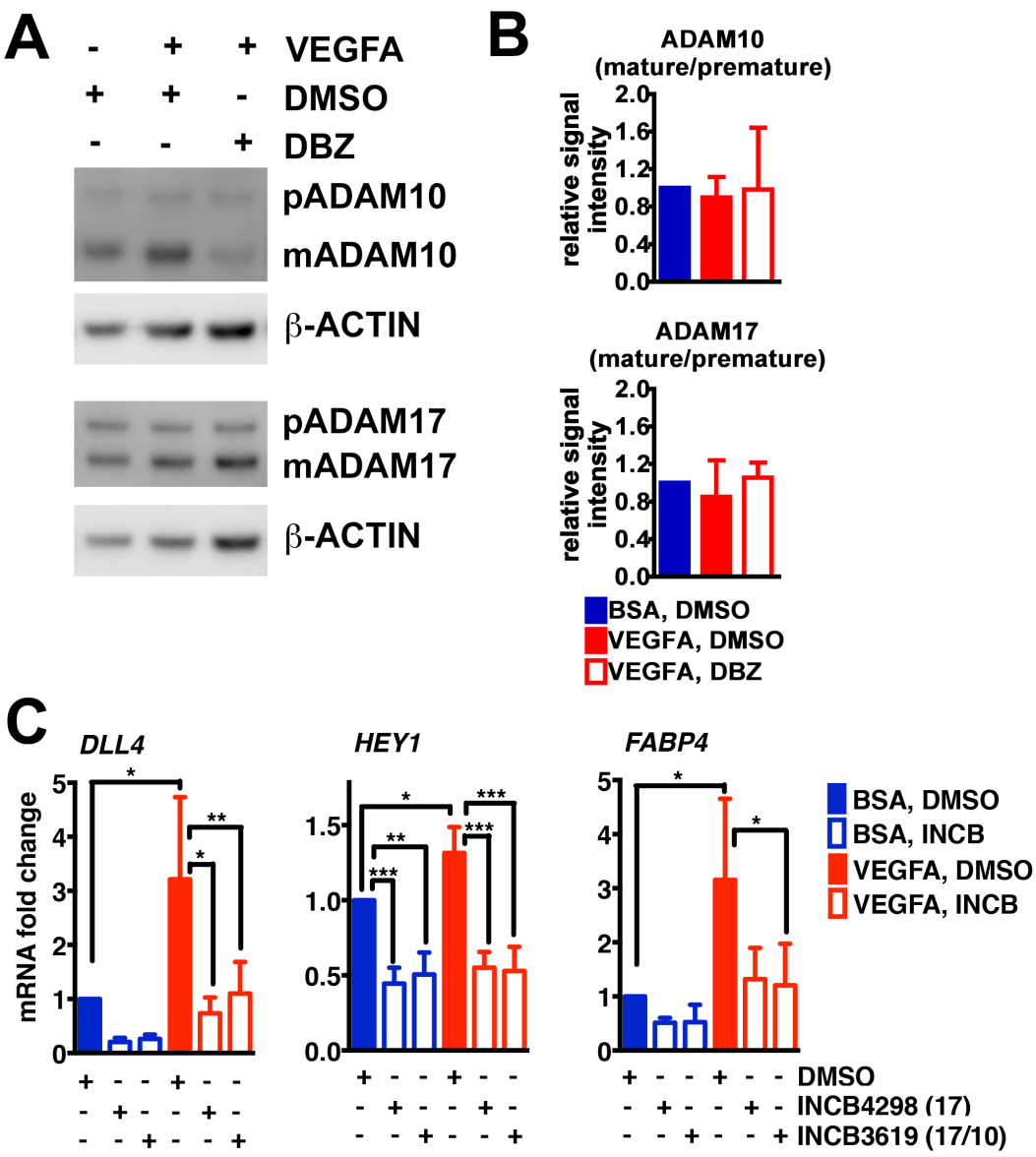


Figure 4.8 Inhibition of ADAM10 and ADAM17 reduces fatty acid binding protein 4 (FABP4) induction by VEGFA. HUVEC were growth factor-starved and stimulated with BSA or VEGFA (50 ng/ml) and treated with dibenzazepine (DBZ) (A, B), INCB4298 (10 μM, targets ADAM17) (C), INCB3619 (5 μM, targets ADAM17/10) (C), or vehicle control (DMSO) as indicated. Cells were harvested and analysed for protein expression of ADAM10 and ADAM17 (A, pre-mature form=pADAM, mature form=mADAM), band intensity (three independent experiments, B), or analysed for mRNA expression of *DLL4, HEY1* and *FABP4* (C). β-ACTIN was used as a loading control (A). Values are expressed as mean +/- S.D., *p<0.05, **p<0.01, ***p<0.001 (B) (n=3, One-way ANOVA, Bonferroni post-hoc test).

4.2.8 DLL4-NOTCH induced FABP4 expression is sensitive to rapamycin

Elmasri *et al*. reported that FABP4 induction was dependent on MTORC1 and activity of its downstream target p70S6 kinase (Elmasri, Ghelfi *et al.* 2012). Therefore it was investigated if this mechanism of regulation was present in the context of DLL4-NOTCH activation. HUVEC were grown on BSAc or DLL4c for 48 h and treated with rapamycin to inhibit MTORC1 or DMSO as a vehicle control. *FABP4* mRNA expression was significantly upregulated in HUVEC with activated DLL4-NOTCH signalling and rapamycin treatment led to a significant downregulation of that induction (Fig. 4.9 A). FABP4 protein expression was upregulated in response to DLL4-NOTCH activation and downregulated in response to rapamycin treatment (Fig. 4.9 B). Target gene expression of the DLL4-NOTCH pathway was investigated in response to rapamycin and there was no significant change of *DLL4*, *VEGFR2*, *HES1, HEY1* or *HEY2* expression (Fig. 4.9 C). *PPARγ* expression was significantly downregulated by rapamycin in DLL4c-treated HUVEC. Overall, these results showed that FABP4 expression was sensitive to MTORC1 inhibition also in the context of DLL4-NOTCH signalling. Canonical DLL4-NOTCH targets were not affected, indicating that the FABP4 regulation by MTORC1 was not occurring upstream of the DLL4-NOTCH pathway. This has been confirmed also in the context of VEGFA stimulation (Fig. 4.10).

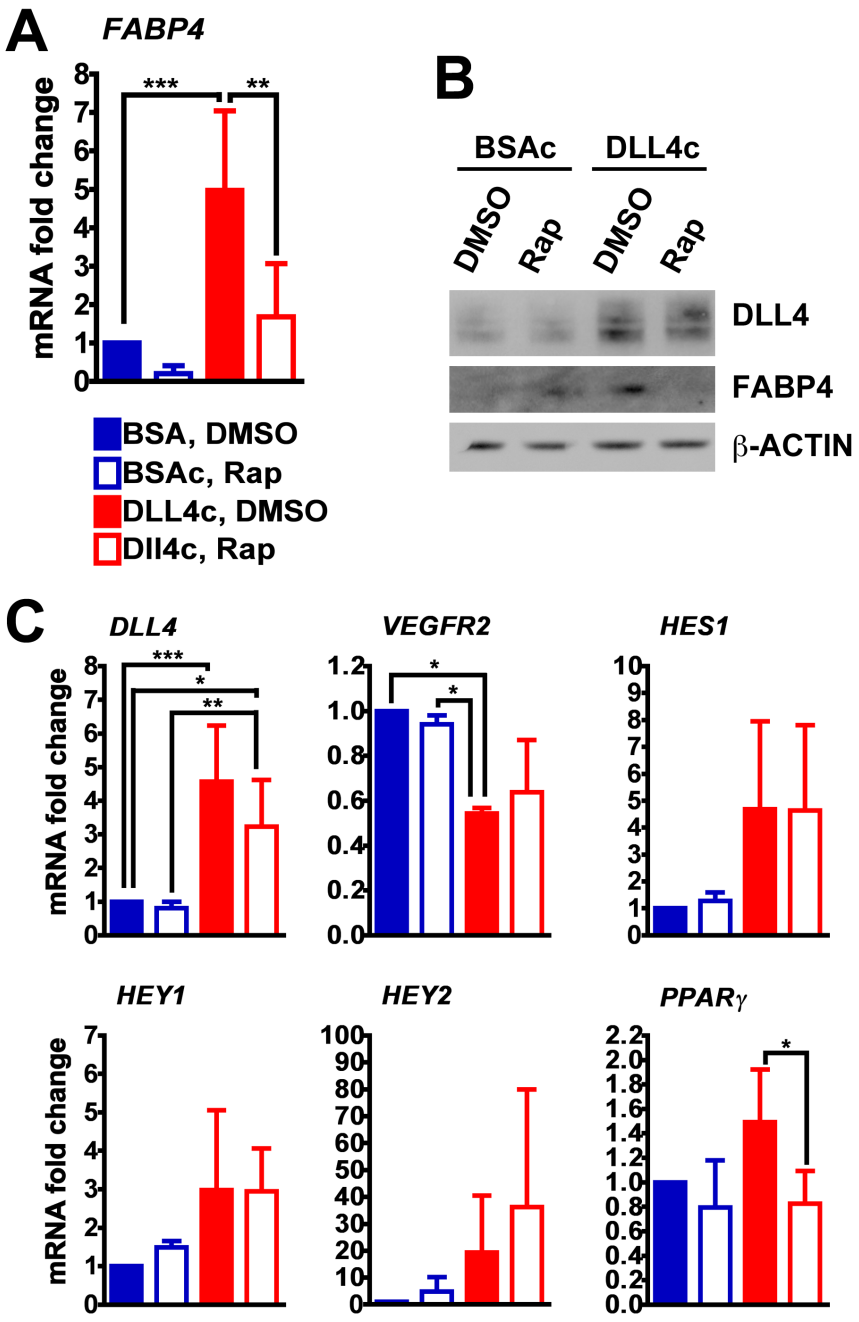


Figure 4.9 DLL4-NOTCH induced fatty acid binding protein 4 (FABP4) expression is sensitive to rapamycin. HUVEC were grown on BSA- or DLL4-coated (BSAc or DLL4c) tissue culture ware and treated with rapamycin (20 nM) or vehicle control (DMSO). Cells were harvested and analysed for mRNA expression of *FABP4* (A), protein expression of DLL4 and FABP4 (B), and mRNA expression of indicated NOTCH target genes (C). β-ACTIN was used as a loading control (B). Values are expressed as mean +/- S.D., *p<0.05, **p<0.01, ***p<0.001 (B; n=3, One-way ANOVA, Bonferroni post-hoc test).

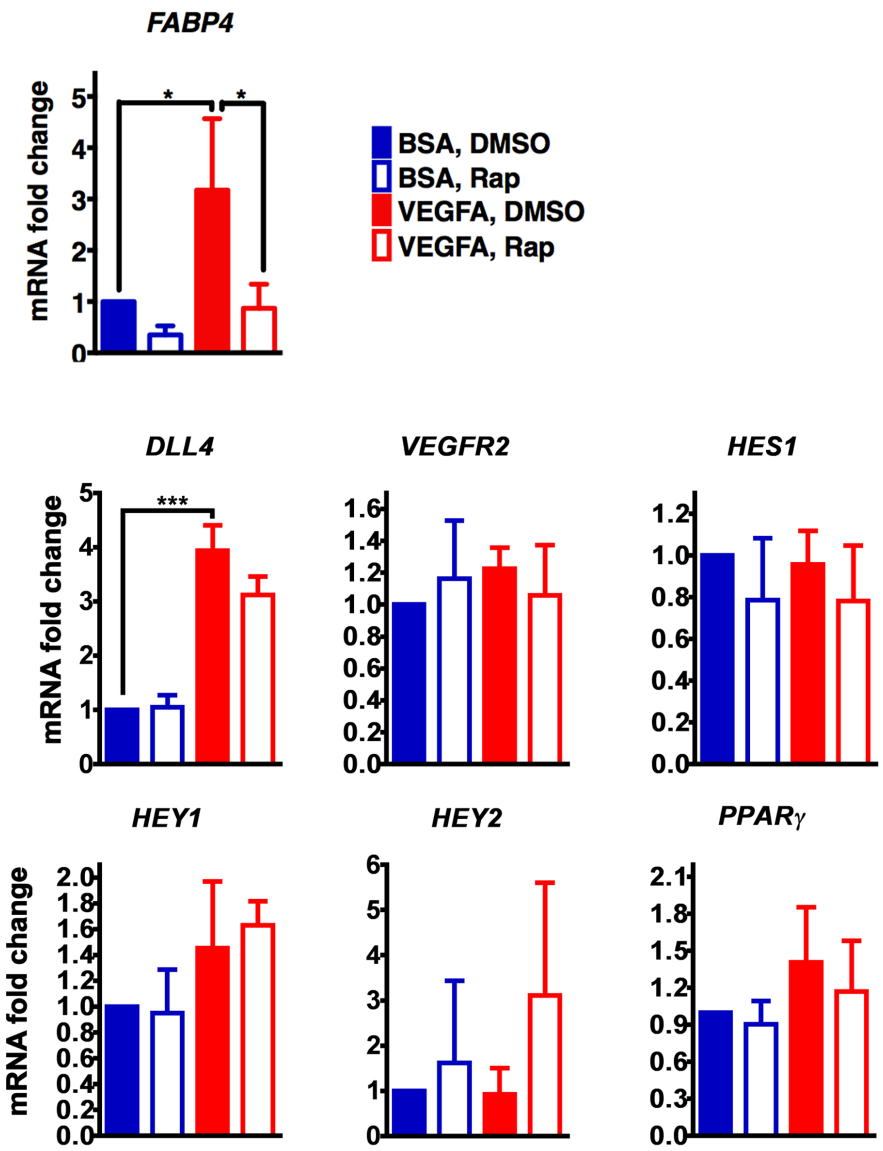


Figure 4.10 VEGFA induced fatty acid binding protein 4 (FABP4) expression is sensitive to rapamycin. HUVEC were growth factor-starved and stimulated with BSA or VEGFA (50 ng/ml), and treated with rapamycin (20 nM) or vehicle control (DMSO). Cells were harvested and analysed for mRNA expression of *FABP4* (upper panel) and mRNA expression of indicated NOTCH target genes (middle and lower panels). Values are expressed as mean +/- S.D.. *p<0.05, ***p<0.001 (B; n=3, One-way ANOVA, Bonferroni post-hoc test).

4.2.9 AKT inhibition increases FABP4 expression

Inhibition of MTORC1 can inhibit a negative feedback loop to AKT kinase (Chen, Liu *et al.* 2010). Because *FABP4* gene expression was repressed in gene expression microarrays of HUVEC overexpressing AKT (Daly, Wong *et al.* 2004), the hypothesis that FABP4 expression was sensitive to changes of AKT activity was investigated. HUVEC stimulated with DLL4c or BSAc were treated with AKT kinase inhibitor X (AKTiX) and analysed for protein expression of FABP4 and the effect on AKT phosphorylation (Fig. 4.11 A). Furthermore, band densitometry analysis was performed of FABP4 compared to the loading control and of phosphorylated AKT compared to total levels of AKT (Fig. 4.11 B). Statistical analysis showed an overall significant change of AKT phosphorylation and FABP4 expression, in response to the treatments (Friedman test $p<0.05$ for phospho-AKT, $p<0.01$ for FABP4, Dunn's post-hoc test not significant). AKTiX treatment led to a consistent decrease of AKT phosphorylation in BSAc treated and DLL4c treated HUVEC. It was observed that DLL4c treatment itself led to a slight decrease of AKT phosphorylation. AKTiX treatment led to a consistent increase of FABP4 expression compared to DMSO in BSAc- or in DLL4c-stimulated cells. These results indicate that the regulation of FABP4 gene and protein expression is dependent on the phosphorylation status of AKT and that increased AKT phosphorylation and activity is a possible mechanism of FABP4 repression.

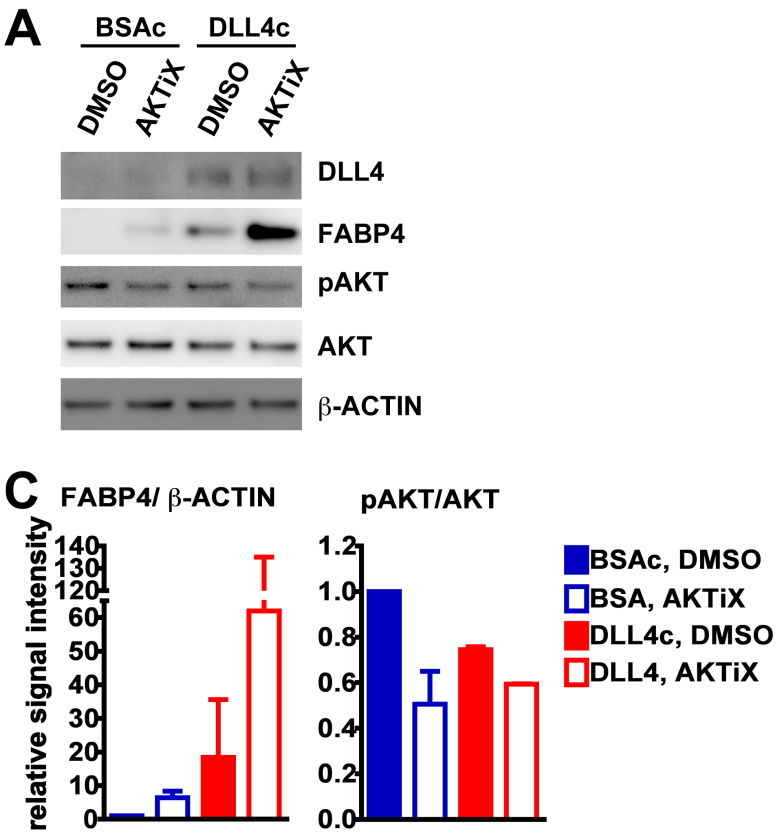


Figure 4.11 AKT inhibition increases fatty acid binding protein 4 (FABP4) expression. HUVEC were grown on BSA- or DLL4-coated (BSAc or DLL4c) tissue culture ware and treated with AKT inhibitor X (AKTiX), or vehicle control (DMSO). Cells were harvested and analysed for protein expression of DLL4, AKT, and FABP4 and for the serine 473 phosphorylation status of AKT (pAKT). β-ACTIN was used as a loading control (A) and band densitometry analysis of three independent experiments was performed (B; n=5, Friedman test FABP4 $p<0.01$, pAKT $p<0.05$, Dunn's post-hoc test not significant).

4.2.10 Regulation of FABP4 downstream of VEGFA or direct DLL4-NOTCH activation is dependent on FOXO1

Activation of AKT signalling leads to phosphorylation of the forkhead transcription factor FOXO1 and renders FOXO1 inactive by trapping it in the cytoplasm (Brunet, Bonni *et al.* 1999). Gene expression microarray studies in HUVEC indicated that AKT and FOXO1 regulate *FABP4* in a reciprocal manner (Daly, Wong *et al.* 2004) and *FABP4* was regulated by FOXO1 in macrophages (Nakae, Cao *et al.* 2008). Therefore, the hypothesis that FOXO1 may be required for *FABP4* transcription in HUVEC was investigated in HUVEC stimulated with BSA or VEGFA stimulated HUVEC (Fig. 4.12 A) or in BSAc or DLL4c stimulated HUVEC (Fig. 4.12 B and C), treated with control or *FOXO1* targeting RNAi. RNAi of *FOXO1* led to >50% reduction of F*OXO1* mRNA in BSA-, VEGFA-, BSAc-, or DLL4c-stimulated cells (Fig. 4.12 A and B). *FABP4* mRNA levels were significantly reduced by *FOXO1* suppression to less than 20% in cells stimulated with BSA or VEGFA, and BSAc or DLL4c (Fig. 4.12 A and B). *DLL4*, and *HEY1* mRNA were significantly downregulated by *FOXO1* suppression and *PPARγ* mRNA was upregulated (Fig. 4.12 D). FABP4 protein levels in response to DLL4c were repressed by *FOXO1* RNAi (Fig. 4.12 C), showing that FOXO1 is required for DLL4-NOTCH-mediated FABP4 induction. The downregulation of DLL4 and HEY1 in response to *FOXO1* RNAi suggests that FOXO1 is needed for either NOTCH signalling transduction or the gene transcriptional induction of other NOTCH targets and needs further investigation.

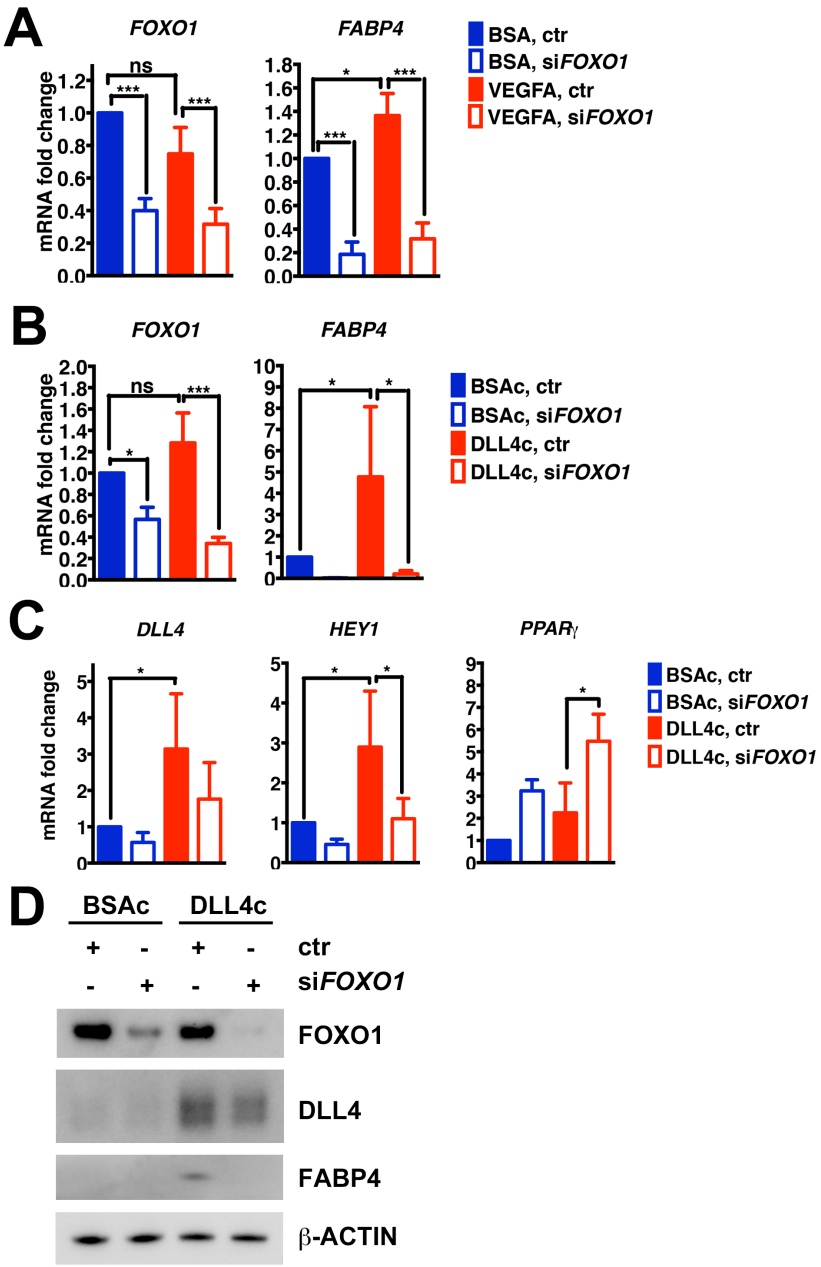


Figure 4.12 Regulation of gene and protein expression of fatty acid binding protein 4 (FABP4) is dependent on FOXO1. HUVEC were growth factor-starved and stimulated with BSA or VEGFA (50 ng/ml) (A) or grown on BSA- or DLL4-coated (BSAc or DLL4c) (B, C) and were transfected with siRNA targeting *FOXO1* (si*FOXO1*) or non-targeting siRNA (control=ctr). Cells were harvested after 48 h and analysed for mRNA expression of *FOXO1* and *FABP4* (A, B), *DLL4*, *HEY1*, and *PPARγ* (C), and protein expression of DLL4, FOXO1 and FABP4 (D). β-ACTIN was used as a loading control (D). Values are expressed as mean +/- S.D., *p<0.05, **p<0.01, ***p<0.001 (A, B; n=3, One-way ANOVA, Bonferroni post-hoc test).

4.2.11 NICD binds to specific FABP4 promoter regions adjacent to the FOXO1 binding motif

In hepatic cells, there is evidence for a NOTCH-FOXO1 co-dependent mechanism of gene transcription (Kitamura, Kitamura *et al.* 2007, Pajvani, Shawber *et al.* 2011). The presented results showed that FOXO1 is required for FABP4 expression in response to DLL4-NOTCH in HUVEC, without significantly affecting canonical NOTCH signalling. Therefore, it was investigated investigated 1) if the *FABP4* gene promoter contains binding sites for the RBPJκ-NICD complex in proximity to FOXO1 binding sites, and if 2) NICD associates with RBPJκ binding sites to promote *FABP4* gene transcription.

In the NICD transcription factor complex, NICD indirectly binds to DNA by associating with the co-factor RBPJκ, which is the DNA binding factor in the complex. Therefore, the promoter region of FABP4 was searched for RBPJκ and FOXO1 binding sites. The motifs were derived from Castel *et al.* and Fan *et al.* (Fan, Morinaga *et al.* 2010, Castel, Mourikis *et al.* 2013), respectively. The *FABP4* gene promoter sequence (gi|42516792) was searched for RBPJκ and FOXO1 binding motifs and their variations. As highlighted in Fig. 4.13 A, a RBPJκ binding motif was present at -2097 bp, directly adjacent to a FOXO1 binding motif (in red). This region is referred to as RBPJκ (R)-FOXO1 (F)-1, (R-F-1). Furthermore, there were RBPJκ binding motifs at -1935 bp (three adjacent repeats, referred to as R-2), and -1284 bp (three repeats, separated by several base pairs, referred to as R-3A, R-3B, and R-3C) (Fig. 4.13 A).

Then the regions R-F-1 and R-2 were investigated in more detail, because of their proximity to the FOXO1 binding motif. To control for the induction of NOTCH target genes in this assay, known RBPJκ binding regions in the promoters of the NOTCH target genes *DLL4* and *HEY1* were analysed as positive controls and a region in the promoter of the *UBC* gene, which is not regulated by NOTCH, as a negative control.

To analyse the association of NICD to the predicted RBPJκ binding sites, ChIP was performed in HUVEC stimulated with DLL4c or BSAc for 16 h and treated with or without

DBZ or DMSO to inhibit NICD release and induction of NOTCH signalling. An antibody targeting NOTCH1 was used to detect NICD. According to the manufacturer's instructions, the antibody used here recognises intracellular epitopes between 2400 and 2500 amino acids of human NOTCH1 and does not detect the extracellular domain of NOTCH1 once it is cleaved by ADAM-like proteases. Rabbit IgG was used as a negative control.

NICD IP and rabbit IgG IP results are shown in one graph for each promoter region of interest (Fig. 4.13 B). The ChIP results of the regions of interests R-F-1 and R-2 are shown in the two upper panels. The ChIP results of the Notch target genes *DLL4* and *HEY1* are shown in the middle two panels, and the results of the *UBC* gene are shown in the lower panel.

ChIP of NICD showed increased binding to R-F-1 and R-2 in response to DLL4c stimulation, compared to BSAc, which was significantly reduced by DBZ treatment (Fig. 4.13 B upper panels). ChIP of NICD also showed increased binding to *DLL4* and *HEY1* promoter regions in DLL4c stimulated HUVEC compared to BSAc that was reduced by DBZ treatment (Fig. 4.13 B middle panels). No increased binding of NICD to the *UBC* promoter in response to DLL4c stimulation was observed (Fig. 4.13 B lower panel). The IP with rabbit IgG showed no significant binding to any of the analysed regions in response to DLL4c-stimulation.

These findings show that NICD associates with RBPJκ binding motifs in the *FABP4* gene promoter, which are directly adjacent to a FOXO1 binding motif. These findings further indicate that *FABP4* transcription is induced by NICD release and its association with the *FABP4* promoter via RBPJκ, and that *FABP4* is a target gene of the DLL4-NOTCH signalling pathway.

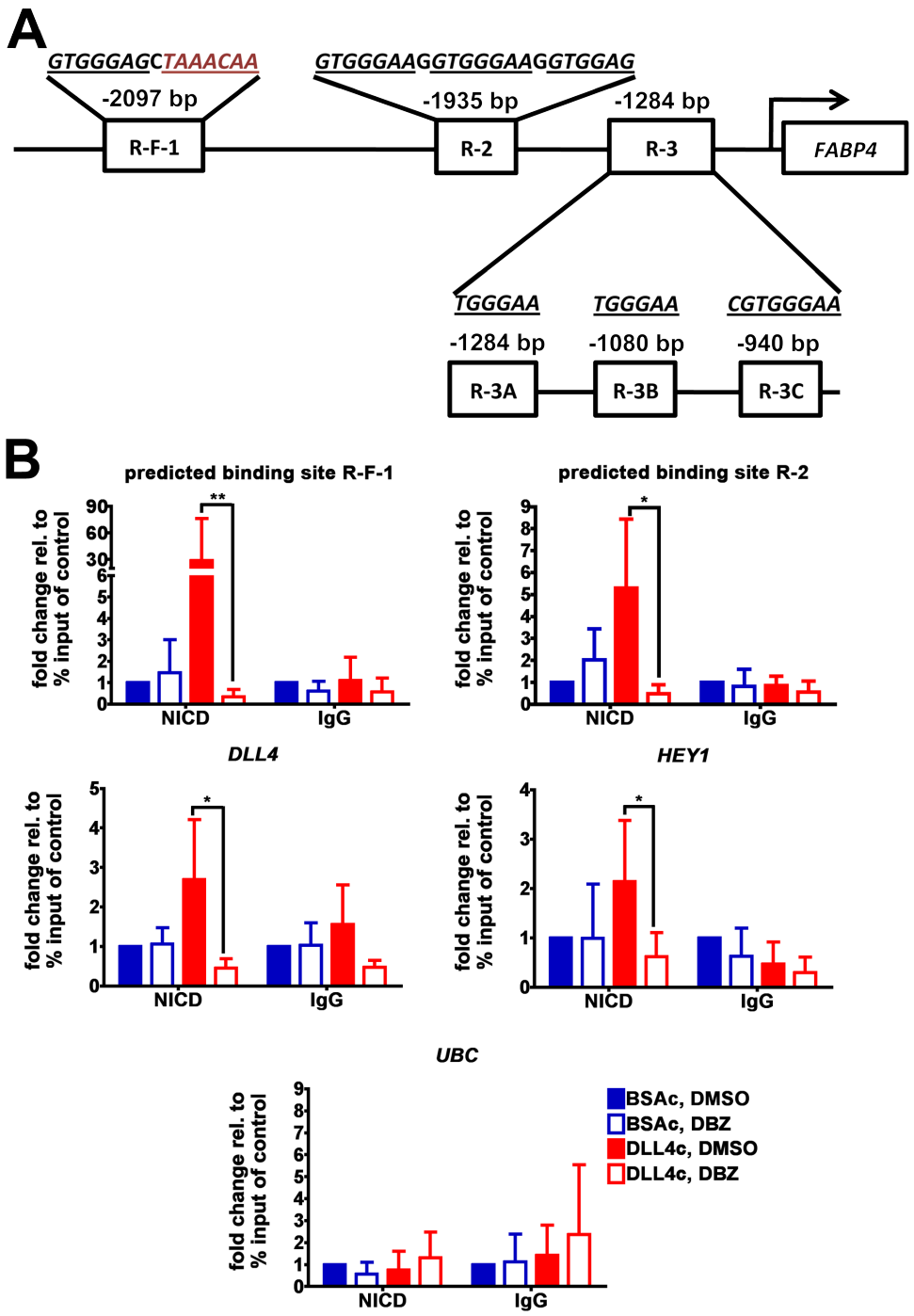


Figure 4.13 NOTCH intracellular domain (NICD) binds to specific fatty acid binding protein 4 (FABP4) promoter regions adjacent to the FOXO1 binding motif. Location of RBPJκ binding motifs (underlined, R-F-1, R-2, R-3A, R-3B, R-3C) or adjacent RBPJκ and FOXO1 binding motifs (R-F-1, FOXO1 binding motif in red) in the *FABP4* promoter sequence are shown (A). HUVEC were grown on BSA- or DLL4-coated (BSAc or DLL4c) for 16 h and were treated with dibenzazepine (DBZ) or vehicle control (DMSO). Cells were fixed, and analysed for NICD binding to the predicted binding sites R-F-1 and R2, known binding sites in *DLL4* and *HEY1* promoters, and a region in *UBC* promoter by chromatin immunoprecipitation (ChIP) (B). Values are expressed relative to % input of the control condition (BSAc, DMSO) and as mean +/- S.D., *p<0.05, **p<0.01, ***p<0.001 (B; n=5, Friedman test, Dunn's post-hoc test).

4.3 Discussion

Previous studies by Elmasri *et al*. have shown that FABP4 is induced by VEGFA and suggested a MTORC1-dependent regulatory axis (Elmasri, Karaaslan *et al.* 2009). However, in this chapter it was found that there are additional regulatory mechanisms of FABP4 induction: VEGFA acts indirectly by inducing DLL4, which then activates NOTCH signalling and initiates *FABP4* gene transcription. FABP4 expression is sensitive to AKT activity. This suggests that an increase of AKT activity renders the transcription factor FOXO1 in the cytoplasm, preventing it from promoting *FABP4* gene transcription. A proposed model of FABP4 regulation in endothelial cells is shown in Fig. 4.14.

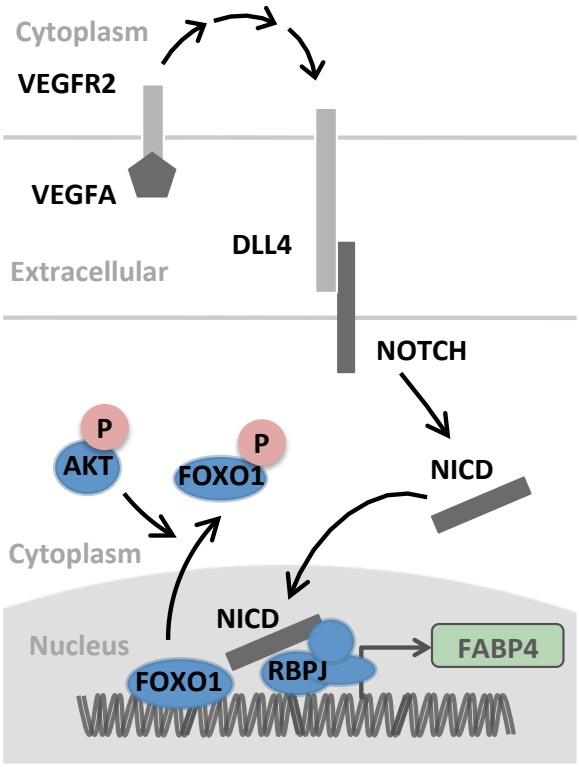


Figure 4.14 Regulation and mechanism of fatty acid binding protein 4 (FABP4) induction in endothelial cells is dependent on DLL4-NOTCH signalling and FOXO1. VEGFA induces DLL4 expression in endothelial cells, thereby promoting the paracrine activation of NOTCH signalling in adjacent cells and inducing indirect binding of NOTCH intracellular domain (NICD) via a transcription factor complex involving RBPJκ to promoter regions of the *FABP4* gene, to induce *FABP4* transcription. Under basal levels of AKT activity, FOXO1 is present in the nucleus and promotes DLL4-NOTCH-dependent *FABP4* transcription. AKT activation induces FOXO1 phosphorylation and cytoplasmic translocation, and diminishes *FABP4* transcription. AKT inhibition leads to FOXO1 being trapped in the nucleus and further promoting *FABP4* transcription.

Inhibition of each step required for NOTCH signalling activation led to reduced induction of FABP4 expression in response to VEGFA. Additionally, inhibition of intracellular cleavage also led to reduction of NICD binding to two specific regions in the *FABP4* promoter, consequently suggesting that DLL4-NOTCH signalling is a direct promoter of *FABP4* gene transcription. Basal levels and VEGFA or DLL4-NOTCH stimulated FABP4 were suppressed by *FOXO1* knockdown and FOXO1 was required for maintaining FABP4 expression.

FABP4 indirectly affects gene transcription by delivering free FAs to the nucleus, which serve as ligands for PPARs and regulate gene transcription (reviewed by Kralisch and Fasshauer 2013). FABP4 also delivers FAs to other compartments of the cell such as the mitochondria for further utilisation. Nieman *et al.* have shown a role of FABP4 in omental ovarian cancer metastasis. FABP4 was required for increased FA oxidation in ovarian cancer cells adjacent to the omentum and upregulated in the adjacent adipocytes. *FABP4* -/- mice injected with ovarian cancer cells had a smaller tumour burden with decreased microvessel density (Nieman, Kenny *et al.* 2011). Additionally, high FABP4 expression has been described in several cancers (Boiteux, Lascombe *et al.* 2009, Cataltepe, Arikan *et al.* 2012), indicating therapeutic relevance.

PPARγ regulates transcription of genes required for adipocyte differentiation and regulates FA storage mainly in adipocytes and macrophages. The *FABP4* gene promoter harbours peroxisome proliferator hormone response elements (PPREs) and is transcriptionally induced by PPARγ (reviewed by Kralisch and Fasshauer 2013). FABP4 in turn delivers PPAR ligands to the nucleus and enhances PPARγ activity, creating a feed-forward loop. However, a more recent study suggests that FABP4 negatively regulates PPARγ expression, by a mechanism that promotes ubiquitination and proteasomal degradation of PPARγ (Garin-Shkolnik, Rudich *et al.* 2014). PPARγ activation has inhibiting effects on tumour growth and differentiation (reviewed by Tontonoz and Spiegelman 2008), whereas FABP4 has tumourigenic effects and is linked to aggressive tumour behavior (Hancke, Grubeck *et al.* 2010, Nieman, Kenny *et al.*

2011, Tucker, Gharpure *et al.* 2014). The results in this chapter did not suggest a strong correlation of FABP4 and PPARγ expression in response to DLL4-NOTCH and even showed an inverse hypoxic regulation of FABP4 and PPARγ by different HIF transcription factors. FOXO1 knockdown led to PPARγ upregulation, which agrees with a negative post-transcriptional PPARγ regulation by FABP4 or suggests a direct regulation by FOXO1. It seems that the DLL4-NOTCH induction of FABP4 may be intertwined with a regulation of PPARγ, but is not co-dependent as previously suggested.

Elmasri *et al.* showed that *FABP4* suppression inhibited VEGFA-induced proliferation, migration, and inhibited sprouting in the aortic ring model. This effect is dependent on changes in gene expression, when FABP4 is inhibited in VEGFA-stimulated cells. In particular, the c-kit pathway plays a major role in this, and exogenous provision of stem cell factor (SCF) restored endothelial function reduced by FABP4 knockdown (Elmasri, Karaaslan *et al.* 2009, Elmasri, Ghelfi *et al.* 2012). The present findings show that, paradoxically, a VEGFA target with pro-angiogenic features is downstream of angiogenesis-restricting NOTCH signalling. Therefore upregulation of FABP4 by increased DLL4-NOTCH and the resulting FABP4 pro-angiogenic effects may overcome effects of VEGFA inhibition in tumour tissue and therefore result in therapy resistance.

Endothelial FABP4 downregulation in hypoxia, that is HIF-1α dependent, may indicate that endothelial FABP4 function becomes significant in (re-) oxygenated areas, when growing tumour blood vessels become perfused and need maintenance. This stresses why a combination of DLL4 blockade and VEGFA inhibition may have additional therapeutic effects in tumour angiogenesis, by blocking endothelial cell proliferation and differentiation.

Elmasri suggested a MTORC1-p70S6kinase-dependent positive regulation of FABP4 (Elmasri, Karaaslan *et al.* 2009), a mechanism which seems to be present also in the DLL4-NOTCH background. However, MTORC1-p70S6kinase inhibition triggers a negative feedback mechanism, resulting in the activation of AKT signalling via IGF-1R/PI3K signalling (Wan, Harkavy *et al.* 2007), and also activation of extracellular signal-regulated

kinase (ERK) (Chen, Liu *et al.* 2010). Upregulation of FOXO1-dependent gene transcription is a candidate mechanism for resistance to therapy targeting AKT and ERK in cancer (Roy, Srivastava *et al.* 2010). In this chapter, AKT inhibition led to upregulation of FABP4 and FABP4 was suppressed by *FOXO1* knockdown. Thus, FABP4 expression induced by DLL4-NOTCH can be modulated by AKT, MTORC1, and potentially ERK signalling pathways, which is important to consider in combination therapies.

FOXO1 and NOTCH regulate hepatic gene transcription of gluconeogenic genes in a co-dependent manner and both FOXO1 and RBPJκ binding sites were required for the induction of target genes (Pajvani, Shawber *et al.* 2011). FOXO1 and NOTCH1 pathways synergise to promote differentiation of myoblasts. FOXO1 binds to RBPJκ in C2C12 cells and is recruited to the *HES1* promoter and is required for expression of the NOTCH target genes *HES1*, *HES5*, and *HEY1*. FOXO1 was also required for NOTCH and MAML1 binding to RBPJκ and promotes co-repressor clearance at the HES1 promoter site. The authors reported that they observed a similar co-operation of FOXO1 and NOTCH in HUVEC (Kitamura, Kitamura *et al.* 2007). FOXO1 limits migratory and sprouting angiogenesis (Potente, Urbich *et al.* 2005). In the present study, the NOTCH targets *DLL4* and *HEY1* were downregulated by *FOXO1* knockdown, which suggests that FOXO1 has a role in NOTCH signalling regulation. A cooperation of NOTCH and FOXO1 signalling in HUVEC would integrate angiogenic and metabolic cues and direct the angiogenic process dependent on the metabolic environment. As recent findings have established that endothelial glucose metabolism is critical for sprouting angiogenesis (De Bock, Georgiadou *et al.* 2013), it is of relevance to investigate if NOTCH and FOXO1 are co-regulators of endothelial gene transcription and FA metabolism and if that is a main pathway for controlling sprouting angiogenesis in development and disease.

In summary this work shows that FABP4 induction by VEGFA is through a DLL4-NOTCH-dependent mechanism and may be modulated by AKT pathways via FOXO1. FABP4 regulation by NOTCH is a candidate mechanism for NOTCH-dependent effects in metabolic

disease such as insulin resistance, atherosclerosis, as well as tumour angiogenesis. It will be exciting to investigate the consequence of NOTCH-dependent mechanisms of FABP4 induction for FA metabolism in tumour endothelial cells. Furthermore, it is possible that there are other genes in the VEGFA transcriptome dependent on this DLL4-feed-forward loop. FOXO1 and NOTCH co-dependent gene regulation, in response to DLL4-NOTCH signal transduction, may be a general mechanism of gene transcription in endothelial cells, which embeds environmental and metabolic cues into the angiogenic process. DLL4-NOTCH-mediated regulation of FABP4 may be integral for its implications in cancer, angiogenesis, and metabolic disease. FABP4 upregulation should be considered in mechanisms of resistance to anti-angiogenic tumour therapy, because of its pro-angiogenic features in VEGFA abundant environments.

5 CHAPTER FIVE

The role of FABP4 in regulating endothelial fatty acid metabolism and angiogenesis

5.1 Introduction

In the previous chapters it was established that DLL4-NOTCH signalling upregulates FA utilisation in endothelial cells. FABP4, an intracellular FA chaperone, was confirmed as a direct target of the DLL4-NOTCH pathway, and regulated in a FOXO1-dependent manner in endothelial cells.

FABP4 is the best-characterised member of the FABP family. Endothelial FABP4 has been shown to have pro-angiogenic effects in response to VEGFA, via induction of the c-kit pathway (Elmasri, Karaaslan *et al.* 2009, Elmasri, Ghelfi *et al.* 2012). The authors showed that FABP4 knockdown in HUVEC leads to enhanced apoptosis and reduced proliferation, migration, and sprouting in response to VEGFA. These effects are dependent on changes in gene expression, because FABP4 knockdown inhibited the c-kit pathway. Exogenous provision of SCF restores the phenotype displayed in FABP4 negative endothelial cells (Elmasri, Karaaslan *et al.* 2009, Elmasri, Ghelfi *et al.* 2012).

FABP4 mRNA and protein levels are induced during adipocyte differentiation and used as a differentiation marker (Bernlohr, Bolanowski *et al.* 1985, Bernlohr, Doering *et al.* 1985). Agonists of PPARγ, a lipoogenic protein induced during adipocyte differentiation, induce FABP4 expression and secretion (Kletzien, Foellmi *et al.* 1992). FABP4 interacts with and activates hormone sensitive lipase via NEFA in its binding pocket, thereby stimulating lipolysis (Shen, Liang *et al.* 2001, Smith, Thompson *et al.* 2007). Genetically or induced obese FABP4-deficient mice show reduced hyperinsulinaemia and insulin resistance without showing weight loss (Hotamisligil, Johnson *et al.* 1996, Shaughnessy, Smith *et al.* 2000). This phenotype is also observed in genetically obese mice treated with the orally available and FABP4 selective inhibitor BMS309403 (from here on referred to as FABP4 inhibitor, F4I; Furuhashi, Tuncman *et al.* (2007)). F4I acts by competitive blocking of the FABP4 FA binding pocket (Sulsky, Magnin *et al.* 2007). Mice deficient in apolipoprotein E develop atherosclerotic lesions (thickened artery walls, accumulation of white blood cells and macrophages that contain cholesterol and TG). FABP4 loss in macrophages leads to defects

in cholesterol accumulation and lipid composition and defects in the pro-inflammatory response, thereby reducing atherosclerosis (Makowski, Brittingham *et al.* 2005). Loss of FABP4 or F4I treatment protects these mice from the development of atherosclerosis (Furuhashi, Tuncman *et al.* 2007). One possible mechanism may be the lack of macrophage lipid accumulation and inflammatory responses when FABP4 is inhibited. Moreover, Nieman *et al*. have shown that ovarian cancer cells preferentially metastasise to the omentum *in vivo* and exhibit increased rates of FA oxidation in co-culture with adipocytes. Adjacent adipocytes have increased rates of lipolysis and release of FAs, which are taken up by adjacent cancer cells. This change of metabolism is dependent on an increase of FABP4 expression in both cell types (Nieman, Kenny *et al.* 2011). In human trophoblasts, FABP4 is required for LD formation when exposed to exogenous FAs, suggesting decreased influx or increased efflux of FAs (Scifres, Chen *et al.* 2011).

Given that FABP4 is a downstream target of the DLL4-NOTCH pathway, it was presently hypothesised that FABP4 is involved in the DLL4-NOTCH mediated promotion of the stalk cell phenotype during sprouting. Furthermore, it was hypothesised that FABP4 may be involved in the upregulation of FA utilisation in response to DLL4-NOTCH (Chapter 3), which might be an important mechanism for stalk cell promotion during sprouting. It was further hypothesised that DLL4-NOTCH upregulation enables endothelial cells to take up and utilise FAs derived directly from adipocytes, in dependence on induction of FABP4. These hypotheses were investigated by employing siRNA-mediated *FABP4* knockdown or F4I-mediated FABP4 inhibition in HUVEC to analyse angiogenesis and the influx of ^{14}C-OA in a single culture or adipocyte co-culture system. However FABP4 also has a major transcriptional role, which was not investigated here.

5.2 Results

5.2.1 Role of FABP4 as a downstream target of DLL4-NOTCH signalling in angiogenesis

5.2.1.1 FABP4 inhibition by RNAi

Four siRNA sequences (si1-4) were tested for their efficiency to reduce *FABP4* expression in response to DLL4-NOTCH activation. A non-targeting siRNA pool (Dharmacon) was used as a negative control (Fig. 5.1 A and B). HUVEC were treated with BSAc or DLL4c to stimulate FABP4 expression. Each of the tested siRNAs led to a significant downregulation of *FABP4* mRNA expression in response to DLL4-NOTCH signalling to less than 30%, compared to the non-targeting siRNA-transfected, DLL4c-stimulated control (Fig. 5.1 A). FABP4 protein expression was downregulated in cells transfected with si1, si2, and si4, compared to control DLL4c-stimulated cells. FABP4 protein expression was downregulated in si3-transfected cells but to a lesser extent than in the other cases. DLL4 protein expression was decreased in response to si2-4 transfection, which was not reflected in the mRNA levels, which were maintained (Fig. 5 A, B). This may be due to a post-translational mechanism. However, mRNA levels of *HEY1* as a downstream target of DLL4 were not changed. The expression of *PPARγ* mRNA was largely unaltered however there was a significant upregulation in si1-transfected, DLL4c-stimulated cells, compared to the DLL4c-stimulated control. This effect was also observed in FOXO1 siRNA-transfected cells, and might be due to the lack of suppression PPARγ expression mediated by FABP4 as reported by Garin-Shkolnik, Rudich *et al.* (2014). *FABP5* mRNA, which has been shown to compensate FABP4 loss in adipocytes (Shaughnessy, Smith *et al.* 2000), was unchanged in response to any treatment (Fig. 5.1 A). Si1 and si2 were used for further experiments.

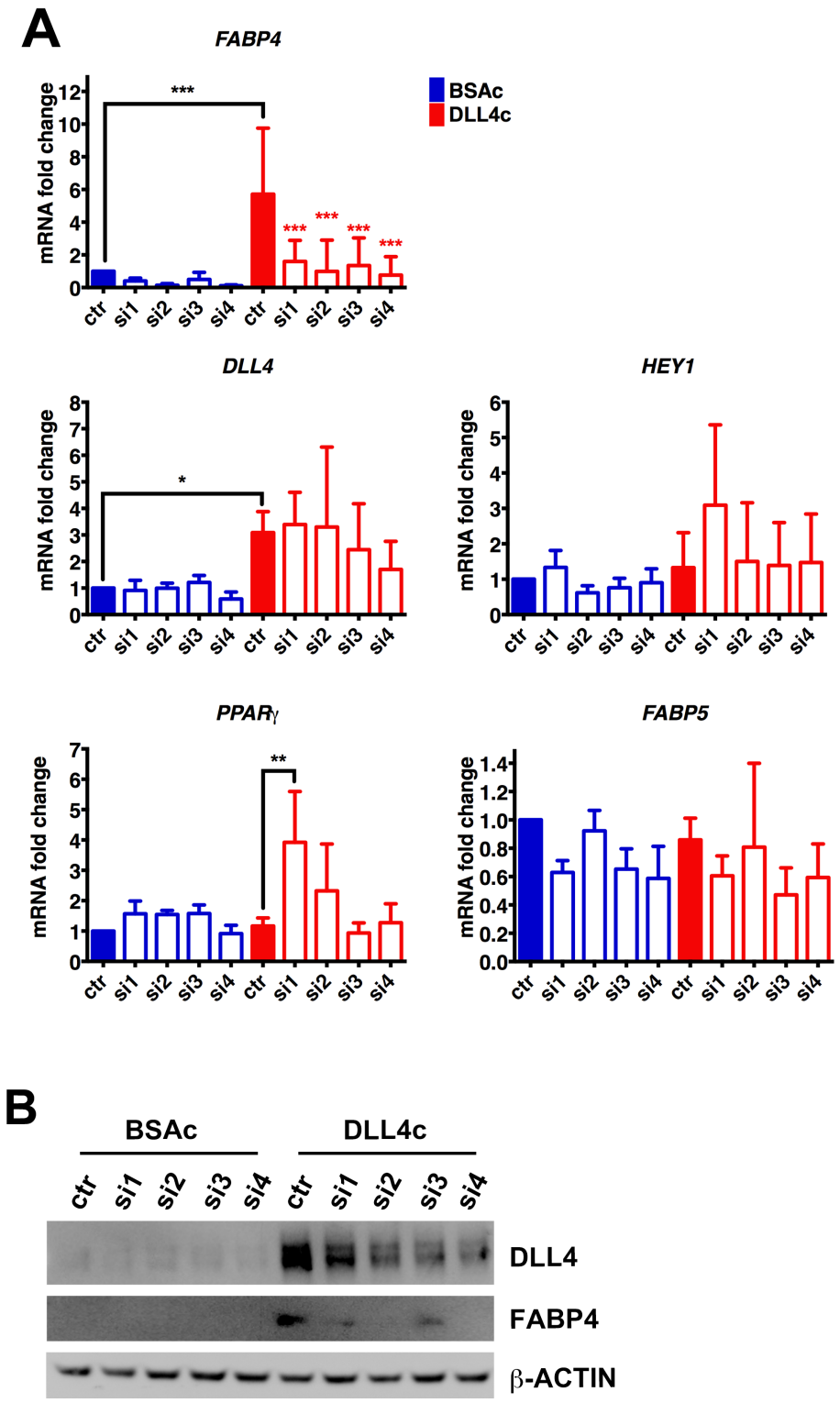


Figure 5.1 Validation of *fatty acid binding protein 4 (FABP4)*-targeting siRNAs. HUVEC were transfected with non-targeting control or four different siRNA sequences targeting *FABP4*, and grown on BSAc or DLL4c for 48 h. Cells were harvested and analysed for mRNA expression of *FABP4, DLL4, HEY1, PPARγ*, or *FABP5* (A), and protein expression of DLL4 and FABP4 (B). Coloured asterisks indicate significant changes compared to non-targeting siRNA-transfected, DLL4c-stimulated control cells (A). Values are expressed as

mean +/- S.D., *p<0.05, **p<0.01, ***p<0.001 (n=3, One-way ANOVA, Bonferroni post-hoc test). β-ACTIN was used as a loading control (C).

5.2.1.2 FABP4 knockdown does not affect angiogenic sprouting in matrigel

It has been shown previously by Elmasri *et al*. that FABP4 following VEGFA stimulation is required for endothelial cell proliferation, migration, and sprouting (Elmasri, Karaaslan *et al.* 2009, Elmasri, Ghelfi *et al.* 2012). Inhibition of DLL4-NOTCH signalling leads to hypersprouting and limits VEGFA-induced angiogenesis. FABP4 as a downstream target of NOTCH might be involved in this phenotype when VEGFA signalling is less dominant. Therefore, the effect of *FABP4* knockdown on sprouting of endothelial cells in basal conditions was investigated without additional VEGFA stimulation (Fig. 5.2). Knockdown of *FABP4* was performed with two different siRNA sequences and compared to non-targeting siRNA. Spheroids were grown overnight and embedded in growth factor-reduced matrigel. After 48 h of sprout growth in matrigel, length, and number of sprouts were determined. Although the sprouts seemed to be thinner when *FABP4* was reduced, there was no significant change in sprout length or number in *FABP4* negative endothelial cells (Fig. 5.2). *FABP4* inhibition in basal conditions without additional VEGFA input does not lead to hypersprouting although being a DLL4-NOTCH target.

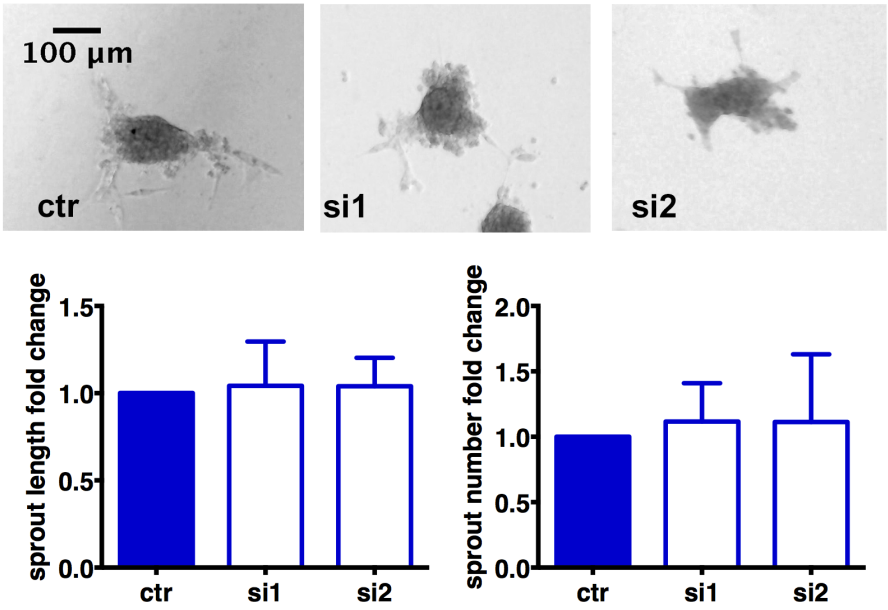


Figure 5.2 ***Fatty acid binding protein 4 (FABP4)*** **knockdown does not affect angiogenic sprouting in matrigel.** HUVEC were transfected with non-targeting control or two different siRNA sequences targeting *FABP4*. After 16 h incubation, HUVEC were subjected to the sprouting assay and grown for 48 h. Sprout number and length were determined. Values are expressed as mean +/- S.D (n=3).

5.2.1.3 FABP4 inhibition by BMS309403 (F4I) and effect on endothelial proliferation, migration, and sprouting

Next, the effect of the FABP4 inhibitor F4I on HUVEC proliferation, migration, and sprouting was tested. The concentration at which 50% of endothelial cell growth was inhibited by F4I was determined (growth EC50) in cells stimulated with BSAc or DLL4c. This was to analyse if DLL4c-stimulated cells, which have higher FABP4 levels, are more sensitive to F4I than BSAc-stimulated cells. HUVEC were grown on BSAc or DLL4c for 96 h and treated with DMSO and increasing concentrations of F4I (Fig. 5.3 A). DLL4c-stimulated cells showed no higher sensitivity towards FABP4 inhibition. Cell growth was inhibited by 50% at 18.20 μM F4I in BSAc treated cells, and at 20.10 μM in DLL4c-stimulated cells. This concentration was in the range of concentrations tested in human trophoblasts, in which 12.5-50 μM F4I correlated to a relative decerase of LD accumulation (Scifres, Chen *et al.* 2011).

To test the ability of F4I to inhibit migration and sprouting, the scratch wound assay and the sprouting assay were performed (Fig. 5.3 B and C). HUVEC were treated with DMSO, 10 μM, 20 μM, or 30 μM F4I. Inhibition of FABP4 by 20 μM or 30 μM F4I led to a significant inhibition of the ability of endothelial cells to migrate. In the sprouting assay, sprouts at 20 μM F4I seemed thinner, but the number of sprouts and sprout length was only significantly inhibited at 30 μM F4I.

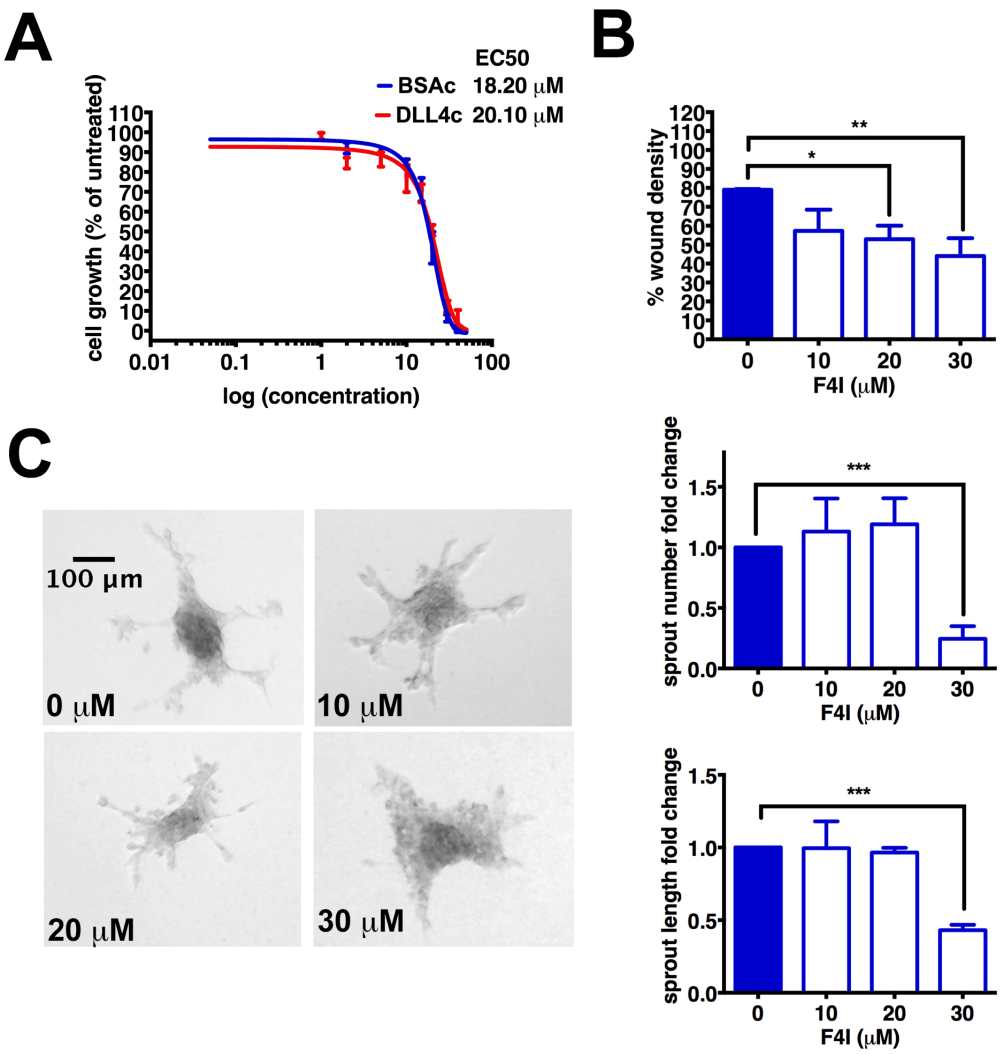


Figure 5.3 Fatty acid binding protein 4 (FABP4) inhibition by BMS309403 (F4I) and effect on endothelial proliferation, migration and sprouting. HUVEC were grown on BSAc or DLL4c and treated with increasing concentrations of F4I for 4 d, and cell growth relative to untreated control was analysed using the CyQuant assay, and the concentrations at which 50% of cell growth was inhibited were calculated (A). HUVEC were subjected to the scratch wound assay and treated with 10, 20 or 30 μM of F4I (B). HUVEC were subjected to the sprouting assay and treated with 10, 20 or 30 μM of F4I for 48 h (C). Sprout number and length were determined. Values are expressed as mean +/- S.D., *p<0.05, **p<0.01, ***p<0.001 (n=3, One-way ANOVA, Bonferroni post-hoc test).

5.2.2 Role of FABP4 as a downstream target of DLL4-NOTCH signalling in FA utilisation

5.2.2.1 FABP4 inhibition by RNAi or F4I does not affect accumulation of ^{14}C derived from extracellular ^{14}C-oleate

The results of chapter 3 indicated an increase of FA utilisation in response to DLL4-NOTCH signalling. FABP4 binds FA and delivers them to sites of utilisation. It was hypothesised that the increase of FABP4 mediates increased FA flux in response to DLL4-NOTCH signalling. Therefore, it was investigated if FABP4 is involved in increased ^{14}C-accumulation derived from extracellular ^{14}C-oleate following DLL4-NOTCH signalling, which is an indicator of FA flux, by modulating *FABP4* expression with RNAi or inhibiting FABP4 with F4I. Because FABP4 is downregulated by *FOXO1* knockdown, and FOXO1 activation is involved in FA uptake and oxidation in muscle cells (Bastie, Nahle *et al.* 2005), *FOXO1* RNAi was performed in addition to *FABP4* RNAi (please also refer to chapter 4). HUVEC were stimulated with BSAc or DLL4c and transfected with si1, si2, or control siRNA, or treated with 10, 20 or 30 μM F4I or DMSO as a control and grown for 48 h. The assay was performed in media containing 50 μM carnitine (co-factor for mitochondrial FA import), 500 μM OA conjugated to FA-free BSA, and 0.05 μCi/ml ^{14}C-OA (Fig. 5.4). DLL4c stimulation indicated an upregulation of ^{14}C-accumulation, but this was not significant. Loss of *FABP4* by si1 or si2 transfection did not lead to a significant downregulation of ^{14}C-accumulation in any condition. *FOXO1* knockdown did not lead to a significant change of ^{14}C-accumulation (Fig. 5.4A). Inhibition of FABP4 with the small molecule inhibitor F4I did not lead to a change of ^{14}C-accumulation in any condition tested (Fig. 5.4B). These results indicated that FABP4 or FOXO1 are not involved in the increase of intracellular ^{14}C derived from ^{14}C-oleate observed in response to DLL4-NOTCH signalling.

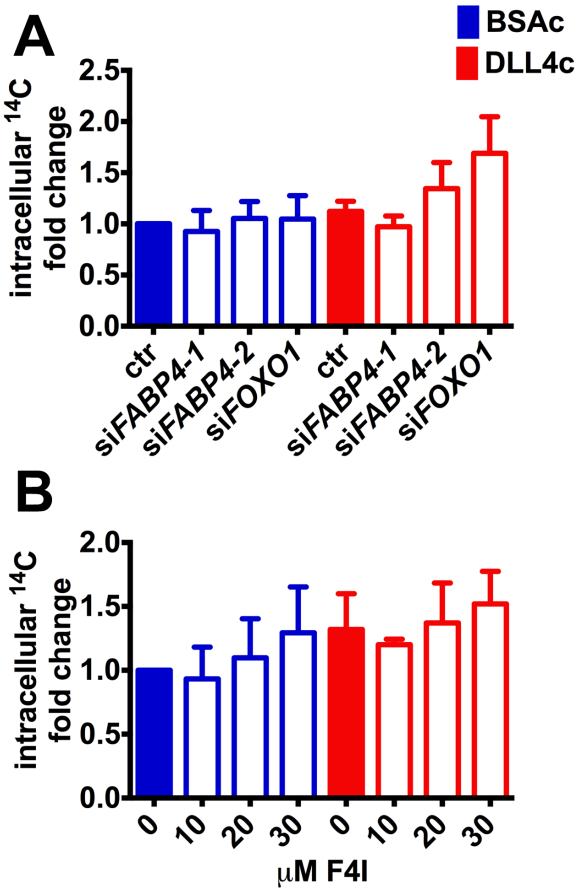


Figure 5.4 FABP4 inhibition by RNAi or by BMS309403 (F4I) does not affect accumulation of ^{14}C derived from extracellular ^{14}C-oleate. HUVEC were transfected with non-targeting control or *FABP4* (*siFABP4-1*, *siFABP4-2*) or *FOXO1* (si*FOXO1*) targeting siRNA, or treated with 0, 10, 20 or 30 μM F4I, and grown on BSAc or DLL4c for 48 h. ^{14}C-uptake assays were performed in assay media containing 50 μM carnitine and 500 μM oleic acid conjugated to FA-free BSA, and 0.05 μCi/ml ^{14}C-oleic acid. Raw values were normalised to cell number. Values are expressed as mean +/- S.D., (n=4, Two-way ANOVA (A), One-way ANOVA (B), Bonferroni post-hoc test).

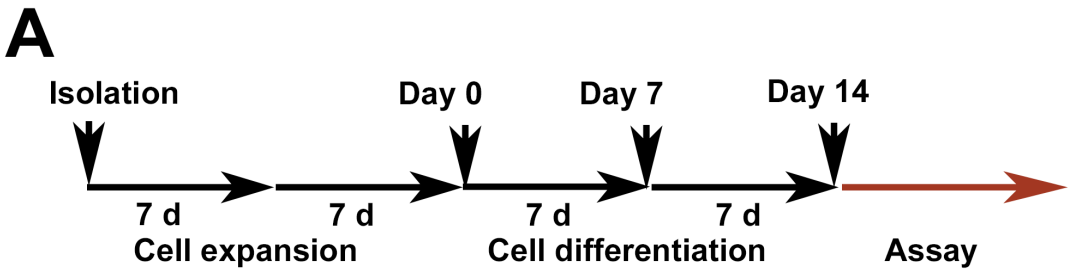
5.2.3 OA-derived ^{14}C-transfer from adipocytes to endothelial cells

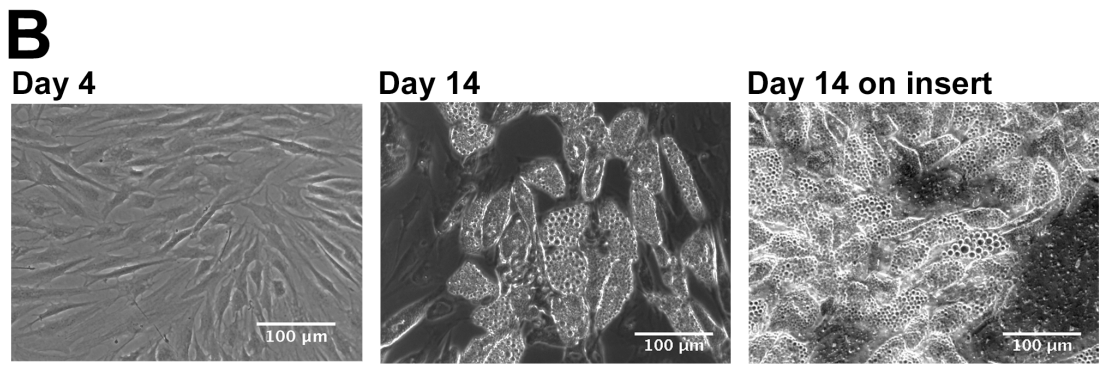
The physiological sources of FAs are either dietary FAs in the plasma or FAs released from adipocytes in fat tissue. In previous experiments, the influx of FAs directly added to the medium was investigated. To investigate the influx of FAs directly derived from adipocytes, HUVEC were co-cultured with differentiated adipocytes and the transfer of pre-labelled FAs from adipocytes to endothelial cells in response to DLL4-NOTCH investigated.

For this, pre-adipocytes were isolated from healthy female volunteers with normal body mass index and grown for 14 days then differentiated for 14 days *in vitro* on tissue culture inserts (Fig. 5.5A). After 7 days of differentiation, a mixture of FAs (25% linoleic acid, 30% palmitic acid, 45% OA) and ^{14}C-OA was added to the media to promote accumulation of lipids and pre-label lipid stores. Figure 5.5A shows a timeline of isolation and differentiation of pre-adipocytes. Figure 5.5B shows photographs of adipocytes at day 4, depicting spindle-like, elongated morphology without visible LD and at day 14, at which time point adipocytes were differentiated and had visible LD. The tissue culture inserts on which adipocytes were grown were then transferred into wells with endothelial cells seeded on BSAc or DLL4c, untreated, or treated with siRNA targeting *FABP4*. The non-transfected cells were cultured for 24 h, 48 h, or 72 h (Fig. 5.5C), and the siRNA-transfected cells were cultured for 48 h (Fig. 5.5D). At each time point, cells were lysed, supernatants were collected, and ^{14}C accumulation in the respective samples was determined. Protein lysates were collected for normalisation.

^{14}C was detected in the adipocytes, supernatants, as well as in the endothelial cells, indicating a release of ^{14}C into the media and uptake by endothelial cells, although the levels of intracellular ^{14}C in endothelial cells were only a fractional amount of that seen in adipocytes (ratio 1/1000). There was no significant change in ^{14}C-levels in adipocytes or supernatants over time in any of the conditions (Fig. 5.5C). At each time point, BSAc and DLL4c-stimulated endothelial cells were compared for their levels of intracellular ^{14}C as an indicator of the influx of FAs derived from adipocytes in co-culture. There was no significant change in the levels of intracellular ^{14}C in BSAc- or DLL4c-treated cells at any given time point. Knockdown of *FABP4* by si1 or si2 did not lead to a significant change of intracellular ^{14}C in

BSAc- or DLL4c-treated (Fig. 5.5D). These results show that adipocytes cultured on tissue culture inserts in co-culture with endothelial cells can act as suppliers of ^{14}C-OA derived species. The influx of ^{14}C-derived species into endothelial cells however was not affected by activation of DLL4-NOTCH signalling or when *FABP4* expression was modulated.


A
Isolation
Day 0
Day 7
Day 14
7 d
7 d
7 d
7 d
Cell expansion
Cell differentiation
Assay


B
Day 4
Day 14
Day 14 on insert
100 µm
100 µm
100 µm

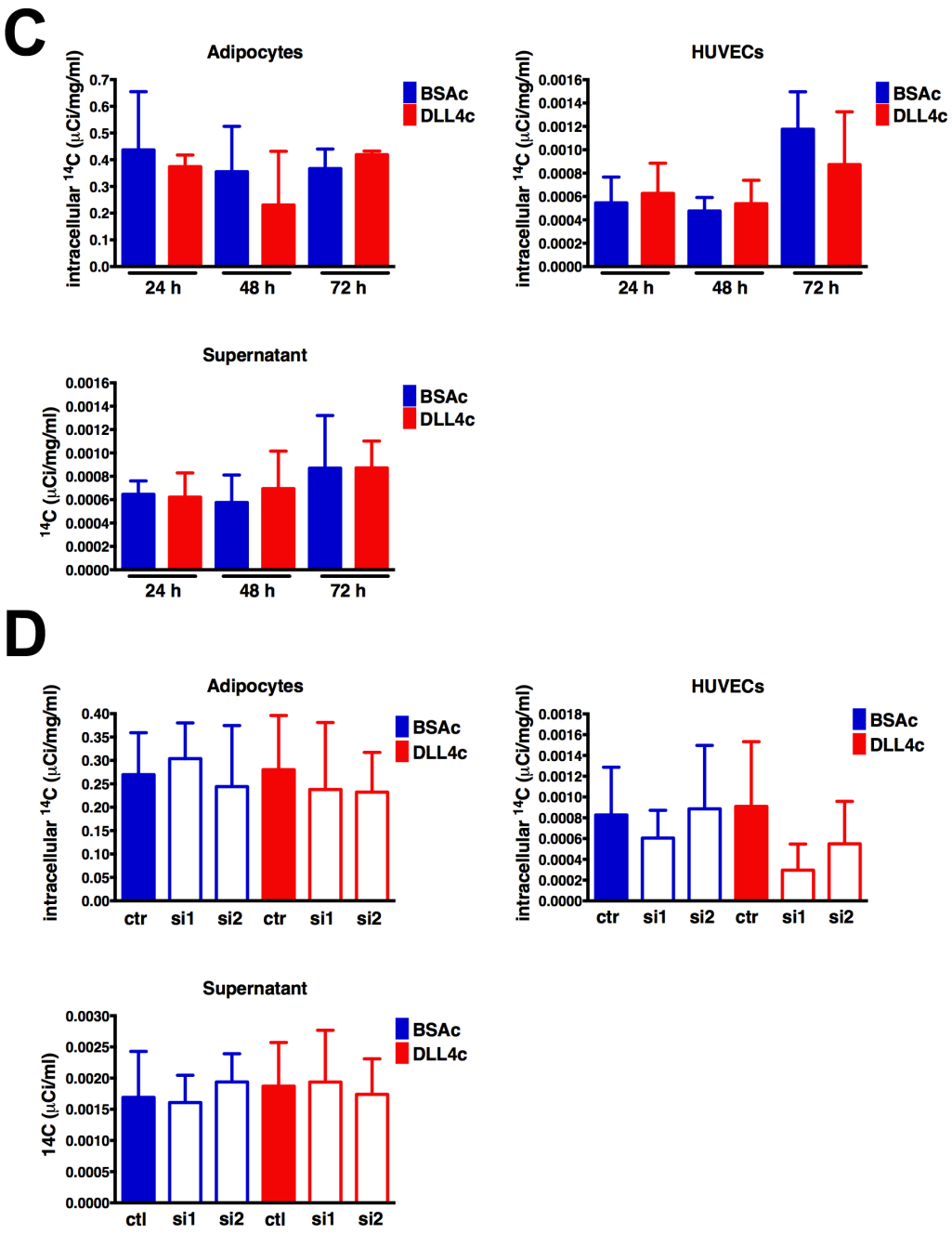


Figure 5.5 Oleic acid-derived ^{14}C-transfer from adipocytes to endothelial cells. Pre-adipocytes were isolated from healthy volunteers and expanded for 14 d. Then, cells were reseeded on tissue culture inserts, and media was changed to media containing differentiation-promoting factors, and incubated for 14 d. After 7 d, 100 µM of BSA-conjugated palmitate, oleate, and linoleate and 0.05 µCi/ml ^{14}C-oleic acid were added (A). Photographs of adipocytes at day 4, and day 14 are shown in (B). The tissue culture inserts with differentiated adipocytes were transferred to wells containing endothelial cells seeded on BSAc or DLL4c, untreated (C) or transfected with non-targeting siRNA or *fatty acid binding protein 4 (FABP4)*-targeting siRNA (D). The cells were grown in EGM2, for 24-72 h (C) or 48 h (D). Cells were harvested, supernatants collected, and analysed for ^{14}C content. Data was normalised to protein concentrations. Values are expressed as mean +/- S.D (C, D).

5.3 Discussion

5.3.1 Role of FABP4 as a downstream target of DLL4-NOTCH in sprouting

In this chapter, it was hypothesised that FABP4, as a downstream effector of DLL4-NOTCH signalling, may promote stalk cell formation during sprouting and that FABP4 inhibition may lead to hypersprouting.

The results presented here do not support this hypothesis. Sprouting was investigated in HUVEC with transient siRNA-mediated knockdown of *FABP4* or F4I treatment in normal EGM2, containing a range of growth factors and cytokines (including epidermal growth factor, VEGF, FGF and IGF-1). When *FABP4* expression was reduced by siRNA by at least 70% (stable for >48 h), there was no change observed in sprout length or number. When FABP4 was inhibited by 20 or 30 μM F4I, proliferation and migration (processes that are increased when DLL4-NOTCH is inhibited) were decreased (this needs validation by transient FABP4 knockdown). At 30 μM F4I, sprout length and number were reduced. However since 30 μM was above the growth EC50 and siRNA transfection did not lead to a similar effect, this may be due to possible toxicity.

5.3.1.1 Limitations of the study

The sprouting assay with siRNA-transfected cells showed very few sprouts in the control condition (Fig. 5.2), possibly indicating that the basic ability of cells to sprout was low. Any change in sprouting ability due to *FABP4* knockdown might have been very subtle because of the already low ability. To control for this, the capacity of the cells to sprout could have been verified by including positive and negative control drug treatments in the sprouting assay: DBZ to inhibit NOTCH signalling, leading to hypersprouting, and Sunitinib to inhibit VEGFA signalling, leading to reduced sprouting. Furthermore, the siRNA transfection might have decreased the cells' ability to sprout. Optimisation of the lipofectamine concentration, the time of incubation, and the siRNA concentrations to knockdown *FABP4* specifically for the sprouting assay might help improve the experiment. A reduction of sprout formation was

not detected, although 20 μM F4I led to inhibition of endothelial proliferation and migration. However, the sprouts were thinner when FABP4 was inhibited, a change which could not be quantified with the current method of analysis. Sprout number and length were analysed using the ImageJ software, by manually tracing the sprout using the line tool and recording sprout length and number of each spheroid. Very subtle changes in sprout length might be masked due to the manual way of analysis and might have been missed. An automated, software-based approach would improve the analysis and help detecting small changes in sprout length and record other parameters like the width of the sprouts. Furthermore, tube formation, maturation, and lumen formation of the vessels were not determined in the present assays and are relevant to determine the function of FABP4 in angiogenesis.

5.3.1.2 Interpretation of the results and possible ways of improving the experimental strategy

In the tested conditions, FABP4 inhibition did not lead to hypersprouting, suggesting that FABP4 is not involved in promoting stalk cell formation downstream of NOTCH during sprouting. Elmasri *et al*. suggested a role of FABP4 in supporting proliferation, migration, and sprout formation. Elmasri investigated sprouting in *FABP4* -/- mouse aortic ring explants in response to bFGF stimulation (Elmasri, Ghelfi *et al.* 2012). A significant reduction of sprout length or number was not observed in the present study, which does not back a pro-angiogenic role of FABP4 as suggested by Elmasri.

Apart from limitations in the experimental setup and analysis method as outlined above, the discrepancy between the present findings and the Elmasri findings may be based on different levels of expression of FABP4 in the two different cell types (mouse versus human)/experimental models used, and/or on different levels of FABP4 inhibition compared to the control. VEGFA or DLL4c stimulation leads to a 4-12-fold induction of FABP4 protein levels in HUVEC (see chapter 4). If FABP4 protein expression was low at the beginning of the sprouting assay and FABP4 levels were not sufficiently induced by the activation of NOTCH signalling during the course of the assay, then a reduction of FABP4 by RNAi or

inhibition by F4I would likely not have a detrimental phenotypic effect. Therefore, a pre-conditioning of the cells with DLL4c to increase FABP4 protein levels prior to the start of the sprouting assay may accentuate the effects of a FABP4 inhibition by RNAi or F4I. Immunofluorescent staining of FABP4 in the sprouts could then be employed to validate FABP4 expression in tip or stalk cells. Because the cells appeared like clusters sometimes, it is worth investigating the induction of apoptosis by staining of apoptotic markers like poly ADP ribose polymerase. Furthermore, removal of the growth factors supplemented in the media and stimulation of the cells with a defined concentration of VEGFA may lead to a cleaner FABP4 induction in addition to DLL4c stimulation. Also, FABP4 induced by NOTCH signalling might be important in later stages of angiogenesis, such as tube formation and maturation of the newly established vascular network. To investigate the ability of endothelial cells to branch and differentiate, the tube formation assay can be employed, and *in vivo* models/assays like the mouse retinal angiogenesis assay, the zebrafish model, and the chicken chorioallantoic membrane angiogenesis assay can be employed to study different stages of angiogenesis in more detail (Staton, Reed *et al.* 2009). The retinal angiogenesis assay and the chorioallantoic membrane assay have now been established in the laboratory and will be used to extend the study of FABP4 in angiogenesis.

5.3.2 Role of FABP4 as a downstream target of DLL4-NOTCH in FA utilisation

5.3.2.1 Limitations of experimental set up used to study FA influx and ways of improving the experimental strategy

FABP4 was the only gene among the FA transport and activation genes investigated in chapter 4 that was significantly upregulated by DLL4-NOTCH. This led to the hypothesis that FABP4 may contribute to increased FA utilisation in endothelial cells in response to DLL4-NOTCH. Inhibition of *FABP4* by *FABP4* or *FOXO1* siRNA transfection or by F4I treatment however did not lead to a decrease of ^{14}C-accumulation from extracellular ^{14}C-OA, as an indicator of FA influx, nor to a change of influx of ^{14}C derived directly from adipocytes. These results do not support the hypothesis that upregulation of FABP4 is a key regulator of

FA influx in endothelial cells. These assays however are only indirect indicators of FA utilisation in cells and do not represent the range of aspects investigated in chapter 3. The role of FABP4 might be in FA partitioning towards only a specific organelle, in regulation of gene expression, or dependent on the presence or absence of other genes and signalling pathways. Furthermore, it might be that FABP4 indeed increases FA accumulation, but that these are used up or secreted at a high turn over rate. Therefore, investigating the change of FA over a shorter time course might be useful.

Niemann *et al.* have shown that FABP4 expression was linked to increased FA uptake and oxidation in ovarian cancer cells (Nieman, Kenny *et al.* 2011). This phenotype is similar to the one presently observed in response to DLL4-NOTCH activation, showing increased FA influx and oxidation. Therefore, a more thorough analysis of FA metabolism when FABP4 is inhibited is needed in order to make more informed assumptions about the role of FABP4 in endothelial cell metabolism in response to DLL4-NOTCH. However this could not be done before submission of this thesis due to time constraints. Detailed analysis of the effect of DLL4-NOTCH and FABP4 inhibition on FA oxidation, and the metabolic fate of FAs by 13C-tracer analysis would be helpful to test this.

Co-culture of adipocytes and endothelial cells, in which the transfer of FAs from adipocytes to endothelial cells at a distance was investigated, was successful in principle in that ^{14}C was detected in endothelial cells derived from adipocyte lipid stores. Adipocytes grown in EGM2 were able to release FAs from intracellular stores, as lipolytic stimulation by isoprenaline or inhibition by insulin in differentiated adipocytes grown in EGM2 showed a 33-fold increase or 0.5-fold decrease of NEFA release, respectively (see Appendix I, Fig. 0.4). However, the concentration of ^{14}C derived from adipocytes was 100 times higher in the adipocyte chamber (tissue culture insert), than in the HUVEC chamber (well), indicating that the media exchange through the membrane was low and consequently HUVEC were exposed to comparably very low concentrations of ^{14}C. Increasing the FA release by adipocytes in the media that endothelial cells are exposed to and creating a steeper concentration gradient, thereby increasing the basal gradient-dependent rates of FA influx might improve the experimental

setup. To achieve this, a membrane with larger pores could be considered to increase the media exchange rates. Alternatively, a direct co-culture with physical contact of the two different cell types could be considered to circumvent the problem observed in the system with two separate chambers, in which the media cannot exchange properly. Another possibility would be to use pre-conditioned media adipocytes have been growing in and add it to HUVEC. Eventually, similar experiments may be performed with tumor cells that have pre-labelled lipid stores, instead of adipocytes. Tumour cells accumulate lipids in hypoxia (Bensaad, Favaro *et al.* 2014), and might release and secrete FAs upon reoxygenation, when endothelial cells revascularise the area.

5.3.2.2 Possible role of FABP4 in VEGFA or NOTCH specific regulation of gene transcriptional programs and crosstalk with other pathways

The effects of DLL4-NOTCH on FA metabolism observed in chapter 3 might also be the collective output of a slight increase of several genes and proteins involved in FA trafficking, activation, and utilisation that happen in response to extracellular fluctuations of nutrients, oxygen, and growth factor concentrations, in which case the targeting of rate-limiting enzymes like CPT1, which is the mitochondrial FA importer and targeted by the drug EX, or FAT/CD36, which is a FA transporter, would be a feasible way forward to study the targeting of FA metabolism as an anti-angiogenic therapy option. The major role of FABP4 in response to DLL4-NOTCH signalling might also not be directly in utilisation through FA delivery to respective sites of degradation or usage, but in activation of lipolytic pathways due to its interaction and activation of hormone-sensitive lipase for example (Shen, Liang *et al.* 2001, Smith, Thompson *et al.* 2007) or in regulating gene expression through ligand delivery to nuclear receptors. For example, when FABP4 binds PPARγ-activating ligands like linoleic acid or troglitazone it translocates to the nucleus for ligand delivery whereby it enhances PPARγ transcriptional activity (ligands like oleate and stearate are bound by FABP but do not lead to FABP4 nuclear translocation) (Ayers, Nedrow *et al.* 2007, Gillilan, Ayers *et al.* 2007).

Elmasri *et al*. have studied changes of gene expression in FABP4-deficient HUVEC, showing that FABP4 affects angiogenesis by regulating the expression of SCF and activating the c-kit pathway, thereby stimulating angiogenesis (Elmasri, Ghelfi *et al.* 2012). SCF stimulation in HUVEC leads to improved survival and promotes migration and tube formation and activation of AKT and ERK signalling in response to SCF contribute to the proangiogenic effects (Matsui, Wakabayashi *et al.* 2004). VEGFA signalling mediates angiogenesis via similar pathways. Signal transduction occurs through activation of VEGFR2, resulting in activation of PI3K, AKT, or ERK signalling pathways and pro-proliferative, pro-migratory, and pro-survival effects. These pathways are intermittently activated and are modified by the level of VEGFR2 activation and VEGF receptor crosstalk. Activation of DLL4-NOTCH signalling has opposing effects to VEGFA signalling. By reducing VEGFR2 and increasing VEGFR1 expression it limits VEGFA signalling (reviewed by Siekmann, Covassin *et al.* 2008). Of note, PI3K/AKT signalling and ERK signalling have been shown to promote DLL4-NOTCH signalling in the context of artery-vein specification (Hong, Kume *et al.* 2008, Deng, Larrivee *et al.* 2013), which may resemble an additional negative feedback mechanism that limits VEGFA signalling also during sprouting angiogenesis.

DLL4-NOTCH promotes the stalk cell phenotype during sprout formation. DLL4-NOTCH signalling is anti-proliferative and limits sprout formation, based on the activation of a transcriptional program that is not yet fully defined. The stalk cell phenotype is more proliferative than the rather migratory tip cell phenotype. This conundrum may be explained by the positive modulation of pro-proliferative WNT signalling by NOTCH in stalk cells, which can overrule the anti-proliferative effects of DLL4-NOTCH. This occurs via a negative feedback loop: DLL4-NOTCH signalling activates the transcription of NOTCH-regulated ankyrin repeat protein (NRARP). NRARP promotes WNT3A/ Catenin (Cadherin-Associated Protein), Beta 1 (CTNNB1) signalling via Lymphoid Enhancer-Binding Factor 1 (LEF1), and limits NOTCH signalling. Loss of NRARP, CTNNB1 or LEF1 leads to decreased endothelial cell proliferation and vessel regression. This indicates that the balance of NOTCH and WNT signalling in endothelial cells determines their proliferative state and is important for stalk

cell proliferation and sprout elongation (Phng, Potente *et al.* 2009). Therefore, it is interesting to hypothesise a pro-proliferative role of NOTCH through activation of FABP4 expression and to speculate about possible crosstalks with the c-kit or WNT signalling pathways. Investigating the effects of *FABP4* knockdown on gene expression in response to DLL4-NOTCH signalling may help to narrow down the endothelial function of FABP4 as part of this pathway and is planned for future experiments.

6 CHAPTER SIX

FABP4 in tumour angiogenesis – a pilot study

6.1 Introduction

The expression of FABP4 in the tumour stroma seems to be a relevant factor for disease progression. FABP4 is higher expressed in high-grade glioblastoma and tumour endothelial cells compared to normal (Cataltepe, Arikan *et al.* 2012) and ovarian cancer xenografts in *FABP4* -/- mice show reduced microvessel density (Nieman, Kenny *et al.* 2011), which implicates a potential role in tumour angiogenesis. DLL4 expression in serous ovarian adenocarcinomas is significantly associated with poor survival and patients responding to anti-VEGFA therapy have lower levels of DLL4 than non-responders. This indicates a role of DLL4 in anti-VEGFA therapy resistance, as was also suggested in previous studies (Hu, Lu *et al.* 2011, Li, Sainson *et al.* 2011). Mice bearing ovarian cancer xenografts and treated with mouse targeting *DLL4* siRNA show decreased microvessel density and increased tumour hypoxia. Anti-VEGFA therapy in tumour xenografts shows the greatest effect when *DLL4* expression is silenced by siRNA in the stroma and tumour compartment of tumour-bearing mice (Hu, Lu *et al.* 2011). Since FABP4 is a direct target of DLL4-NOTCH in endothelial cells, it was hypothesised that FABP4 expression in tumour endothelial cells of ovarian cancer is associated with expression of DLL4 and NOTCH. To test this hypothesis, FABP4 expression levels were investigated in human specimen of serous ovarian adenocarcinoma of different type and stage in relation to NOTCH, DLL4, and VEGFR2 expression.

Serous ovarian adenocarcinomas can be broadly classified in low-grade serous carcinomas (LGSC) (making up <5% of total ovarian carcinomas) or high-grade serous carcinomas (HGSC, SA) (70% of total). LGSC and HGSC are different tumour types and have a different genetic make-up. Serous borderline tumours (SBT), which are not classified as malignant yet, show abnormal proliferation, no stromal invasion, and a better prognosis.

Ovarian carcinoma metastases occur via cell detachment from the primary tumour in the ovary or the fallopian tube. Detached cancer cells are transported passively by the peritoneal fluid and disseminate in the peritoneal cavity. The most common site of dissemination is the omentum. SBT can disseminate and form implants on peritoneal surfaces and progress to

LGSC. The implants can be non-invasive (NII) or invasive (II). LGSC can arise from SBT, and usually do not harbor *TP53* or *Breast Cancer 1, Early Onset gene (BRCA)* mutations. HGSC are not associated with SBT, and harbor *TP53* and *BRCA* mutations (reviewed by Vang, Shih Ie *et al.* (2009), Lengyel (2010), and Prat (2012)). Peritoneal metastases of HGSC are referred to as deposits (HGCS-D) in the following text.

6.2 Results

6.2.1 Expression of FABP4, NOTCH, DLL4 and VEGFR2 in ovarian tumours

The expression levels of FABP4 in relation to NOTCH, DLL4, and VEGFR2 were investigated in patient samples of different borderline or malignant serous ovarian tumours by immunohistochemistry (IHC). All antibodies used have been validated previously, except for the FABP4 targeting antibody, which has been validated in this study (Jubb, Turley *et al.* (2009), Smith, Baker *et al.* (2010), Sliwa, Awsa *et al.* (2014); see Appendix I, Fig. 0.5). Expression patterns in SBT were compared to NII and I, and HGSC were compared to HGSC-D (Fig. 6.1 for intensity scores, Fig. 6.2 for extent). Representative images of the IHC stainings in epithelium, epithelium-associated stroma, or epithelium-associated vessels are shown in Fig. 6.3, 6.4 or 6.5, respectively. The staining in adipose-tissue associated stroma or vessels was not quantified because of the very high expression of FABP4 in these compartments and the difficulty in differentiation between vessels and adipocytes in FABP4-stained sections.

FABP4 expression was detected in all compartments of all tumour types. The intensity of FABP4 expression was equally moderate to strong (extent 10-100%) in the tumour epithelium of SBT, NII or II, and HGSC or HGSC-D (Fig. 6.3). A difference of FABP4 signal intensity in tumour epithelium close to adipose tissue or at a distance was not observed. The intensity of FABP4 expression was stronger in the stromal department of NII or II compared to the expression in the stromal department of SBT ($p<0.05$), with a higher percentage of cells positively stained (Fig. 6.4). There was a high intensity and extensive staining of FABP4 in HGSC and HGSC-D and no change between the two. FABP4 staining in the vascular department was present in most tumour cases (Fig. 6.5). In the tumour cases in which vessels were stained, FABP4 staining was more intense and extensive in NII and II compared to SBT and of equal intensity and extent in HGSC-D and HGSC.

NOTCH expression was detected in all compartments in every tumour type. The intensity of NOTCH staining in the epithelial department was moderate to strong in all tumour types investigated (Fig. 6.3). The percentage of NOTCH positively stained cells in NII and II was higher (up to >50%) than in SBT (<10%) and >10% cells were positively stained for NOTCH in HGSC-D or HGSC. NOTCH expression in the stromal department was weak in all tumours investigated, but more extensive in NII and II compared to SBT ($p<0.05$), and >10% cells were positively stained for NOTCH in HGSC-D or HGSC (Fig. 6.4). NOTCH expression in the vascular department was strong, with a higher percentage of cells stained in NII and II compared to SBT. NOTCH staining in the vessels of HGSC-D and HGSC was very strong and extensive with up to >50% of cells stained (Fig. 6.5).

DLL4 expression was weak or absent in the epithelial and stromal compartment of all cases investigated. The intensity of DLL4 staining in the vessels was stronger in NII and II compared to SBT and very strong in HGSC-D and HGSC, with a high percentage of cells positively stained (NII, II>SBT, HGSC-D=HGSC).

VEGFR2 expression was detected in all tumour types and all compartments. There was moderate to strong staining in NII and II, compared to weak to moderate staining in the epithelium, with more cells positively stained in NII and II compared to SBT. The extent of staining in HGSC-D and HGSC was high, but the staining only weak to moderate (Fig. 6.3). VEGFR2 expression in the stroma was weak to very strong in NII and II, where up to >50% of cells were positively stained, compared to weak to moderate and less extensive staining in SBT stroma ($p<0.05$ for intensity and extent) (Fig. 6.4). VEGFR2 staining in the vessels of SBT and NII was weak to moderate, and weak to strong in II ($p<0.05$). Staining in NII and II was more extensive than in SBT. VEGFR2 staining was stronger and more extensive in HGSC-D compared to HGSC, where it was weak or absent (Fig. 6.5).

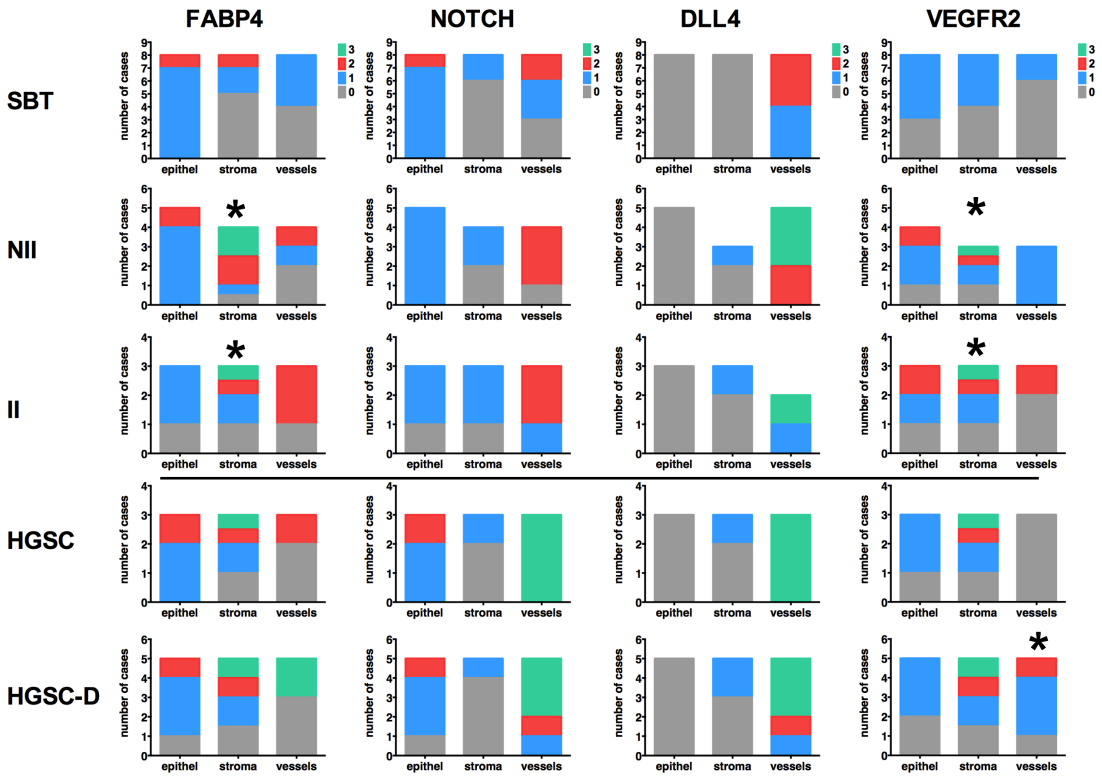


Figure 6.1 Intensity scoring of immunohistochemial stainings of serial sections of human ovarian cancer specimen. Sections stained for fatty acid binding protein 4 (FABP4), NOTCH, DLL4 or VEGFR2 were scored (0=negative/ weak, 1=moderate, 2=strong, 3=very strong) for intensity in the epithelial, stromal, or vessel compartment. Statistical analysis was performed using the Chi-Square test (*$p<0.05$). Scores of serous borderline tumours (SBT) were compared to scores of non-invasive implants (NII) and invasive implants (II). Scores of high-grade serous adenocarcinomas (HGSC) were compared to scores of peritoneal deposits of HGSC (HGSC-D).

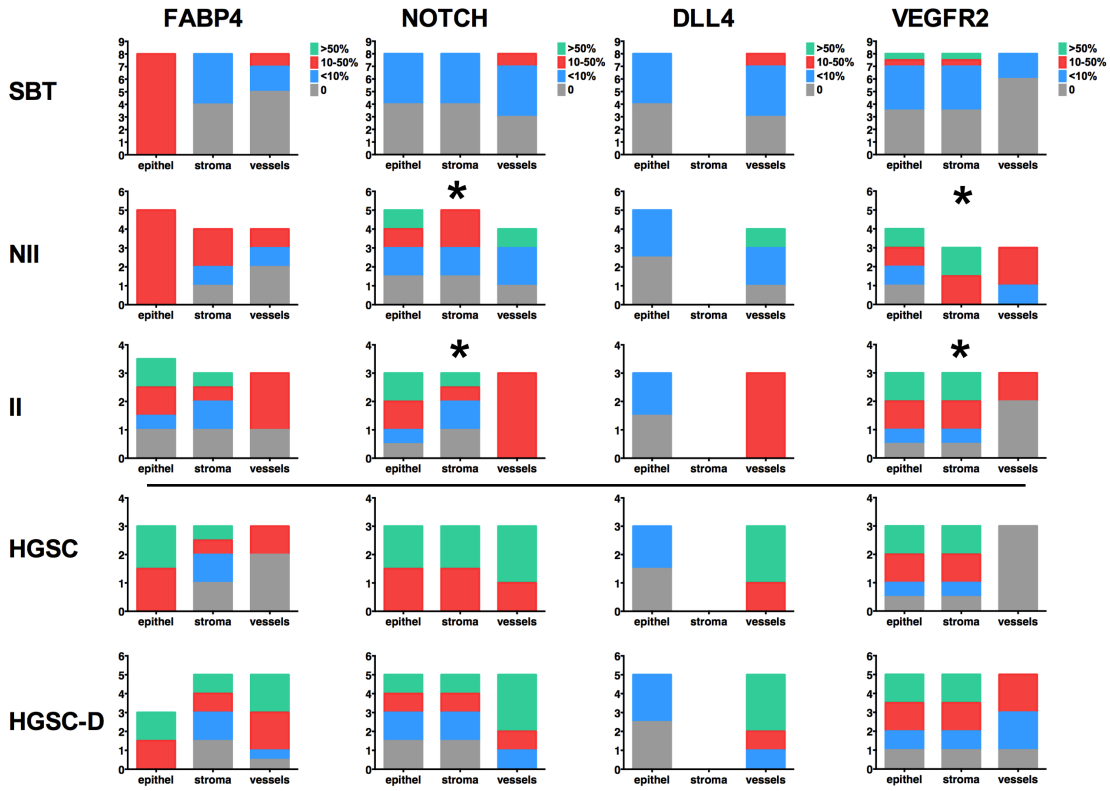


Figure 6.2 Extent scoring of immunohistochemial stainings of serial sections of human ovarian cancer specimen. Sections stained for fatty acid binding protein 4 (FABP4), NOTCH, DLL4 or VEGFR2 were scored for extent of positively stained cells in the epithelial, stromal, or vessel compartment. Statistical analysis was performed using the Chi-Square test (*$p<0.05$). Scores of serous borderline tumours (SBT) were compared to the accumulative scores of non-invasive implants (NII) and invasive implants (II). Scores of high-grade serous adenocarcinomas (HGSC) were compared to scores of peritoneal deposits of HGSC (HGSC-D).

6.2.1.1 Epithelium

FABP4 in the epithelial compartment was present in the cytoplasm of columnal (yellow arrows) and polygonal cells (red arrows). Polygonal cells are secretory cells that are more likely to detach and invade than columnal epithelial cells. It was observed that the staining in polygonal cells was more diffuse than in columnal cells. VEGFR2 and NOTCH staining was similar to FABP4 staining in the epithelial compartment, and was detected in polygonal and columnal cells. NOTCH staining was present in the cytoplasm (Fig. 6.3, top middle panel) and at the membrane (Fig. 6.3, bottom middle panel). VEGFR2 staining was mainly at the membrane. DLL4 was not detected in the epithelial compartment (Fig. 6.3).

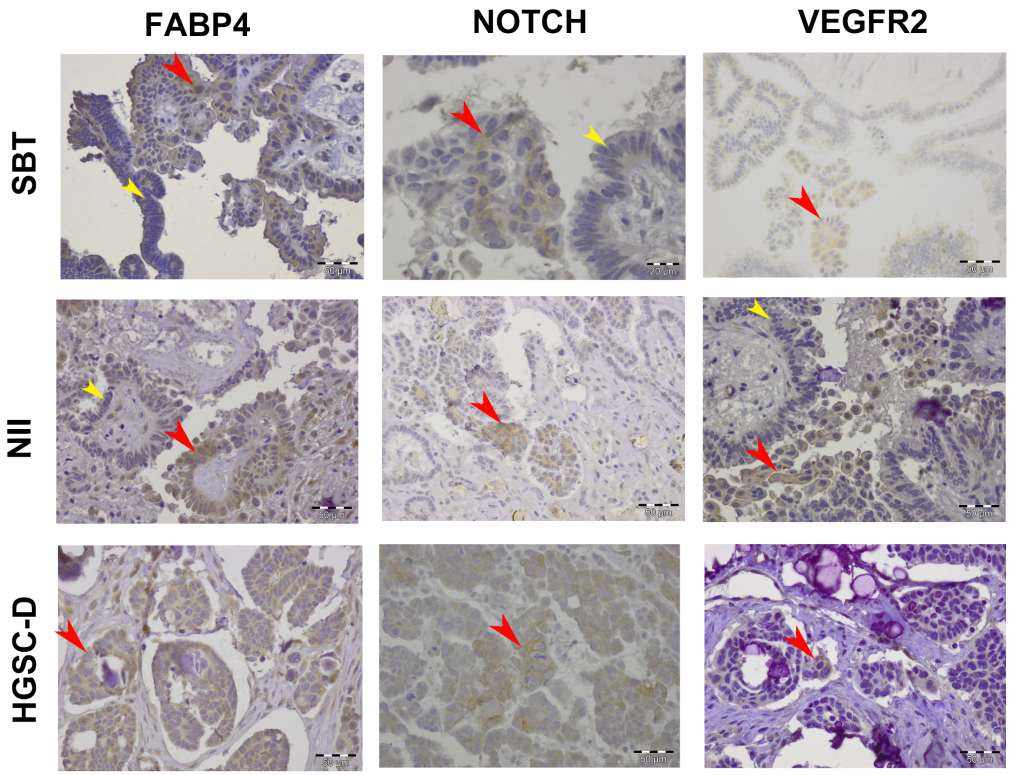


Figure 6.3 Representative immunohistochemical staining for fatty acid binding protein 4 (FABP4), NOTCH and VEGFR2 in epithelium of serial sections of ovarian serous borderline tumours (SBT), invasive implants (NII), and high grade serous carcinomas deposits (HGSC-D). Red arrows indicate polygonal cells, yellow arrows indicate columnal cells.

6.2.1.2 Epithelium-associated stroma

The stromal compartment (red arrow, epithelial compartment yellow arrows) in SBT stained very weakly for FABP4, VEGFR2, or NOTCH. In more advanced or aggressive tumours like NII, or HGSC, the stromal compartment was strongly stained for FABP4 and VEGFR2. NICD was stained in parts of the stromal compartment but not as extensive as FABP4 and VEGFR2. It was observed that VEGFR2 was not consistently stained in the vessels, however the specificity of the antibody used has been validated previously (Smith, Baker *et al.* 2010, Molhoek, Erdag *et al.* 2011). DLL4 was not detected or was very weakly stained in the stromal compartment (Fig. 6.4).

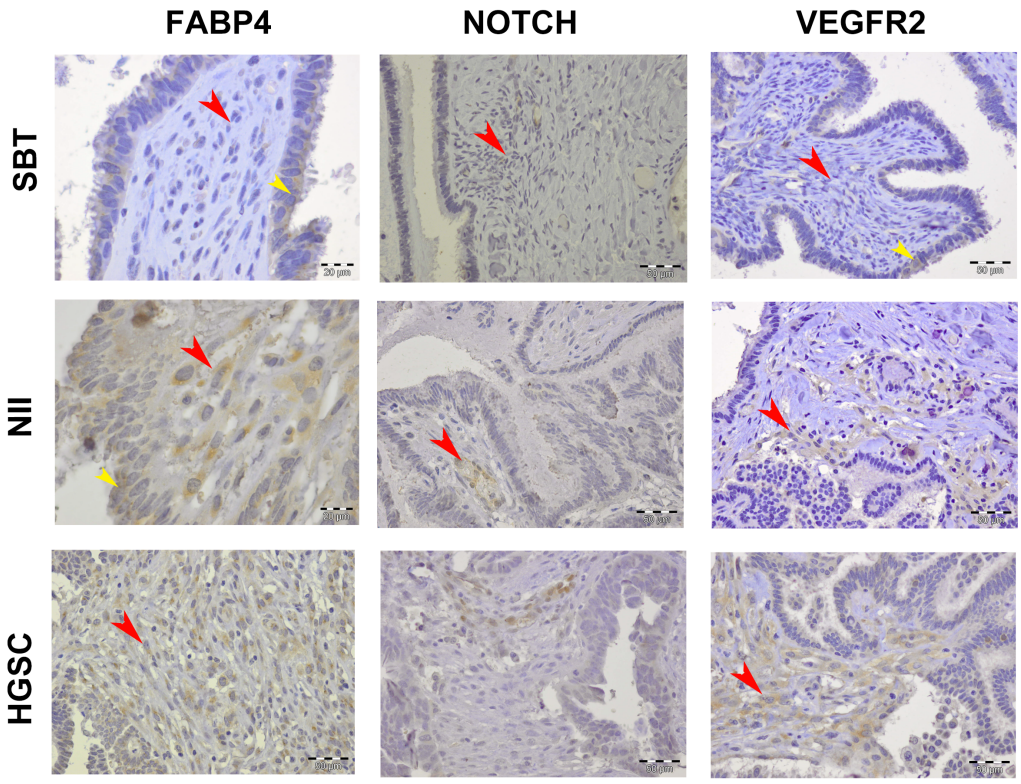


Figure 6.4 Representative immunohistochemical staining for fatty acid binding protein 4 (FABP4), NOTCH and VEGFR2 in epithelium-associated stroma of serial sections of ovarian serous borderline tumours (SBT), non-invasive implants (NII), and high greade serous carcinomas (HGSC). Red arrows indicate stromal cells, yellow arrows indicate epithelial cells.

6.2.1.3 Epithelium-associated vessels

FABP4 was present in the vessels of all tumour types and stronger in NII than in SBT. VEGFR2 was present but not changed. NOTCH and DLL4 were stained stronger and more extensive in vessels of more NII or HGSC compared to SBT, but also present in SBT.

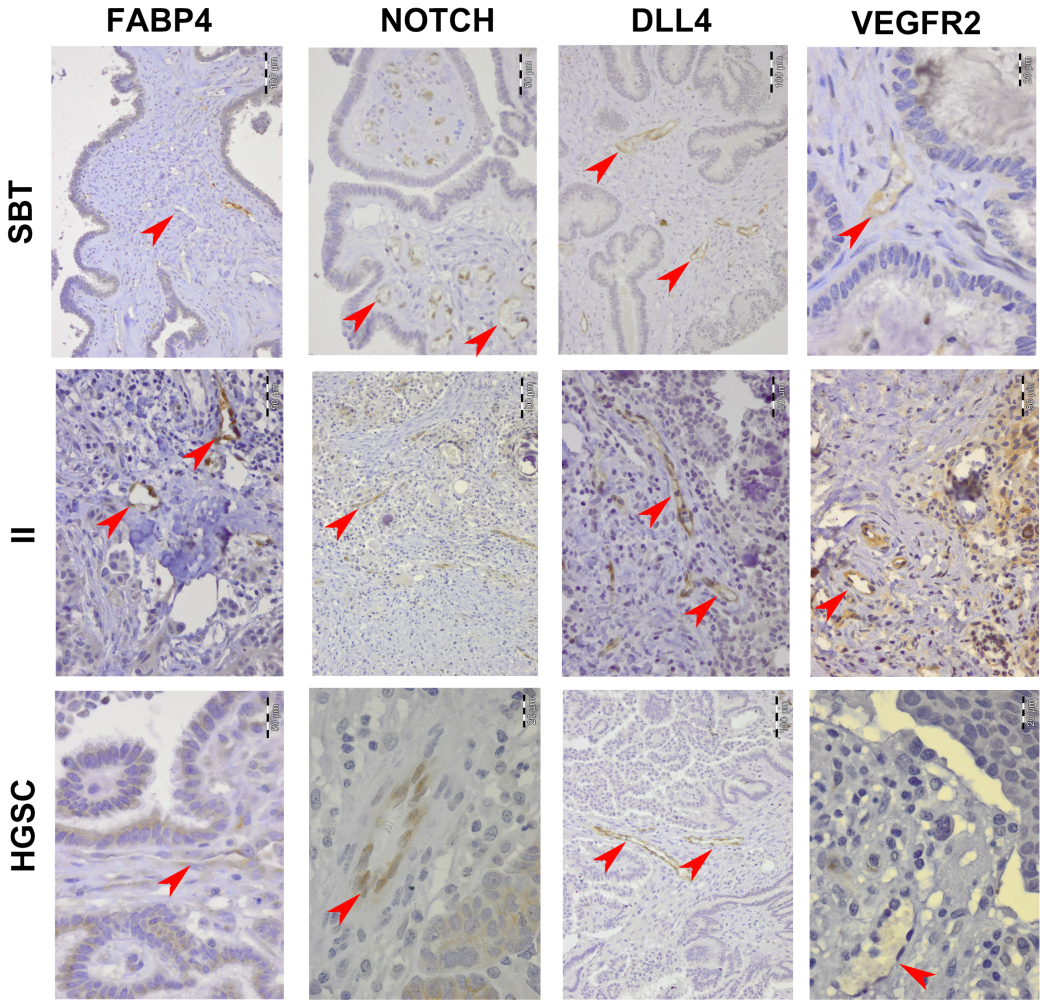


Figure 6.5 Representative immunohistochemical staining for fatty acid binding protein 4 (FABP4), NOTCH, DLL4 and VEGFR2 in epithelium-associated vessels of serial sections of ovarian serous borderline tumours (SBT), invasive implants (NII), and high-grade serous carcinoma (HGSC). Red arrows indicate vessels.

6.3 Discussion

This chapter investigated the hypothesis that FABP4 expression in tumour endothelial cells of ovarian cancer is associated with the expression of DLL4 and NOTCH. An IHC pilot study was performed in which the FABP4 expression in patient samples of human ovarian cancer in relation to expression of NOTCH, DLL4 and VEGFR2 was investigated.

Nieman *et al.* reported that FABP4 was upregulated in tumour cells in omental metastases compared to the primary tumour in the ovary (Nieman, Kenny *et al.* 2011). They described that the expression of FABP4 was stronger in tumour epithelium close to adipose tissue, compared to distant tumour epithelium. In the present study, FABP4 was expressed in the tumour epithelium of primary tumours and metastasised tumours and there was no significant change in expression. The expression patterns of FABP4, VEGFR2, and NICD in the different cells of the epithelial compartment (columnal and polygonal cells) were strikingly similar. Therefore it could be speculated that there is a functional connection of FABP4 induction and NOTCH or VEFGR2 signalling in tumour cells. Loss of FABP4 is associated with urothelial carcinoma progression (Ohlsson, Moreira *et al.* 2005). *In vitro*, prostate and breast cancer cells show a downregulation of expression compared to normal tissue, indicating a possible tumour suppressor function of FABP4 (Das, Hammamieh *et al.* 2001, Hammamieh, Chakraborty *et al.* 2005). Overexpression of FABP4 in prostate cancer cells leads to increased apoptosis, although the mechanism is unknown (De Santis, Hammamieh *et al.* 2004). Since there is no study *in vivo* about the functional significance of tumour epithelial FABP4 expression for tumour growth, this is a field that requires further investigation.

The tumour microenvironment contains a population of cancer-associated fibroblasts that have higher proliferation rates than normal fibroblasts and contribute to tumour progression through secretion of factors that stimulate angiogenesis, inflammation, and oncogenesis (reviewed by Madar, Goldstein *et al.* (2013)). An interesting observation was therefore the strong expression of FABP4 and VEGFR2 and partly NICD, in the stromal non-adipose tissue of invading tumours, compared to SBT. This has not been reported before. The expression of

FABP4 and VEGFR2 in the stroma of progressed ovarian cancer raises speculation about a possible role of these proteins in the activation of this phenotype in resident fibroblasts and its tumour-promoting activity. In *FABP4* -/- mice, growth and metastasis of ovarian cancer xenografts is accelerated, which Nieman *et al.* attributed to the lack of FABP4 expression in adipose tissue and the lack of FABP4 mediated cancer cell-adipocyte interaction (Nieman, Kenny *et al.* 2011). However, the expression of FABP4 in cancer-associated fibroblasts that is here reported may be contributing to the acceleration of tumour growth in the *FABP4* -/- model. Furthermore, FABP4 expression has been reported in macrophages and is associated with the modulation of inflammatory responses. FABP4 silencing interferes with the production of pro-inflammatory cytokines such as interleukin 1β, tumour-necrosis factor-α, and monocyte chemoattractant protein 1, and with the function of inducible nitric oxide synthase (iNOS), cyclooxygenase 2, and the activity of the inhibitor of kappa kinase (IKK)-nuclear factor κB (NF- κB) pathway (Makowski, Brittingham *et al.* 2005). FABP4 expression in cancer-associated fibroblasts might contribute to the promotion of pro-inflammatory signalling pathways and cytokines and promote tumour growth via paracrine stimulation of angiogenesis, inflammation, and tumour cell proliferation. In this regard, it would be interesting to investigate the expression of FABP4 in tumour-associated macrophages and determine the role of FABP4 in tumour-associated inflammatory responses.

DLL4 induces NOTCH signalling in macrophages and is upregulated by pro-inflammatory stimuli. It has been shown to induce inflammatory signalling pathways like NF-kB and iNOS (Fung, Tang *et al.* 2007). The mechanism of FABP4 induction in cancer-associated fibroblasts or macrophages may be paracrine and dependent on DLL4-NOTCH signalling, which needs further investigation. In addition, epithelial mesenchymal transition (tumour epithelial cells acquiring mesenchymal-like properties, EMT), which contributes to the population of cancer-associated fibroblasts and cancer stem cells, is regulated by NOTCH in lung cancer and pancreatic cancer (Bao, Wang *et al.* 2011, Xie, Zhang *et al.* 2012). Interestingly, FABP4 gene expression is downregulated in the stromal compartment of pre-

invasive and invasive breast cancer compared to normal breast tissue (Ma, Dahiya *et al.* 2009). Increased plasma levels of FABP4 are associated with increased breast cancer risk (Hancke, Grubeck *et al.* 2010, Holm, Ueland *et al.* 2011, Djousse and Gaziano 2012). This indicates a potential correlation of FABP4 expression in adipose tissue, its secretion, and breast cancer progression and that the role of FABP4 in the tumour microenvironment may be dependent on the tumour type.

The intensity of vascular FABP4 expression was high in the tumours investigated. Interestingly, the extent of FABP4 positively stained cells was highest in HGSC-D, which are omental metastases of HGSC. NICD and DLL4 expression in vessels was strongest in invading or metastasising tumours, suggesting a potential link between DLL4-NOTCH signalling induction and FABP4 expression in these vessels. Since both FABP4 and DLL4 have been linked independently to tumour angiogenesis in ovarian cancer, this is an interesting observation that needs further studies to define the functional relationship between DLL4-NOTCH signalling and FABP4 in tumour angiogenesis.

The expression of FABP4 in the stromal and vascular compartment of ovarian tumours correlated with the expression pattern of VEGFR2 and NOTCH in the stroma and partly with that of DLL4 and NOTCH in endothelial cells. These observations point to a possible relation between the activation of DLL4 expression by VEGFA via VEGFR2 and NOTCH in tumour endothelial cells, and the activation of NOTCH signalling in the tumour stroma and endothelium, potentially leading to increased expression of FABP4. However, there are only a small number of cases and the analysis will be expanded in the near future.

7 CHAPTER SEVEN

Concluding remarks and future directions

In 2009, the number of studies investigating tumour angiogenesis in relation to metabolism was limited to three. These studies had investigated the effects of lactate, which is high in the tumour tissue, on angiogenesis (Hunt, Aslam *et al.* 2007, Vegran, Boidot *et al.* 2011), the effects of glycogen degradation as a rapidly accessible source for glucose, and the pentose phosphate pathway activity in response to VEGFA and bFGF (Vizan, Sanchez-Tena *et al.* 2009). Most recently, the Carmeliet research group has shown great interest in the detailed investigation of major metabolic pathways that are required for angiogenesis. Since DLL4-NOTCH signalling was found to inhibit glycolysis (De Bock, Georgiadou *et al.* 2013), the researchers hypothesised that the "regulation of metabolism is a (perhaps even "the") key activity of NOTCH driving stalk cell formation". This puts emphasis on the present study to meet the emerging interest and contribute significantly to the field of endothelial metabolism as a therapeutic target.

7.1 Summary

Figure 7.1 shows a summary of the findings and hypotheses derived from this thesis, which will be described in the following paragraphs. The aims of this thesis were firstly to characterise the metabolism in endothelial cells in response to the activation of the DLL4-NOTCH signalling pathway and to investigate the effect of metabolic interference on angiogenesis. Certain aspects of FA metabolism were found to be upregulated when DLL4-NOTCH signalling was activated, whereas glycolysis was downregulated. In particular, FA storage and oxidation were upregulated in certain conditions, indicating that DLL4-NOTCH signalling leads to a shift in metabolism from glucose to the utilisation of FAs in endothelial cells. Inhibition of FA oxidation by EX led to reduced sprouting of endothelial cells and caudal vein plexus formation in zebrafish. Secondly, this thesis aimed at developing an understanding of potential pathways involved and investigating potential targets of NICD mediated transcription that may drive the observed metabolic phenotype. The regulation of candidate genes involved in FA transport and activation were investigated. Among those investigated, FABP4 was the only one found to be significantly induced by DLL4-NOTCH.

Further investigation showed that FABP4 was regulated by NOTCH on the level of gene transcription, which was dependent on the presence of the transcription factor FOXO1. Thirdly, this thesis analysed the effect of DLL4-NOTCH mediated effects on metabolism and FABP4 in angiogenesis using relevant coculture models and IHC staining of FABP4 in human tumour tissue. Although a strong candidate for regulation of the phenotypic changes observed when DLL4-NOTCH was activated, a direct link between FABP4 upregulation and FA utilisation could not be confirmed in this thesis. In tumour tissue, FABP4 expression in vessels of progressed ovarian cancer was correlated with increased expression of DLL4-NOTCH. FABP4 expression may contribute to resistance to anti-VEGFA therapy observed when DLL4-NOTCH is upregulated in tumours.

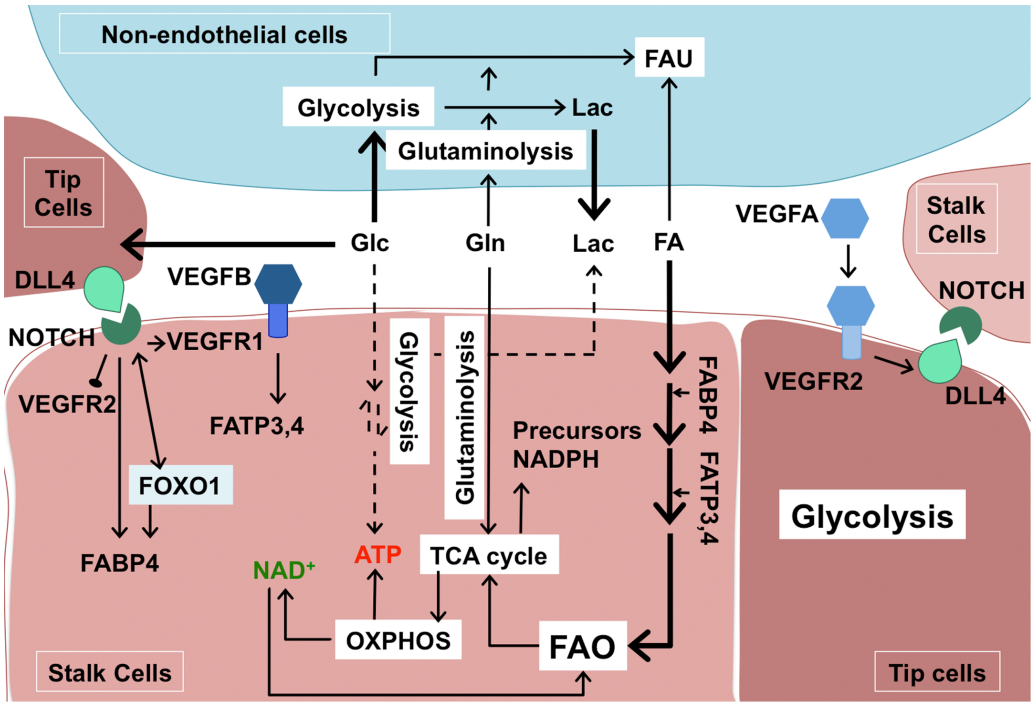


Figure 7.1 DLL4-NOTCH-induced endothelial cell metabolism in relation to the tumour metabolic environment. Cells in the tumour microenvironment such as tumour cells and fibroblasts can be highly glycolytic and glutaminolytic and have increased glucose (glc) uptake and increased lactate (lac) secretion. Fatty acids (FAs) are utilised (FAU) by non-endothelial cells for lipid synthesis, FA oxidation, etc. In tumour tissue VEGFA secretion and binding to VEGF receptor 2 (VEGFR2) on endothelial cells leads to tumour angiogenesis. VEGFA/VEGFR2 signalling promotes the tip cell phenotype and induces Delta-like ligand 4 (DLL4). DLL4-NOTCH signalling in adjacent cells promotes the stalk cell phenotype and regulates expression of VEGFR2 (inhibition) and VEGFR1 (activation). Oxidative phosphorylation (OxPhos) leads to increased NAD+, which is required for FA oxidation (FAO). FAO is activated in response to DLL4-NOTCH signalling, and related to increased FA influx, possibly promoted by expression of FA binding protein 4 (FABP4), FA transport protein 3 (FATP3) and FATP4 in the stalk cells *in vivo*. DLL4-NOTCH signalling induces transcription of FABP4, which requires the presence of FOXO1, possibly resembling a co-dependent regulatory mechanism by NOTCH and FOXO1. VEGFB binding to VEGFR1 promotes FATP3 and FATP4 expression. DLL4-NOTCH signalling decreases glc uptake and lac secretion, thereby reducing the glycolytic rate. Glutamine (gln) uptake and glutaminolysis is at least maintained in response to DLL4-NOTCH signalling. Increased FAO may promote the synthesis of precursor molecules for DNA and protein synthesis and NADPH regeneration via the tricarboxylic acid (TCA) cycle, and ATP production and NAD+ regeneration via the TCA cycle and OxPhos.

7.2 FA metabolism - a metabolic niche for tumour endothelial cells?

Given the notion that tumour cells are generally highly glycolytic, a decreased dependence of endothelial cells on glycolysis during sprouting or maintenance processes, with a shift towards other energy substrates, would potentially be an advantage. Tumour tissues are highly plastic and heterogeneous and subpopulations of tumour tissues can differ in their metabolic phenotype and might even support each other (e.g. reverse Warburg effect: tumour cells support aerobic glycolysis in cancer-associated fibroblasts, and the produced lactate is taken up by tumour cells and used for OxPhos, Pavlides, Whitaker-Menezes *et al.* (2009)). The Nieman study further demonstrates the plasticity of tumour cells and their ability to adapt to different microenvironments (Nieman, Kenny *et al.* 2011). Tumour endothelial cells are exposed to intermittent hypoxia and expected to form new sprouts in hypoxic regions. Hypoxia further increases glycolysis and FA synthesis is slightly increased in hypoxia (Furuta, Pai *et al.* 2008). However, Bensaad *et al.* showed that hypoxic tumour cells have greatly increased FA uptake and incorporation into TG, which can be accessed and used for FA oxidation to promote cell survival upon re-oxygenation. This increase in uptake accounts for the majority of FA increase in hypoxia, rather than synthesis. This effect was higher in breast tumour cells than in glioma cells (Bensaad, Favaro *et al.* 2014). The extent of exogenous FA availability for angiogenesis in non-perfused areas will therefore vary in different tumour types and depend on surrounding tissues. In perfused areas, endothelial cells have the most immediate access to dietary FAs. Given the high plasticity of endothelial cells and their intrinsic capacity to defer glycolysis in favour of FA oxidation (Dagher, Ruderman *et al.* 2001), the function of FA metabolism in vessel development and maintenance and its possible targeting in the tumour tissue is crucial to understand.

7.3 Integration of FA metabolism by signalling pathways in the vasculature

It seems a paradox that DLL4-NOTCH signalling, although anti-proliferative, increases FA oxidation, thereby contributing to the proliferation of stalk cells during sprouting. The stalk cell promoting signalling network consists of multiple players with the WNT and NOTCH signalling pathways possibly being at the core. However, other pathways have emerged whose role in metabolism may be a considerable factor in the observed metabolic phenotype in response to NOTCH.

7.3.1 VEGFB

VEGFB has (limited) mitogenic properties in endothelial cells and acts as a survival factor for endothelial cells, vascular smooth muscle cells, and pericytes that stabilise the vasculature. It protects these cells from apoptosis in conditions of oxidative stress or serum starvation (Olofsson, Korpelainen *et al.* 1998, Zhang, Tang *et al.* 2009). VEGFB withdrawal inhibits choroidal and retinal neovascularisation (Zhang, Tang *et al.* 2009). Gene expression profiling of smooth muscle cells shows an inhibition of apoptosis related genes by VEGFB and VEGFR1 signalling (Li, Zhang *et al.* 2008). VEGFB stimulation leads to upregulation of DLL4 (Bry, Kivela *et al.* 2010), possibly promoting DLL4-NOTCH signalling, which upregulates VEGFR1, as part of a feed-forward loop.

VEGFB has been shown to promote FA uptake in endothelial cells via upregulation of FATP3 and FATP4. This effect is dependent on its binding and signalling via neuropilin 1 and VEGFR1 and may be important for cross-endothelial transport of FA to peripheral tissues (Hagberg, Falkevall *et al.* 2010). VEGFB expression is correlated with mitochondrial gene expression, indicating that cells that are producing and secreting VEGFB are simultaneously prepared for increased mitochondrial oxidation of incoming FAs. This notion was investigated in a type 2 diabetes mouse model and high-fat diet rats, in which pathological lipid deposition in peripheral tissue and lipid-induced insulin resistance in muscle tissue

occurs. Inhibition of VEGFB by genetic deletion or administration of a VEGFB neutralising antibody led to improvement of insulin resistance and decreased dyslipidemia, showing that targeting VEGFB and the vasculature as a FA transport barrier is a valid therapy option for metabolic disease (Hagberg, Mehlem *et al.* 2013).

The role of VEGFB in tumour biology is less well studied. VEGFB is expressed in breast tumours, melanoma, and head and neck tumours, in tumour cells as well as in tumour endothelial cells (Salven, Lymboussaki *et al.* 1998). VEGFB expression correlates with lymph node metastasis in breast cancer and is present in tumour cells and occasionally in stromal and endothelial cells in breast cancer and correlates with microvessel density in head and neck tumours (Gunningham, Currie *et al.* 2001, Shintani, Li *et al.* 2004, reviewed by Fischer, Mazzone *et al.* 2008). VEGFR1 is upregulated by DLL4 and increased in DLL4-overexpressing, anti-VEGFA therapy resistant tumour xenografts (Harrington, Sainson *et al.* 2008, Li, Sainson *et al.* 2011). VEGFR1 induction by NOTCH increases endothelial cell sensitivity to the VEGFR1 ligand PlGF, indicating that VEGFR1 may not simply act as a 'VEGFA sink', but contribute to NOTCH signalling during angiogenic sprouting (Funahashi, Shawber *et al.* 2010). It is tempting to speculate that DLL4-NOTCH signalling sensitises endothelial cells to VEGFB signalling via upregulation of VEGFR1 and promotes FA uptake via this pathway as well (see also Fig. 7.1). Since VEGFB is not a component of endothelial culture media, this mechanism is not contributing to the regulation of FA influx investigated in this thesis, but may potentiate it, and come into effect *in vivo*.

7.3.2 PGC-1α

PGC-1α is a transcriptional co-activator that functions in cells that experience nutrient and oxygen deprivation and stimulates vascularisation of the deprived areas. PGC-1α binds to and activates several transcriptional factors and, depending on the factor, and the tissue, promotes the expression of gluconeogenesis (hepatocytes), respiratory chain (muscle, heart), and/or FA oxidation (muscle, heart) genes (Herzig, Long *et al.* 2001, Russell, Mansfield *et al.* 2004). The function of endothelial PGC-1α has been studied only to a limited extent and seems to be

anti-angiogenic at least in part through activation of NOTCH via ADAMTS10 (A Disintegrin-Like And Metalloprotease (Reprolysin Type) With Thrombospondin Type 1 Motif, 10), as overexpression inhibits capillary sprout formation and HUVEC migration, which is rescued by γ-secretase inhibition. VEGFA stimulation inhibits PGC-1α expression in endothelial cells (Sawada, Jiang *et al.* 2014). Furthermore, PGC-1α controls expression of FOXO1, VEGFA, Angiopoietin 2 and VEGFB and several long chain FA transporters in different cell types (reviewed by Hagberg, Mehlem *et al.* 2013).

7.3.3 Nitric oxide (NO)

NO acts as a vasodilator and signalling molecule, regulating angiogenesis, blood flow, vascular permeability, leukocyte–endothelial interaction, platelet aggregation, and microlymphatic flow. NO production is a target in anti-vascular tumour therapy. Tumour blood flow can be maintained and dynamically altered by NO level modulation. NO has also been shown to regulate vascular permeability (reviewed by Fukumura, Kashiwagi *et al.* 2006). In the established tumour vasculature, blood flow can be intermittent, thereby hampering the delivery of chemotherapeutic agents, changing cellular responsiveness, and promoting resistance to therapy.

DLL4-NOTCH signalling promotes genes involved in vasoconstriction and blood flow, thereby controlling post-angiogenic vascular morphology (Lobov, Cheung *et al.* 2011). Endothelial cells are the main producers of NO and express endothelial NO synthase (eNOS). NOTCH and FABP4 have been independently linked to promoting eNOS expression (Elmasri, Ghelfi *et al.* 2012, Patenaude, Fuller *et al.* 2014). Endothelial cell specific inhibition of NOTCH leads to reduced function of the tumour vasculature and reduced tumour growth, an effect dependent on eNOS modulation by NOTCH (Patenaude, Fuller *et al.* 2014). Moreover, eNOS and NO may be involved in controlling FA metabolism, as it has been shown that *eNOS* knock out mice have reduced FA oxidation in isolated mitochondria and reduced expression of FA uptake and/ or oxidation related genes like FATP, FABP3 and CPT1 (Le Gouill, Jimenez *et al.* 2007).

7.4 Potential of FA oxidation as a target in tumour therapy

This study shows that endothelial DLL4-NOTCH signalling upregulates FA storage and oxidation, indicating that DLL4-NOTCH signalling leads to a shift in metabolism from glucose to the utilisation of FAs in endothelial cells. Inhibition of FA oxidation by EX led to reduced sprouting of endothelial cells and caudal vein plexus formation in zebrafish.

Drugs inhibiting FA oxidation have been under clinical investigation for the treatment of heart diseases. Although EX has shown hepatotoxicity in clinical trials, other CPT1 inhibitors like perhexiline are already approved in some countries for the treatment of heart disease (Holubarsch, Rohrbach *et al.* 2007). The drugs trimetazidine and ranolazine inhibit the final enzymatic step of FA oxidation and have been approved for the treatment of angina in Europe, Asia and the US (Kantor, Lucien *et al.* 2000, Nash and Nash 2008, reviewed by Carracedo, Cantley *et al.* 2013). Endothelial FA oxidation as a potential target in tumour therapy is an interesting strategy worthy of further investigation. Research shows that inhibition of FA oxidation by EX or other drugs *in vitro* and *in vivo* leads to effects that can be beneficial in tumour therapy (Hernlund, Ihrlund *et al.* 2008, Samudio, Harmancey *et al.* 2010, Pike, Smift *et al.* 2011, Tirado-Velez, Joumady *et al.* 2012, Currie, Schulze *et al.* 2013, Schlaepfer, Rider *et al.* 2014).

7.4.1 Anti-inflammatory and pro-apoptotic properties of EX

EX is under investigation for targeting inflammation-related disease, because the activation of immune cells is related to the activation of FA metabolism. The transition of T cells from effector to memory T cells is characterised by a metabolic switch from glucose to FAs as a primary source for energy and monocytes isolated from patients with infection have increased levels of acyl-carnitine, which is imported into mitochondria by CPT1 for oxidation (Cress, Fraker *et al.* 1989, Pearce, Walsh *et al.* 2009). EX treatment inhibits pro-inflammatory

cytokine production and promotes apoptosis in activated T cells in a mouse model of multiple sclerosis (Shriver and Manchester 2011).

In tumour therapy, EX is being tested as a combination therapy with FA synthesis inhibitors or chemotherapeutics, or as a single therapy. Tumour cells that are resistant to chemotherapy or radiation are associated with higher FA catabolism than therapy-sensitive cells, which are mainly glycolytic (Harper, Antoniou *et al.* 2002). Combination of EX with chemotherapeutic drugs leads to potentiation of their anti-proliferative effects (Hernlund, Ihrlund *et al.* 2008) and EX or ranolazine treatment can sensitise to the induction of apoptosis in leukemia cells (Samudio, Harmancey *et al.* 2010). Parallel inhibition of FA oxidation and *de novo* FA synthesis in tumours with high FA synthesis rates was suggested recently and trialled as a therapeutic strategy *in vitro*, leading to a reduction in the proliferation rates of prostate tumour and myeloma cells (Tirado-Velez, Joumady *et al.* 2012, Currie, Schulze *et al.* 2013, Schlaepfer, Rider *et al.* 2014). Glioblastoma cells treated with EX alone have decreased ATP levels, accompanied by a reduction of NADPH levels and glutathione production. The cells showed increased levels of apoptosis, which is likely due to the increase of ROS following EX treatment and suggests that FA oxidation contributes to the production of NADPH (via reaction of acetyl-CoA and oxalocaetate to citrate in the TCA cycle, its export to the cytoplasm via the citrate shuttle, and step-wise conversion to pyruvate, which regenerates two NADPH) and ROS protection (Pike, Smift *et al.* 2011). However, the underlying mechanism for increased ROS may also be that FA oxidation inhibition leads to activation of the unfolded protein response (UPR), which is accompanied by an impaired defense against oxidative stress in hepatocytes (Tyra, Spitz *et al.* 2012). Two studies showed that EX reduces tumour growth *in vivo*, however there are no reports on microvessel density in EX-treated mice (Samudio, Harmancey *et al.* 2010, Schlaepfer, Rider *et al.* 2014).

7.4.2 Anti-angiogenic proterties of EX

The present study is the first to show the potential of EX to reduce angiogenesis by targeting FA oxidation. There have been several studies investigating the contribution of FA oxidation

to endothelial cell homeostasis, mostly indicating that it is minor. However, the caveat with comparing and interpreting endothelial metabolism studies in regards to FA oxidation is the difference in the experimental set up, the endothelial cell types tested, and the difference in culture, such as the time of pre-labelling FAs and the concentration of metabolic substrates or co-factors like glucose, FAs, and carnitine.

It has been suggested before that FAs are likely incorporated into TG stores before being oxidized (Dagenais, Tancredi *et al.* 1976), which was confirmed by Dagher *et al.*, who found that FA oxidation rates of labeled FAs are increased when the cells are pre-labeled 24 h prior to the assay, instead of 2 h. Our studies show that NOTCH signalling upregulates intracellular TG and FA oxidation, which supports a FA channeling into TG prior to their oxidation.

Glucose-depleted cells are able to maintain their ATP levels, likely due to an increase in FA oxidation (Dagher, Ruderman *et al.* 2001). Induction of energy stress by an AMP kinase inhibitor leads to a 3 fold upregulation of FA oxidation and an increase from 14% to 36% contribution to total ATP levels (Dewhirst, Kimura *et al.* 1996). This shows that intracellular TG stores are readily available for endothelial cells to increase FA oxidation rates and thereby maintain cellular homeostasis in conditions of nutrient depletion or energy stress, likely more so than glycogen stores do (Dagher, Ruderman *et al.* 2001). In the present study, DLL4-NOTCH upregulates FA oxidation by an undefined mechanism, downregulates glycolysis possibly via direct regulation of glycolytic genes, and (maybe even therefore) inhibits cell growth of endothelial cells, while maintaining ATP levels. However, this might also be due to a cell growth-related decrease of ATP-consuming reactions.

EX targets the FA oxidation rate-limiting CPT1, which uses carnitine as a co-subsubstrate. The presence of carnitine in the media is required for cells to perform FA oxidation. Addition of 50 μM carnitine increases FA oxidation rates (Dagher, Ruderman *et al.* 1999, Dagher, Ruderman *et al.* 2001). The concentration of carnitine in FCS or rat serum is 30-40 μM (Ling, Aziz *et al.* 2012, Kienesberger, Pordes *et al.* 2014), and the final concentration in culture media with 2% FCS would be only 0.8 μM. Considering that endothelial cells, at least in fully

established vessels, are in closest proximity to the blood, they have access to up to 40 μM carnitine and to physiological plasma FA concentrations (>400 μM) (Kidwell, Monaco *et al.* 1978, Lagarde, Sicard *et al.* 1984, Hodson, Skeaff *et al.* 2008). If carnitine and FA concentrations are far below the physiological level, the level of FA oxidation and its contribution to cell homeostasis is likely to be underestimated. This might partly explain the different ranges of FA oxidation rates and contribution to endothelial cell homeostasis (14-70%) stated in published studies (Hulsmann and Dubelaar 1988, Culic, Gruwel *et al.* 1997, Dagher, Ruderman *et al.* 1999, Dagher, Ruderman *et al.* 2001, De Bock, Georgiadou *et al.* 2013).

FA oxidation contributes to endothelial cell growth and proliferation during sprouting *in vitro*, as presented in this study. Since ATP levels were not changed at moderate EX concentrations, the mechanism of reducing cell growth may be caused by

1) changes in biomass production from TCA cycle intermediates, which might indirectly affect the activity of the pentose phosphate pathway, DNA/ RNA synthesis etc.,
2) decreased NADPH production and higher ROS sensitivity,
3) increased UPR and higher ROS sensitivity,

which need to be evaluated in future studies. Additional studies *in vivo* are required to validate the extent of FA oxidation that is required in endothelial cells to establish and maintain a functional vasculature. Up to date there are no reports on the effect of FA oxidation inhibition on the tumour vasculature *in vivo* and it is an interesting and promising avenue to pursue.

7.5 Perspectives and future studies

It is of interest to investigate how the balance of activation of the described signalling networks may contribute to the regulation of metabolism during angiogenesis and in the established vasculature. For example, Sawada *et al*. suggest that PGC-1α may inhibit glycolysis and promote mitochondrial oxidation during sprouting angiogenesis, thereby contributing to stalk cell phenotype formation and promoting endothelial cell quiescence, similar to NOTCH signalling. The effect of VEGFB in conjunction with NOTCH on FA utilisation is another avenue worth investigating. The effects on FA metabolism seen in response to NOTCH may be a consequence of interrelated changes in gene expression and metabolite production and it may be challenging to denote a sole cause for the observed changes, considering the complexity of signalling that is occurring during angiogenesis. Although FABP4 was identified as a strong candidate for regulation of the metabolic phenotypic changes observed when DLL4-NOTCH signalling was activated, a direct link between FABP4 upregulation and FA utilisation was not observed. However, in tumour tissue, FABP4 expression in vessels of progressed ovarian cancer may correlate with increased expression of DLL4-NOTCH. FABP4 expression may also contribute to mechanisms of resistance to anti-VEGFA therapy when DLL4-NOTCH signalling is upregulated in tumours.

The present study was carried out in HUVEC as the main model system. The tumour vasculature is composed of microvessels, and it would be advantageous to validate main findings in microvascular cells and, ideally, tumour endothelial cells. However, the study of tumour endothelial cells is hampered by the difficulty in isolating and culturing sufficient amounts for analysis. The experiments done in this study were partly performed in conditions that mimicked the tumour microenvironment in the sense of glucose starvation and increased lactate concentrations. Since endothelial cells enter hypoxic areas in the tumour tissue, it would be of interest to extend the study to include conditions of hypoxia or HIF-1α

overexpression in HUVEC and study the effects on metabolism in response to DLL4-NOTCH.

Furthermore, to validate the significance of the present findings the following issues need to be addressed and further investigated.

1) The extent of DLL4-NOTCH mediated FA utilisation needs further investigation by
    a) 13-tracer flux analysis of FAs to determine if DLL4-NOTCH increases FA injection into the TCA cycle and thereby provides substrates for nucleotide synthesis
    b) LD staining in mouse retinas to determine LD in tip or stalk cells
    c) LD staining in DLL4-overexpressing tumour xenografts to determine a change of lipid droplet levels in vessels with active NOTCH signalling
    d) investigation of the effect of FA oxidation inhibition on NADPH, ROS production, cell cycle, and apoptosis in HUVEC
    e) investigation of the effect of FA oxidation inhibition *in vivo* (mouse retina angiogenesis assay, chicken chorioallantoic membrane angiogenesis assay, tumour xenograft)
2) The role of FABP4 in the DLL4-NOTCH pathway has not been fully elucidated, and needs further investigation by the
    a) study of FABP4 inhibition after pre-stimulation of the DLL4-NOTCH pathway *in vitro* and effect on sprouting, network formation, tube formation, flow, and regulation of global gene expression, possibly in co-culture models
    b) study of FABP4 expression in breast tumour xenografts and in DLL4-overexpressing tumour xenografts treated with anti-VEGFA therapy
    c) study of *FABP4* knockdown effect *in vivo* (mouse retina angiogenesis assay, chicken chorioallantoic membrane angiogenesis assay, tumour xenografts)

APPENDIX I

Supplementary data

MitoStress Test optimisation

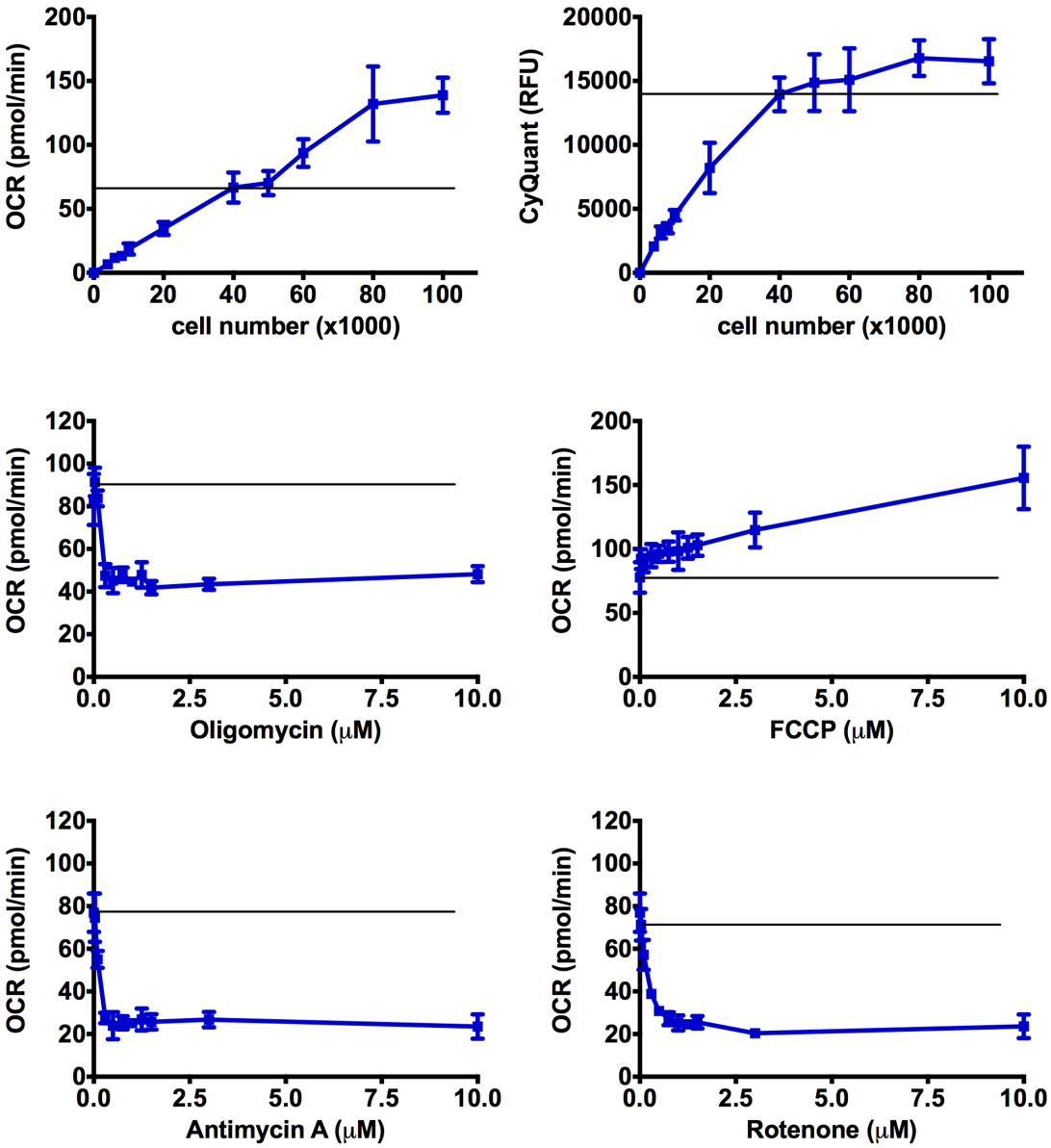


Figure 0.1 Optimisation of cell density and drug concentration for the MitoStress Test. HUVEC were seeded in increasing cell densities on Seahorse XF96 Cell Culture microplates overnight. Oxygen consumption rates (OCR) were measured to identify the cell density at which the basal OCR is between 50 and 100 pmol/min. A density of 40,000 cells per well were selected for further experiments, as the OCR was at 80 pmol/min (upper right panel) and the RFU for CyQuant (upper left panel), which is used to normalise OCR, for this density was in the still in the linear detection range. Oligomycin (middle right panel), FCCP (middle left panel), Antimycin A (bottom left panel), and rotenone (bottom right panel) were tested at increasing concentrations to identify the concentrations that leads to maximal OCR repression (Oligomycin, Antimycin A, Rotenone), or maximal OCR increase (FCCP).

Etomoxir effect on endothelial sprouting in fibrin gel

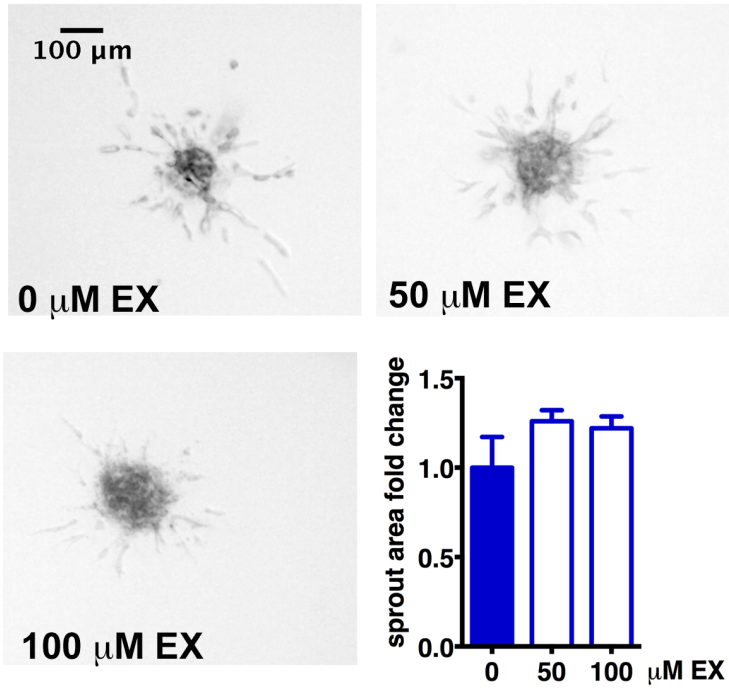


Figure 0.2 Sprouting angiogenesis is decreased by EX in fibrin gel. HUVEC were grown as spheroids overnight and were embedded in fibrin gel and grown in 5 mM glucose with 0, 50, or 100 µM EX (vehicle DMSO) for 48 h. Then the cells were analysed by brightfield microscopy and sprout area was quantified. Values are expressed as mean +/- S.D..

Gene expression data LDHA and SLC1A4

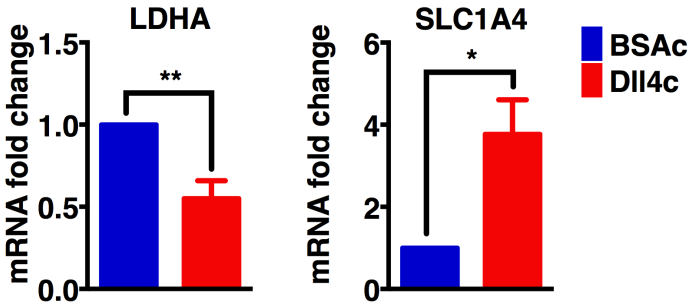


Figure 0.3 DLL4-NOTCH signalling regulates lactate dehydrogenase A (LDHA) and the membranal glutamine transporter SLC1A4. HUVEC were grown on BSA- or DLL4-coated (BSAc or DLL4c) dishes for the indicated time points. Cells were harvested and analysed for mRNA expression of LDHA and SLC1A4. Values are expressed as mean +/- S.D., *p<0.05, **p<0.01.

Lipolytic capacity of differentiated adipocytes

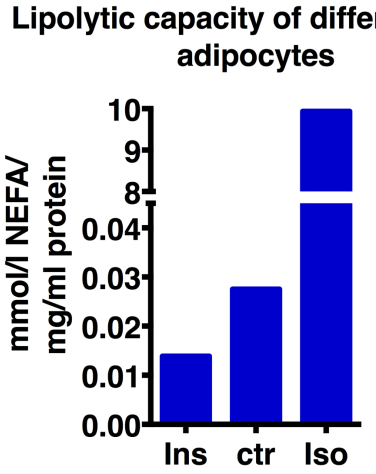


Figure 0.4 Lipolytic capacity of differentiated adipocytes used in coculture. Pre-adipocytes were expanded for 14 days, and then differentiated for another 14 days (see Fig. 5.3). A replicate of adipocytes was grown to test for the ability to release non-esterified fatty acids (NEFA) into the media. 24 h prior to the assay, the media was changed to EGM2. Adipocytes were treated with insulin (0.1 μM) to inhibit lipolysis or isoprenaline (1 μM) for 2 h. The supernatants were collected, and NEFAs were measured. Raw values were normalised to protein concentrations.

FABP4 antibody validation for IHC staining

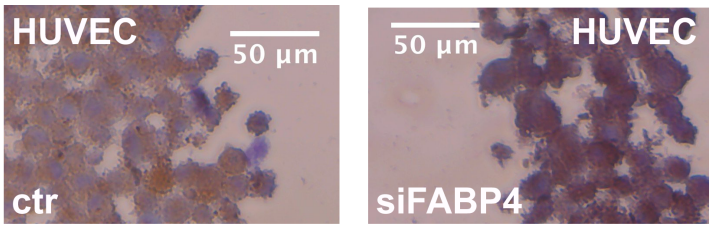


Figure 0.5 Validation of immunohistochemical staining for human fatty acid binding protein 4 (FABP4). HUVEC were transfected with non-targeting control siRNA (ctr) or *FABP4* targeting siRNA (siFABP4), and grown for 48 h. The cell pellets were fixed in 10% formaldehyde, paraffinembedded, and sections were immunohistochemically stained using anti-human FABP4 antibody produced in rabbit (Prestige antibody, Sigma, see Material and Methods for details).

APPENDIX II

List of publications related to this thesis

Harjes, U*., et al.* (2012). "Endothelial cell metabolism and implications for cancer therapy." Br J Cancer **107**(8): 1207-1212.

Harjes, U*., et al.* (2014). "Fatty Acid-binding Protein 4, a Point of Convergence for Angiogenic and Metabolic Signaling Pathways in Endothelial Cells." J Biol Chem **289**(33): 23168-23176.

REFERENCES

Aragones, G., P. Saavedra, M. Heras, A. Cabre, J. Girona and L. Masana (2012). "Fatty acid-binding protein 4 impairs the insulin-dependent nitric oxide pathway in vascular endothelial cells." Cardiovasc Diabetol **11**: 72.

Ayers, S. D., K. L. Nedrow, R. E. Gillilan and N. Noy (2007). "Continuous nucleocytoplasmic shuttling underlies transcriptional activation of PPAR gamma by FABP4." Biochemistry **46**(23): 6744-6752.

Bao, B., Z. Wang, S. Ali, D. Kong, Y. Li, A. Ahmad, S. Banerjee, A. S. Azmi, L. Miele and F. H. Sarkar (2011). "Notch-1 induces epithelial-mesenchymal transition consistent with cancer stem cell phenotype in pancreatic cancer cells." Cancer Lett **307**(1): 26-36.

Bastie, C. C., Z. Nahle, T. McLoughlin, K. Esser, W. Zhang, T. Unterman and N. A. Abumrad (2005). "FoxO1 stimulates fatty acid uptake and oxidation in muscle cells through CD36-dependent and -independent mechanisms." J Biol Chem **280**(14): 14222-14229.

Baudino, T. A., C. McKay, H. Pendeville-Samain, J. A. Nilsson, K. H. Maclean, E. L. White, A. C. Davis, J. N. Ihle and J. L. Cleveland (2002). "c-Myc is essential for vasculogenesis and angiogenesis during development and tumor progression." Genes Dev **16**(19): 2530-2543.

Beets, K., D. Huylebroeck, I. M. Moya, L. Umans and A. Zwijsen (2013). "Robustness in angiogenesis: notch and BMP shaping waves." Trends Genet **29**(3): 140-149.

Bellot, G., R. Garcia-Medina, P. Gounon, J. Chiche, D. Roux, J. Pouyssegur and N. M. Mazure (2009). "Hypoxia-induced autophagy is mediated through hypoxia-inducible factor induction of BNIP3 and BNIP3L via their BH3 domains." Mol Cell Biol **29**(10): 2570-2581.

Bensaad, K., E. Favaro, C. A. Lewis, B. Peck, S. Lord, J. M. Collins, K. E. Pinnick, S. Wigfield, F. M. Buffa, J. L. Li, Q. Zhang, M. J. Wakelam, F. Karpe, A. Schulze and A. L. Harris (2014). "Fatty Acid Uptake and Lipid Storage Induced by HIF-1alpha Contribute to Cell Growth and Survival after Hypoxia-Reoxygenation." Cell Rep.

Berg, J. M., J. L. Tymoczko, L. Stryer and L. Stryer (2002). Biochemistry. New York, W.H. Freeman.

Bernlohr, D. A., M. A. Bolanowski, T. J. Kelly, Jr. and M. D. Lane (1985). "Evidence for an increase in transcription of specific mRNAs during differentiation of 3T3-L1 preadipocytes." J Biol Chem **260**(9): 5563-5567.

Bernlohr, D. A., T. L. Doering, T. J. Kelly, Jr. and M. D. Lane (1985). "Tissue specific expression of p422 protein, a putative lipid carrier, in mouse adipocytes." Biochem Biophys Res Commun **132**(2): 850-855.

Bettenhausen, B. and A. Gossler (1995). "Efficient isolation of novel mouse genes differentially expressed in early postimplantation embryos." Genomics **28**(3): 436-441.

Bickel, P. E., J. T. Tansey and M. A. Welte (2009). "PAT proteins, an ancient family of lipid droplet proteins that regulate cellular lipid stores." Biochim Biophys Acta **1791**(6): 419-440.

Boiteux, G., I. Lascombe, E. Roche, M. L. Plissonnier, A. Clairotte, H. Bittard and S. Fauconnet (2009). "A-FABP, a candidate progression marker of human transitional cell carcinoma of the bladder, is differentially regulated by PPAR in urothelial cancer cells." Int J Cancer **124**(8): 1820-1828.

Bridges, E., C. E. Oon and A. Harris (2011). "Notch regulation of tumor angiogenesis." Future Oncol **7**(4): 569-588.

Brunet, A., A. Bonni, M. J. Zigmond, M. Z. Lin, P. Juo, L. S. Hu, M. J. Anderson, K. C. Arden, J. Blenis and M. E. Greenberg (1999). "Akt promotes cell survival by phosphorylating and inhibiting a Forkhead transcription factor." Cell **96**(6): 857-868.

Bry, M., R. Kivela, T. Holopainen, A. Anisimov, T. Tammela, J. Soronen, J. Silvola, A. Saraste, M. Jeltsch, P. Korpisalo, P. Carmeliet, K. B. Lemstrom, M. Shibuya, S. Yla-Herttuala, L. Alhonen, E. Mervaala, L. C. Andersson, J. Knuuti and K. Alitalo (2010). "Vascular endothelial growth factor-B acts as a coronary growth factor in transgenic rats without inducing angiogenesis, vascular leak, or inflammation." Circulation **122**(17): 1725-1733.

Burdge, G. C., P. Wright, A. E. Jones and S. A. Wootton (2000). "A method for separation of phosphatidylcholine, triacylglycerol, non-esterified fatty acids and cholesterol esters from plasma by solid-phase extraction." Br J Nutr **84**(5): 781-787.

Cairns, R. A., I. S. Harris and T. W. Mak (2011). "Regulation of cancer cell metabolism." Nat Rev Cancer **11**(2): 85-95.

Caolo, V., N. M. van den Akker, S. Verbruggen, M. M. Donners, G. Swennen, H. Schulten, J. Waltenberger, M. J. Post and D. G. Molin (2010). "Feed-forward signaling by membrane-bound ligand receptor circuit: the case of NOTCH DELTA-like 4 ligand in endothelial cells." J Biol Chem **285**(52): 40681-40689.

Carmeliet, P., Y. Dor, J. M. Herbert, D. Fukumura, K. Brusselmans, M. Dewerchin, M. Neeman, F. Bono, R. Abramovitch, P. Maxwell, C. J. Koch, P. Ratcliffe, L. Moons, R. K. Jain, D. Collen and E. Keshert (1998). "Role of HIF-1alpha in hypoxia-

mediated apoptosis, cell proliferation and tumour angiogenesis." Nature **394**(6692): 485-490.

Carracedo, A., L. C. Cantley and P. P. Pandolfi (2013). "Cancer metabolism: fatty acid oxidation in the limelight." Nat Rev Cancer **13**(4): 227-232.

Casanovas, O., D. J. Hicklin, G. Bergers and D. Hanahan (2005). "Drug resistance by evasion of antiangiogenic targeting of VEGF signaling in late-stage pancreatic islet tumors." Cancer Cell **8**(4): 299-309.

Castel, D., P. Mourikis, S. J. Bartels, A. B. Brinkman, S. Tajbakhsh and H. G. Stunnenberg (2013). "Dynamic binding of RBPJ is determined by Notch signaling status." Genes Dev **27**(9): 1059-1071.

Cataltepe, O., M. C. Arikan, E. Ghelfi, C. Karaaslan, Y. Ozsurekci, K. Dresser, Y. Li, T. W. Smith and S. Cataltepe (2012). "Fatty acid binding protein 4 is expressed in distinct endothelial and non-endothelial cell populations in glioblastoma." Neuropathol Appl Neurobiol **38**(5): 400-410.

Chen, X. G., F. Liu, X. F. Song, Z. H. Wang, Z. Q. Dong, Z. Q. Hu, R. Z. Lan, W. Guan, T. G. Zhou, X. M. Xu, H. Lei, Z. Q. Ye, E. J. Peng, L. H. Du and Q. Y. Zhuang (2010). "Rapamycin regulates Akt and ERK phosphorylation through mTORC1 and mTORC2 signaling pathways." Mol Carcinog **49**(6): 603-610.

Cress, A. P., P. J. Fraker and L. L. Bieber (1989). "Carnitine and acylcarnitine levels of human peripheral blood lymphocytes and mononuclear phagocytes." Biochim Biophys Acta **992**(2): 135-139.

Culic, O., M. L. Gruwel and J. Schrader (1997). "Energy turnover of vascular endothelial cells." Am J Physiol **273**(1 Pt 1): C205-213.

Currie, E., A. Schulze, R. Zechner, T. C. Walther and R. V. Farese, Jr. (2013). "Cellular fatty acid metabolism and cancer." Cell Metab **18**(2): 153-161.

Dagenais, G. R., R. G. Tancredi and K. L. Zierler (1976). "Free fatty acid oxidation by forearm muscle at rest, and evidence for an intramuscular lipid pool in the human forearm." J Clin Invest **58**(2): 421-431.

Dagher, Z., N. Ruderman, K. Tornheim and Y. Ido (1999). "The effect of AMP-activated protein kinase and its activator AICAR on the metabolism of human umbilical vein endothelial cells." Biochem Biophys Res Commun **265**(1): 112-115.

Dagher, Z., N. Ruderman, K. Tornheim and Y. Ido (2001). "Acute regulation of fatty acid oxidation and amp-activated protein kinase in human umbilical vein endothelial cells." Circ Res **88**(12): 1276-1282.

Daly, C., V. Wong, E. Burova, Y. Wei, S. Zabski, J. Griffiths, K. M. Lai, H. C. Lin, E. Ioffe, G. D. Yancopoulos and J. S. Rudge (2004). "Angiopoietin-1 modulates

endothelial cell function and gene expression via the transcription factor FKHR (FOXO1)." Genes Dev **18**(9): 1060-1071.

Dang, C. V. (2013). "MYC, metabolism, cell growth, and tumorigenesis." Cold Spring Harb Perspect Med **3**(8).

Das, R., R. Hammamieh, R. Neill, M. Melhem and M. Jett (2001). "Expression pattern of fatty acid-binding proteins in human normal and cancer prostate cells and tissues." Clin Cancer Res **7**(6): 1706-1715.

De Bock, K., M. Georgiadou, S. Schoors, A. Kuchnio, B. W. Wong, A. R. Cantelmo, A. Quaegebeur, B. Ghesquiere, S. Cauwenberghs, G. Eelen, L. K. Phng, I. Betz, B. Tembuyser, K. Brepoels, J. Welti, I. Geudens, I. Segura, B. Cruys, F. Bifari, I. Decimo, R. Blanco, S. Wyns, J. Vangindertael, S. Rocha, R. T. Collins, S. Munck, D. Daelemans, H. Imamura, R. Devlieger, M. Rider, P. P. Van Veldhoven, F. Schuit, R. Bartrons, J. Hofkens, P. Fraisl, S. Telang, R. J. Deberardinis, L. Schoonjans, S. Vinckier, J. Chesney, H. Gerhardt, M. Dewerchin and P. Carmeliet (2013). "Role of PFKFB3-driven glycolysis in vessel sprouting." Cell **154**(3): 651-663.

De Santis, M. L., R. Hammamieh, R. Das and M. Jett (2004). "Adipocyte-fatty acid binding protein induces apoptosis in DU145 prostate cancer cells." J Exp Ther Oncol **4**(2): 91-100.

DeBerardinis, R. J., A. Mancuso, E. Daikhin, I. Nissim, M. Yudkoff, S. Wehrli and C. B. Thompson (2007). "Beyond aerobic glycolysis: transformed cells can engage in glutamine metabolism that exceeds the requirement for protein and nucleotide synthesis." Proc Natl Acad Sci U S A **104**(49): 19345-19350.

Deng, Y., B. Larrivee, Z. W. Zhuang, D. Atri, F. Moraes, C. Prahst, A. Eichmann and M. Simons (2013). "Endothelial RAF1/ERK activation regulates arterial morphogenesis." Blood **121**(19): 3988-3996, S3981-3989.

Dewhirst, M. W., H. Kimura, S. W. Rehmus, R. D. Braun, D. Papahadjopoulos, K. Hong and T. W. Secomb (1996). "Microvascular studies on the origins of perfusion-limited hypoxia." Br J Cancer Suppl **27**: S247-251.

Djousse, L. and J. M. Gaziano (2012). "Plasma levels of FABP4, but not FABP3, are associated with increased risk of diabetes." Lipids **47**(8): 757-762.

Duarte, A., M. Hirashima, R. Benedito, A. Trindade, P. Diniz, E. Bekman, L. Costa, D. Henrique and J. Rossant (2004). "Dosage-sensitive requirement for mouse Dll4 in artery development." Genes Dev **18**(20): 2474-2478.

Dunwoodie, S. L., D. Henrique, S. M. Harrison and R. S. Beddington (1997). "Mouse Dll3: a novel divergent Delta gene which may complement the function of other Delta homologues during early pattern formation in the mouse embryo." Development **124**(16): 3065-3076.

Dwarakanath, B. and V. Jain (2009). "Targeting glucose metabolism with 2-deoxy-D-glucose for improving cancer therapy." Future Oncol **5**(5): 581-585.

Elkin, M., A. Orgel and H. K. Kleinman (2004). "An angiogenic switch in breast cancer involves estrogen and soluble vascular endothelial growth factor receptor 1." J Natl Cancer Inst **96**(11): 875-878.

Ellisen, L. W., J. Bird, D. C. West, A. L. Soreng, T. C. Reynolds, S. D. Smith and J. Sklar (1991). "TAN-1, the human homolog of the Drosophila notch gene, is broken by chromosomal translocations in T lymphoblastic neoplasms." Cell **66**(4): 649-661.

Elmasri, H., E. Ghelfi, C. W. Yu, S. Traphagen, M. Cernadas, H. Cao, G. P. Shi, J. Plutzky, M. Sahin, G. Hotamisligil and S. Cataltepe (2012). "Endothelial cell-fatty acid binding protein 4 promotes angiogenesis: role of stem cell factor/c-kit pathway." Angiogenesis **15**(3): 457-468.

Elmasri, H., C. Karaaslan, Y. Teper, E. Ghelfi, M. Weng, T. A. Ince, H. Kozakewich, J. Bischoff and S. Cataltepe (2009). "Fatty acid binding protein 4 is a target of VEGF and a regulator of cell proliferation in endothelial cells." FASEB J **23**(11): 3865-3873.

Endres, K., A. Anders, E. Kojro, S. Gilbert, F. Fahrenholz and R. Postina (2003). "Tumor necrosis factor-alpha converting enzyme is processed by proprotein-convertases to its mature form which is degraded upon phorbol ester stimulation." Eur J Biochem **270**(11): 2386-2393.

Escudier, B., T. Eisen, W. M. Stadler, C. Szczylik, S. Oudard, M. Siebels, S. Negrier, C. Chevreau, E. Solska, A. A. Desai, F. Rolland, T. Demkow, T. E. Hutson, M. Gore, S. Freeman, B. Schwartz, M. Shan, R. Simantov, R. M. Bukowski and T. S. Group (2007). "Sorafenib in advanced clear-cell renal-cell carcinoma." N Engl J Med **356**(2): 125-134.

Fan, W., H. Morinaga, J. J. Kim, E. Bae, N. J. Spann, S. Heinz, C. K. Glass and J. M. Olefsky (2010). "FoxO1 regulates Tlr4 inflammatory pathway signalling in macrophages." EMBO J **29**(24): 4223-4236.

Farhang Ghahremani, M., S. Goossens, D. Nittner, X. Bisteau, S. Bartunkova, A. Zwolinska, P. Hulpiau, K. Haigh, L. Haenebalcke, B. Drogat, A. Jochemsen, P. P. Roger, J. C. Marine and J. J. Haigh (2013). "p53 promotes VEGF expression and angiogenesis in the absence of an intact p21-Rb pathway." Cell Death Differ **20**(7): 888-897.

Favaro, E., K. Bensaad, M. G. Chong, D. A. Tennant, D. J. Ferguson, C. Snell, G. Steers, H. Turley, J. L. Li, U. L. Gunther, F. M. Buffa, A. McIntyre and A. L. Harris (2012). "Glucose utilization via glycogen phosphorylase sustains proliferation and prevents premature senescence in cancer cells." Cell Metab **16**(6): 751-764.

Ferrara, N. (2004). "Vascular endothelial growth factor as a target for anticancer therapy." Oncologist **9 Suppl 1**: 2-10.

Ferrara, N. (2010). "Pathways mediating VEGF-independent tumor angiogenesis." Cytokine Growth Factor Rev **21**(1): 21-26.

Ferrara, N., H. P. Gerber and J. LeCouter (2003). "The biology of VEGF and its receptors." Nat Med **9**(6): 669-676.

Fessel, J. P., R. Hamid, B. M. Wittmann, L. J. Robinson, T. Blackwell, Y. Tada, N. Tanabe, K. Tatsumi, A. R. Hemnes and J. D. West (2012). "Metabolomic analysis of bone morphogenetic protein receptor type 2 mutations in human pulmonary endothelium reveals widespread metabolic reprogramming." Pulm Circ **2**(2): 201-213.

Fischer, C., M. Mazzone, B. Jonckx and P. Carmeliet (2008). "FLT1 and its ligands VEGFB and PlGF: drug targets for anti-angiogenic therapy?" Nat Rev Cancer **8**(12): 942-956.

Flavin, R., S. Peluso, P. L. Nguyen and M. Loda (2010). "Fatty acid synthase as a potential therapeutic target in cancer." Future Oncol **6**(4): 551-562.

Folch, J., M. Lees and G. H. Sloane Stanley (1957). "A simple method for the isolation and purification of total lipides from animal tissues." J Biol Chem **226**(1): 497-509.

Folkman, J., E. Merler, C. Abernathy and G. Williams (1971). "Isolation of a tumor factor responsible for angiogenesis." J Exp Med **133**(2): 275-288.

Forsythe, J. A., B. H. Jiang, N. V. Iyer, F. Agani, S. W. Leung, R. D. Koos and G. L. Semenza (1996). "Activation of vascular endothelial growth factor gene transcription by hypoxia-inducible factor 1." Mol Cell Biol **16**(9): 4604-4613.

Fukuda, R., K. Hirota, F. Fan, Y. D. Jung, L. M. Ellis and G. L. Semenza (2002). "Insulin-like growth factor 1 induces hypoxia-inducible factor 1-mediated vascular endothelial growth factor expression, which is dependent on MAP kinase and phosphatidylinositol 3-kinase signaling in colon cancer cells." J Biol Chem **277**(41): 38205-38211.

Fukumura, D., S. Kashiwagi and R. K. Jain (2006). "The role of nitric oxide in tumour progression." Nature reviews Cancer **6**(7): 521-534.

Fukumura, D., L. Xu, Y. Chen, T. Gohongi, B. Seed and R. K. Jain (2001). "Hypoxia and acidosis independently up-regulate vascular endothelial growth factor transcription in brain tumors in vivo." Cancer Res **61**(16): 6020-6024.

Funahashi, Y., C. J. Shawber, M. Vorontchikhina, A. Sharma, H. H. Outtz and J. Kitajewski (2010). "Notch regulates the angiogenic response via induction of VEGFR-1." J Angiogenes Res **2**(1): 3.

Fung, E., S. M. Tang, J. P. Canner, K. Morishige, J. F. Arboleda-Velasquez, A. A. Cardoso, N. Carlesso, J. C. Aster and M. Aikawa (2007). "Delta-like 4 induces notch signaling in macrophages: implications for inflammation." Circulation **115**(23): 2948-2956.

Furuhashi, M., G. Tuncman, C. Z. Gorgun, L. Makowski, G. Atsumi, E. Vaillancourt, K. Kono, V. R. Babaev, S. Fazio, M. F. Linton, R. Sulsky, J. A. Robl, R. A. Parker and G. S. Hotamisligil (2007). "Treatment of diabetes and atherosclerosis by inhibiting fatty-acid-binding protein aP2." Nature **447**(7147): 959-965.

Furuta, E., S. K. Pai, R. Zhan, S. Bandyopadhyay, M. Watabe, Y.-Y. Mo, S. Hirota, S. Hosobe, T. Tsukada, K. Miura, S. Kamada, K. Saito, M. Iiizumi, W. Liu, J. Ericsson and K. Watabe (2008). "Fatty acid synthase gene is up-regulated by hypoxia via activation of Akt and sterol regulatory element binding protein-1." Cancer Res **68**(4): 1003-1011.

Gale, N. W., M. G. Dominguez, I. Noguera, L. Pan, V. Hughes, D. M. Valenzuela, A. J. Murphy, N. C. Adams, H. C. Lin, J. Holash, G. Thurston and G. D. Yancopoulos (2004). "Haploinsufficiency of delta-like 4 ligand results in embryonic lethality due to major defects in arterial and vascular development." Proc Natl Acad Sci U S A **101**(45): 15949-15954.

Galzio, R., L. Cristiano, A. Fidoamore, M. G. Cifone, E. Benedetti, B. Cinque, P. Menghini, S. Raysi Dehcordi, R. Ippoliti, A. Giordano and A. Cimini (2012). "Hypoxia modulation of peroxisome proliferator-activated receptors (PPARs) in human glioblastoma stem cells. Implications for therapy." J Cell Biochem **113**(11): 3342-3352.

Garin-Shkolnik, T., A. Rudich, G. S. Hotamisligil and M. Rubinstein (2014). "FABP4 attenuates PPARgamma and adipogenesis and is inversely correlated with PPARgamma in adipose tissues." Diabetes **63**(3): 900-911.

Gerhardt, H. (2008). "VEGF and endothelial guidance in angiogenic sprouting." Organogenesis **4**(4): 241-246.

Gillilan, R. E., S. D. Ayers and N. Noy (2007). "Structural basis for activation of fatty acid-binding protein 4." Journal of Molecular Biology **372**(5): 1246-1260.

Gordon, W. R., K. L. Arnett and S. C. Blacklow (2008). "The molecular logic of Notch signaling--a structural and biochemical perspective." J Cell Sci **121**(Pt 19): 3109-3119.

Gottlieb, E. and K. H. Vousden (2010). "p53 regulation of metabolic pathways." Cold Spring Harb Perspect Biol **2**(4): a001040.

Guarani, V., G. Deflorian, C. A. Franco, M. Kruger, L. K. Phng, K. Bentley, L. Toussaint, F. Dequiedt, R. Mostoslavsky, M. H. Schmidt, B. Zimmermann, R. P. Brandes, M. Mione, C. H. Westphal, T. Braun, A. M. Zeiher, H. Gerhardt, S.

Dimmeler and M. Potente (2011). "Acetylation-dependent regulation of endothelial Notch signalling by the SIRT1 deacetylase." Nature **473**(7346): 234-238.

Gunningham, S. P., M. J. Currie, C. Han, B. A. Robinson, P. A. Scott, A. L. Harris and S. B. Fox (2001). "VEGF-B expression in human primary breast cancers is associated with lymph node metastasis but not angiogenesis." J Pathol **193**(3): 325-332.

Hagberg, C., A. Mehlem, A. Falkevall, L. Muhl and U. Eriksson (2013). "Endothelial fatty acid transport: role of vascular endothelial growth factor B." Physiology (Bethesda) **28**(2): 125-134.

Hagberg, C. E., A. Falkevall, X. Wang, E. Larsson, J. Huusko, I. Nilsson, L. A. van Meeteren, E. Samen, L. Lu, M. Vanwildemeersch, J. Klar, G. Genove, K. Pietras, S. Stone-Elander, L. Claesson-Welsh, S. Yla-Herttuala, P. Lindahl and U. Eriksson (2010). "Vascular endothelial growth factor B controls endothelial fatty acid uptake." Nature **464**(7290): 917-921.

Hammamieh, R., N. Chakraborty, M. Barmada, R. Das and M. Jett (2005). "Expression patterns of fatty acid binding proteins in breast cancer cells." J Exp Ther Oncol **5**(2): 133-143.

Hanahan, D. and R. A. Weinberg (2000). "The hallmarks of cancer." Cell **100**(1): 57-70.

Hanahan, D. and R. A. Weinberg (2011). "Hallmarks of cancer: the next generation." Cell **144**(5): 646-674.

Hancke, K., D. Grubeck, N. Hauser, R. Kreienberg and J. M. Weiss (2010). "Adipocyte fatty acid-binding protein as a novel prognostic factor in obese breast cancer patients." Breast Cancer Res Treat **119**(2): 367-367.

Hanrahan, V., M. J. Currie, S. P. Gunningham, H. R. Morrin, P. A. Scott, B. A. Robinson and S. B. Fox (2003). "The angiogenic switch for vascular endothelial growth factor (VEGF)-A, VEGF-B, VEGF-C, and VEGF-D in the adenoma-carcinoma sequence during colorectal cancer progression." J Pathol **200**(2): 183-194.

Harjes, U., K. Bensaad and A. L. Harris (2012). "Endothelial cell metabolism and implications for cancer therapy." Br J Cancer **107**(8): 1207-1212.

Harjes, U., E. Bridges, A. McIntyre, B. A. Fielding and A. L. Harris (2014). "Fatty Acid-binding Protein 4, a Point of Convergence for Angiogenic and Metabolic Signaling Pathways in Endothelial Cells." J Biol Chem **289**(33): 23168-23176.

Harper, M. E., A. Antoniou, E. Villalobos-Menuey, A. Russo, R. Trauger, M. Vendemelio, A. George, R. Bartholomew, D. Carlo, A. Shaikh, J. Kupperman, E. W. Newell, I. A. Bespalov, S. S. Wallace, Y. Liu, J. R. Rogers, G. L. Gibbs, J. L. Leahy, R. E.

Camley, R. Melamede and M. K. Newell (2002). "Characterization of a novel metabolic strategy used by drug-resistant tumor cells." FASEB J **16**(12): 1550-1557.

Harrington, L. S., R. C. Sainson, C. K. Williams, J. M. Taylor, W. Shi, J. L. Li and A. L. Harris (2008). "Regulation of multiple angiogenic pathways by Dll4 and Notch in human umbilical vein endothelial cells." Microvasc Res **75**(2): 144-154.

Harris, A. L. (2002). "Hypoxia--a key regulatory factor in tumour growth." Nat Rev Cancer **2**(1): 38-47.

Herbert, S. P. and D. Y. Stainier (2011). "Molecular control of endothelial cell behaviour during blood vessel morphogenesis." Nat Rev Mol Cell Biol **12**(9): 551-564.

Hernlund, E., L. S. Ihrlund, O. Khan, Y. O. Ates, S. Linder, T. Panaretakis and M. C. Shoshan (2008). "Potentiation of chemotherapeutic drugs by energy metabolism inhibitors 2-deoxyglucose and etomoxir." Int J Cancer **123**(2): 476-483.

Herzig, S., F. Long, U. S. Jhala, S. Hedrick, R. Quinn, A. Bauer, D. Rudolph, G. Schutz, C. Yoon, P. Puigserver, B. Spiegelman and M. Montminy (2001). "CREB regulates hepatic gluconeogenesis through the coactivator PGC-1." Nature **413**(6852): 179-183.

Hiratsuka, S., O. Minowa, J. Kuno, T. Noda and M. Shibuya (1998). "Flt-1 lacking the tyrosine kinase domain is sufficient for normal development and angiogenesis in mice." Proc Natl Acad Sci U S A **95**(16): 9349-9354.

Hodson, L., C. M. Skeaff and B. A. Fielding (2008). "Fatty acid composition of adipose tissue and blood in humans and its use as a biomarker of dietary intake." Prog Lipid Res **47**(5): 348-380.

Holderfield, M. T., A. M. Henderson Anderson, H. Kokubo, M. T. Chin, R. L. Johnson and C. C. Hughes (2006). "HESR1/CHF2 suppresses VEGFR2 transcription independent of binding to E-boxes." Biochem Biophys Res Commun **346**(3): 637-648.

Holm, S., T. Ueland, T. B. Dahl, A. E. Michelsen, M. Skjelland, D. Russell, S. H. Nymo, K. Krohg-Sorensen, O. P. Clausen, D. Atar, J. L. Januzzi, P. Aukrust, J. K. Jensen and B. Halvorsen (2011). "Fatty Acid binding protein 4 is associated with carotid atherosclerosis and outcome in patients with acute ischemic stroke." PLoS One **6**(12): e28785.

Holubarsch, C. J., M. Rohrbach, M. Karrasch, E. Boehm, L. Polonski, P. Ponikowski and S. Rhein (2007). "A double-blind randomized multicentre clinical trial to evaluate the efficacy and safety of two doses of etomoxir in comparison with placebo in patients with moderate congestive heart failure: the ERGO (etomoxir for the recovery of glucose oxidation) study." Clin Sci (Lond) **113**(4): 205-212.

Hong, C. C., T. Kume and R. T. Peterson (2008). "Role of crosstalk between phosphatidylinositol 3-kinase and extracellular signal-regulated kinase/mitogen-activated protein kinase pathways in artery-vein specification." Circ Res **103**(6): 573-579.

Hotamisligil, G. S., R. S. Johnson, R. J. Distel, R. Ellis, V. E. Papaioannou and B. M. Spiegelman (1996). "Uncoupling of obesity from insulin resistance through a targeted mutation in aP2, the adipocyte fatty acid binding protein." Science **274**(5291): 1377-1379.

Hu, G. H., H. Liu, P. Lai, Z. F. Guo, L. Xu, X. D. Yao, J. H. Zheng, M. Liu and Y. F. Xu (2014). "Delta-like ligand 4 (Dll4) predicts the prognosis of clear cell renal cell carcinoma, and anti-Dll4 suppresses tumor growth in vivo." Int J Clin Exp Pathol **7**(5): 2143-2152.

Hu, W., C. Lu, H. H. Dong, J. Huang, D. Y. Shen, R. L. Stone, A. M. Nick, M. M. Shahzad, E. Mora, N. B. Jennings, S. J. Lee, J. W. Roh, K. Matsuo, M. Nishimura, B. W. Goodman, R. B. Jaffe, R. R. Langley, M. T. Deavers, G. Lopez-Berestein, R. L. Coleman and A. K. Sood (2011). "Biological roles of the Delta family Notch ligand Dll4 in tumor and endothelial cells in ovarian cancer." Cancer Res **71**(18): 6030-6039.

Hulsmann, W. C. and M. L. Dubelaar (1988). "Aspects of fatty acid metabolism in vascular endothelial cells." Biochimie **70**(5): 681-686.

Hunt, T. K., R. S. Aslam, S. Beckert, S. Wagner, Q. P. Ghani, M. Z. Hussain, S. Roy and C. K. Sen (2007). "Aerobically derived lactate stimulates revascularization and tissue repair via redox mechanisms." Antioxid Redox Signal **9**(8): 1115-1124.

Hurwitz, H., L. Fehrenbacher, W. Novotny, T. Cartwright, J. Hainsworth, W. Heim, J. Berlin, A. Baron, S. Griffing, E. Holmgren, N. Ferrara, G. Fyfe, B. Rogers, R. Ross and F. Kabbinavar (2004). "Bevacizumab plus irinotecan, fluorouracil, and leucovorin for metastatic colorectal cancer." N Engl J Med **350**(23): 2335-2342.

Ishigami, S., T. Arigami, Y. Uenosono, H. Okumura, H. Kurahara, Y. Uchikado, T. Setoyama, Y. Kita, Y. Kijima, Y. Nishizono, A. Nakajo, T. Owaki, S. Ueno and S. Natsugoe (2013). "Clinical implications of DLL4 expression in gastric cancer." J Exp Clin Cancer Res **32**: 46.

Jain, R. K., D. G. Duda, J. W. Clark and J. S. Loeffler (2006). "Lessons from phase III clinical trials on anti-VEGF therapy for cancer." Nat Clin Pract Oncol **3**(1): 24-40.

Jakobsson, L., C. A. Franco, K. Bentley, R. T. Collins, B. Ponsioen, I. M. Aspalter, I. Rosewell, M. Busse, G. Thurston, A. Medvinsky, S. Schulte-Merker and H. Gerhardt (2010). "Endothelial cells dynamically compete for the tip cell position during angiogenic sprouting." Nat Cell Biol **12**(10): 943-953.

Jiao, M. and K. J. Nan (2012). "Activation of PI3 kinase/Akt/HIF-1alpha pathway contributes to hypoxia-induced epithelial-mesenchymal transition and chemoresistance in hepatocellular carcinoma." Int J Oncol **40**(2): 461-468.

Jubb, A. M., H. Turley, H. C. Moeller, G. Steers, C. Han, J. L. Li, R. Leek, E. Y. Tan, B. Singh, N. J. Mortensen, I. Noguera-Troise, F. Pezzella, K. C. Gatter, G. Thurston, S. B. Fox and A. L. Harris (2009). "Expression of delta-like ligand 4 (Dll4) and markers of hypoxia in colon cancer." Br J Cancer **101**(10): 1749-1757.

Kantor, P. F., A. Lucien, R. Kozak and G. D. Lopaschuk (2000). "The antianginal drug trimetazidine shifts cardiac energy metabolism from fatty acid oxidation to glucose oxidation by inhibiting mitochondrial long-chain 3-ketoacyl coenzyme A thiolase." Circ Res **86**(5): 580-588.

Kidwell, W. R., M. E. Monaco, M. S. Wicha and G. S. Smith (1978). "Unsaturated fatty acid requirements for growth and survival of a rat mammary tumor cell line." Cancer Res **38**(11 Pt 2): 4091-4100.

Kienesberger, K., A. G. Pordes, T. G. Volk and R. Hofbauer (2014). "L-carnitine and PPARalpha-agonist fenofibrate are involved in the regulation of Carnitine Acetyltransferase (CrAT) mRNA levels in murine liver cells." BMC Genomics **15**: 514.

Kitamura, T., Y. I. Kitamura, Y. Funahashi, C. J. Shawber, D. H. Castrillon, R. Kollipara, R. A. DePinho, J. Kitajewski and D. Accili (2007). "A Foxo/Notch pathway controls myogenic differentiation and fiber type specification." J Clin Invest **117**(9): 2477-2485.

Kletzien, R. F., L. A. Foellmi, P. K. Harris, B. M. Wyse and S. D. Clarke (1992). "Adipocyte fatty acid-binding protein: regulation of gene expression in vivo and in vitro by an insulin-sensitizing agent." Mol Pharmacol **42**(4): 558-562.

Konerding, M. A., E. Fait and A. Gaumann (2001). "3D microvascular architecture of pre-cancerous lesions and invasive carcinomas of the colon." Br J Cancer **84**(10): 1354-1362.

Kontomanolis, E., M. Panteliadou, A. Giatromanolaki, S. Pouliliou, E. Efremidou, V. Limberis, G. Galazios, E. Sivridis and M. I. Koukourakis (2014). "Delta-like ligand 4 (DLL4) in the plasma and neoplastic tissues from breast cancer patients: correlation with metastasis." Med Oncol **31**(5): 945.

Kopan, R. (2012). "Notch signaling." Cold Spring Harb Perspect Biol **4**(10).

Koukourakis, M. I., A. Giatromanolaki, A. L. Harris and E. Sivridis (2006). "Comparison of metabolic pathways between cancer cells and stromal cells in colorectal carcinomas: a metabolic survival role for tumor-associated stroma." Cancer Res **66**(2): 632-637.

Koukourakis, M. I., A. Giatromanolaki, E. Sivridis, K. C. Gatter and A. L. Harris (2013). "High DLL4 expression in tumour-associated vessels predicts for favorable radiotherapy outcome in locally advanced squamous cell head-neck cancer (HNSCC)." Angiogenesis **16**(2): 343-351.

Kralisch, S. and M. Fasshauer (2013). "Adipocyte fatty acid binding protein: a novel adipokine involved in the pathogenesis of metabolic and vascular disease?" Diabetologia **56**(1): 10-21.

Krebs, L. T., J. R. Shutter, K. Tanigaki, T. Honjo, K. L. Stark and T. Gridley (2004). "Haploinsufficient lethality and formation of arteriovenous malformations in Notch pathway mutants." Genes Dev **18**(20): 2469-2473.

Krebs, L. T., Y. Xue, C. R. Norton, J. R. Shutter, M. Maguire, J. P. Sundberg, D. Gallahan, V. Closson, J. Kitajewski, R. Callahan, G. H. Smith, K. L. Stark and T. Gridley (2000). "Notch signaling is essential for vascular morphogenesis in mice." Genes Dev **14**(11): 1343-1352.

Krutzfeldt, A., R. Spahr, S. Mertens, B. Siegmund and H. M. Piper (1990). "Metabolism of exogenous substrates by coronary endothelial cells in culture." J Mol Cell Cardiol **22**(12): 1393-1404.

Kuemmerle, N. B., E. Rysman, P. S. Lombardo, A. J. Flanagan, B. C. Lipe, W. A. Wells, J. R. Pettus, H. M. Froehlich, V. A. Memoli, P. M. Morganelli, J. V. Swinnen, L. A. Timmerman, L. Chaychi, C. J. Fricano, B. L. Eisenberg, W. B. Coleman and W. B. Kinlaw (2011). "Lipoprotein lipase links dietary fat to solid tumor cell proliferation." Mol Cancer Ther **10**(3): 427-436.

Lagarde, M., B. Sicard, M. Guichardant, O. Felisi and M. Dechavanne (1984). "Fatty acid composition in native and cultured human endothelial cells." In Vitro **20**(1): 33-37.

Landau, B. R., J. Laszlo, J. Stengle and D. Burk (1958). "Certain metabolic and pharmacologic effects in cancer patients given infusions of 2-deoxy-D-glucose." J Natl Cancer Inst **21**(3): 485-494.

Landor, S. K. J., A. P. Mutvei, V. Mamaeva, S. B. Jin, M. Busk, R. Borra, T. J. Gronroos, P. Kronqvist, U. Lendahl and C. M. Sahlgren (2011). "Hypo- and hyperactivated Notch signaling induce a glycolytic switch through distinct mechanisms." Proc Natl Acad Sci U S A **108**(46): 18814-18819.

Lardelli, M., J. Dahlstrand and U. Lendahl (1994). "The novel Notch homologue mouse Notch 3 lacks specific epidermal growth factor-repeats and is expressed in proliferating neuroepithelium." Mech Dev **46**(2): 123-136.

Laughner, E., P. Taghavi, K. Chiles, P. C. Mahon and G. L. Semenza (2001). "HER2 (neu) signaling increases the rate of hypoxia-inducible factor 1alpha (HIF-1alpha) synthesis: novel mechanism for HIF-1-mediated vascular endothelial growth factor expression." Mol Cell Biol **21**(12): 3995-4004.

Le Gouill, E., M. Jimenez, C. Binnert, P.-Y. Jayet, S. Thalmann, P. Nicod, U. Scherrer and P. Vollenweider (2007). "Endothelial nitric oxide synthase (eNOS) knockout mice have defective mitochondrial beta-oxidation." Diabetes **56**(11): 2690-2696.

Lengyel, E. (2010). "Ovarian cancer development and metastasis." Am J Pathol **177**(3): 1053-1064.

Li, J. L., R. C. Sainson, C. E. Oon, H. Turley, R. Leek, H. Sheldon, E. Bridges, W. Shi, C. Snell, E. T. Bowden, H. Wu, P. S. Chowdhury, A. J. Russell, C. P. Montgomery, R. Poulsom and A. L. Harris (2011). "DLL4-Notch signaling mediates tumor resistance to anti-VEGF therapy in vivo." Cancer Res **71**(18): 6073-6083.

Li, Y., F. Zhang, N. Nagai, Z. Tang, S. Zhang, P. Scotney, J. Lennartsson, C. Zhu, Y. Qu, C. Fang, J. Hua, O. Matsuo, G. H. Fong, H. Ding, Y. Cao, K. G. Becker, A. Nash, C. H. Heldin and X. Li (2008). "VEGF-B inhibits apoptosis via VEGFR-1-mediated suppression of the expression of BH3-only protein genes in mice and rats." J Clin Invest **118**(3): 913-923.

Lim, J. H., E. S. Lee, H. J. You, J. W. Lee, J. W. Park and Y. S. Chun (2004). "Ras-dependent induction of HIF-1alpha785 via the Raf/MEK/ERK pathway: a novel mechanism of Ras-mediated tumor promotion." Oncogene **23**(58): 9427-9431.

Lindsell, C. E., C. J. Shawber, J. Boulter and G. Weinmaster (1995). "Jagged: a mammalian ligand that activates Notch1." Cell **80**(6): 909-917.

Ling, B., C. Aziz and J. Alcorn (2012). "Systematic Evaluation of Key L-Carnitine Homeostasis Mechanisms during Postnatal Development in Rat." Nutr Metab (Lond) **9**(1): 66.

Liu, Z. J., M. Xiao, K. Balint, K. S. Smalley, P. Brafford, R. Qiu, C. C. Pinnix, X. Li and M. Herlyn (2006). "Notch1 signaling promotes primary melanoma progression by activating mitogen-activated protein kinase/phosphatidylinositol 3-kinase-Akt pathways and up-regulating N-cadherin expression." Cancer Res **66**(8): 4182-4190.

Lobov, I. B., E. Cheung, R. Wudali, J. Cao, G. Halasz, Y. Wei, A. Economides, H. C. Lin, N. Papadopoulos, G. D. Yancopoulos and S. J. Wiegand (2011). "The Dll4/Notch pathway controls postangiogenic blood vessel remodeling and regression by modulating vasoconstriction and blood flow." Blood **117**(24): 6728-6737.

Ma, X. J., S. Dahiya, E. Richardson, M. Erlander and D. C. Sgroi (2009). "Gene expression profiling of the tumor microenvironment during breast cancer progression." Breast Cancer Res **11**(1): R7.

Madar, S., I. Goldstein and V. Rotter (2013). "'Cancer associated fibroblasts'--more than meets the eye." Trends in molecular medicine **19**(8): 447-453.

Mailhos, C., U. Modlich, J. Lewis, A. Harris, R. Bicknell and D. Ish-Horowicz (2001). "Delta4, an endothelial specific notch ligand expressed at sites of physiological and tumor angiogenesis." Differentiation **69**(2-3): 135-144.

Makowski, L., K. C. Brittingham, J. M. Reynolds, J. Suttles and G. S. Hotamisligil (2005). "The fatty acid-binding protein, aP2, coordinates macrophage cholesterol trafficking and inflammatory activity. Macrophage expression of aP2 impacts peroxisome proliferator-activated receptor gamma and IkappaB kinase activities." J Biol Chem **280**(13): 12888-12895.

Mashek, D. G. and R. A. Coleman (2006). "Cellular fatty acid uptake: the contribution of metabolism." Curr Opin Lipidol **17**(3): 274-278.

Mashek, D. G., M. A. McKenzie, C. G. Van Horn and R. A. Coleman (2006). "Rat long chain acyl-CoA synthetase 5 increases fatty acid uptake and partitioning to cellular triacylglycerol in McArdle-RH7777 cells." J Biol Chem **281**(2): 945-950.

Masood, R., J. Cai, T. Zheng, D. L. Smith, D. R. Hinton and P. S. Gill (2001). "Vascular endothelial growth factor (VEGF) is an autocrine growth factor for VEGF receptor-positive human tumors." Blood **98**(6): 1904-1913.

Matsui, J., T. Wakabayashi, M. Asada, K. Yoshimatsu and M. Okada (2004). "Stem cell factor/c-kit signaling promotes the survival, migration, and capillary tube formation of human umbilical vein endothelial cells." J Biol Chem **279**(18): 18600-18607.

Medes, G., A. Thomas and S. Weinhouse (1953). "Metabolism of neoplastic tissue. IV. A study of lipid synthesis in neoplastic tissue slices in vitro." Cancer Res **13**(1): 27-29.

Metallo, C. M., P. A. Gameiro, E. L. Bell, K. R. Mattaini, J. Yang, K. Hiller, C. M. Jewell, Z. R. Johnson, D. J. Irvine, L. Guarente, J. K. Kelleher, M. G. Vander Heiden, O. Iliopoulos and G. Stephanopoulos (2012). "Reductive glutamine metabolism by IDH1 mediates lipogenesis under hypoxia." Nature **481**(7381): 380-384.

Michelakis, E. D., G. Sutendra, P. Dromparis, L. Webster, A. Haromy, E. Niven, C. Maguire, T. L. Gammer, J. R. Mackey, D. Fulton, B. Abdulkarim, M. S. McMurtry and K. C. Petruk (2010). "Metabolic modulation of glioblastoma with dichloroacetate." Sci Transl Med **2**(31): 31ra34.

Miller, K., M. Wang, J. Gralow, M. Dickler, M. Cobleigh, E. A. Perez, T. Shenkier, D. Cella and N. E. Davidson (2007). "Paclitaxel plus bevacizumab versus paclitaxel alone for metastatic breast cancer." N Engl J Med **357**(26): 2666-2676.

Mohanti, B. K., G. K. Rath, N. Anantha, V. Kannan, B. S. Das, B. A. Chandramouli, A. K. Banerjee, S. Das, A. Jena, R. Ravichandran, U. P. Sahi, R. Kumar, N. Kapoor, V. K. Kalia, B. S. Dwarakanath and V. Jain (1996). "Improving cancer radiotherapy with 2-deoxy-D-glucose: phase I/II clinical trials on human cerebral gliomas." Int J Radiat Oncol Biol Phys **35**(1): 103-111.

Molhoek, K. R., G. Erdag, J. K. Rasamny, C. Murphy, D. Deacon, J. W. Patterson, C. L. Slingluff, Jr. and D. L. Brautigan (2011). "VEGFR-2 expression in human melanoma: revised assessment." Int J Cancer **129**(12): 2807-2815.

Motzer, R. J., T. E. Hutson, P. Tomczak, M. D. Michaelson, R. M. Bukowski, O. Rixe, S. Oudard, S. Negrier, C. Szczylik, S. T. Kim, I. Chen, P. W. Bycott, C. M. Baum and R. A. Figlin (2007). "Sunitinib versus interferon alfa in metastatic renal-cell carcinoma." N Engl J Med **356**(2): 115-124.

Moya, I. M., L. Umans, E. Maas, P. N. Pereira, K. Beets, A. Francis, W. Sents, E. J. Robertson, C. L. Mummery, D. Huylebroeck and A. Zwijsen (2012). "Stalk cell phenotype depends on integration of Notch and Smad1/5 signaling cascades." Dev Cell **22**(3): 501-514.

Mullen, A. R., W. W. Wheaton, E. S. Jin, P. H. Chen, L. B. Sullivan, T. Cheng, Y. Yang, W. M. Linehan, N. S. Chandel and R. J. DeBerardinis (2012). "Reductive carboxylation supports growth in tumour cells with defective mitochondria." Nature **481**(7381): 385-388.

Nakae, J., Y. Cao, M. Oki, Y. Orba, H. Sawa, H. Kiyonari, K. Iskandar, K. Suga, M. Lombes and Y. Hayashi (2008). "Forkhead transcription factor FoxO1 in adipose tissue regulates energy storage and expenditure." Diabetes **57**(3): 563-576.

Nash, D. T. and S. D. Nash (2008). "Ranolazine for chronic stable angina." Lancet **372**(9646): 1335-1341.

Nieman, K. M., H. A. Kenny, C. V. Penicka, A. Ladanyi, R. Buell-Gutbrod, M. R. Zillhardt, I. L. Romero, M. S. Carey, G. B. Mills, G. S. Hotamisligil, S. D. Yamada, M. E. Peter, K. Gwin and E. Lengyel (2011). "Adipocytes promote ovarian cancer metastasis and provide energy for rapid tumor growth." Nat Med **17**(11): 1498-1503.

Noguera-Troise, I., C. Daly, N. J. Papadopoulos, S. Coetzee, P. Boland, N. W. Gale, H. C. Lin, G. D. Yancopoulos and G. Thurston (2006). "Blockade of Dll4 inhibits tumour growth by promoting non-productive angiogenesis." Nature **444**(7122): 1032-1037.

Nomura, D. K., J. Z. Long, S. Niessen, H. S. Hoover, S. W. Ng and B. F. Cravatt (2010). "Monoacylglycerol lipase regulates a fatty acid network that promotes cancer pathogenesis." Cell **140**(1): 49-61.

Ohlsson, G., J. M. Moreira, P. Gromov, G. Sauter and J. E. Celis (2005). "Loss of expression of the adipocyte-type fatty acid-binding protein (A-FABP) is associated with progression of human urothelial carcinomas." Mol Cell Proteomics **4**(4): 570-581.

Olofsson, B., E. Korpelainen, M. S. Pepper, S. J. Mandriota, K. Aase, V. Kumar, Y. Gunji, M. M. Jeltsch, M. Shibuya, K. Alitalo and U. Eriksson (1998). "Vascular

endothelial growth factor B (VEGF-B) binds to VEGF receptor-1 and regulates plasminogen activator activity in endothelial cells." Proc Natl Acad Sci U S A **95**(20): 11709-11714.

Pajvani, U. B., C. J. Shawber, V. T. Samuel, A. L. Birkenfeld, G. I. Shulman, J. Kitajewski and D. Accili (2011). "Inhibition of Notch signaling ameliorates insulin resistance in a FoxO1-dependent manner." Nat Med **17**(8): 961-967.

Parra-Bonilla, G., D. F. Alvarez, A. B. Al-Mehdi, M. Alexeyev and T. Stevens (2010). "Critical role for lactate dehydrogenase A in aerobic glycolysis that sustains pulmonary microvascular endothelial cell proliferation." Am J Physiol Lung Cell Mol Physiol **299**(4): L513-522.

Patel, N. S., M. S. Dobbie, M. Rochester, G. Steers, R. Poulsom, K. Le Monnier, D. W. Cranston, J. L. Li and A. L. Harris (2006). "Up-regulation of endothelial delta-like 4 expression correlates with vessel maturation in bladder cancer." Clin Cancer Res **12**(16): 4836-4844.

Patel, N. S., J. L. Li, D. Generali, R. Poulsom, D. W. Cranston and A. L. Harris (2005). "Up-regulation of delta-like 4 ligand in human tumor vasculature and the role of basal expression in endothelial cell function." Cancer Res **65**(19): 8690-8697.

Patenaude, A., M. Fuller, L. Chang, F. Wong, G. Paliouras, R. Shaw, A. H. Kyle, P. Umlandt, J. H. E. Baker, E. Diaz, J. Tong, A. I. Minchinton and A. Karsan (2014). "Endothelial-specific Notch blockade inhibits vascular function and tumor growth through an eNOS-dependent mechanism." Cancer Res **74**(9): 2402-2411.

Pavlides, S., D. Whitaker-Menezes, R. Castello-Cros, N. Flomenberg, A. K. Witkiewicz, P. G. Frank, M. C. Casimiro, C. Wang, P. Fortina, S. Addya, R. G. Pestell, U. E. Martinez-Outschoorn, F. Sotgia and M. P. Lisanti (2009). "The reverse Warburg effect: aerobic glycolysis in cancer associated fibroblasts and the tumor stroma." Cell Cycle **8**(23): 3984-4001.

Pearce, E. L., M. C. Walsh, P. J. Cejas, G. M. Harms, H. Shen, L. S. Wang, R. G. Jones and Y. Choi (2009). "Enhancing CD8 T-cell memory by modulating fatty acid metabolism." Nature **460**(7251): 103-107.

Perdomo, G., S. R. Commerford, A. M. Richard, S. H. Adams, B. E. Corkey, R. M. O'Doherty and N. F. Brown (2004). "Increased beta-oxidation in muscle cells enhances insulin-stimulated glucose metabolism and protects against fatty acid-induced insulin resistance despite intramyocellular lipid accumulation." J Biol Chem **279**(26): 27177-27186.

Phng, L. K., M. Potente, J. D. Leslie, J. Babbage, D. Nyqvist, I. Lobov, J. K. Ondr, S. Rao, R. A. Lang, G. Thurston and H. Gerhardt (2009). "Nrarp coordinates endothelial Notch and Wnt signaling to control vessel density in angiogenesis." Dev Cell **16**(1): 70-82.

Pike, L. S., A. L. Smift, N. J. Croteau, D. A. Ferrick and M. Wu (2011). "Inhibition of fatty acid oxidation by etomoxir impairs NADPH production and increases reactive oxygen species resulting in ATP depletion and cell death in human glioblastoma cells." Biochim Biophys Acta **1807**(6): 726-734.

Potente, M., H. Gerhardt and P. Carmeliet (2011). "Basic and therapeutic aspects of angiogenesis." Cell **146**(6): 873-887.

Potente, M., L. Ghaeni, D. Baldessari, R. Mostoslavsky, L. Rossig, F. Dequiedt, J. Haendeler, M. Mione, E. Dejana, F. W. Alt, A. M. Zeiher and S. Dimmeler (2007). "SIRT1 controls endothelial angiogenic functions during vascular growth." Genes Dev **21**(20): 2644-2658.

Potente, M., C. Urbich, K. Sasaki, W. K. Hofmann, C. Heeschen, A. Aicher, R. Kollipara, R. A. DePinho, A. M. Zeiher and S. Dimmeler (2005). "Involvement of Foxo transcription factors in angiogenesis and postnatal neovascularization." J Clin Invest **115**(9): 2382-2392.

Prat, J. (2012). "New insights into ovarian cancer pathology." Annals of Oncology **23**: 111-117.

Prows, D. R., E. J. Murphy and F. Schroeder (1995). "Intestinal and liver fatty acid binding proteins differentially affect fatty acid uptake and esterification in L-cells." Lipids **30**(10): 907-910.

Puente, X. S., M. Pinyol, V. Quesada, L. Conde, G. R. Ordonez, N. Villamor, G. Escaramis, P. Jares, S. Bea, M. Gonzalez-Diaz, L. Bassaganyas, T. Baumann, M. Juan, M. Lopez-Guerra, D. Colomer, J. M. Tubio, C. Lopez, A. Navarro, C. Tornador, M. Aymerich, M. Rozman, J. M. Hernandez, D. A. Puente, J. M. Freije, G. Velasco, A. Gutierrez-Fernandez, D. Costa, A. Carrio, S. Guijarro, A. Enjuanes, L. Hernandez, J. Yague, P. Nicolas, C. M. Romeo-Casabona, H. Himmelbauer, E. Castillo, J. C. Dohm, S. de Sanjose, M. A. Piris, E. de Alava, J. San Miguel, R. Royo, J. L. Gelpi, D. Torrents, M. Orozco, D. G. Pisano, A. Valencia, R. Guigo, M. Bayes, S. Heath, M. Gut, P. Klatt, J. Marshall, K. Raine, L. A. Stebbings, P. A. Futreal, M. R. Stratton, P. J. Campbell, I. Gut, A. Lopez-Guillermo, X. Estivill, E. Montserrat, C. Lopez-Otin and E. Campo (2011). "Whole-genome sequencing identifies recurrent mutations in chronic lymphocytic leukaemia." Nature **475**(7354): 101-105.

Quintero, M., S. L. Colombo, A. Godfrey and S. Moncada (2006). "Mitochondria as signaling organelles in the vascular endothelium." Proc Natl Acad Sci U S A **103**(14): 5379-5384.

Rak, J., Y. Mitsuhashi, L. Bayko, J. Filmus, S. Shirasawa, T. Sasazuki and R. S. Kerbel (1995). "Mutant ras oncogenes upregulate VEGF/VPF expression: implications for induction and inhibition of tumor angiogenesis." Cancer Res **55**(20): 4575-4580.

Rao, P. K., M. Dorsch, T. Chickering, G. Zheng, C. Jiang, A. Goodearl, T. Kadesch and S. McCarthy (2000). "Isolation and characterization of the notch ligand delta4." Exp Cell Res **260**(2): 379-386.

Reedijk, M., S. Odorcic, L. Chang, H. Zhang, N. Miller, D. R. McCready, G. Lockwood and S. E. Egan (2005). "High-level coexpression of JAG1 and NOTCH1 is observed in human breast cancer and is associated with poor overall survival." Cancer Res **65**(18): 8530-8537.

Reihill, J. A., M. A. Ewart and I. P. Salt (2011). "The role of AMP-activated protein kinase in the functional effects of vascular endothelial growth factor-A and -B in human aortic endothelial cells." Vasc Cell **3**: 9.

Ridgway, J., G. Zhang, Y. Wu, S. Stawicki, W. C. Liang, Y. Chanthery, J. Kowalski, R. J. Watts, C. Callahan, I. Kasman, M. Singh, M. Chien, C. Tan, J. A. Hongo, F. de Sauvage, G. Plowman and M. Yan (2006). "Inhibition of Dll4 signalling inhibits tumour growth by deregulating angiogenesis." Nature **444**(7122): 1083-1087.

Roy, S. K., R. K. Srivastava and S. Shankar (2010). "Inhibition of PI3K/AKT and MAPK/ERK pathways causes activation of FOXO transcription factor, leading to cell cycle arrest and apoptosis in pancreatic cancer." J Mol Signal **5**: 10.

Russell, L. K., C. M. Mansfield, J. J. Lehman, A. Kovacs, M. Courtois, J. E. Saffitz, D. M. Medeiros, M. L. Valencik, J. A. McDonald and D. P. Kelly (2004). "Cardiac-specific induction of the transcriptional coactivator peroxisome proliferator-activated receptor gamma coactivator-1alpha promotes mitochondrial biogenesis and reversible cardiomyopathy in a developmental stage-dependent manner." Circ Res **94**(4): 525-533.

Salven, P., A. Lymboussaki, P. Heikkila, H. Jaaskela-Saari, B. Enholm, K. Aase, G. von Euler, U. Eriksson, K. Alitalo and H. Joensuu (1998). "Vascular endothelial growth factors VEGF-B and VEGF-C are expressed in human tumors." Am J Pathol **153**(1): 103-108.

Samudio, I., R. Harmancey, M. Fiegl, H. Kantarjian, M. Konopleva, B. Korchin, K. Kaluarachchi, W. Bornmann, S. Duvvuri, H. Taegtmeyer and M. Andreeff (2010). "Pharmacologic inhibition of fatty acid oxidation sensitizes human leukemia cells to apoptosis induction." J Clin Invest **120**(1): 142-156.

Sandler, A., R. Gray, M. C. Perry, J. Brahmer, J. H. Schiller, A. Dowlati, R. Lilenbaum and D. H. Johnson (2006). "Paclitaxel-carboplatin alone or with bevacizumab for non-small-cell lung cancer." N Engl J Med **355**(24): 2542-2550.

Sawada, N., A. Jiang, F. Takizawa, A. Safdar, A. Manika, Y. Tesmenitsky, K. T. Kang, J. Bischoff, H. Kalwa, J. L. Sartoretto, Y. Kamei, L. E. Benjamin, H. Watada, Y. Ogawa, Y. Higashikuni, C. W. Kessinger, F. A. Jaffer, T. Michel, M. Sata, K. Croce, R. Tanaka and Z. Arany (2014). "Endothelial PGC-1alpha mediates vascular dysfunction in diabetes." Cell Metab **19**(2): 246-258.

Scehnet, J. S., W. Jiang, S. R. Kumar, V. Krasnoperov, A. Trindade, R. Benedito, D. Djokovic, C. Borges, E. J. Ley, A. Duarte and P. S. Gill (2007). "Inhibition of Dll4-mediated signaling induces proliferation of immature vessels and results in poor tissue perfusion." Blood **109**(11): 4753-4760.

Schlaepfer, I. R., L. Rider, L. U. Rodrigues, M. A. Gijon, C. T. Pac, L. Romero, A. Cimic, S. J. Sirintrapun, L. M. Glode, R. H. Eckel and S. D. Cramer (2014). "Lipid Catabolism via CPT1 as a Therapeutic Target for Prostate Cancer." Mol Cancer Ther.

Scifres, C. M., B. Chen, D. M. Nelson and Y. Sadovsky (2011). "Fatty acid binding protein 4 regulates intracellular lipid accumulation in human trophoblasts." J Clin Endocrinol Metab **96**(7): E1083-1091.

Seghezzi, G., S. Patel, C. J. Ren, A. Gualandris, G. Pintucci, E. S. Robbins, R. L. Shapiro, A. C. Galloway, D. B. Rifkin and P. Mignatti (1998). "Fibroblast growth factor-2 (FGF-2) induces vascular endothelial growth factor (VEGF) expression in the endothelial cells of forming capillaries: an autocrine mechanism contributing to angiogenesis." J Cell Biol **141**(7): 1659-1673.

Shaughnessy, S., E. R. Smith, S. Kodukula, J. Storch and S. K. Fried (2000). "Adipocyte metabolism in adipocyte fatty acid binding protein knockout mice (aP2-/-) after short-term high-fat feeding: functional compensation by the keratinocyte [correction of keritinocyte] fatty acid binding protein." Diabetes **49**(6): 904-911.

Shawber, C., D. Nofziger, J. J. Hsieh, C. Lindsell, O. Bogler, D. Hayward and G. Weinmaster (1996). "Notch signaling inhibits muscle cell differentiation through a CBF1-independent pathway." Development **122**(12): 3765-3773.

Shen, W. J., Y. Liang, R. Hong, S. Patel, V. Natu, K. Sridhar, A. Jenkins, D. A. Bernlohr and F. B. Kraemer (2001). "Characterization of the functional interaction of adipocyte lipid-binding protein with hormone-sensitive lipase." J Biol Chem **276**(52): 49443-49448.

Shintani, S., C. Li, T. Ishikawa, M. Mihara, K. Nakashiro and H. Hamakawa (2004). "Expression of vascular endothelial growth factor A, B, C, and D in oral squamous cell carcinoma." Oral Oncol **40**(1): 13-20.

Shriver, L. P. and M. Manchester (2011). "Inhibition of fatty acid metabolism ameliorates disease activity in an animal model of multiple sclerosis." Sci Rep **1**: 79.

Shutter, J. R., S. Scully, W. Fan, W. G. Richards, J. Kitajewski, G. A. Deblandre, C. R. Kintner and K. L. Stark (2000). "Dll4, a novel Notch ligand expressed in arterial endothelium." Genes Dev **14**(11): 1313-1318.

Siekmann, A. F., L. Covassin and N. D. Lawson (2008). "Modulation of VEGF signalling output by the Notch pathway." Bioessays **30**(4): 303-313.

Sliwa, T., S. Awsa, M. Vesely, D. Rokitte, P. Grossschmidt, R. Jilch, W. Ulrich and K. Geissler (2014). "Hyperexpression of NOTCH-1 is found in immature acute myeloid leukemia." Int J Clin Exp Pathol **7**(3): 882-889.

Smith, A. J., B. R. Thompson, M. A. Sanders and D. A. Bernlohr (2007). "Interaction of the adipocyte fatty acid-binding protein with the hormone-sensitive lipase: regulation by fatty acids and phosphorylation." J Biol Chem **282**(44): 32424-32432.

Smith, N. R., D. Baker, N. H. James, K. Ratcliffe, M. Jenkins, S. E. Ashton, G. Sproat, R. Swann, N. Gray, A. Ryan, J. M. Jurgensmeier and C. Womack (2010). "Vascular endothelial growth factor receptors VEGFR-2 and VEGFR-3 are localized primarily to the vasculature in human primary solid cancers." Clin Cancer Res **16**(14): 3548-3561.

Sonveaux, P., T. Copetti, C. J. De Saedeleer, F. Vegran, J. Verrax, K. M. Kennedy, E. J. Moon, S. Dhup, P. Danhier, F. Frerart, B. Gallez, A. Ribeiro, C. Michiels, M. W. Dewhirst and O. Feron (2012). "Targeting the lactate transporter MCT1 in endothelial cells inhibits lactate-induced HIF-1 activation and tumor angiogenesis." PLoS One **7**(3): e33418.

Sonveaux, P., F. Vegran, T. Schroeder, M. C. Wergin, J. Verrax, Z. N. Rabbani, C. J. De Saedeleer, K. M. Kennedy, C. Diepart, B. F. Jordan, M. J. Kelley, B. Gallez, M. L. Wahl, O. Feron and M. W. Dewhirst (2008). "Targeting lactate-fueled respiration selectively kills hypoxic tumor cells in mice." J Clin Invest **118**(12): 3930-3942.

Staton, C. A., M. W. Reed and N. J. Brown (2009). "A critical analysis of current in vitro and in vivo angiogenesis assays." Int J Exp Pathol **90**(3): 195-221.

Stransky, N., A. M. Egloff, A. D. Tward, A. D. Kostic, K. Cibulskis, A. Sivachenko, G. V. Kryukov, M. S. Lawrence, C. Sougnez, A. McKenna, E. Shefler, A. H. Ramos, P. Stojanov, S. L. Carter, D. Voet, M. L. Cortes, D. Auclair, M. F. Berger, G. Saksena, C. Guiducci, R. C. Onofrio, M. Parkin, M. Romkes, J. L. Weissfeld, R. R. Seethala, L. Wang, C. Rangel-Escareno, J. C. Fernandez-Lopez, A. Hidalgo-Miranda, J. Melendez-Zajgla, W. Winckler, K. Ardlie, S. B. Gabriel, M. Meyerson, E. S. Lander, G. Getz, T. R. Golub, L. A. Garraway and J. R. Grandis (2011). "The mutational landscape of head and neck squamous cell carcinoma." Science **333**(6046): 1157-1160.

Sulsky, R., D. R. Magnin, Y. Huang, L. Simpkins, P. Taunk, M. Patel, Y. Zhu, T. R. Stouch, D. Bassolino-Klimas, R. Parker, T. Harrity, R. Stoffel, D. S. Taylor, T. B. Lavoie, K. Kish, B. L. Jacobson, S. Sheriff, L. P. Adam, W. R. Ewing and J. A. Robl (2007). "Potent and selective biphenyl azole inhibitors of adipocyte fatty acid binding protein (aFABP)." Bioorg Med Chem Lett **17**(12): 3511-3515.

Swendeman, S., K. Mendelson, G. Weskamp, K. Horiuchi, U. Deutsch, P. Scherle, A. Hooper, S. Rafii and C. P. Blobel (2008). "VEGF-A stimulates ADAM17-dependent

shedding of VEGFR2 and crosstalk between VEGFR2 and ERK signaling." Circ Res **103**(9): 916-918.

Swietach, P., R. D. Vaughan-Jones and A. L. Harris (2007). "Regulation of tumor pH and the role of carbonic anhydrase 9." Cancer Metastasis Rev **26**(2): 299-310.

Talks, K. L., H. Turley, K. C. Gatter, P. H. Maxwell, C. W. Pugh, P. J. Ratcliffe and A. L. Harris (2000). "The expression and distribution of the hypoxia-inducible factors HIF-1alpha and HIF-2alpha in normal human tissues, cancers, and tumor-associated macrophages." Am J Pathol **157**(2): 411-421.

Therade-Matharan, S., E. Laemmel, J. Duranteau and E. Vicaut (2004). "Reoxygenation after hypoxia and glucose depletion causes reactive oxygen species production by mitochondria in HUVEC." Am J Physiol Regul Integr Comp Physiol **287**(5): R1037-1043.

Thurston, G., I. Noguera-Troise and G. D. Yancopoulos (2007). "The Delta paradox: DLL4 blockade leads to more tumour vessels but less tumour growth." Nat Rev Cancer **7**(5): 327-331.

Tirado-Velez, J. M., I. Joumady, A. Saez-Benito, I. Cozar-Castellano and G. Perdomo (2012). "Inhibition of fatty acid metabolism reduces human myeloma cells proliferation." PLoS One **7**(9): e46484.

Tontonoz, P. and B. M. Spiegelman (2008). "Fat and beyond: the diverse biology of PPARgamma." Annu Rev Biochem **77**: 289-312.

Tretyakov, A. V. and H. W. Farber (1995). "Endothelial cell tolerance to hypoxia. Potential role of purine nucleotide phosphates." J Clin Invest **95**(2): 738-744.

Tucker, S. L., K. Gharpure, S. M. Herbrich, A. K. Unruh, A. M. Nick, E. K. Crane, R. L. Coleman, J. Guenthoer, H. J. Dalton, S. Y. Wu, R. Rupaimoole, G. Lopez-Berestein, B. Ozpolat, C. Ivan, W. Hu, K. A. Baggerly and A. K. Sood (2014). "Molecular biomarkers of residual disease after surgical debulking of high-grade serous ovarian cancer." Clin Cancer Res **20**(12): 3280-3288.

Tyra, H. M., D. R. Spitz and D. T. Rutkowski (2012). "Inhibition of fatty acid oxidation enhances oxidative protein folding and protects hepatocytes from endoplasmic reticulum stress." Mol Biol Cell **23**(5): 811-819.

Vang, R., M. Shih Ie and R. J. Kurman (2009). "Ovarian low-grade and high-grade serous carcinoma: pathogenesis, clinicopathologic and molecular biologic features, and diagnostic problems." Adv Anat Pathol **16**(5): 267-282.

Vegran, F., R. Boidot, C. Michiels, P. Sonveaux and O. Feron (2011). "Lactate influx through the endothelial cell monocarboxylate transporter MCT1 supports an NF-kappaB/IL-8 pathway that drives tumor angiogenesis." Cancer Res **71**(7): 2550-2560.

Veikkola, T. and K. Alitalo (1999). "VEGFs, receptors and angiogenesis." Semin Cancer Biol **9**(3): 211-220.

Viatour, P., U. Ehmer, L. A. Saddic, C. Dorrell, J. B. Andersen, C. Lin, A. F. Zmoos, P. K. Mazur, B. E. Schaffer, A. Ostermeier, H. Vogel, K. G. Sylvester, S. S. Thorgeirsson, M. Grompe and J. Sage (2011). "Notch signaling inhibits hepatocellular carcinoma following inactivation of the RB pathway." J Exp Med **208**(10): 1963-1976.

Villa, N., L. Walker, C. E. Lindsell, J. Gasson, M. L. Iruela-Arispe and G. Weinmaster (2001). "Vascular expression of Notch pathway receptors and ligands is restricted to arterial vessels." Mech Dev **108**(1-2): 161-164.

Vizan, P., S. Sanchez-Tena, G. Alcarraz-Vizan, M. Soler, R. Messeguer, M. D. Pujol, W. N. Lee and M. Cascante (2009). "Characterization of the metabolic changes underlying growth factor angiogenic activation: identification of new potential therapeutic targets." Carcinogenesis **30**(6): 946-952.

Wan, X., B. Harkavy, N. Shen, P. Grohar and L. J. Helman (2007). "Rapamycin induces feedback activation of Akt signaling through an IGF-1R-dependent mechanism." Oncogene **26**(13): 1932-1940.

Warburg, O. (1956). "On respiratory impairment in cancer cells." Science **124**(3215): 269-270.

Weis, S. M. and D. A. Cheresh (2011). "Tumor angiogenesis: molecular pathways and therapeutic targets." Nat Med **17**(11): 1359-1370.

Weng, A. P., A. A. Ferrando, W. Lee, J. P. t. Morris, L. B. Silverman, C. Sanchez-Irizarry, S. C. Blacklow, A. T. Look and J. C. Aster (2004). "Activating mutations of NOTCH1 in human T cell acute lymphoblastic leukemia." Science **306**(5694): 269-271.

Westhoff, B., I. N. Colaluca, G. D'Ario, M. Donzelli, D. Tosoni, S. Volorio, G. Pelosi, L. Spaggiari, G. Mazzarol, G. Viale, S. Pece and P. P. Di Fiore (2009). "Alterations of the Notch pathway in lung cancer." Proc Natl Acad Sci U S A **106**(52): 22293-22298.

Wiley, D. M., J. D. Kim, J. Hao, C. C. Hong, V. L. Bautch and S. W. Jin (2011). "Distinct signalling pathways regulate sprouting angiogenesis from the dorsal aorta and the axial vein." Nat Cell Biol **13**(6): 686-692.

Williams, C. K., J. L. Li, M. Murga, A. L. Harris and G. Tosato (2006). "Up-regulation of the Notch ligand Delta-like 4 inhibits VEGF-induced endothelial cell function." Blood **107**(3): 931-939.

Wise, D. R., R. J. DeBerardinis, A. Mancuso, N. Sayed, X. Y. Zhang, H. K. Pfeiffer, I. Nissim, E. Daikhin, M. Yudkoff, S. B. McMahon and C. B. Thompson (2008). "Myc regulates a transcriptional program that stimulates mitochondrial

glutaminolysis and leads to glutamine addiction." Proc Natl Acad Sci U S A **105**(48): 18782-18787.

Wise, D. R. and C. B. Thompson (2010). "Glutamine addiction: a new therapeutic target in cancer." Trends Biochem Sci **35**(8): 427-433.

Xie, M., L. Zhang, C. S. He, F. Xu, J. L. Liu, Z. H. Hu, L. P. Zhao and Y. Tian (2012). "Activation of Notch-1 enhances epithelial-mesenchymal transition in gefitinib-acquired resistant lung cancer cells." J Cell Biochem **113**(5): 1501-1513.

Yeh, W. L., C. J. Lin and W. M. Fu (2008). "Enhancement of glucose transporter expression of brain endothelial cells by vascular endothelial growth factor derived from glioma exposed to hypoxia." Mol Pharmacol **73**(1): 170-177.

Yun, H., M. Lee, S. S. Kim and J. Ha (2005). "Glucose deprivation increases mRNA stability of vascular endothelial growth factor through activation of AMP-activated protein kinase in DU145 prostate carcinoma." J Biol Chem **280**(11): 9963-9972.

Zaugg, K., Y. Yao, P. T. Reilly, K. Kannan, R. Kiarash, J. Mason, P. Huang, S. K. Sawyer, B. Fuerth, B. Faubert, T. Kalliomaki, A. Elia, X. Luo, V. Nadeem, D. Bungard, S. Yalavarthi, J. D. Growney, A. Wakeham, Y. Moolani, J. Silvester, A. Y. Ten, W. Bakker, K. Tsuchihara, S. L. Berger, R. P. Hill, R. G. Jones, M. Tsao, M. O. Robinson, C. B. Thompson, G. Pan and T. W. Mak (2011). "Carnitine palmitoyltransferase 1C promotes cell survival and tumor growth under conditions of metabolic stress." Genes Dev **25**(10): 1041-1051.

Zhang, F., Z. Tang, X. Hou, J. Lennartsson, Y. Li, A. W. Koch, P. Scotney, C. Lee, P. Arjunan, L. Dong, A. Kumar, T. T. Rissanen, B. Wang, N. Nagai, P. Fons, R. Fariss, Y. Zhang, E. Wawrousek, G. Tansey, J. Raber, G. H. Fong, H. Ding, D. A. Greenberg, K. G. Becker, J. M. Herbert, A. Nash, S. Yla-Herttuala, Y. Cao, R. J. Watts and X. Li (2009). "VEGF-B is dispensable for blood vessel growth but critical for their survival, and VEGF-B targeting inhibits pathological angiogenesis." Proc Natl Acad Sci U S A **106**(15): 6152-6157.

Zhao, Y. Z., X. L. Liu, G. M. Shen, Y. N. Ma, F. L. Zhang, M. T. Chen, H. L. Zhao, J. Yu and J. W. Zhang (2014). "Hypoxia induces peroxisome proliferator-activated receptor gamma expression via HIF-1-dependent mechanisms in HepG2 cell line." Arch Biochem Biophys **543**: 40-47.

Zhong, H., A. M. De Marzo, E. Laughner, M. Lim, D. A. Hilton, D. Zagzag, P. Buechler, W. B. Isaacs, G. L. Semenza and J. W. Simons (1999). "Overexpression of hypoxia-inducible factor 1alpha in common human cancers and their metastases." Cancer Res **59**(22): 5830-5835.

Zu, X. L. and M. Guppy (2004). "Cancer metabolism: facts, fantasy, and fiction." Biochem Biophys Res Commun **313**(3): 459-465.

Zundel, W., C. Schindler, D. Haas-Kogan, A. Koong, F. Kaper, E. Chen, A. R. Gottschalk, H. E. Ryan, R. S. Johnson, A. B. Jefferson, D. Stokoe and A. J. Giaccia (2000). "Loss of PTEN facilitates HIF-1-mediated gene expression." Genes Dev **14**(4): 391-396.